New Techniques for High Orders in Scattering Amplitudes

Prifysgol Abertawe
Swansea University

Joseph Strong

College of Science
Department of Physics

Primary supervisor
Dr Warren Perkins

Submitted in 2022 to Swansea University for the fulfilment of the requirements for the Degree of Doctor of Philosophy in Physics

Abstract

This thesis uses four-dimensional unitarity and augmented recursion to calculate a selection of Yang-Mills amplitudes. This selection consists of the full-colour, two-loop, all-plus helicity amplitudes for five- and six-points; a conjecture for an n-point sub-subleading in colour two-loop amplitude; calculation of the cut-constructible piece of the full-colour, two-loop, all-plus helicity n-point amplitude. A new technique for calculating the cut constructible part of the leading in colour two-loop, five-point, single-minus helicity amplitude is presented. The correct infrared divergent piece of this single-minus amplitude was calculated, as well as the correct transcendental two pieces at finite order. Logarithms containing Mandelstam variables including only positive helicity legs were unable to be correctly calculated, but the calculation of this final amplitude uncovered many new relations involving generalised hypergeometric functions such as the Appell functions.

Declaration

This work has not previously been accepted in substance for any degree and is not being concurrently submitted in candidature for any degree.
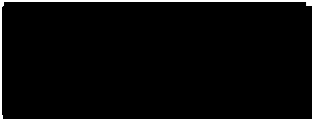
Signed: ████████████ Dated: 20/06/2022

This thesis is the result of my own investigations, except where otherwise stated. Other sources are acknowledged by footnotes giving explicit references. A bibliography is appended.

Signed: ████████████ Dated: 20/06/2022

I hereby give consent for my thesis, if accepted, to be available for photocopying and for inter-library loan, and for the title and summary to be made available to outside organisations.

Signed: ████████████ Dated: 20/06/2022

The University's ethical procedures have been followed and, where appropriate, that ethical approval has been granted.

Signed: ████████████ Dated: 20/06/2022

Contents

Acknowledgements

List of Figures

List of Tables

Chapter 1

Introduction

Physics is an exploratory science which may be split into two broad areas: theory and experiment. They have historically been heavily intertwined, where most theory was developed to explain observable phenomena on a classical scale, and there was even a time where it was thought that physics was almost solved. Clearly with a modern view this is emphatically untrue, and since the advent of quantum mechanics and general relativity, a new epoch of theoretical and experimental physics has begun.

This new epoch has seen the emergence of scattering amplitudes, a subject which aims to both probe mathematics and also to provide results that are needed in experiments. Collider experiments such as those performed at the Large Hadron Collider (LHC) seek to investigate the standard model of physics and indeed, what lies *beyond* the standard model. A typical collider experiment fires beams of high energy protons at each other, creating large numbers of product particles that hit the boundary detectors, and whose signatures are detected and measured. These measurements relate the total number of detected events, N_{events}, to the luminosity, L, and the cross section, σ, via

$$N_{\text{events}} = \int \mathrm{d}t \frac{\mathrm{d}N_{\text{events}}}{\mathrm{d}t} = \sigma \int \mathrm{d}t L = \sigma L_{int} \tag{1.1}$$

where L_{int} is the integrated luminosity. The cross section σ describes the probability of all possible interactions that can occur. The experiment can tune the integrated luminosity, aiming to increase both the luminosity and the time the experiment runs for, and then measure the number of events and calculate the cross section from these. The measured cross section can then be compared to the theoretical cross section which is related to scattering amplitudes (using a $2 \to 2$ process as an example) via

$$\sigma = \int_0^{2\pi} \mathrm{d}\theta \int_0^{\pi} \mathrm{d}\phi \frac{\mathrm{d}\sigma}{\mathrm{d}\Omega} \sin\theta = \int_0^{2\pi} \mathrm{d}\theta \int_0^{\pi} \mathrm{d}\phi |\mathcal{A}|^2 \sin\theta, \tag{1.2}$$

where Ω is the solid angle and $\mathcal{A}$ is the scattering amplitude. It is the calculation of scattering amplitudes that this thesis focuses on. These calculations provide a clear link between experiment and theory for high energy particle physics interactions.

The strong force is colour-charged and asymptotically free. Colour confinement tells us that no colour-charged particle can exist in an isolated state and must form colourless clumps of particles called hadrons. Asymptotic freedom means that at high energy the coupling constant of the theory is weak, and so colliding high energy protons produces, initially, quarks and gluons which fire off from the collision. Confinement then means that, in order to keep

these colour charged quarks and gluons in colourless clumps, additional quarks and gluons get pulled from the vacuum to create a new high energy hadron, which in turn separates into individual particles which pull quarks and gluons from the vacuum and so on. This process results in a tight cone of hadrons called a jet which eventually reach low energy scales.

As experimental precision and accuracy increases, we must reduce the theoretical uncertainties at each stage of the above processes. At the high energy scale we may perturbatively expand a given scattering amplitude and therefore break the calculation into an expansion in the coupling constant. If we are then to detect any new interactions or to test the interactions of the Standard Model, we need to understand the background that is produced during hadronization to a sufficiently high degree of accuracy, with sufficiency being determined by the accuracy of the experiment.

In this thesis, we wish to push the accuracy of the gluon-gluon interactions further and so we will calculate pure Yang-Mills theory [3]. Within pure Yang-Mills, the perturbative expansion of an n-gluon scattering amplitude is written as an expansion in the gauge coupling constant g

$$\mathcal{A}_n = ig^{n-2} \sum_{\ell \geq 0} a^\ell \mathcal{A}_n^{(\ell)}, \tag{1.3}$$

where $a = \frac{g^2 e^{-\epsilon \gamma_E}}{(4\pi)^{2-\epsilon}}$, γ_E is the Euler–Mascheroni constant, ϵ here is the dimensional regularisation constant [4] which we will discuss shortly. $\mathcal{A}^{(\ell)}$ is the ℓ'th loop amplitude. Traditionally these were calculated using Feynman diagrams [5] where the loop here refers to the number of closed, internal momentum loops present in the diagrams that are needed for each loop amplitude. This is the way most students will be introduced to Quantum Field Theory calculations at an undergraduate level; it involves drawing every allowed diagram in accordance to the Lagrangian of the theory, each vertex and internal propagator corresponding to a mathematical object. For tree-level diagrams, the momentum conservation at vertices allows the internal momenta to be constrained in terms of external momenta, which for uniformity in later discussions we will take to all be outgoing. For loop diagrams, there are momenta which cannot be uniquely specified and so must be integrated over.

While this was successful for tree-level and low multiplicity (i.e. small numbers of gluons), problems quickly develop, not least being the sheer number of diagrams needed to be summed over. For a four-point tree amplitude, there are only 4 diagrams so this is not an issue. However, by ten-point you need $10,525,900$ diagrams. Oh dear. This exponential increase goes up both with added gluons but also with added loops, comparing the $2,485$ diagrams needed for the seven-point, tree-level gluon amplitude with the $227,585$ diagrams needed for the one-loop, seven-point gluon amplitude. Another issue is that each Feynman diagram is gauge dependent with gauge independence only being restored in the full sum. Gauge dependent terms cancelling each other out implies redundancies and indeed, there are a huge number of them. Here is our first clue that these calculations could be vastly improved.

One way of improving this would be to find gauge invariant subsets, necessarily negating the need for gauge dependent terms cancelling. The first way of finding these gauge invariant subsets was inspired by string theory and the emergence of Chan-Paton factors [6], where an analogous decomposition was made for tree-level gluon amplitudes and applied to the six-point calculation [7, 8]. This decomposition allowed one to rewrite the amplitude for a

2

given helicity assignment as

$$\mathcal{A}_n^{(0)}(1^{\lambda_1}, 2^{\lambda_2}, ..., n^{\lambda_n}) = \sum_{\sigma \in S_n/Z_n} \text{Tr}(T^{a_{\sigma(1)}} T^{a_{\sigma(2)}} \cdots T^{a_{\sigma(n)}}) A_n^{(0)}(\sigma(1)^{\lambda_{\sigma(1)}}, \sigma(2)^{\lambda_{\sigma(2)}}, ..., \sigma(n)^{\lambda_{\sigma(n)}})$$

(1.4)

where the notation 1^{λ_1} refers to a labelling of gluon 1 with momentum p_1 and helicity λ_1, and the sum is over all non-cyclic permutations with S_n and Z_n being the set of all permutations and all cyclic permutations respectively. T^{a_i} are the 8×8 matrices in the adjoint representation of SU(3) and the traces are the equivalent of the Chan-Paton factors. We will hereby generalise SU(3) to SU(N_c) and indeed we will later take this to U(N_c) - however, that will become clearer in a later section. Helicity for a massless particle is a Lorentz invariant quantity which describes the spin projected onto the axis of the particle's three-momentum. This is given by

$$h := \frac{\mathbf{p} \cdot \mathbf{S}}{|\mathbf{p}|},$$

(1.5)

and decomposing the amplitude into a sum over all helicity configurations allows us to further fine grain the problem into more manageable pieces. These $A_n^{(0)}$ partial amplitudes have the same cyclic and flip symmetries of the trace of colour matrices they multiply,

$$A_n^{(0)}(1^{\lambda_1}, 2^{\lambda_2}, \cdots, n^{\lambda_n}) = A_n^{(0)}(2^{\lambda_2}, \cdots, n^{\lambda_n}, 1^{\lambda_1})$$

(1.6)

$$A_n^{(0)}(1^{\lambda_1}, 2^{\lambda_2}, \cdots, n^{\lambda_n}) = (-1)^n A_n^{(0)}(n^{\lambda_n}, (n-1)^{\lambda_{(n-1)}}, \cdots, 1^{\lambda_1})$$

(1.7)

and contain all of the kinematic information for that particular subset, motivating a view of (colour × kinematics). This colour decomposition is now a widely used convention and we will discuss how it extends beyond tree-level later. We will hereby simplify our notation by suppressing the σ's, writing the decomposition

$$\mathcal{A}_n^{(0)}(1^{\lambda_1}, 2^{\lambda_2}, ..., n^{\lambda_n}) = \sum_{S_n/Z_n} \text{Tr}(1, 2, \cdots, n) A_n^{(0)}(1^{\lambda_1}, 2^{\lambda_2}, \cdots, n^{\lambda_n})$$

(1.8)

to mean the same thing as (1.4).

The partial amplitudes are dependent on the external momenta and the helicites of the external particles. Indeed, the results of [7, 8] are presented in a compact notation that was introduced in [9–15] called the spinor helicity formalism, where [9–14] focused on QED calculations and [15] extended it to non-abelian gauge theories. This formalism allows one to rewrite four-vectors that transform under SO$^+$(1, 3) in terms of two Weyl spinors that transform under SL(2, $\mathbb{C}$). The next section of this chapter will review this formalism. We will then expand upon this, introducing the building blocks needed to create colour ordered Feynman rules. These rules are dependent on momentum and polarization vectors of the gluons and have the colour dependence stripped from them. We will then present some results that may be derived from these rules before continuing onto more modern techniques used in these calculations such as recursion and unitarity.

1.1 Spinor-Helicity Formalism

We have thus far seen that we can reduce the huge redundancies in the Feynman diagram approach to QCD by decomposing the amplitudes into gauge invariant subsets. These early

results can be presented in a compact form using the spinor-helicity formalism. This section reviews this formalism, wherein we present the four-momenta and polarisation vectors of massless particles in terms of products of two spinors. The remainder of this chapter can be found in more detail in [16].

First we should begin by covering some conventions. We choose the Weyl/chiral representation of the γ^μ matrix

$$\gamma^\mu = \begin{pmatrix} 0 & \sigma^\mu \\ \overline{\sigma}^\mu & 0 \end{pmatrix} \tag{1.9}$$

where $\sigma_\mu^{\dot{\alpha}\alpha} \equiv (\mathbb{1}, \sigma^i)$, $\overline{\sigma}_\mu^{\dot{\alpha}\alpha} = (\mathbb{1}, -\sigma^i)$ and σ^i are the Pauli matrices. We may use σ^μ to rewrite the four-momentum as

$$p^\mu \sigma_\mu^{\dot{\alpha}\alpha} = p^{\dot{\alpha}\alpha} = \begin{pmatrix} p^0 + p^3 & p^1 - ip^2 \\ p^1 + ip^2 & p^0 - p^3 \end{pmatrix}, \tag{1.10}$$

where the determinant of the matrix gives

$$\det(p^{\dot{\alpha}\alpha}) = p_0^2 - \sum_i p_i^2 = m^2. \tag{1.11}$$

The rank of a 2×2 matrix is at most two, but in the case of massless particles the rank reduces to one due to the vanishing determinant. This allows us to write the null four-momentum matrix as

$$p^{\dot{\alpha}\alpha} = \tilde{\lambda}^{\dot{\alpha}} \lambda^\alpha. \tag{1.12}$$

This can be extended to the massive case using a similar rank-two decomposition as a sum of two spinor biproducts, but again we will be focusing on pure Yang-Mills which is a massless theory. For real momenta we require $(\lambda^\alpha)^* = \pm \tilde{\lambda}^{\dot{\alpha}}$ where the sign depends on the sign of the energy of the four-momentum. An example solution for these spinors is

$$\lambda^\alpha = \frac{t}{\sqrt{p^0 + p^3}} \begin{pmatrix} p^0 + p^3 \\ p^1 + ip^2 \end{pmatrix}, \qquad \tilde{\lambda}^{\dot{\alpha}} = \frac{t^{-1}}{\sqrt{p^0 + p^3}} \begin{pmatrix} p^0 + p^3 \\ p^1 - ip^2 \end{pmatrix}, \tag{1.13}$$

where t is an overall convention dependent phase and it is apparent that $\sqrt{p^0 + p^3}$ is real/imaginary depending on whether p^0 is positive/negative because $|p^0| > |p^3|$, giving rise to the ± 1 factor. We will later need to extend the momentum to the complex plane in which case λ and $\tilde{\lambda}$ are independent. We will also be dealing with multiple gluons and thus we will assign a label $p_i^{\alpha\dot{\alpha}} = \lambda_i^\alpha \tilde{\lambda}_i^{\dot{\alpha}}$ for the i'th gluon. The freedom to rescale using t is generated by a helicity operator,

$$h = \sum_{i=1}^n \left(-\lambda_i^\alpha \frac{\partial}{\partial \lambda_i^\alpha} + \tilde{\lambda}_i^{\dot{\alpha}} \frac{\partial}{\partial \tilde{\lambda}_i^{\dot{\alpha}}} \right), \tag{1.14}$$

where we have assigned helicity -1 to λ and helicity $+1$ to $\tilde{\lambda}$. We see that these helicity spinors encode information both about the particle momentum but also about their helicity. We will see an example of how the helicity scaling can be useful further on within the thesis.

4

We can use standard spinor manipulations, raising and lowering spinor indices with the Levi-Civita tensor, and we can use Lorentz-invariant products to form the building blocks of our results

$$\langle i\,j \rangle := \lambda_i^\alpha \lambda_{j\alpha} = \epsilon_{\alpha\beta} \lambda_i^\alpha \lambda_j^\beta = -\langle j\,i \rangle$$
$$[i\,j] := \tilde{\lambda}_{i\dot\alpha} \tilde{\lambda}_j^{\dot\alpha} = -\epsilon_{\dot\alpha\dot\beta} \tilde{\lambda}_i^{\dot\alpha} \tilde{\lambda}_j^{\dot\beta} = -[j\,i]. \tag{1.15}$$

We may write the Mandelstam variables s_{ij} involving two massless particles i and j as

$$s_{ij} = (p_i + p_j)^2 = 2p_i \cdot p_j = p_i^{\alpha\dot\alpha} p_{j\alpha\dot\alpha} = \langle i\,j \rangle [j\,i], \tag{1.16}$$

where the conversion to spinor products can derived using

$$\bar\sigma_\mu^{\alpha\dot\alpha} \bar\sigma_\nu^{\beta\dot\beta} \epsilon_{\alpha\beta} \epsilon_{\dot\alpha\dot\beta} = 2\eta_{\mu\nu} \tag{1.17}$$

and

$$p_i^{\alpha\dot\alpha} p_j^{\beta\dot\beta} \epsilon_{\alpha\beta} \epsilon_{\dot\alpha\dot\beta} = p_i^\mu p_j^\nu \bar\sigma_\mu^{\alpha\dot\alpha} \bar\sigma_\nu^{\beta\dot\beta} \epsilon_{\alpha\beta} \epsilon_{\dot\alpha\dot\beta} = 2p_i^\mu p_j^\nu \eta_{\mu\nu} = 2p_i \cdot p_j. \tag{1.18}$$

It is clear here that $\langle i\,i \rangle = [i\,i] = 0$ and we see from $2p_i^2 = \langle i\,i \rangle [i\,i] = 0$ that the massless condition is encoded directly into these spinor products. We can also view the helicity spinors λ^α and $\tilde{\lambda}^{\dot\alpha}$ as solutions of the massless Dirac equation

$$|p\rangle := u_+(p) = v_-(p) = \begin{pmatrix} \lambda_\alpha \\ 0 \end{pmatrix}, \qquad |p] := u_-(p) = v_+(p) = \begin{pmatrix} 0 \\ \tilde{\lambda}^{\dot\alpha} \end{pmatrix}, \tag{1.19}$$

where we introduce the bracket notation $|i\rangle$ and $|i]$ for convenience later. $u_\pm$ and $v_\pm$ are chiral projections of the solutions of the massless Dirac equation, where $u_\pm(p) = \frac{1}{2}(1 \pm \gamma_5) u(p)$ and $v_\mp = \frac{1}{2}(1 \pm \gamma_5) v(p)$. The difference between u and v is only present for the massive Dirac equation but we keep both here for consistency with common notation. We note here that

$$\not{p}|p\rangle = p_\mu \gamma^\mu |p\rangle = \begin{pmatrix} 0 & p_{\alpha\dot\alpha} \\ p^{\dot\alpha\alpha} & 0 \end{pmatrix} \begin{pmatrix} \lambda_\alpha \\ 0 \end{pmatrix} = \not{p}|p] = 0, \tag{1.20}$$

showing that they satisfy the massless Dirac equation. Finally, with the introduction of a Schouten identity

$$\langle 1\,2 \rangle \lambda_3 + \langle 2\,3 \rangle \lambda_1 + \langle 3\,1 \rangle \lambda_2 = 0, \tag{1.21}$$

we now have the basics of the spinor helicity formalism. This Schouten identity comes from the fact that the spinors live in a two-space and so any three of them must have linear dependence. For example, we may write $\lambda_3 = \alpha\lambda_1 + \beta\lambda_2$, assuming $\lambda_1 \neq k\lambda_2$ for some constant k, and the Schouten identity becomes explicit,

$$\langle 1\,2 \rangle \lambda_3 + \langle 2\,3 \rangle \lambda_1 + \langle 3\,1 \rangle \lambda_2 = \langle 1\,2 \rangle \left(\alpha\lambda_1 + \beta\lambda_2 \right) + \alpha \langle 2\,1 \rangle \lambda_1 + \beta \langle 2\,1 \rangle \lambda_2 = 0. \tag{1.22}$$

Recalling that this formalism was used to present compact analytic results for the partial amplitudes in the colour-decomposed, gauge invariant subsets of the full amplitude (1.8), we seek a way to write down colour-stripped Feynman rules.

1.1.1 Helicity and Polarization Vectors for Gluons

We have introduced helicity spinors which contain information about a particle's momentum and its helicity. We have defined the helicity generators in (1.14), where we choose the convention of assigning the objects $\tilde{\lambda}/\lambda$ a helicity of $1/-1$. Alternative conventions assign $\pm\frac{1}{2}$ to the generators in (1.14) if dealing with other types of particles, but we only consider gluons in this thesis which are spin-1 particles. We wish to form modified Feynman rules that are stripped of colour information and to do so we will need another gluonic object, the polarization vectors $\varepsilon_\pm^\mu(p)$. These satisfy the relations

$$p \cdot \varepsilon_\pm = 0, \qquad \varepsilon_+(p) \cdot \varepsilon_+(p) = \varepsilon_-(p) \cdot \varepsilon_-(p) = 0, \tag{1.23}$$

and can be written in helicity spinor form for particle i as

$$\varepsilon_{+,i}^{\alpha\dot\alpha} = -\frac{\tilde{\lambda}_i^{\dot\alpha}\eta^\alpha}{\langle\lambda_i\,\eta_i\rangle}, \qquad \varepsilon_{-,i}^{\alpha\dot\alpha} = \frac{\lambda_i^\alpha\tilde{\eta}^{\dot\alpha}}{[\lambda_i\,\eta]}, \tag{1.24}$$

where η and $\tilde{\eta}$ are arbitrary reference spinors. It is easy to show the relations (1.23) are satisfied by this and that they are eigenvectors of the helicity operator with eigenvalues ± 1 for $\varepsilon_\pm^\mu$. It can be shown that with a shift of $\eta \to \eta + \delta\eta$, we have $\delta\varepsilon_+^{\alpha\dot\alpha}(p) \propto p^\mu$ and it can be shown that $\delta\varepsilon_+^\mu\mathcal{A}_{\mu\nu_1\ldots}(p, q_1, \ldots) = 0$. In this sense changing η corresponds to a gauge transformation and we see consistency in claiming that these partial amplitudes are gauge independent. Now that we have the gluon polarizations we may start looking at colour ordered Feynman rules.

1.2 Yang-Mills and Colour Ordered Feynman Rules

We have seen that we can colour decompose an amplitude into gauge invariant subsets, that the results can be presented in compact spinor helicity formalism and that we can present polarization vectors in this formalism. We will now apply these concepts to pure Yang-Mills theory and present some of the earliest results that used these techniques.

We define the field strength tensor as

$$F_{\mu\nu} = \partial_\mu A_\nu - \partial_\nu A_\mu - ig[A_\mu, A_\nu], \tag{1.25}$$

where A^μ is the gluon-field, and we can then decompose it in terms of the Lie algebra generators T^a of $\mathrm{SU}(N_c)$, such that $F_{\mu\nu} = F_{\mu\nu}^a T^a$, with

$$A_\mu^a = \mathrm{Tr}[T^a A_\mu] \tag{1.26}$$

and

$$F_{\mu\nu}^a = \partial_\mu A_\nu^a - \partial_\nu A_\mu^a + igf^{abc}A_\mu^b A_\nu^c, \tag{1.27}$$

where we take T^a to be the traceless, antihermitian generators of the fundamental representation of $\mathrm{SU}(N_c)$. In the adjoint representation the entries of the matrices are just the structure constants $(T^a)_{bc} = f^{abc}$. The Lagrangian for pure Yang-Mills is then

$$\mathcal{L} = -\frac{1}{4}\mathrm{Tr}[F_{\mu\nu}F^{\mu\nu}]. \tag{1.28}$$

where we take the trace over the colour indices to keep it gauge invariant. We need to add a gauge fixing term

$$\mathcal{L}_{g.f} = -\frac{1}{2\xi}(\partial^\mu A_\mu^a)^2 \tag{1.29}$$

and, given this is a non-Abelian gauge theory, we should also need ghosts. We will discuss later that we use unitarity methods which involve only on-shell particles in the S-matrix, and so these ghosts play no part in practice. From here we can write down the momentum space Feynman rules where the gluon propagator is given by

$$\Delta_{\mu\nu}^{ab}(k) = \frac{\delta^{ab}}{k^2 + i\delta}\left(\eta_{\mu\nu} + (\xi - 1)\frac{k_\mu k_\nu}{k^2 + i\delta}\right), \tag{1.30}$$

where the $i\delta$ term regularised the $k^2 \to 0$ limit of the propagator. We have the three/four point vertices, again with all outgoing gluons, are given by
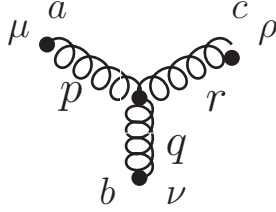
$$iV_{\mu\nu\rho}^{abc}(p, q, r) = gf^{abc}\left[(q - r)_\mu \eta_{\nu\rho} + (r - p)_\nu \eta_{\rho\mu} + (p - q)_\rho \eta_{\mu\nu}\right] \tag{1.31}$$

and
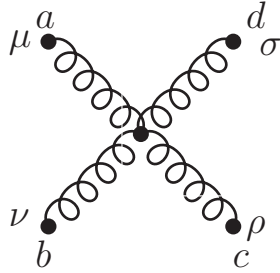
$$\begin{aligned}
iV_{\mu\nu\rho\sigma}^{abcd} = -\,ig^2\Big[&f^{abe}f^{cde}(\eta_{\mu\rho}\eta_{\nu\sigma} - \eta_{\mu\sigma}\eta_{\nu\rho}) \\
&+ f^{ace}f^{dbe}(\eta_{\mu\sigma}\eta_{\nu\rho} - \eta_{\mu\nu}\eta_{\rho\sigma}) \\
&+ f^{ade}f^{bce}(\eta_{\mu\nu}\eta_{\rho\sigma} - \eta_{\mu\rho}\eta_{\nu\sigma})\Big].
\end{aligned} \tag{1.32}$$

We can then disentangle the colour and kinematic degrees of freedom by rewriting the structure constants on a given diagram in terms of traces of strings of generator matrices,

$$f^{abc} = \text{Tr}(T^a[T^b, T^c]), \tag{1.33}$$

normalised to

$$\mathrm{Tr}[T^a T^b] = \delta^{ab}. \tag{1.34}$$

Summing over all diagrams after rewriting the colour factors like this leads to the decomposition (1.8). With the separation of colour and kinematics we can write down colour ordered Feynman rules which make use of the already discussed polarization vectors, with the propagator being given by

$$D_{\mu\nu}(p) = -\frac{i}{p^2 + i\delta}\eta_{\mu\nu}, \tag{1.35}$$

and three/four point vertices being given by

$$V_3 = -g[(\varepsilon_1 \cdot \varepsilon_2)((p_1 - p_2) \cdot \varepsilon_3) + (\varepsilon_2 \cdot \varepsilon_3)((p_2 - p_3) \cdot \varepsilon_1) + (\varepsilon_3 \cdot \varepsilon_1)((p_3 - p_1) \cdot \varepsilon_2] \tag{1.36}$$

and

$$V_4 = g^2[2(\varepsilon_1 \cdot \varepsilon_3)(\varepsilon_2 \cdot \varepsilon_4) - (\varepsilon_1 \cdot \varepsilon_2)(\varepsilon_3 \cdot \varepsilon_4) - (\varepsilon_1 \cdot \varepsilon_4)(\varepsilon_2 \cdot \varepsilon_3)]. \tag{1.37}$$

With these colour ordered Feynman rules, the number of diagrams which contribute to a specific colour structure is vastly reduced and one can start deriving simple tree amplitudes. We will briefly outline the calculation of the vanishing amplitudes and the four-point tree amplitudes, before presenting an n-point amplitude. This will demonstrate the simplification of the colour decomposition and the power of the compact spinor helicity formalism.

1.2.1 Initial Tree Amplitudes

Firstly, we will present some n-point vanishing results. We choose a uniform, massless reference momentum $\eta = \lambda_\eta \tilde{\lambda}_\eta$ to be used in the polarization vectors for all external gluons, which immediately yields the relations

$$\varepsilon_{+,i} \cdot \varepsilon_{+,j} = \varepsilon_{-,i} \cdot \varepsilon_{-,j} = 0. \tag{1.38}$$

It can be easily argued that an n-leg tree graph contains at least one polarization contraction of the form $\varepsilon_i \cdot \varepsilon_j$. Therefore, we immediately conclude that "all-plus" tree amplitudes vanish,

$$A_n^{(0)}(a^+, b^+, \ldots, n^+) = 0, \tag{1.39}$$

as there necessarily is at least one $\varepsilon_{+,i} \cdot \varepsilon_{+,j}$. The amplitude with opposite helicities are related by parity transformations and so the "all-minus" trees vanish. We will henceforth consider mostly positive helicity amplitudes due to this relation. For the "single-minus" tree amplitude, $A^{(0)}(a^-, b^+, c^+, \ldots, n^+)$, we can make a different choice of reference momenta within the polarization vectors such that,

$$q_a = q \neq p_a, \qquad q_b = q_c = \ldots = q_n = p_a, \tag{1.40}$$

where q is arbitrary and p_a is the external, null, four momentum for gluon a. We therefore still have any term with $\varepsilon_{+,i} \cdot \varepsilon_{+,j} = 0$, and now we have $\varepsilon_{+,i} \cdot \varepsilon_{-,a} = 0$, we can write

$$A_n^{(0)}(a^-, b^+, c^+, \ldots, n^+) = 0. \tag{1.41}$$

Again, the single-plus tree amplitudes must also vanish. It should be noted that while we can always make a choice of η like this, once the choice has been made for an amplitude it must be used for all diagrams.

We next want to consider "maximally helicity violating" (MHV) amplitudes with two minus legs and the remainder positive (the conjugate of this being called $\overline{\text{MHV}}$ or a "googly" amplitude). This is named as such because in super-Yang-Mills (SYM) theory the all-plus and single minus amplitudes vanish to all loop orders, and so it is the first non-zero amplitude that maximises the sum of all helicities. This is also true at tree-level for YM theory.

For the four-point interaction these MHV amplitudes are the only non-zero contributions and we will briefly calculate them here. We can make the choice of reference momenta $\{q_a, q_b, q_c, q_d\} = \{p_d, p_d, p_a, p_a\}$ which gives the only contractible polarization vectors as

$$\varepsilon_{-,b} \cdot \varepsilon_{+,c} = -\frac{\langle \eta_c \, \lambda_b \rangle \, [\eta_b \, \lambda_c]}{\langle \lambda_c \, \eta_c \rangle \, [\lambda_b \, \eta_b]} = -\frac{\langle a \, b \rangle \, [c \, d]}{\langle a \, c \rangle \, [b \, d]}. \tag{1.42}$$

The only surviving diagram that contributes to this trace structure with this choice of reference momenta, and therefore the total contribution to this partial amplitude, is given by Figure 1.1
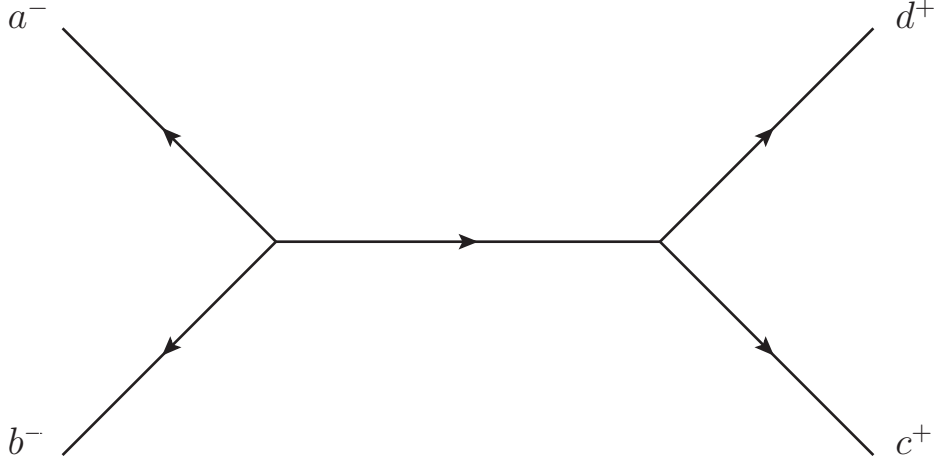
Figure 1.1: Non-zero contribution to $A^{(0)}(a^-, b^-, c^+, d^+)$

where we will hereby use these lines and arrows to represent momentum flow of gluonic propagators, given that there are no other particles in this theory. Using the colour ordered Feynman rules, this leads to

$$
\begin{aligned}
A^{(0)}&(a^-, b^-, c^+, d^+) \\
&= \frac{\eta_{\mu\nu}}{s_{ab}} \left[\varepsilon^\mu_{-,b}(2p_b + p_a) \cdot \varepsilon_{-,a} - \varepsilon^\mu_{-,a}(2p_a + p_b) \cdot \varepsilon_{-,b} \right] \\
&\times \left[\varepsilon^\nu_{+,d}(2p_d + p_c) \cdot \varepsilon_{+,c} - \varepsilon^\nu_{+,c}(2p_c + p_d) \cdot \varepsilon_{+,d} \right] \\
&= -\frac{4}{s_{ab}} (\varepsilon_{-,b} \cdot \varepsilon_{+,c})(p_b \cdot \varepsilon_{-,a})(p_c \cdot \varepsilon_{+,d}) \\
&= -\frac{4}{s_{ab}} \left(-\frac{\langle a \, b \rangle \, [c \, d]}{\langle a \, c \rangle \, [b \, d]} \right) \left(\frac{1}{2} \frac{\langle a \, b \rangle \, [b \, d]}{[a \, d]} \right) \left(\frac{1}{2} \frac{\langle a \, c \rangle \, [c \, d]}{[d \, a]} \right) \\
&= -\frac{\langle a \, b \rangle \, [c \, d]^2}{[a \, b] \, \langle a \, d \rangle \, [d \, a]}. \tag{1.43}
\end{aligned}
$$

We can use overall momentum conservation for outgoing gluons to rewrite $s_{cd} = \langle c\,d \rangle [d\,c] = s_{ab}$, and we can use

$$\sum_{i=1}^{n} p_i^\mu = \sum_{i=1}^{n} \lambda_i^\alpha \tilde{\lambda}_i^{\dot\alpha} = \sum_{i=1}^{n} \langle x\,i \rangle [i\,y] = 0, \tag{1.44}$$

where x and y here are arbitrary, to rewrite the amplitude as

$$A^{(0)}(a^-, b^-, c^+, d^+) = -\frac{\langle a\,b \rangle [c\,d]^2}{[a\,b] \langle a\,d \rangle [d\,a]} \times \frac{\langle d\,c \rangle}{\langle d\,c \rangle} = -\frac{\langle a\,b \rangle^2 [c\,d]}{\langle b\,c \rangle \langle d\,a \rangle [b\,a]} \times \frac{\langle d\,c \rangle}{\langle d\,c \rangle} = \frac{\langle a\,b \rangle^3}{\langle b\,c \rangle \langle c\,d \rangle \langle d\,a \rangle}. \tag{1.45}$$

We would then like to calculate $A^{(0)}(a^-, b^+, c^-, d^+)$ but we can show this is dependent on (1.45) by introducing photon decoupling identities. There is no interaction between photons and gluons (as seen by the vanishing structure constants) and we know that the Lie algebras satisfy $u(N_c) \equiv su(N_c) \times u(1)$, therefore the U($N_c$) and SU($N_c$) amplitudes are identical. If we then set one of the legs to be this U(1) "photon" with colour generator,

$$T^a\Big|_{\mathrm{U}(1)} = \frac{1}{\sqrt{N_c}} \mathbb{1}_{N_c \times N_c}, \tag{1.46}$$

and extract the resulting common trace structure from the full colour sum we find

$$A_n^{(0)}(1, 2, 3, \ldots, n) + A_n^{(0)}(2, 1, 3, \ldots, n) + \ldots + A_n^{(0)}(2, 3, \ldots, (n-1), 1, n) = 0. \tag{1.47}$$

We have set leg 1 as the U(1) photon here but it works for any leg. This is the tree-level decoupling identity and there are equivalent identities derived in the same way at loop orders but we will cover these later. This means we can write,

$$\begin{aligned}
A_4^{(0)}(a^-, b^+, c^-, d^+) &= -A_4^{(0)}(a^-, b^+, d^+, c^-) - A_4^{(0)}(a^-, d^+, b^+, c^-) \\
&= \frac{\langle c\,a \rangle^4}{\langle a\,b \rangle \langle b\,c \rangle \langle c\,d \rangle \langle d\,a \rangle} \left(\frac{\langle d\,a \rangle \langle b\,c \rangle + \langle a\,b \rangle \langle d\,c \rangle}{\langle b\,d \rangle \langle c\,a \rangle} \right) \\
&= \frac{\langle c\,a \rangle^4}{\langle a\,b \rangle \langle b\,c \rangle \langle c\,d \rangle \langle d\,a \rangle},
\end{aligned} \tag{1.48}$$

where we have used the Schouten identity (1.21) with the free λ contracted so it is equivalently written as

$$\langle w\,x \rangle \langle y\,z \rangle + \langle x\,y \rangle \langle w\,z \rangle + \langle y\,w \rangle \langle x\,z \rangle = 0. \tag{1.49}$$

These results can be generalised to the form

$$A_4^{(0)}(a, b, c, d; i^-, j^-) = \frac{\langle i\,j \rangle^4}{\langle a\,b \rangle \langle b\,c \rangle \langle c\,d \rangle \langle d\,a \rangle} \tag{1.50}$$

where i and j are whichever of $\{a, b, c, d\}$ have the negative helicities. We earlier said how the amplitude was decomposed with colour into gauge invariant subsets and presented in spinor helicity formalism in [7, 8]. In these papers there were two more results presented

$$A_5^{(0)}(a, b, c, d, e; i^-, j^-) = \frac{\langle i\,j \rangle^4}{\langle a\,b \rangle \langle b\,c \rangle \langle c\,d \rangle \langle d\,e \rangle \langle e\,a \rangle} \tag{1.51}$$

10

and

$$A_6^{(0)}(a, b, c, d, e, f; i^-, j^-) = \frac{\langle i\,j\rangle^4}{\langle a\,b\rangle\,\langle b\,c\rangle\,\langle c\,d\rangle\,\langle d\,e\rangle\,\langle e\,f\rangle\,\langle f\,a\rangle}, \tag{1.52}$$

which is suggestive of an n-point result

$$A_n^{(0)}(a, b, \ldots, n; i^-, j^-) = \frac{\langle i\,j\rangle^4}{\langle a\,b\rangle\,\langle b\,c\rangle\cdots\langle n-1\,n\rangle\,\langle n\,a\rangle}. \tag{1.53}$$

This is the Parke-Taylor amplitude [17] and, while it was originally presented in terms of the squared amplitude and scalar products, it easily translates to the spinor helicity formalism. This result was not proven until [18] where recursion relations were used to prove this result by induction. We will discuss recursion shortly, but first let us look closer at this result and see what features it satisfies and how the spinor helicity formalism lends itself to easy checks. To start with, the cyclic and flip symmetries are clearly manifest, recalling that $\langle x\,y\rangle = -\langle y\,x\rangle$. Another property it must satisfy is the correct momentum weight. We can see from $p^{\alpha\dot\alpha} = \lambda^\alpha\tilde\lambda^{\dot\alpha}$ and $\tilde\lambda = (\lambda)^*$ that each $\lambda/\tilde\lambda$ spinor carries a momentum weight of $\frac{1}{2}$. Each spinor bracket therefore has overall momentum weight of 1. An n-point amplitude has $4 - n$ powers of momentum, and so the overall momentum weight is clearly satisfied.

We also can check the little group scaling. We saw from (1.13) that the spinors may be rescaled arbitrarily without changing the momentum, this little group scale being given by t. We can then see from (1.24) then that

$$\varepsilon_+ \sim t^{-2}, \qquad \varepsilon_- \sim t^2 \tag{1.54}$$

and this gives another check on the amplitude. Looking at $A_4^{(0)}(a^-, b^-, c^+, d^+)$ as an example and recognising that $|x] \sim t^{-1}$ and $|x\rangle \sim t$, if we label the little group scaling of a gluon i as t_i we see

$$\frac{\langle a\,b\rangle^3}{\langle b\,c\rangle\,\langle c\,d\rangle\,\langle d\,a\rangle} \sim \frac{t_a^3 t_b^3}{t_b t_c \times t_c t_d \times t_d t_a} = t_a^2 t_b^2 t_c^{-2} t_d^{-2}. \tag{1.55}$$

These properties serve as quick, straightforward and easy to read checks on results and, as we will see later, provide some limits on what types of functions we may expect to see. This Parke-Taylor amplitude was the first non-trivial n-point amplitude for a non-abelian gauge theory and clearly demonstrates the shortcomings of the original Feynman diagram approach, where the exponential increase in complexity discussed earlier can all be reduced to a single term. It also demonstrates how more modern techniques have overcome many of these shortcomings, where recursion and the factorisation properties of tree amplitudes were used to prove this formula. The next section introduces the basics of recursion.

1.3 Factorisation and Complex Recursion

We have discussed how the spinor helicity formalism provides compact analytic forms for amplitudes. In this notation there are physical properties that can sometimes be read straight from the amplitude; one such property is the amplitude's analytic structure. We see in (1.53) that if any adjacent momenta become collinear, for example if $p_{i+1} = k \times p_i$ where k is some constant, then $(p_i + p_{i+1})^2 = (1 + k)^2 p_i^2 = (1 + k)^2 \langle i\,i\rangle\,[i\,i] = 0$, and this manifests itself as

a simple pole in the amplitude. One must be wary of the presence of unphysical "spurious" poles appearing in the results of calculations, in which the numerator also goes to zero on an apparent pole. This will be discussed more later but as there are no spurious poles in (1.53), we can press on.

These collinear limits are a subset of kinematic regions where internal propagators go on shell. These regions provide a strong consistency check on a given amplitude. In such a region where the propagator has more than two gluons on each side of the propagator, the amplitude factorises into products of lower point amplitudes,

$$\lim_{P_{1...i}^2 \to 0} A_n^{(0)}(1, \ldots, i, i+1, \ldots, n) = \sum_\lambda A_{i+1}^{(0)}(1, \ldots, i, P_{1...i}^\lambda) \times \frac{-1}{P_{1...i}^2} A_{n-i+1}^{(0)}(-P_{1...i}^{-\lambda}, i+1, \ldots, n)$$
(1.56)

where $i \geq 3$ and we introduce the notation

$$P_{i...j} = p_i + p_{i+1} + \ldots + p_{j-1} + p_j.$$
(1.57)

We assign helicity to $P_{1...i}$ as in the collinear limit this momentum goes null and we must sum over both helicity configurations. This sum over helicities originates from rewriting the metric tensor from the connecting propagator in terms of a sum of polarization vectors due to the completeness relation,

$$\sum_\lambda \varepsilon^{\mu, \lambda} (\varepsilon^{\nu, \lambda})^* \sim -\eta^{\mu\nu}.$$
(1.58)

If we know the lower order amplitudes then this provides a strong check which can be implemented analytically or numerically on the n-point amplitude.

In the case of $i = 2$, this necessarily means the two external particles are collinear. This leads to a universal behaviour

$$\lim_{i||i+1} A_n^{(0)}(1, 2, \ldots, i, i+1, \ldots, n)$$
$$= \sum_\lambda \text{Split}_\lambda^{(0)}(i, i+1; z) A_{n-1}^{(0)}(1, 2, \ldots, i-1, k^{-\lambda}, i+2, \ldots, n),$$
(1.59)

where $\text{Split}_\lambda^{(\ell)}$ are splitting functions and z here is a parameter that can relate the collinear gluons via

$$p_i = (1 - z)k, \qquad p_{i+1} = zk,$$
(1.60)

where $k^2 = (p_i + p_{i+1})^2 = 0$. This discussion will be extended to loop order later but for now the tree-level splitting functions are [17, 19, 20]

$$\text{Split}_+^{(0)}(i^+, j^-) = \frac{1}{\langle i \, j \rangle} \frac{(1-z)^2}{\sqrt{z(1-z)}}$$

$$\text{Split}_-^{(0)}(i^+, j^-) = \frac{1}{[j \, i]} \frac{z^2}{\sqrt{z(1-z)}}$$

$$\text{Split}_-^{(0)}(i^+, j^+) = \frac{1}{\langle i \, j \rangle} \frac{1}{\sqrt{z(1-z)}}$$

$$\text{Split}_-^{(0)}(i^-, j^-) = 0.$$
(1.61)

We may relate the remaining splitting functions to these via conjugation. Other factorising behaviour may be exhibited in the soft limit of an external momentum [19, 20]. This is when one of the external momenta goes to zero $p_i \to 0$ and factorises the amplitude as

$$\lim_{p_s \to 0} A_n^{(0)}(1, 2, \ldots, s-1, s^{\lambda_s}, s+1, \ldots, n)$$
$$= \text{Soft}^{(0)}(s-1, s^{\lambda_s}, s+1) A_{n-1}^{(0)}(1, 2, \ldots, s-1, s+1, \ldots, n) \quad (1.62)$$

where

$$\text{Soft}^{(0)}(i, s^+, j) = \left(\text{Soft}^{(0)}(i, s^-, j)\right)^* = \frac{\langle i\, j \rangle}{\langle i\, s \rangle \langle s\, j \rangle}. \quad (1.63)$$

We can make good use of factorisation properties of amplitudes to implement powerful tools for calculation. One such tool is complex recursion, used to construct rational parts of amplitudes using complex analysis and factorisation theorems. This involves shifting select external momenta into the complex plane, introducing some complex variable z (different to the splitting function variable z above) and looking at the rational parts of the amplitude as a meromorphic function of z. The poles in z are then associated with internal propagators going on shell. The residues of the highest order singularities in the Laurent series around these propagator z poles are the factorisations of the amplitude.

This observation was first made in [21, 22] and was used to generate a set of recursion relations which can be used to build higher point tree amplitudes as we will now discuss.

1.3.1 Britto-Cachazo-Feng-Witten (BCFW) Recursion

We have shown how colour ordering Feynman rules and colour decomposing the amplitudes can reduce redundancy, yet we still see the use of Feynman diagrams. We will now discuss how the factorisation properties may be used to develop recursion relations, massively reducing redundancies as we can now write the amplitude as a sum of products of on-shell, gauge invariant amplitudes. This significantly reduces algebraic cancellations by eliminating gauge redundancy. In this thesis, when we talk about applying recursion to the calculation of amplitudes, we really only mean the rational parts of the amplitudes although this will only become relevant at loop order.

We start by considering an n-point amplitude and perform a complex shift of two neighbouring legs, for example 1 and n,

$$\lambda_1 \to \hat{\lambda}_1(z) = \lambda_1 - z\lambda_n,$$
$$\tilde{\lambda}_n \to \hat{\tilde{\lambda}}_n(z) = \tilde{\lambda}_n + z\tilde{\lambda}_1, \quad (1.64)$$

where $z \in \mathbb{C}$. The momentum then gets complexified via

$$p_1^{\alpha\dot{\alpha}} \to \hat{p}_1^{\alpha\dot{\alpha}}(z) = (\lambda_1 - z\lambda_n)^\alpha \tilde{\lambda}_1^{\dot{\alpha}},$$
$$p_n^{\alpha\dot{\alpha}} \to \hat{p}_n^{\alpha\dot{\alpha}}(z) = \lambda_n^\alpha (\tilde{\lambda}_n + z\tilde{\lambda}_1)^{\dot{\alpha}}, \quad (1.65)$$

where the deformation preserves momentum conservation and on-shell conditions,

$$\hat{p}_1^2 = \hat{p}_n^2 = 0, \qquad \hat{p}_1 + \hat{p}_n = p_1 + p_n. \quad (1.66)$$

As previously mentioned, this shift effectively turns the amplitude into a meromorphic function of z, $A_n(z)$. Propagator poles become poles in z whose locations need to be analysed. The residue of the highest order pole in the Laurent series corresponds to products of lower order tree amplitudes, with emphasis here on the highest order pole as we will show later that at loop order we see the emergence of double poles. This type of recursion can then provide the double pole contribution but it fails to provide the full simple pole piece. We also need to analyse the large z behaviour of $A(z)$, requiring it to vanish for a given shift at large z so that we may perform a suitable contour integral.

For tree-level these simple poles are easy enough to find. Consider the factorisation in Figure 1.2,
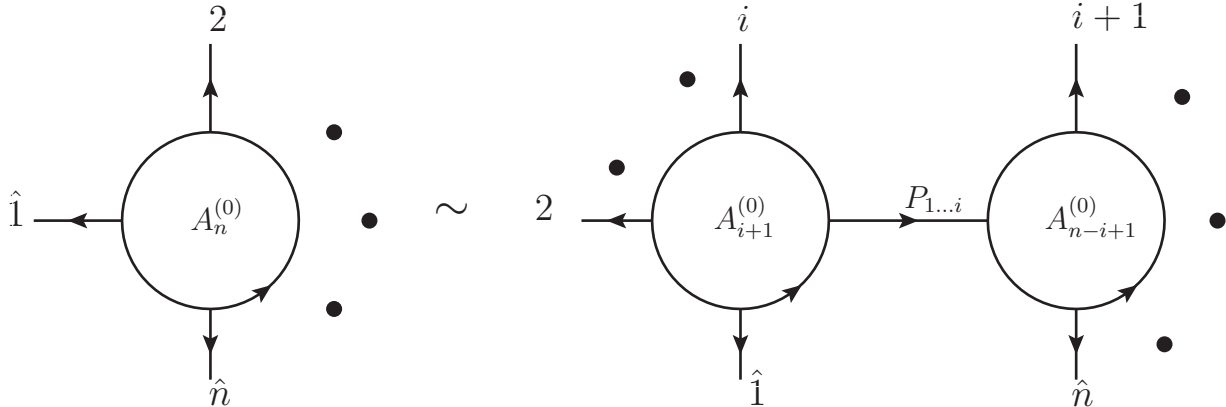
Figure 1.2: Factorisation of the n-point amplitude $A_n^{(0)}$ on the propagator pole $z_{P_{1\ldots i}}$ corresponding to the sum $p_1 + p_2 + \ldots + p_i$ going on-shell.

where we have a factorisation connected by the propagator

$$\frac{1}{\hat{P}_{1\ldots i}^2} = \frac{1}{(\hat{p}_1 + p_2 + \ldots + p_i)^2} = \frac{1}{P_{1\ldots i}^2 - z[1|P_{1\ldots i}|n\rangle}, \qquad (1.67)$$

where we introduce the notation $[1|P_{1\ldots i}|n\rangle = \lambda_{n\alpha} P_{1\ldots i}^{\alpha\dot\alpha} \tilde\lambda_{1\dot\alpha} = \sum_{j=1}^{i}[1|j|n\rangle$. It is important that $\hat{p}_1$ and $\hat{p}_n$ are on different sides of the factorisation as the sum of the two is independent of z and so no poles are present. This shift clearly breaks the cyclic symmetry of the problem and later we will see recovering this cyclic symmetry becomes a highly non-trivial check on results. Pressing on, we see that $A_n(z)$ has simple poles in z at,

$$z_i = \frac{P_{1\ldots i}^2}{[1|P_{1\ldots i}|n\rangle}, \qquad (1.68)$$

where $i \in [2, n-2]$. In [22] it was proven that the residue of this pole corresponds to a sum of lower point amplitudes and so we can write

$$\lim_{z \to z_i} A_n(z) = \frac{1}{z - z_i} \frac{-1}{[1|P_{1\ldots i}|n\rangle} \sum_{\lambda} A_{i+1}^{(0)} \left(\hat{1}(z_i), 2, \ldots, i, \hat{P}_{1\ldots i}^{\lambda}(z_i) \right)$$

$$\times A_{n-i+1}^{(0)} \left(-\hat{P}_{1\ldots i}^{-\lambda}(z_i), i+1, \ldots, n-1, \hat{n}(z_i) \right). \qquad (1.69)$$

It is possible to prove this factorisation, but it is easy to convince yourself that the clusters on each side of the factorisation contain all of the Feynman diagrams necessary to calculate that particular lower-point amplitude, and that the propagator goes on shell so this becomes

14

a product of two on-shell sub-amplitudes. The sum over λ is again over both helicities of the now on-shell $\hat{P}_{1\ldots i}(z_i)$; if one were to consider other theories we would also need to consider the full particle content that could run between the factorisations.

The amplitude we are interested in is $A_n(z = 0)$ and so with our eye on Cauchy's residue theorem we would like a pole at $z = 0$. This does not correspond to any propagator pole and so we must include the pole manually. This can be simply done by considering the contour integral

$$\mathcal{I}(z) = \frac{1}{2\pi i} \oint_\gamma \frac{A^{(0)}(z)}{z} \mathrm{d}z, \tag{1.70}$$

where dividing by z inserts a $z = 0$ pole and γ is a circular contour that we take to infinity, containing all propagator poles and the pole at $z = 0$. Cauchy's residue theorem then gives us

$$\mathcal{I}(z) = A_n^{(0)}(0) + \sum_{z_i \neq 0} \mathrm{Res}\left[\frac{A_n^{(0)}(z)}{z}, z_i\right], \tag{1.71}$$

and if $\lim_{z\to\infty} A(z) = 0$ then the contour integral vanishes, allowing us to write the desired amplitude as

$$A_n^{(0)}(0) = -\sum_{z_i} \mathrm{Res}\left[\frac{A_n^{(0)}(z)}{z}, z_i\right]. \tag{1.72}$$

We can then combine (1.69) and (1.72) to write

$$A_n^{(0)} = \sum_{i=2}^{n-2} \sum_\lambda A_{i+1}^{(0),\lambda}(z_i) \frac{1}{P_{1\ldots i}^2} A_{n-i+1}^{(0),-\lambda}(z_i). \tag{1.73}$$

This is a key result of recursion. It clearly scales significantly better with higher multiplicity than the Feynman diagram approach, which has factorial scaling. There are still some algebraic redundancies present, as can be seen when considering the Parke-Taylor formula (1.53) compared to (1.73), but it is a huge improvement and can be used to prove the conjecture (1.53).

For this to work, we need to know the large z behaviour of the amplitude. This can be considered by analysing generic graphs and seeing how propagators, interaction vertices and polarisation vectors behave with z. Simple analysis of the worst case scenario leads to the scaling for the BCFW shift,

$$A(\hat{1}^+, \hat{n}^-) \sim \frac{1}{z}, \qquad A(\hat{1}^+, \hat{n}^+) \sim z,$$
$$A(\hat{1}^-, \hat{n}^-) \sim z, \qquad A(\hat{1}^-, \hat{n}^+) \sim z^3. \tag{1.74}$$

For the majority of amplitudes, the BCFW shift (1.65) can be used as it clearly vanishes with large z. The all-plus case does not have this shift as an option and so the BCFW shift fails. This is fine as there are other shifts available and the discussion is the same. The Risager shift [23] acts on three momenta p_a, p_b and p_c to give

$$\lambda_a \to \hat{\lambda}_a = \lambda_a + z\,[b\,c]\,\lambda_\eta,$$
$$\lambda_b \to \hat{\lambda}_b = \lambda_b + z\,[c\,a]\,\lambda_\eta,$$
$$\lambda_c \to \hat{\lambda}_c = \lambda_c + z\,[a\,b]\,\lambda_\eta, \tag{1.75}$$

where η is some arbitrary reference that has the condition $\langle a\,\eta \rangle \neq$ etc but is otherwise unconstrained. This shift has the correct large z behaviour for a^+, b^+ and c^+ and so can be used for an all-plus calculation. This will be important in later chapters where we will calculate two-loop, all-plus, full-colour amplitudes.

The discussion so far has been entirely focused on tree order amplitudes. We will now move our discussion to loop order and start to specialise to the amplitudes relevant for the remainder of this thesis.

1.4   Loop Amplitudes

We have thus far focused our discussion on tree amplitudes, outlining the development of techniques which significantly improve the efficiency of these calculations. As previously discussed, the momentum conservation at vertices in tree amplitudes allows the internal momenta to be entirely constrained. For loop diagrams, there are momenta which cannot be uniquely specified and so must be integrated over. There are regions of this loop momenta integral which cause divergences, namely ultraviolet (UV) divergences for high energy regions, and infrared (IR) divergences which appear for low energy and collinear parts of the integration region. These need to be regularised and in some cases one can renormalize the bare parameters in the Lagrangian which absorb these divergences.

For an n-point, Yang-Mills amplitude one can have at worst a loop integral with n propagators and n powers of loop momentum in the numerator. Traditionally, these amplitudes would be set up with Feynman diagrams and integrated but, as with the tree amplitudes, this is hugely inefficient and difficult. There now exists integral reduction methods [24–31] for one-loop integrals which reduce the problem to a more simple basis of integrals. These basis integrals are built of functions containing branch cut singularities, and the discontinuities across such branch cuts are utilised to construct the amplitude in a highly constrained method.

This following section will outline how the amplitudes are regularised, introduce the colour decomposition and colour relations used to build gauge invariant subsets at loop orders, before going on to discuss integral reduction techniques. We will then go on to discuss how we use branch cut singularities and discontinuities to constrain the problem, significantly reducing the calculational intensity. These techniques will later be implemented in this thesis to calculate the cut-constructible part of the n-point, full-colour, two-loop, all-plus helicity amplitude. We will also calculate the cut constructible part of the planar five-point, single-minus amplitude for two-loops.

1.4.1   Dimensional Regularisation and renormalization

Feynman integrals may diverge in the UV or IR integration regions. For example the bubble integral

$$I_2^{D=4}(P^2) = \int \frac{\mathrm{d}^4\ell}{(2\pi)^4} \frac{1}{\ell^2(\ell-P)^2}, \tag{1.76}$$

diverges as $\ell \to \infty$ in four dimensions but is finite in the IR $\ell \to 0$ limit. We define these integrals in the "mostly minus" Minkowski space with metric

$$\eta_{\mu\nu} = \begin{pmatrix} 1 & 0 & 0 & 0 \\ 0 & -1 & 0 & 0 \\ 0 & 0 & -1 & 0 \\ 0 & 0 & 0 & -1 \end{pmatrix}. \tag{1.77}$$

We take the Feynman propagators off the real axis using $1/(\ell - P + i\delta)^2$ where we will drop the explicit $i\delta$ unless it becomes relevant. These types of integrals can be regularised by analytically continuing the integration dimension to $D = 4 - 2\epsilon$, a process called dimensional regularisation [4]. This allows both UV and IR divergences to be regularised simultaneously although usually one has to keep $\epsilon > 0$ so that one can perform UV renormalization of the bare parameters in the Lagrangian and then continue to $\epsilon < 0$ in order to renormalize the IR divergences. The loop integration measure becomes

$$\int \frac{\mathrm{d}^4\ell}{(2\pi)^4} \to \mu^{4-D} \int \frac{\mathrm{d}^D\ell}{(2\pi)^D}, \tag{1.78}$$

where μ is an arbitrary mass scale to keep the units consistent. We will set $\mu \to 1$ for ease of notation but we must be mindful of its presence. There are subtleties about whether or not keeping the numerator loop momenta in four-dimensions is valid (it in fact misses terms) but as we will discuss later there are ways around this. The most common way of course would be to just take the internal loop momenta into D-dimensions but we will return to this later.

The counter-term for the coupling constant can be viewed as an expansion,

$$g \to g + \frac{\delta g}{\epsilon}, \tag{1.79}$$

where $\frac{\delta g}{\epsilon}$ is $\mathcal{O}(\epsilon^{-1})$ as it is required to renormalize UV divergences. We expand this within the perturbation expansion as

$$\begin{aligned} \mathcal{A}_n = &\left(\frac{g}{4\pi}\right)^{n-2} \mathcal{A}_n^{(0)} + \left(\frac{g}{4\pi}\right)^n \mathcal{A}_n^{(1)} + \left(\frac{g}{4\pi}\right)^{n+2} \mathcal{A}_n^{(2)} \\ &+ (n-2)\left(\frac{g}{4\pi}\right)^{n-3} \frac{\delta g}{\epsilon} \mathcal{A}_n^{(0)} + n\left(\frac{g}{4\pi}\right)^{n-1} \frac{\delta g}{\epsilon} \mathcal{A}_n^{(1)} + \dots \end{aligned} \tag{1.80}$$

We need the counter term δg to cancel the UV part of the one-loop amplitude but firstly we must note that the UV divergence starts a loop order higher than the *first non-zero* amplitude, which does not necessarily mean the tree amplitude. Pressing on, the counter term in the $\overline{\text{MS}}$ scheme for one-loop amplitudes is [32]

$$\mathcal{A}_n^{(1)}\Big|_{\text{UV}} = -\frac{(n-2)(4\pi)^\epsilon}{2\epsilon\Gamma[1-\epsilon]} \left(\frac{g}{4\pi}\right)^2 \beta_0 \mathcal{A}_n^{(0)}, \qquad \beta_0\Big|_{\text{Yang−Mills}} = \frac{11N_c}{3}, \tag{1.81}$$

and from the perturbative expansion we need

$$\left(\frac{g}{4\pi}\right)^n \left[\mathcal{A}_n^{(1)}\Big|_{\text{UV}} + (n-2)\left(\frac{g}{4\pi}\right)^{-3} \frac{\delta g}{\epsilon} \mathcal{A}_n^{(0)}\right] = 0 \tag{1.82}$$

We therefore find

$$\delta g = \frac{(4\pi)^\epsilon}{2\Gamma[1-\epsilon]} \left(\frac{g}{4\pi}\right)^5 \beta_0. \tag{1.83}$$

For the all-plus and single-minus helicity configurations (which are the configurations that are investigated in this thesis), the tree-level amplitudes vanish and so the UV divergence first appears at two loops. We can therefore write

$$\left(\frac{g}{4\pi}\right)^{n+2} \left[\mathcal{A}_n^{(2)} \Big|_{\text{UV}} + n \left(\frac{g}{4\pi}\right)^{-3} \frac{\delta g}{\epsilon} \mathcal{A}_n^{(1)} \right] = 0, \tag{1.84}$$

and given δg is now fixed we have

$$\mathcal{A}_n^{(2)} \Big|_{\text{UV}} = -n \frac{(4\pi)^\epsilon}{2\epsilon\Gamma[1-\epsilon]} \beta_0 \left(\frac{g}{4\pi}\right)^2 \mathcal{A}_n^{(1)}. \tag{1.85}$$

This in itself is not so remarkable but when compared with the collinear divergences for these helicity configurations at two-loops [32] we see

$$\mathcal{A}_n^{(2)} \Big|_{\text{collinear}} = -\left(\frac{g}{4\pi}\right)^2 \frac{n\gamma(g)}{\epsilon} \mathcal{A}_n^{(1)}, \tag{1.86}$$

where for gluons in pure Yang-Mills $\gamma(g) = \beta_0/2$. In the full cross section and upon expanding in ϵ, the UV and collinear IR divergences cancel, leaving just the soft IR divergences. We will therefore leave our amplitudes unrenormalized for this thesis. The soft IR divergences for these amplitudes are already known [33] but before we can discuss them properly we must first introduce the colour decomposition at loop order and the functional content of these amplitudes.

1.4.2 Colour relations and Loop Order Colour Decomposition

We would like to extend the discussion of colour decomposition to that of loop order amplitudes. We have already mentioned that we extend the $\text{SU}(N_c)$ of Yang-Mills theory to $\text{U}(N_c)$ and how the non-zero amplitudes in $\text{SU}(N_c)$ are equal kinematically to that of $\text{U}(N_c)$. We work in $\text{U}(N_c)$ for colour dressing purposes as it largely simplifies the colour algebra. It is also the source of the decoupling identities and we will see later that the combination of colour dressing and the use of decoupling identities allowed for simplifications in the calculation at the expense of introducing new redundancies in the final answer.

The $\text{U}(N_c)$ generators T^a have non-zero traces unlike the $\text{SU}(N_c)$ generators and so there are N_c^2 of them. The generators span the colour space and have the normalisations given by (1.34). The $\text{U}(N_c)$ colour algebra makes use of the Fierz identity,

$$T_{ij}^a T_{kl}^a = \delta_{il}\delta_{jk}, \tag{1.87}$$

allowing us to derive relations such as

$$\text{Tr}[T^a X]Tr[T^a Y] = X_{ji}Y_{ij} = \text{Tr}[XY],$$
$$\text{Tr}[T^a X T^a Y] = \text{Tr}[X]\text{Tr}[Y],$$

and

$$\text{Tr}[XT^aT^aY] = \delta_{kk}\text{Tr}[XY] = N_c\text{Tr}[XY]. \tag{1.88}$$

One can write down all possible diagrams and assign colour vertices according to the Feynman rules, rewrite the structure constants as strings of traces using (1.33) and, after repeated application of the above colour relations (remembering that we sum over all colour contributions of the internal gluons), we derive the colour decompositions of the amplitudes. This works for the tree decomposition (1.8) but also works to loop order, giving the colour decomposition for one-loop,

$$\mathcal{A}_n^{(1)}(a, b, \ldots, n) = N_c \sum_{S_n/\mathcal{P}_{n:1}} \text{Tr}[T^{a_1} \cdots T^{a_n}]A_{n:1}^{(1)}(a_1, a_2, \cdots a_n)$$

$$+ \sum_{r=2}^{\lfloor n/2 \rfloor+1} \sum_{S_n/\mathcal{P}_{n:r}} \text{Tr}[T^{a_1} \cdots T^{a_{r-1}}]\text{Tr}[T^{b_r}T^{b_{r+1}} \cdots T^{b_n}]A_{n:r}^{(1)}(a_1 \cdots a_{r-1}; b_r \cdots b_n), \tag{1.89}$$

and for two-loop,

$$\mathcal{A}_n^{(2)}(a, b, \ldots, n) = N_c^2 \sum_{S_n/\mathcal{P}_{n:1}} \text{Tr}[T^{a_1} \cdots T^{a_n}]A_{n:1}^{(2)}(a_1, a_2, \cdots a_n)$$

$$+N_c \sum_{r=2}^{\lfloor n/2 \rfloor+1} \sum_{S_n/\mathcal{P}_{n:r}} \text{Tr}[T^{a_1} \cdots T^{a_{r-1}}]\text{Tr}[T^{b_r}T^{b_{r+1}} \cdots T^{b_n}]A_{n:r}^{(2)}(a_1 \cdots a_{r-1}; b_r \cdots b_n)$$

$$+\sum_{s=1}^{\lfloor n/3 \rfloor} \sum_{t=s}^{\lfloor (n-s)/2 \rfloor} \sum_{S_n/\mathcal{P}_{n:s,t}} \text{Tr}[T^{a_1} \cdots T^{a_s}]\text{Tr}[T^{b_{s+1}} \cdots T^{b_{s+t}}]\text{Tr}[T^{c_{s+t+1}} \cdots T^{c_n}]$$

$$\times A_{n:s,t}^{(2)}(a_1, \cdots, a_s; b_{s+1}, \cdots, b_{s+t}; c_{s+t+1}, \cdots, c_n)$$

$$+ \sum_{S_n/\mathcal{P}_{n:1}} \text{Tr}[T^{a_1} \cdots T^{a_n}]A_{n:1B}^{(2)}(a_1, a_2, \cdots a_n). \tag{1.90}$$

We have introduced here the "subleading in colour" amplitudes $A_{n:r}$ and at two-loop we have "sub-subleading in colour" amplitudes $A_{n:s,t}$ and $A_{n:1B}$. These amplitudes follow the cyclic symmetry of the multiplying trace structure, as well as a flip symmetry

$$A_{n:r}^{\ell}(a, b, \ldots, r-1; r, \ldots, n) = (-1)^n A_{n:r}^{\ell}(r-1, \ldots, b, a; n, n-1, \ldots, r), \tag{1.91}$$

and similarly for the $A_{n:s,t}$ amplitudes. This flip symmetry can be derived from the antihermitian group generators

$$\text{Tr}[a, b, \ldots, n]^{\dagger} = (-1)^n \text{Tr}[n, \ldots, b, a]. \tag{1.92}$$

It can also be shown to be true if one chooses the hermitian convention by counting the number of flip-antisymmetric three point interaction vertices which apply to each amplitude. We have also introduced the notation $\mathcal{P}_{n:c}$ which are the symmetry sets of the amplitude. This ensures every colour structure is counted exactly once and they are given by (for $r > 1$, $r-1 \neq \frac{n}{2}$, $s \neq t$, $t \neq \frac{n-s}{2}$ and $3s \neq m, n$),

$$\begin{aligned}
\mathcal{P}_{n:1} &= Z_n[a, b, \ldots, n], \\
\mathcal{P}_{n:r} &= Z_{r-1}[a, b, \ldots, r-1] \times Z_{n+1-r}[r, \ldots, n], \\
\mathcal{P}_{n:s,t} &= Z_s[a, b, \ldots, s] \times Z_t[s+1, \ldots, s+t] \times Z_{n-s-t}[s+t+1, \ldots, n]. \tag{1.93}
\end{aligned}$$

For cases with equal length sets we have,

$$
\begin{aligned}
\mathcal{P}_{2m:m+1} &= Z_m[a,b,\ldots,m] \times Z'_m[m+1,\ldots,2m] \times Z_2[Z_m, Z'_m], \\
\mathcal{P}_{n:s,s} &= Z_s[a,b,\ldots,s] \times Z'_s[s+1,\ldots,2s] \times Z_{n-2s}[2s+1,\ldots,n] \times Z_2[Z_s, Z'_s], \\
\mathcal{P}_{3m:m,m} &= Z_m[a,b,\ldots,m] \times Z'_m[m+1,\ldots,2m] \times Z''_m[2m+1,\ldots,3m] \times S_3[Z_m, Z'_m, Z''_m], \\
\mathcal{P}_{2m:2s,m-s} &= Z_{2s}[a,b,\ldots,2s] \times Z_{m-s}[2s+1, s+m] \times Z'_{m-s}[s+m+1,\ldots,2m] \\
&\quad \times Z_2[Z_{m-s}, Z'_{m-s}].
\end{aligned}
\tag{1.94}
$$

For example at six-point with $A_{6:2,2}(a,b;c,d;e,f)$ the manifest symmetry is

$$
\mathcal{P}_{6:2,2} = Z_2[a,b] \times Z_2[c,d] \times Z_2[e,f] \times S_3[\{a,b\},\{c,d\},\{e,f\}].
\tag{1.95}
$$

These subamplitudes have gauge invariance just as with tree-level and therefore many of the redundancies are eliminated. These colour decompositions are the same for both $\mathrm{U}(N_c)$ and $\mathrm{SU}(N_c)$, although any terms with a single generator $\mathrm{Tr}[T^a]$ vanish for $\mathrm{SU}(N_c)$ as these generators are traceless. We will give examples of the colour dressing in a later chapter, but if one considers all colour dressed diagrams, we recover these full colour structures and the calculation of the single trace term allows us to use decoupling identities to check the $\mathrm{SU}(N_c)$ amplitudes. We will later see that one can write all of the single trace terms as sums of $\mathrm{SU}(N_c)$ amplitudes and so this provides another numerical check on our results as these relations are highly non-trivial. The simplest case is seen by setting gluon 1 to be $\mathrm{U}(1)$

$$
A_{n:2}^{(\ell)}(1;2,\ldots,n) = - \sum_{\sigma \in \mathcal{P}_{n:2}} A_{n:1}^{(\ell)}(1,\sigma),
\tag{1.96}
$$

where as a reminder $\mathcal{P}_{n:2}$ is the group of cyclic symmetries $Z_{n-1}[2,3,\ldots,n]$ as opposed to the non-cyclic $S_n/\mathcal{P}_{n:2}$ that we see in the colour decomposition. We therefore have tools for colour dressing, the colour decomposition and will later use $\mathrm{U}(N_c)$ relations for tests and simplifications. We see that the colour decomposition has different powers of N_c on different structures, introducing the concept of "leading-in-colour" terms $A_{n:1}$. These are "maximally planar" amplitudes, planar in every definition of the word whether it is being able to bring external gluons to infinity without crossing any internal gluons on the graph or when considering colour dressing having no colour lines crossing. See Figure 1.3 for an example.

20
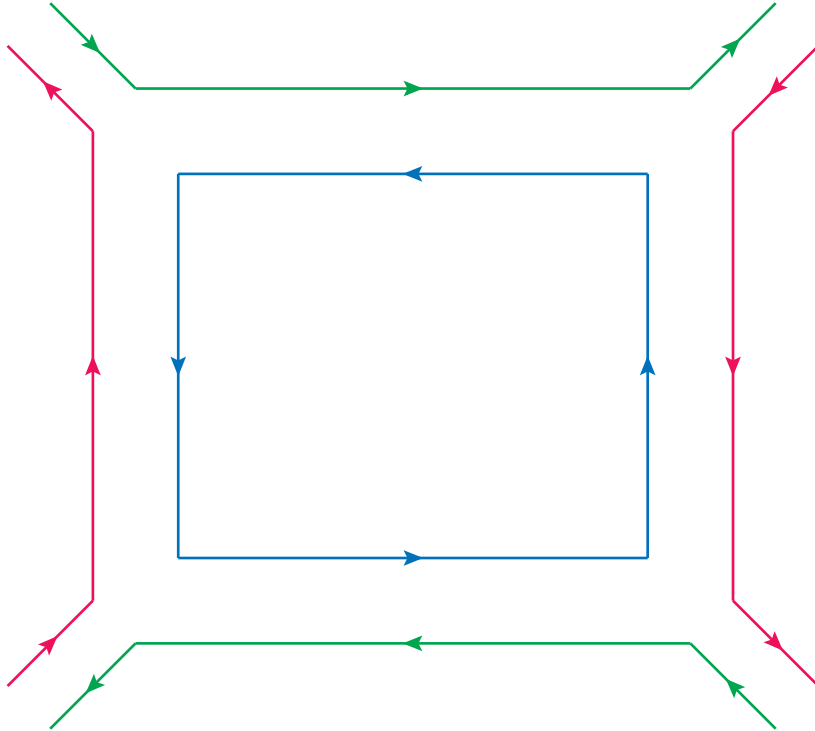
Figure 1.3: A one-loop box ribbon diagram contributing to the planar "leading-in-colour" amplitude. The closed colour loop in the middle contributes a factor of N_c to the colour structure.

Planar diagrams are easier to calculate and so for a given helicity structure the first calculation tends to be the "large N_c limit" [34] where we consider this planar contribution. When we calculate the single-minus configuration we will focus on the leading-in-colour amplitude. We will also consider the "maximally non-planar" amplitudes $A^{(2)}_{n:1B}$ in a later chapter. This is not the only colour decomposition available to us [35–37] and studying the relations between different decompositions has been used to derive new group theory identities for the partial amplitudes [38, 39]. We will look at these more closely in Chapter 2 but they allow us to write $A^{(2)}_{5:1B}$ in terms of $A^{(2)}_{5:3}$ and $A^{(2)}_{5:1}$, though we see this is not possible at six-point or higher.

In the previous section we talked about how the soft IR divergences are already known but we needed to first introduce colour notation. Now that this is done we can look at the soft IR divergences for the full colour amplitudes. First defining the divergent piece

$$I_{i,j} \equiv -\frac{(s_{ij})^{-\epsilon}}{\epsilon^2}, \tag{1.97}$$

the leading in colour IR soft term is [33]

$$U^{(1)}_{n:1}(1, 2, \ldots, n) \equiv A^{(0)}_{n:1}(1, 2, \ldots, n) \sum_{i=1}^{n} I_{i,i+1}, \tag{1.98}$$

where $I_{n,n+1} \equiv I_{n,1}$. Importantly here $\ell = 0$ refers to the first non-zero loop order which for all-plus and single-minus amplitudes is one-loop. This means (1.98) is valid at two-loops for these helicity configurations. To extend this to full colour we write the IR soft term in the

more telling form of [40]

$$I_{a,b} \times f^{aij} f^{bik} \times \mathcal{A}_n^{(1)}(j, k, \ldots, n), \tag{1.99}$$

and we wish to disentangle this simple equation into the color-ordered components. When considering n-point full colour calculations, it will be convenient to use a list notation for the partial amplitudes where we use

$$A_n^{(l)}(S) = A_n^{(l)}(\{a_1, a_2, \cdots a_n\}) \equiv A_{n:1}^{(l)}(a_1, a_2, \cdots a_n), \tag{1.100}$$

$A_n^{(l)}(S_1; S_2)$ for $A_{n:r}^{(l)}$ and $A_n^{(l)}(S_1; S_2; S_3)$ for $A_{n:s,t}^{(l)}$.

We then have for a list $S = \{a_1, a_2, a_3, \cdots, a_r\}$,

$$I_r[S] = \sum_{i=1}^{r} I_{a_i, a_{i+1}} \tag{1.101}$$

where the term $I_{a_r, a_{r+1}} \equiv I_{a_r, a_1}$ is included in the sum. We also define $I_j[S_1, S_2]$ and $I_k[S_1, S_2]$,

$$I_j[S_1, S_2] = I_j[\{a_1, a_2 \cdots a_r\}, \{b_1, b_2, \cdots b_s\}] \equiv (I_{a_1, a_r} + I_{b_1, b_s} - I_{a_1, b_1} - I_{a_r, b_s}),$$
$$I_k[S_1, S_2] = I_k[\{a_1, a_2 \cdots a_r\}, \{b_1, b_2, \cdots b_s\}] \equiv (I_{a_1, b_s} + I_{b_1, a_r} - I_{a_1, b_1} - I_{a_r, b_s}), \tag{1.102}$$

giving

$$I_r[S_1 \oplus S_2] = I_r[S_1] + I_r[S_2] + I_k[S_1, S_2] - I_j[S_1, S_2] \tag{1.103}$$

where $\{a_1 \cdots a_r\} \oplus \{b_1 \cdots b_s\} = \{a_1 \cdots a_r, b_1 \cdots b_s\}$. In this language the leading and sub-leading IR singularities at one-loop are

$$\begin{aligned}
A_n^{(1)}(S) &= A_n^{(0)}(S) \times I_r[S], \\
A_n^{(1)}(S_1; S_2) &= \sum_{S_1' \in Z(S_1)} \sum_{S_2' \in Z(S_2)} A_n^{(0)}(S_1' \cup S_2') \times I_j[S_1', S_2'].
\end{aligned} \tag{1.104}$$

The set $Z(S)$ is again the set of cyclic permutations of S.

At two-loops, for vanishing tree amplitude helicities, we have

$$\begin{aligned}
A_n^{(2)}(S) &= A_n^{(1)}(S) \times I_r[S], \\
A_n^{(2)}(S_1; S_2) &= A_n^{(1)}(S_1; S_2) \times (I_r[S_1] + I_r[S_2]) \\
&\quad + \sum_{S_1' \in Z(S_1)} \sum_{S_2' \in Z(S_2)} A_n^{(1)}(S_1' \cup S_2') \times I_j[S_1', S_2'], \\
A_n^{(2)}(S_1; S_2; S_3) &= \sum_{S_2' \in Z(S_2)} \sum_{S_3' \in Z(S_3)} A_n^{(1)}(S_1; S_2' \cup S_3') \times I_j[S_2', S_3'] \\
&\quad + \sum_{S_1' \in Z(S_1)} \sum_{S_3' \in Z(S_3)} A_n^{(1)}(S_2; S_1' \cup S_3') \times I_j[S_1', S_3'] \\
&\quad + \sum_{S_1' \in Z(S_1)} \sum_{S_2' \in Z(S_2)} A_n^{(1)}(S_3; S_1' \cup S_2') \times I_j[S_1', S_2'], \\
A_{n,B}^{(2)}(S) &= \sum_{U(S)} A_n^{(1)}(S_1'; S_2') \times I_k[S_1', S_2'],
\end{aligned} \tag{1.105}$$

where $U(S)$ is the set of all distinct pairs of lists satisfying $S_1' \oplus S_2' \in Z(S)$ where the size of S_i' is greater than one. For example

$$U(\{1, 2, 3, 4, 5\}) = \Big\{ (\{1, 2\}, \{3, 4, 5\}), (\{2, 3\}, \{4, 5, 1\}), (\{3, 4\}, \{5, 1, 2\}),$$

$$(\{4, 5\}, \{1, 2, 3\}), (\{5, 1\}, \{2, 3, 4\}) \Big\}. \tag{1.106}$$

We have now seen how the amplitudes decompose, and we know the universal IR pieces, and so we can review some techniques that have been developed to improve calculations at loop order.

1.5   One-Loop Integral Reduction

For an n-point amplitude we can have up to n powers of loop momenta in the numerator and n propagators. A general Feynman integral with N propagators and rank r is

$$\int \frac{\mathrm{d}^D \ell}{(2\pi)^D} \frac{\ell^{\mu_1} \dots \ell^{\mu_r}}{\ell^2 (\ell - P_1)^2 \dots (\ell - P_{N-1})^2}, \tag{1.107}$$

and at one-loop level this can be simplified greatly to $\mathcal{O}(\epsilon^0)$ by use of integral reduction techniques [24–27]. This can be achieved using Passarino-Veltman reduction [25] in which one can use the linear dependence of the loop and external momenta to rewrite the numerator as a sum of inverse propagators and scalar factors which depend only on the external momenta. This can reduce (1.107) to scalar integrals with arbitrary numbers of propagators.

One can then on a case by case basis keep reducing these integrals by building new bases and systems of equations and rewriting the loop momenta until we are left with a basis of integrals,

$$I_N^{(1)}(a, b, \dots, n) = \sum_i c_{4,i} \mathcal{I}_{4,i} + \sum_i c_{3,i} \mathcal{I}_{3,i} + \sum_i c_{2,i} \mathcal{I}_{2,i} + \sum_i c_{1,i} \mathcal{I}_{1,i} + \mathcal{R}, \tag{1.108}$$

where, for $\mathcal{I}_{n,i}$, n refers to the set of n-point scalar one-loop integral functions, i labels the kinematically distinct n-point integrals within each set and $c_{n,i}$ is a rational, kinematic coefficient of this function. $\mathcal{R}$ is the totally rational kinematic contribution. We will be using four-dimensional unitarity in this thesis which has advantage of simplicity in the interactions of the internal and external gluons, but has the disadvantage that some rational contributions get lost when we perform these sorts of reductions in the $D = 4$ limit. At loop level the recursion techniques we have covered also fail as there exist double poles, but we will later introduce a method called augmented recursion which bypasses this issue.

The tadpole diagrams $I_{1,i}$ vanish in four-dimensions with massless particles so this entire contribution vanishes. The remaining integral functions are known in analytic form and are given in Chapter 2 and so the problem becomes determining $c_{n,i}$. One could of course manually perform these reductions and keep track of all contributions until we have the reduction for each integral. This is a very intensive process but one can instead make use of the branch cut singularities present in the amplitude to massively simplify this process. This technique is known as unitarity.

1.6 Unitarity

We have discussed that the problem of calculating one-loop integrals is now reduced to determining coefficients of scalar boxes, triangles and bubble integral functions, and additionally a rational contribution. These coefficients are then built by exploiting the factorising properties of the amplitude itself along with the discontinuities along branch cut singularities in the integral functions. This process is called generalised unitarity and can be motivated by looking at the optical theorem of quantum field theory.

The optical theorem can be understood by analysing the S-matrix [41], an object which describes the trajectory of a particle propagating from the times $t = -\infty$ to $t = \infty$ with possible interactions occurring in some finite time within these limits. This is written as

$$S = \mathbb{1} + iT \tag{1.109}$$

where the identity matrix is the path with no scattering, and T describes the interaction states which contribute to scattering. The elements of the S-matrix determine the probability of a given interaction occurring and this means they must sum to 1, imposing the condition

$$SS^\dagger = \mathbb{1}, \tag{1.110}$$

and this, along with (1.109), gives us

$$-i(T - T^\dagger) = TT^\dagger. \tag{1.111}$$

We can perturbably expand T and extract coefficients of different powers of the coupling constant g to find the relations,

$$T^{(0)\dagger} = T^{(0)}, \qquad -i(T^{(1)} - T^{(1)\dagger}) = T^{(0)}T^{(0)}. \tag{1.112}$$

We define elements of T between asymptotic states which we call $T_{oi} \equiv \langle \text{out}|T|\text{in}\rangle$ such that

$$\langle \text{out}|T^\dagger|\text{in}\rangle = \langle \text{in}|T|\text{out}\rangle^* \equiv (T_{io})^* = (T_{oi})^*, \tag{1.113}$$

where the last part is true due to time reversal invariance. This leads us to Cutkosky's rule [42]

$$-i(T_{oi}^{(1)} - T_{io}^{(1)*}) = \int \mathrm{d}\mu\, T_{0\mu}^{(0)} T_{\mu i}^{(0)}, \tag{1.114}$$

where $\int \mathrm{d}\mu$ refers to the sum over all helicities and phase-space integrals over all intermediate on-shell states. If one extended to other theories this would also be a sum over different particle contents but importantly it only includes on-shell external states which eliminates ghosts.

The left hand side of this equation is then twice the imaginary part of $T_{oi}^{(1)}$, which we may relate to branch cut discontinuities in the integral functions. These integral functions are made up of polylogarithms and other special functions which can have these branch cut discontinuities. These discontinuities arise in the regions of loop-momenta integrations when a virtual gluon goes on shell, and therefore a propagator becomes purely imaginary and can be thought of as being "cut". To exploit the factorisation property of the amplitude, we need to perform two cuts as shown in Figure 1.4.

24
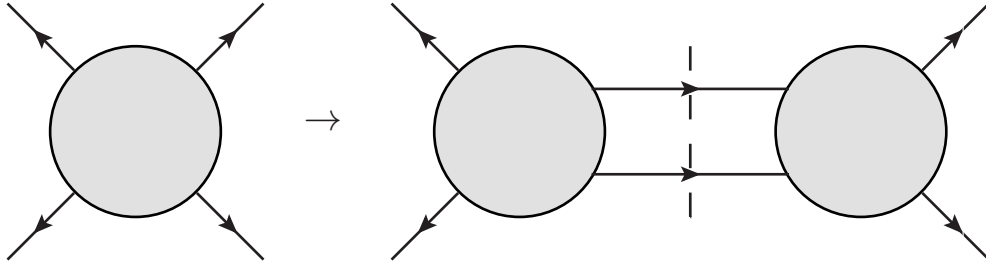
Figure 1.4: Schematic diagram of the optical theorem. The LHS being a generic one-loop amplitude and the RHS how it factorises into two tree-level amplitudes on a two-particle cut, represented by the dashed lines over the internal propagators.

To practically implement a cut, we rewrite the propagator via the distribution relation

$$\lim_{\delta \to 0} \frac{1}{p^2 + i\delta} = P\left(\frac{1}{p^2}\right) - i\pi\delta(p^2), \tag{1.115}$$

where P is the principle part. We can see that the discontinuity of the one-loop amplitude can be computed for a given channel by replacing the two relevant propagators with $\delta(p_i^2)$, thus introducing discontinuities within the integrand. The dimension of this δ function determines whether we use four-dimensional unitarity or D-dimensional unitarity. We will be using four-dimensional unitarity but the most common method is to use D-dimensions [43–49]. This involves decomposing the loop momentum into a four-dimensional component and a -2ϵ component,

$$\ell = \ell^{[4]} + \ell^{[-2\epsilon]} = \tilde{\ell} + \mu, \qquad \ell^2 = \tilde{\ell}^2 - \mu^2, \tag{1.116}$$

with the integration measure

$$\int \frac{\mathrm{d}^D \ell}{(2\pi)^D} = \int \frac{\mathrm{d}^4 \tilde{\ell}}{(2\pi)^4} \int \frac{\mathrm{d}^{-\epsilon}\mu^2}{(2\pi)^{-2\epsilon}}. \tag{1.117}$$

This technique has the benefit of calculating the full amplitude, including the whole rational contribution, at the expense of more complicated algebra and a larger set of master integrals. We will not discuss D-dimensional unitarity further in this thesis.

Our discussion of unitarity has thus far been limited to two-particle cuts, but we would like to extend this method to allow us to calculate the coefficients $c_{n,i}$ of (1.108). We do this by extending unitarity to higher order cuts in the technique known as generalised unitarity.

1.6.1 Generalised Unitarity

We have introduced unitarity via the optical theorem but we would like to calculate the coefficients $c_{n,i}$ for the scalar integral functions in the decomposition (1.108). This can be achieved by generalising unitarity to higher numbers of particle cuts. If one performs four cuts then triangles and bubbles are eliminated, allowing one to calculate the box coefficient as was initially done for $\mathcal{N} = 4$ SYM [50]. One can then perform a triple cut to isolate the triangle coefficient, being careful to subtract the box contributions and so on.

We will cover the practical applications when we need them in later chapters, but for now we will briefly discuss quadruple cuts for pedagogical purposes. Note that on a cut we may

rewrite the loop momenta in the spinor helicity formalism $\ell = \lambda_\ell \tilde{\lambda}_\ell$. This momentum has four degrees of freedom and therefore on a quadruple cut we can use momentum conservation and the cut conditions to fully constrain ℓ in terms of external gluon spinors at one-loop. The quadruple cut factorises the amplitude into a product of four trees as shown schematically by Figure 1.5,
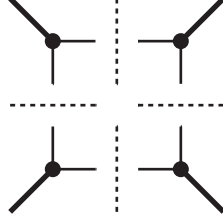
Figure 1.5: Schematic quadruple cut, each corner represents a tree amplitude. Thick external lines means the corner might have one null leg or many null legs.

$$
\begin{aligned}
A_n^{(1)}(1, 2, \ldots, n)\Big|_{\text{cut}} = \frac{1}{2} \sum_\lambda \; & A^{(0)}\left(-\ell_4^{-\lambda_{\ell_4}}, 1, \ldots, i, \ell_0^{\lambda_{\ell_0}}\right) \times A^{(0)}\left(-\ell_1^{-\lambda_{\ell_1}}, i+1, \ldots, j, \ell_2^{\lambda_{\ell_2}}\right) \\
& \times A^{(0)}\left(-\ell_2^{-\lambda_{\ell_2}}, j+1, \ldots, k, \ell_3^{\lambda_{\ell_3}}\right) \times A^{(0)}\left(-\ell_3^{-\lambda_{\ell_3}}, k+1, \ldots, n, \ell_4^{\lambda_{\ell_4}}\right) \\
& \times \mathcal{I}_4[P_{1\ldots i}^2, P_{i+1\ldots j}^2, P_{j+1\ldots k}^2, P_{k+1\ldots n}^2]\Big|_{\text{cut}},
\end{aligned}
\tag{1.118}
$$

where the sum is over all internal helicity configurations and $\mathcal{I}_4[K_1, K_2, K_3, K_4]$ is the scalar one-loop box integral whose arguments are the masses on each corner. There are two solutions for the loop momentum on the cuts which need "averaging over", a fact which comes from extracting the Jacobian factor that is equal on both sides of this equation and hence the factor of 2 in the denominator.

Inserting the fully constrained loop momenta into the right hand side of (1.118) gives the coefficient of this particular box in (1.108). One then needs to sum over all configurations and cuts. Many of these subamplitudes might vanish depending on helicities. Triple cuts will leave one degree of freedom unconstrained. There are various simple methods of dealing with this but specific implementations will be further discussed in later chapters.

This decomposition into scalar boxes, triangles and bubbles only works for one-loop integrals (emphasis on integrals here, as we will see in the next chapter that certain two-loop amplitudes may be reduced to one-loop integrals using unitarity). For two-loop amplitudes there is no universal decomposition such as (1.108), but there are reduction techniques which exist, such as integration by parts (IBP) relations which can reduce a given problem to a smaller set of master integrals for beyond one-loop [51–62].

We will later use unitarity in a two-loop setting in order to constrain the problem to a general set of numerators for a series of propagators, and these are integrated by hand. We argue that our technique should scale well with higher multiplicities but clearly this is still not the most efficient method given the relative simplicity of the final results. Throughout this introduction we have talked about methods of calculation which begin as incredibly inefficient but over time make use of symmetries and functional properties to eliminate large swathes of redundancies. The two loop techniques presented in Chapter 5 still exhibit cancellations

and redundancies. We will highlight this as it is suggestive of undiscovered techniques which may exist to further simplify these loop calculations.

Before we continue on to new calculations there remains one more problem for us to address, namely the existence of double poles in rational parts of some amplitudes. We will be performing four-dimensional unitarity in this thesis and as such we will lose rational terms. For the amplitudes whose rational terms contain at worst simple poles, we may use complex recursion to recover the entire rational piece. The recursion we have covered so far only gives leading contributions to the Laurent series and so, for amplitudes containing double poles and higher, this method fails. We will now briefly review an augmented recursion technique which bypasses this problem.

1.7 Augmented Recursion

BCFW recursion looks at factorisations of an amplitude and how we can build amplitudes from these factorisations. We have already stated that this only provides the leading poles in the Laurent expansion and so anything with double poles will miss rational contributions if one uses standard recursion. Lets now go into detail about what this means.

At tree-level, the MHV amplitude has the form (1.53). When we talk about simple poles, we really mean poles in z after a complex deformation of the external momenta. This has been discussed in more detail in Section 1.3.1 but this means for poles where $\langle i\,j \rangle \to 0$ we can rephrase it as $\frac{c_i}{(z-z_i)}$. The complex deformation changes the amplitude to a complex function $A(z)$ and we would like to recover $A(0)$ from this. We therefore want to invoke Cauchy's theorem and find a $z = 0$ contribution by looking at $A(z)/z$, forcing the existence of a $z = 0$ pole. For example, the one-loop all-plus amplitude is known to any multiplicity [63],

$$A_n^{(1)}(1^+, 2^+, \ldots, n^+) = -\frac{1}{3} \frac{1}{\langle 1\,2 \rangle \langle 2\,3 \rangle \ldots \langle n\,1 \rangle} \sum_{1 \leq i < j < k < l \leq n} \mathrm{Tr}_-[ijkl] + \mathcal{O}(\epsilon) \qquad (1.119)$$

where $\mathrm{Tr}_-[ijkl] \equiv \mathrm{Tr}\left(\frac{(1-\gamma_5)}{2} \slashed{k}_i \slashed{k}_j \slashed{k}_k \slashed{k}_l\right) = \langle i\,j \rangle [j\,k] \langle k\,l \rangle [l\,i]$ and we use the normalisation in (1.3). For $n > 4$ this only contains simple poles but for $n = 4$ we see the emergence of double poles in the form $\langle 2\,3 \rangle^2$ after rewriting the amplitude using four-point kinematics. Recalling that loop-level amplitudes contain polylogarithmic terms, diverging terms and finite rational terms, we call the finite rational part of the amplitude $R(z)$ and so

$$\frac{R(z)}{z} = \frac{c_{-2}}{z(z-z_i)^2} + \frac{c_{-1}}{z(z-z_i)} + \mathcal{O}\left((z-z_i)^0\right), \qquad (1.120)$$

where c_j are the coefficients of $(z-z_i)^j$ in the Laurent expansion around the $z_i \neq 0$ propagator pole. We can rewrite the pole as $\delta = z - z_i$ and Taylor expand

$$\frac{R(z)}{z} = \frac{c_{-2}}{(\delta + z_i)\delta^2} + \frac{c_{-1}}{(\delta + z_i)\delta} + \mathcal{O}(\delta^0) \approx \frac{c_{-2}}{z_i\delta^2} + \frac{1}{\delta}\left(-\frac{c_{-2}}{z_i^2} + \frac{c_{-1}}{z_i}\right) + \mathcal{O}(\delta^0). \qquad (1.121)$$

We therefore see that the residue around this pole is given by

$$\mathrm{Res}\left[\frac{R(z)}{z}\right]\Bigg|_{z_j} = -\frac{c_{-2}}{z_i^2} + \frac{c_{-1}}{z_i} \qquad (1.122)$$

and this is what is used for (1.72). The problem is that while c_{-2} (or whichever the leading pole in z_i is) is given by factorisations, as we saw with BCFW recursion, there are no universal results for c_{-1}. We therefore implement a technique called "augmented recursion" [64], which has been used to calculate rational parts of various one-loop and two-loop amplitudes [64–71], where the latter two references are part of chapters 2 and 3.

This technique makes use of the axial gauge formalism [72–74] to extract the "pole under the pole" term so that we may use recursion. For the all-plus, two-loop helicity amplitudes, the origin of the double pole can be traced to the factorisation in Figure 1.6 for complex momenta, where there are one-loop contributions on both sides,
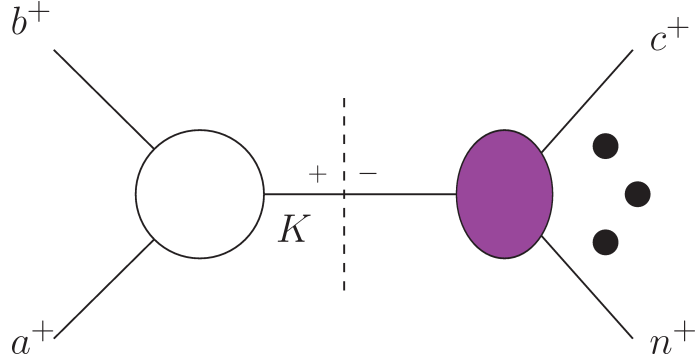
Figure 1.6: The origin of the double pole. The double pole corresponds to the coincidence of the singularity arising in the three-point, one-loop integral from the left hand side, with the factorisation corresponding to $K^2 = s_{ab} \to 0$. The RHS of the factorisation here can be an any loop-level, $(n-1)$-point amplitude, depending on the overall amplitude that is factorising.

and we can build diagrams of the form presented in Figure 1.7 where the internal legs, α and β, are taken off shell using axial gauge techniques.
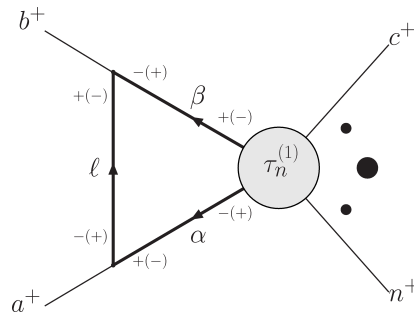
Figure 1.7: Diagram containing the leading and sub-leading poles as $s_{ab} \to 0$. The axial gauge construction permits the off-shell continuation of the internal legs.

In this formalism we can assign helicity labels to the internal off-shell legs and vertices by rewriting the off-shell momenta as a sum of two nullified momenta

$$K = K^\flat + \frac{K^2}{2K \cdot q} q = K^\flat + K^\sharp, \tag{1.123}$$

where q is a massless but otherwise arbitrary reference momenta. The two off-shell legs are given by

$$\alpha = \alpha(\ell) = \ell + a, \qquad \beta = \beta(\ell) = b - \ell, \tag{1.124}$$

where $P_{\alpha\beta} = \alpha + \beta = a + b = P_{ab}$ is independent of the loop momentum ℓ. For now we will keep the discussion to leading in colour and so the diagram may be written as

$$\int d\Lambda(-\alpha^{-\lambda_\alpha}, a^+, b^+, -\beta^{-\lambda_\beta})\tau_{n:1}^{(1)}(\alpha^{\lambda_\alpha}, \beta^{\lambda_\beta}, c^+, d^+, \ldots, n^+), \tag{1.125}$$

where

$$\int d\Lambda(-\alpha^{-\lambda_\alpha}, a^+, b^+, -\beta^{-\lambda_\beta}) = \frac{i}{c_\Gamma(2\pi)^D} \int \frac{d^D\ell}{\ell^2\alpha^2\beta^2}\mathcal{V}(\alpha, a, \ell)\mathcal{V}(\ell, b, \beta), \tag{1.126}$$

and we can build the vertices $\mathcal{V}$ using the axial gauge formalism and these are dependent on the helicites of the arguments.

$\tau_{n:1}^{(1)}$ is a doubly off-shell current and is the key to augmented recursion. We are only interested in the residue on the $s_{ab} \to 0$ pole and so, when building the current, we only need two conditions to be satisfied:

(C1) It reproduces the leading singularities as $s_{\alpha\beta} \to 0$ with $\alpha^2, \beta^2 \neq 0$,

(C2) It must reproduce the one-loop amplitude $\tau_{n:1}^{(1)}(\alpha, \beta, c, \ldots, n) \to A_{n:1}^{(1)}(\alpha, \beta, c, \ldots, n)$ in the on-shell limit $\alpha^2, \beta^2 \to 0$, $s_{\alpha\beta} \neq 0$.

In this thesis we build the current by starting with the on-shell amplitude, written in terms of $\alpha^\flat$ and $\beta^\flat$ from (1.123). Historically the reference momentum q has been chosen to relate to one of the external legs for simplification, but we will keep q general as this helps with the full colour calculations. We then rewrite the amplitude in such a way that gives the factorisations in Figure 1.8 which give the leading singularities for (C1).
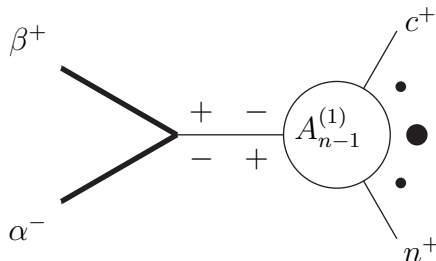
Figure 1.8: The leading singularities to be found within the current. Both helicities of the internal propagator need to be accounted for.

We emphasise these factorisations must be built for the $s_{\alpha\beta} \to 0$ pole, recalling that $\langle \alpha \, \beta \rangle [\beta \, \alpha] = (\alpha^\flat + \beta^\flat)^2 \neq s_{\alpha\beta}$ and so care must be taken when taking things off-shell in this way. These manipulations can make use of $s_{\alpha\beta} << 1$ and add in terms that are proportional

to α^2 and β^2 for free. Once we have the leading factorisations, we should be left with a piece that is of order $\mathcal{O}(s_{\alpha\beta}^{-1})$ that came from the double pole manipulations. This is the "pole under the pole" piece we seek. Any additional terms that do not contribute a pole can be discarded, so we do not need the full current. The final step is to then perform the integration, sum over all contributing integrated currents and perform recursion alongside all other channels that do not contribute double poles and we obtain the full rational piece.

In this thesis we build several currents for full-colour, all-plus helicity amplitudes and so there will be examples of this process given in Chapters 2 and 3. We use the Risager shift (1.75) for the all-plus amplitude and this breaks the cyclic symmetry of whichever colour structure we calculate. The axial gauge also makes a gauge choice but the final result should be gauge invariant. These provide very strong numerical checks on results, and we can test that the result is independent of the choice of q and that the cyclic symmetries are recovered. These are tested numerically because the expression calculated reads as a large function of q and so the independence is highly non-trivial. We then fit analytic expressions to this rational piece, a process which will be described in detail in Chapter 3.

We again see a large intermediate expression reduced to much smaller analytic expressions ($\sim$Mb in size to $\sim$kb in size) which is indicative of some undiscovered technique for calculating these pieces. This is still relatively efficient and allows us to make use of the much simpler four-dimensional unitarity to calculate cut-constructible pieces. We have now schematically introduced all of the techniques that will be used throughout this thesis. We have motivated modern techniques being vastly more efficient than traditional methods but with an eye of improving calculations in the future. We are now therefore ready to move onto new calculations.

The remainder of this thesis is organised as follows: Chapter 2 extends previously developed four-dimensional unitarity and augmented recursion techniques to a full colour setting. We then use this colour-dressed technology to calculate the full-colour, two-loop, five-point, all-plus helicity amplitude. This is published work [70]. Chapter 3 calculates the same amplitude but at six-point. This was a new result at the time of publishing [71] and so we also discuss functional reconstruction methods used to fit the rational piece of this amplitude. Chapter 4 discusses n-point amplitudes, calculating the full-colour, cut-constructible part of the n-point, two-loop, all-plus helicity amplitude. We then provide a conjecture for the rational part of the $A_{n:1B}^{(2)}$ colour-amplitude which has been tested numerically for up to seven-point. This is the first partial amplitude conjectured to n-points for pure Yang-Mills, which both has agreement with the explicit calculation for seven-point while also obeying non-trivial symmetry checks to even higher points. This is also published work [75]. Chapter 5 is unpublished and extends four-dimensional unitarity to calculate the cut-constructible piece of the two-loop, five-point, single-minus, leading in colour amplitude. This result is already known [2], but this is the first time four-dimensional unitarity has been used to attempt to calculate such a configuration and, as we argue throughout, once this technique has been full automated it will scale well to higher multiplicities. We also derive many useful relations along the way, from generalised hypergeometric relations to a very convenient scalar box integral result with general powers on the propagators and also under a Mellin-Barnes transformation. Finally, summarises what has been learned in these calculations and discusses what the author would like to see explored in future calculations.

Chapter 2

Colour Dressed Unitarity and Recursion: a Five Point Amplitude

2.1 Introduction

In Chapter 1 we discussed how experimental results in particle physics may be explored with theoretical calculations. Calculating perturbative scattering not only decreases the theoretical uncertainty in these tests but reveals deeper insights and understanding into symmetries and properties of the theories that are not present in the Lagrangian approach. This perturbative expansion is given by (1.3) and we can further expand each loop amplitude in terms of colour structures, C^λ

$$\mathcal{A}_n^{(\ell)} = \sum_c A_{n:c}^{(\ell)} C^c \,, \tag{2.1}$$

separating the colour and kinematics of the amplitude. The colour structures C^λ may be organised in terms of powers of N_c.

There has been much progress in computing leading tree and one-loop amplitudes. For two-loops progress has been considerable in theories with highly extended supersymmetry, both at the integrated [76] and integrand level [77]. However for pure gauge theory, progress has been restricted to amplitudes with a small number of external legs. Specifically full results are only available analyically for four gluons [78, 79], and in [80] these results are presented to all orders in dimensional regularisation.

The first amplitude to be computed at five point was the leading in colour part of the amplitude with all positive helicity external gluons (the all-plus amplitude) which was computed using D-dimensional unitarity methods [81, 82] and was subsequently presented in a very elegant and compact form [83]. In [67], it was shown how four-dimensional unitarity techniques could be used to regenerate the five-point leading in color amplitude. The leading in colour five-point amplitudes have been computed for the remaining helicities [2, 84]. Full colour amplitudes are significantly more complicated requiring a larger class of master integrals incorporating non-planar integrals [85, 86]. In [87] the first full colour five-point amplitude was presented in QCD -for the case of all-plus helicities. Beyond five-point, the leading in color all-plus amplitudes for six- and seven-points are known [68, 69] and indeed in [71] and in Chapter 3 we calculate a full-colour, six-point amplitude.

In this chapter we examine the one and two-loop partial amplitudes using a $U(N_c)$ colour trace basis where the fundamental objects are traces of colour matrices T^a rather than contractions of the structure constants f^{abc}. We examine the all-plus amplitude, $\mathcal{A}_n(1^+, \cdots n^+)$.

This amplitude is fully crossing symmetric which makes computation relatively more tractable but nonetheless is a valuable laboratory for studying the properties of gluon scattering. We compute directly all the colour trace structures for the five-point all-plus two-loop amplitude. The singular part is known from general theorems so we focus on the finite remainder. Our results are in complete agreement with the results computed by Badger et. al. [87] and are consistent with constraints imposed by group theoretical arguments [38, 39].

Our methodology involves computing the polylogarithmic and rational parts of the finite remainder by a combination of techniques. The polylogarithms are computed using four dimensional unitarity cuts and the rational parts are determined by recursion. We use augmented recursion [88] to overcome the issues associated with the presence of double poles. These concepts have already been introduced in the previous chapter but we will now discuss them in more detail.

2.2   One-Loop Sub-leading Amplitudes

The full one-loop n-point amplitude can be expanded as shown in (1.89), with the manifest symmetries given in (1.93) and (1.94). This colour decomposition is both a U(N_c) and an SU(N_c) expression. The $A_{n:2}^{(1)}$ is absent (or zero) in the SU(N_c) case. If any external gluons in the U(N_c) case are the U(1) gluon then the amplitude must vanish. This imposes *decoupling identities* amongst the partial amplitudes. For example setting leg 1 to be U(1) and extracting the coefficient of $\text{Tr}[T^2 T^3 \cdots T^n]$ implies

$$A_{n:2}^{(1)}(1; 2, 3, \cdots n) + A_{n:1}^{(1)}(1, 2, 3, \cdots n) + A_{n:1}^{(1)}(2, 1, 3, \cdots n) + \cdots A_{n:1}^{(1)}(2, \cdots, 1, n) = 0 \quad (2.2)$$

and consequently the $A_{n:2}^{(1)}$ can be expressed as a sum of $(n-1)$ of the $A_{n:1}^{(1)}$. By repeated application of the decoupling identities all the $A_{n:r}^{(1)}$ can be expressed as sums over the $A_{n:1}^{(1)}$ and we obtain,

$$A_{n;r}^{(1)}(1, 2, \ldots, r-1; r, r+1, \ldots, n) \;=\; (-1)^{r-1} \sum_{\sigma \in COP\{\bar{\alpha}\}\{\beta\}} A_{n;1}^{(1)}(\sigma) \qquad (2.3)$$

where $\alpha_i \in \{\bar{\alpha}\} \equiv \{r-1, r-2, \ldots, 2, 1\}$, $\beta_i \in \{\beta\} \equiv \{r, r+1, \ldots, n-1, n\}$ [Note that the ordering of the first set of indices is reversed with respect to the second]. $COP\{\alpha\}\{\beta\}$ is the set of all permutations of $\{1, 2, \ldots, n\}$ with n held fixed that preserve the cyclic ordering of the α_i within $\{\alpha\}$ and of the β_i within $\{\beta\}$, while allowing for all possible relative orderings of the α_i with respect to the β_i. For example if $\{\alpha\} = \{2, 1\}$ and $\{\beta\} = \{3, 4, 5\}$, then $COP\{\alpha\}\{\beta\}$ contains the twelve elements (where $\{\alpha\}$ is made bold for clarity)

$(\mathbf{2}, \mathbf{1}, 3, 4, 5)$, $(\mathbf{2}, 3, \mathbf{1}, 4, 5)$, $(\mathbf{2}, 3, 4, \mathbf{1}, 5)$, $(3, \mathbf{2}, \mathbf{1}, 4, 5)$, $(3, \mathbf{2}, 4, \mathbf{1}, 5)$, $(3, 4, \mathbf{2}, \mathbf{1}, 5)$,
$(\mathbf{1}, \mathbf{2}, 3, 4, 5)$, $(\mathbf{1}, 3, \mathbf{2}, 4, 5)$, $(\mathbf{1}, 3, 4, \mathbf{2}, 5)$, $(3, \mathbf{1}, \mathbf{2}, 4, 5)$, $(3, \mathbf{1}, 4, \mathbf{2}, 5)$, $(3, 4, \mathbf{1}, \mathbf{2}, 5)$.

The simplest one-loop QCD n-gluon helicity amplitude is all-plus helicity amplitude (1.119). This expression is correct up to order ϵ but all-ϵ expression exist for the first few

amplitudes in this series [46],

$$A_{4;1}^{(1)}(1^+, 2^+, 3^+, 4^+) = \frac{2}{\langle 1\,2 \rangle \langle 2\,3 \rangle \langle 3\,4 \rangle \langle 4\,1 \rangle} \frac{\epsilon(1-\epsilon)}{(4\pi)^{2-\epsilon}} \times s_{12}s_{23}I_4^{D=8-2\epsilon},$$

$$A_{5;1}^{(1)}(1^+, 2^+, 3^+, 4^+, 5^+) = \frac{1}{\langle 1\,2 \rangle \langle 2\,3 \rangle \langle 3\,4 \rangle \langle 4\,5 \rangle \langle 5\,1 \rangle} \frac{\epsilon(1-\epsilon)}{(4\pi)^{2-\epsilon}}$$
$$\times \left[s_{23}s_{34}I_4^{(1),D=8-2\epsilon} + s_{34}s_{45}I_4^{(2),D=8-2\epsilon} + s_{45}s_{51}I_4^{(3),D=8-2\epsilon} \right.$$
$$\left. + \; s_{51}s_{12}I_4^{(4),D=8-2\epsilon} + s_{12}s_{23}I_4^{(5),D=8-2\epsilon} + (4-2\epsilon)\varepsilon(1,2,3,4)I_5^{D=10-2\epsilon} \right],$$

$$A_{6;1}^{(1)}(1^+, 2^+, 3^+, 4^+, 5^+, 6^+) = \frac{1}{2 \langle 1\,2 \rangle \langle 2\,3 \rangle \langle 3\,4 \rangle \langle 4\,5 \rangle \langle 5\,6 \rangle \langle 6\,1 \rangle} \frac{\epsilon(1-\epsilon)}{(4\pi)^{2-\epsilon}} \left[\right.$$
$$- \sum_{1 \le i_1 < i_2 \le 6} \text{Tr}[\not{k}_{i_1}\not{P}_{i_1+1,i_2-1}\not{k}_{i_2}\not{P}_{i_2+1,i_1-1}]I_{4:i_1;i_2}^{D=8-2\epsilon}$$
$$+(4-2\epsilon) \; \text{Tr}[123456] \, I_6^{D=10-2\epsilon}$$
$$\left. +(4-2\epsilon) \sum_{i=1}^{6} \varepsilon(i+1, i+2, i+3, i+4)I_5^{(i),D=10-2\epsilon} \right].$$

In principle, all the $A_{n;r}^{(1)}$ amplitudes for the all-plus case may be expressed in terms of the leading colour however the number of terms grows quite rapidly. The number of terms in a single $A_{n;1}^{(1)}$ grows as

$$\frac{1}{24}n(n-1)(n-2)(n-3) \tag{2.4}$$

and the summation over COP terms grows with n as

$$\sim \frac{(n-1)!}{(r-2)!(n-r)!}. \tag{2.5}$$

Although the number of terms in (2.3) is growing very rapidly with n and r, there is considerable simplification. We demonstrate how useful the spinor-helicity formalism is here; by simply thinking of which expressions have the correct momentum weight, little group scaling and symmetries, and by making use of previously conjectured sums to guess which kind of sums appear, we can obtain simple all-n formulae for the subleading terms.

$$A_{n;1}^{(1)}(1^+, 2^+, 3^+, \cdots, n^+) = -\frac{1}{3}\frac{\sum_{i<j<k<l} \text{Tr}_-(ijkl)}{\langle 1\,2 \rangle \langle 2\,3 \rangle \cdots \langle n\,1 \rangle}$$

$$A_{n;2}^{(1)}(1^+; 2^+, 3^+, \cdots, n^+) = -\frac{\sum_{i<j}[1|ij|1]}{\langle 2\,3 \rangle \langle 3\,4 \rangle \cdots \langle n\,2 \rangle}$$

$$A_{n;3}^{(1)}(1^+, 2^+; 3^+, \cdots, n^+) = 2\frac{[1\,2]^2}{\langle 3\,4 \rangle \langle 4\,5 \rangle \cdots \langle n\,3 \rangle}$$

$$A_{n;r}^{(1)}(1^+, 2^+, 3^+, \cdots, (r-1)^+; r^+ \cdots n^+) = -2\frac{(P_{1\ldots r-1}^2)^2}{(\langle 1\,2 \rangle \langle 2\,3 \rangle \cdots \langle (r-1)\,1 \rangle)(\langle r\,(r+1) \rangle \cdots \langle n\,r \rangle)}$$

where $P_{1\ldots r-1}$ denotes the usual $\sum_{i=1}^{r-1} k_i$ and $r \ge 3$. These expressions have been tested numerically against the decoupling identities for up to $n = 12$. These expressions are remarkably simple given the large number of terms one would expect from the decoupling identities.

Another complication we have discussed at loop order are double poles. They occur in amplitudes at complex momenta when the factorisation shown in Figure 1.6 occurs. The factorisation takes the form

$$V(a^+, b^+, K^+) \times \frac{1}{s_{ab}^2} A_{n-1}^{(0)}(K^-, \cdots) \sim \frac{[a\,b]}{\langle a\,b \rangle^2} \times A_{n-1}^{(0)}(K^-, \cdots) \qquad (2.6)$$

where

$$\frac{V^{(1)}(a^+, b^+, K^+)}{s_{ab}} = -\frac{1}{3} \frac{[a\,b]\,[b\,K]\,[K\,a]}{s_{ab}}. \qquad (2.7)$$

is the one-loop three-point vertex [89]. As we previously discussed, the all-plus one-loop amplitude does not contain double poles for $n > 4$ since the tree amplitude on the RHS of the factorisation vanishes. The single minus amplitude does have double poles which can be seen explicitly in the five-point case [90]

$$A_{5:1}^{(1)}(1^-, 2^+, 3^+, 4^+, 5^+) = \frac{1}{3} \frac{1}{\langle 3\,4 \rangle^2} \left[-\frac{[2\,5]^3}{[1\,2]\,[5\,1]} + \frac{\langle 1\,4 \rangle^3\,[4\,5]\,\langle 3\,5 \rangle}{\langle 1\,2 \rangle\,\langle 2\,3 \rangle\,\langle 4\,5 \rangle^2} - \frac{\langle 1\,3 \rangle^3\,[3\,2]\,\langle 4\,2 \rangle}{\langle 1\,5 \rangle\,\langle 5\,4 \rangle\,\langle 2\,3 \rangle^2} \right], \quad (2.8)$$

where there are $\langle a\,b \rangle^{-2}$ singularities for $\langle a\,b \rangle = \langle 2\,3 \rangle$, $\langle 3\,4 \rangle$ and $\langle 4\,5 \rangle$.

The naive application of (2.3) obscures the simplicity of the sub-leading terms. In particular, there are no double poles in the one-loop sub-leading partial amplitudes for $n > 4$. This can be derived from decoupling identities, for example in the $A_{n:2}^{(1)}(a; b, c, \ldots, n)$ case, rewriting this in terms of the $A_{n:1}^{(1)}$ as in (1.96) then the double pole in $\langle a\,b \rangle$ will only occur in the first two terms and will be of the form

$$\frac{V(a^+, b^+, K^+)}{s_{ab}^2} \times A_{n-1:1}^{(0)}(K^-, c, \cdots n) + \frac{V(b^+, a^+, K^+)}{s_{ab}^2} \times A_{n-1:1}^{(0)}(K^-, c, \cdots n) = 0 \qquad (2.9)$$

since $V(a, b, K)$ is antisymmetric. The double pole in s_{bc} for $A_{n:2}^{(1)}(a; b, c, \ldots, n)$ vanishes via a decoupling identity. In the summation only the second term does not contribute and we obtain

$$\frac{V(b^+, c^+, K^+)}{s_{bc}^2} \times \left(A_{n-1:1}^{(0)}(a, K^-, d, \cdots n) + A_{n-1:1}^{(0)}(K^-, a, d, \cdots n) \right.$$
$$\left. + \cdots + A_{n-1:1}^{(0)}(K^-, d, \cdots a, n) \right) \qquad (2.10)$$

This vanishes due to the decoupling identity for the tree amplitude $A_{n-1:1}^{(0)}$. Similar arguments show the vanishing of double poles for all $A_{n:r}^{(1)}$ for $r > 1$. Importantly this argument is independent of the helicities outside of the three-point vertex and so is true for all configurations considered in this thesis, including the single-minus amplitude.

The simplifications in the sub-leading terms allow us to present some compact n-point expressions for the single minus configuration. Explicitly, we can find all-n formulae for $A_{n:2}^{(1)}(1^-; 2^+, \cdots n^+)$ and $A_{n:3}^{(1)}(1^-, 2^+; 3^+, \cdots n^+)$:

$$A_{n:2}^{(1)}(1^-; 2^+, 3^+, \cdots, n^+) = \frac{-\sum_{2 \leq i < j \leq n} \langle 1|ij|1 \rangle}{\langle 2\,3 \rangle\,\langle 3\,4 \rangle \cdots \langle (n-1)\,n \rangle\,\langle n\,2 \rangle} \qquad (2.11)$$

34

and

$$A_{n:3}^{(1)}(1^-, 2^+; 3^+, \cdots, n^+) = \sum_{Z_{(3 \cdots n)}} \frac{\sum_{2 \leq i < j \leq n} \langle 1 | ij | 1 \rangle}{\langle 2\,3 \rangle \langle 3\,4 \rangle \cdots \langle (n-1)\,n \rangle \langle n\,2 \rangle} \tag{2.12}$$

where $Z_{(3 \cdots n)}$ is the set of cyclic permutations of the set $(3, \cdots n)$.

The vanishing of the $\langle b\,c \rangle$ double poles in (2.10) uses a tree level identity, so we do not expect the argument to extend beyond one-loop. Specifically if we consider the double pole in $A_{n:2}^{(2)}(a; b, c, \ldots, n)$, a formula for the double pole in $\langle b\,c \rangle$ akin to (2.10) will exist but with the tree amplitudes $A_{n-1:1}^{(0)}$ replaced by their one-loop equivalents $A_{n-1:1}^{(1)}$. The combination of $A_{n-1:1}^{(1)}$ is that of the decoupling identity (1.96) so the double pole does not vanish but instead is proportional to

$$\frac{V^{(1)}(b^+, c^+, K^+)}{s_{bc}^2} \times A_{n-1:2}^{(1)}(a; K^-, d, \cdots n). \tag{2.13}$$

These simplified subleading in colour amplitudes will prove to be very useful in calculating the two-loop, all-plus amplitudes.

2.3 Two-Loop Amplitudes

A general two-loop amplitude may be expanded as in (1.90). For five-point amplitudes this reduces to

$$\begin{aligned}
\mathcal{A}_5^{(2)}(a, b, c, d, e) &= N_c^2 \sum_{S_5/\mathcal{P}_{5:1}} \mathrm{Tr}(abcde) A_{5:1}^{(2)}(a, b, c, d, e) \\
&+ N_c \sum_{S_5/\mathcal{P}_{5:2}} \mathrm{Tr}(a)\,\mathrm{Tr}(bcde) A_{5:2}^{(2)}(a; b, c, d, e) \\
&+ N_c \sum_{S_5/\mathcal{P}_{5:3}} \mathrm{Tr}(ab)\,\mathrm{Tr}(cde) A_{5:3}^{(2)}(a, b; c, d, e) \\
&+ \sum_{S_5/\mathcal{P}_{5:1,1}} \mathrm{Tr}(a)\,\mathrm{Tr}(b)\,\mathrm{Tr}(cde) A_{5:1,1}^{(2)}(a; b; c, d, e) \\
&+ \sum_{S_5/(\mathcal{P}_{5:1,2}} \mathrm{Tr}(a)\,\mathrm{Tr}(bc)\,\mathrm{Tr}(de) A_{5:1,2}^{(2)}(a; b; c, d, e) \\
&+ \sum_{S_5/\mathcal{P}_{5:1}} \mathrm{Tr}(abcde) A_{5:1B}^{(2)}(a, b, c, d, e) \tag{2.14}
\end{aligned}$$

where we again suppress σ notation, similar to going from (1.4) to (1.8) and we have defined all of the summation sets in Chapter 1. For an $\mathrm{SU}(N_c)$ gauge group, this simplifies to

$$\begin{aligned}
\mathcal{A}_5^{(2)}(a, b, c, d, e) &= N_c^2 \sum_{S_5/\mathcal{P}_{5:1}} \mathrm{Tr}(abcde) A_{5:1}^{(2)}(a, b, c, d, e) \\
&+ N_c \sum_{S_5/\mathcal{P}_{5:3}} \mathrm{Tr}(ab)\,\mathrm{Tr}(cde) A_{5:3}^{(2)}(a, b; c, d, e) \\
&+ \sum_{S_5/\mathcal{P}_{5:1}} \mathrm{Tr}(abcde) A_{5:1B}^{(2)}(a, b, c, d, e) , \tag{2.15}
\end{aligned}$$

35

which gives three separate functions needing to be determined: $A_{5:1}^{(2)}$, $A_{5:3}^{(2)}$ and $A_{5:1B}^{(2)}$. By themselves the U(1) decoupling identities do not determine any of the three however they can be used to obtain the specifically U(1) functions $A_{5:2}^{(2)}$, $A_{5:1,1}^{(2)}$ and $A_{5:1,2}^{(2)}$.

$$A_{5:2}^{(2)}(a; b, c, d, e) = -A_{5:1}^{(2)}(a, b, c, d, e) - A_{5:1}^{(2)}(b, a, c, d, e) - A_{5:1}^{(2)}(b, c, a, d, e) - A_{5:1}^{(2)}(b, c, d, a, e),$$

$$
\begin{aligned}
A_{5:1,1}^{(2)}(d; e; a, b, c) &= \Big(-A_{5:2}^{(2)}(e; a, b, c, d) - A_{5:2}^{(2)}(e; a, b, d, c) - A_{5:2}^{(2)}(e; a, d, b, c) \\
&\quad - \frac{1}{2} A_{5:3}^{(2)}(d, e; a, b, c) \Big) + \{d \leftrightarrow e\} \\
&= \sum_{\sigma \in COP\{d,e\}\{a,b,c\}} A_{5:1}^{(2)}(\sigma) - A_{5:3}^{(2)}(d, e; a, b, c)
\end{aligned}
$$

(2.16)

and

$$
\begin{aligned}
A_{5:1,2}^{(2)}&(1; 2, 3; 4, 5) \\
&= -A_{5:3}^{(2)}(2, 3; 1, 4, 5) - A_{5:3}^{(2)}(2, 3; 1, 5, 4) - A_{5:3}^{(2)}(4, 5; 1, 2, 3) - A_{5:3}^{(2)}(4, 5; 1, 3, 2) \\
&= 0.
\end{aligned}
$$

(2.17)

Decoupling identities do not relate the $A_{n:1B}^{(2)}$ to the other terms but do impose a tree-like identity,

$$A_{n:1B}^{(2)}(a, b, c, \cdots n) + A_{n:1B}^{(2)}(b, a, c, \cdots n) + \cdots A_{n:1B}^{(2)}(b, \cdots, a, n) = 0,$$ (2.18)

which in itself does not specify $A_{n:1B}^{(2)}$ completely. There are however further colour restrictions beyond the decoupling identities [38,39] which may be obtained by recursive methods. These, together with eq. (2.18) determine the $A_{5:1B}^{(2)}$:

$$
\begin{aligned}
A_{5:1B}^{(2)}(a, b, c, d, e) &= -A_{5:1}^{(2)}(a, b, d, c, e) + 2A_{5:1}^{(2)}(a, b, e, c, d) + A_{5:1}^{(2)}(a, b, e, d, c) \\
&\quad -A_{5:1}^{(2)}(a, c, b, d, e) + 2A_{5:1}^{(2)}(a, c, d, b, e) - 5A_{5:1}^{(2)}(a, c, e, b, d) \\
&\quad -2A_{5:1}^{(2)}(a, c, e, d, b) + 2A_{5:1}^{(2)}(a, d, b, c, e) + A_{5:1}^{(2)}(a, d, c, b, e) \\
&\quad +2A_{5:1}^{(2)}(a, d, e, b, c) + A_{5:1}^{(2)}(a, d, e, c, b) \\
&\quad - \frac{1}{2} \sum_{Z_5(a,b,c,d,e)} \Big(A_{5:3}^{(2)}(a, b; c, d, e) - A_{5:3}^{(2)}(a, c; b, d, e) \Big).
\end{aligned}
$$

(2.19)

Our calculation determines $A_{5:1B}^{(2)}$ and we use (2.19) as a consistency check. We will now review the functional content of these amplitudes.

2.4   The Cut Constructible Piece

We can split amplitudes into a piece containing branch cut singularities and a rational piece,

$$A_{n:c}^{(2)} = P_{n:c}^{(2)} + R_{n:c}^{(2)},$$ (2.20)

where P refers to cut constructible pieces and R refers to the rational piece that will lose terms in four-dimensional unitarity. We label it P as we will hereby refer to this as "polylogarithmic" although this also refers to divergent pieces and hypergeometric functions. We use

c here to indicate the different colour structures. We can then split P into diverging parts and IR finite pieces

$$P_{n:c}^{(2)} = U_{n:c}^{(2)} + F_{n:c}^{(2)}. \tag{2.21}$$

$U_{n:c}^{(2)}$ contains a IR singular structure which is determined by general theorems (1.106) as already discussed. Given the general expressions for $U_{n:c}^{(2)}$ are known, the challenge is to compute the finite parts of the amplitude $F_n^{(2)}$.

2.4.1 Unitarity

D-dimensional unitarity techniques can be used to generate the integrands [81] for the five-point amplitude which can then be integrated to give the result [83]. We would like to use four-dimensional unitarity and cut the two-loop diagrams that contribute to $\mathcal{A}_5^{(2)}(a^+, b^+, c^+, d^+, e^+)$. We can categorise two-loop diagrams into two types: what we call "genuine two-loop diagrams" where you must cut more than one internal propagator to reduce the diagram to two sub-diagrams (cut and reduce here being in a topological sense) and (one-loop)^2 which are reducible with a single cut. Figure 2.1 gives an example of each type, introducing the "tricorner box" which will become very important in Chapter 5.

Figure 2.1: (Top) The tricorner box falls under the genuine two-loop category. (Bottom) An example of a (one-loop)^2 diagram, where topologically cutting the connecting propagator would reduce the diagram to two one-loop diagrams.
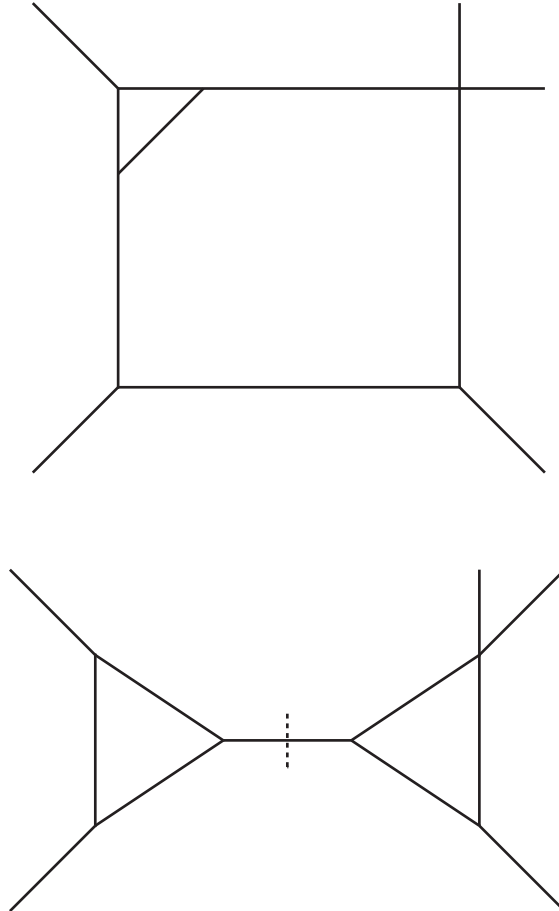
We can use unitarity to distinguish between the two types, utilising continuous triple cuts like the one in Figure 2.2 which factorises the amplitude into $A^{(0)} \times A^{(0)}$. A very useful result of this is that for the all-plus configuration these are all zero. This is because there are no ways of distributing negative helicities on the cut loop-momenta that will give two non-zero amplitudes. When we look at the single-minus amplitude there are non-zero cuts as you can then have two negative helicities on two loop momenta in one amplitude and two negative helicities from the remaining loop momentum and also from the external negative helicity leg.
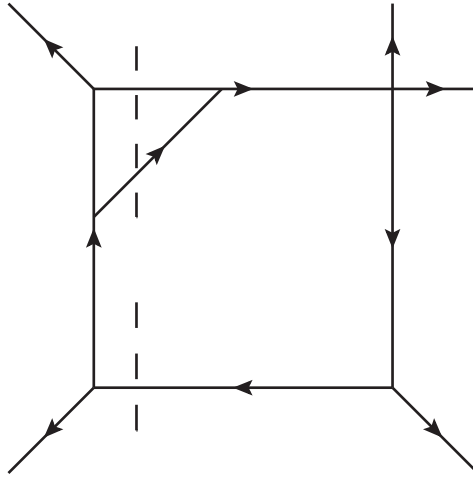
Figure 2.2: Triple cut contributing to a (tree)×(tree) factorisation.

We therefore find unitarity reduces the problem to only the (one-loop)^2 diagrams. These can then be viewed as loop insertions. This is particularly useful as it ties up one of the loop integrals and effectively reduces this two-loop amplitude to a one-loop problem, allowing the use of Passerino-Veltman reduction techniques to reduce it to a sum of scalar boxes, triangles and bubbles such as in (1.108).

Another good indicator that this is valid is by looking at three-point corners with a loop insert. We would expect on a quadruple cut for the amplitude to factorise into $A^{(1)} \times A^{(0)} \times A^{(0)} \times A^{(0)}$ as opposed to four trees. While there is not a three-point, one-loop amplitude as such, we may use the one-loop vertex (2.7) as the insertion to test the behaviour. We find that any quadruple cut containing these inserts vanish, further indicating this method is valid (compare to the single-minus configuration later where some of these cuts diverge, further suggesting the presence of genuine two-loop contributions and invalidating this approach). The non-vanishing four dimensional cuts are therefore shown in Figure 2.3.
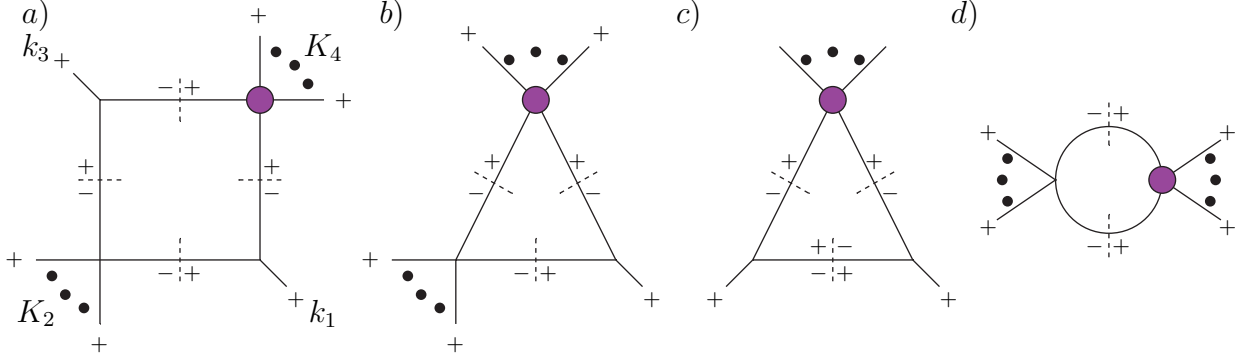
Figure 2.3: Four dimensional cuts of the two-loop all-plus amplitude involving an all-plus one-loop vertex (indicated by •) In the boxes K_2 may be null but K_4 must contain at least two external legs.

The cuts allow us to determine the coefficients, $c_{j,i}$, of box, triangle and bubble functions in the amplitude. The integral functions are

$$\mathcal{I}_2(K^2) = \frac{(-K^2)^{-\epsilon}}{\epsilon(1-2\epsilon)}, \tag{2.22}$$

$$\mathcal{I}_3^{1m}(K^2) = \frac{1}{\epsilon^2}(-K^2)^{-1-\epsilon}, \quad \mathcal{I}_3^{2m}(K_1^2, K_2^2) = \frac{1}{\epsilon^2}\frac{(-K_1^2)^{-\epsilon} - (-K_2^2)^{-\epsilon}}{(-K_1^2) - (-K_2^2)}, \tag{2.23}$$

and

$$
\begin{aligned}
\mathcal{I}_4^{2m}(s, t, K_2^2, K_4^2) &= -\frac{2}{st - K_2^2 K_4^2}\left[-\frac{1}{\epsilon^2}\left[(-s)^{-\epsilon} + (-t)^{-\epsilon} - (-K_2^2)^{-\epsilon} - (-K_4^2)^{-\epsilon}\right]\right. \\
&+ \mathrm{Li}_2\left(1 - \frac{K_2^2}{s}\right) + \mathrm{Li}_2\left(1 - \frac{K_2^2}{t}\right) + \mathrm{Li}_2\left(1 - \frac{K_4^2}{s}\right) + \mathrm{Li}_2\left(1 - \frac{K_4^2}{t}\right) \\
&\left. - \mathrm{Li}_2\left(1 - \frac{K_2^2 K_4^2}{st}\right) + \frac{1}{2}\log^2\left(\frac{s}{t}\right) + \frac{\pi^2}{6}\right]
\end{aligned}
\tag{2.24}
$$

where $s = (k_1 + K_4)^2$ and $t = (k_1 + K_2)^2$.

The bubbles in principle would determine the $(-s)^\epsilon/\epsilon$ infinities. However, explicit calculation using, for example, a canonical basis approach [91] shows that they have zero coefficient. The triangles only contain contributions to $U_{n:\lambda}^{(2)}$, while the box functions contribute to both the IR terms and the finite polylogarithms. Separating these pieces we have

$$I_4^{2m}(s, t, K_2^2, K_4^2) = I_4^{2m}\Big|_{IR} - \frac{2}{st - K_2^2 K_4^2}\mathrm{F}^{2m}[s, t, K_2^2, K_4^2] \tag{2.25}$$

where F^{2m} is a dimensionless combination of polylogarithms.

The IR terms combine to give the correct IR singularities [92],

$$\left(\sum c_{4,i}\mathcal{I}_{4,i}^{2m}\Big|_{IR} + \sum c_{3,i}^{2m}\mathcal{I}_{3,i}^{2m} + \sum c_{3,i}^{1m}\mathcal{I}_{3,i}^{1m}\right)_c = U_{n:c}^{(2),\epsilon^0}(1^+, 2^+, \cdots, n^+) \tag{2.26}$$

39

where $U_{n,c}^{(2),\epsilon^0}(1^+, 2^+, \cdots, n^+)$ is the order ϵ^0 truncation and $n : c$ labels the colour structure, for example it might mean $n : 1$ or $n : s, t$ etc. The sum over i is simply the sum over all relevant configurations of boxes and triangles that will contribute to the colour structure c.

We have checked the relation of (2.26) by using four dimensional unitarity techniques to compute the coefficients and then comparing to the expected form of $U_n^{(2)}$ given by (1.106) for n up to 10 points. Given these just give results of a known theorem we leave discussion of triple and double cut calculations for Chapter 5.

The remaining parts of the box integral functions become the finite polylogarithms. The expression for $F_n^{(2)}$ is [92]

$$F_n^{(2)} = \sum_i c_i \mathrm{F}_i^{2m} \tag{2.27}$$

where where the i sum is simply over all boxes, and

$$\mathrm{F}^{2m}[s, t, K_2^2, K_4^2] = \quad \mathrm{Li}_2[1 - \tfrac{K_2^2}{s}] + \mathrm{Li}_2[1 - \tfrac{K_2^2}{t}] + \mathrm{Li}_2[1 - \tfrac{K_4^2}{s}]$$
$$+ \quad \mathrm{Li}_2[1 - \tfrac{K_4^2}{t}] - \mathrm{Li}_2[1 - \tfrac{K_2^2 K_4^2}{st}] + \tfrac{1}{2}\ln^2(s/t) + \tfrac{\pi^2}{6} \tag{2.28}$$

and, in the specific case where $K_2^2 = 0$,

$$\mathrm{F}^{1m}[s, t, K_4^2] \equiv \mathrm{F}^{2m}[s, t, 0, K_4^2] = \quad \mathrm{Li}_2[1 - \tfrac{K_4^2}{s}] + \mathrm{Li}_2[1 - \tfrac{K_4^2}{t}] + \tfrac{1}{2}\ln^2(s/t) + \tfrac{\pi^2}{3} \ . \tag{2.29}$$

Let us now consider the specific five-point case where only the $K_2^2 = 0$ case occurs.
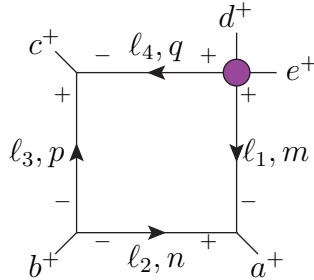
Figure 2.4: The labelling and internal helicities of the quadruple cut.

In this case the one-loop corner is a four-point amplitude. The colour partial amplitudes simplify the case since

$$A_{4:1}^{(1)}(1234) = A_{4:1}^{(1)}(1243) = A_{4:1}^{(1)}(1324) \tag{2.30}$$

which implies from the decoupling identities that,

$$A_{4:2}^{(1)}(1; 234) = -3A_{4:1}^{(1)}(1234), \qquad A_{4:3}^{(1)}(12; 34) = 6A_{4:1}^{(1)}(1234) \tag{2.31}$$

which means the full colour amplitude factorises into colour and kinematics as

$$\mathcal{A}_4^{(1)}(\ell_1, \ell_4, d, e) = \mathcal{C} \times A_{4:1}^{(1)}(\ell_4, d, e, \ell_1) \tag{2.32}$$

Since the three-point tree amplitudes also factorise, the quadruple cut of this box function will be

$$\mathcal{C}' \times A_3^{(0)}(a, \ell_2, \ell_1) A_3^{(0)}(b, \ell_3, \ell_2) A_3^{(0)}(c, \ell_4, \ell_3) A_{4:1}^{(1)}(\ell_4, d, e, \ell_1) \tag{2.33}$$

40

We then just need the solution to the quadruple cuts. The following works for n-point one-mass boxes with all-plus helicity legs.
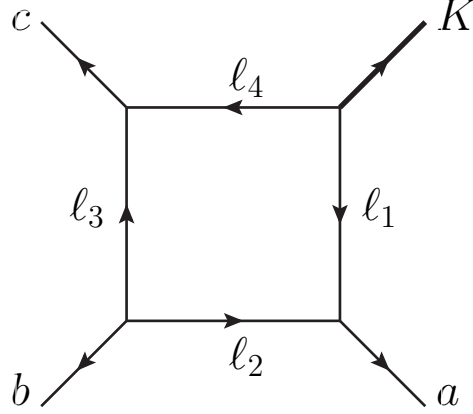
Figure 2.5: A general one-mass box with $a^2 = b^2 = c^2 = 0$ and $K^2 \neq 0$. On a quadruple cut, $\ell_i^2 = 0$ for $i \in \{1, 2, 3, 4\}$.

For the configuration in Figure 2.5 we have

$$\ell_2 + \ell_1 = a$$
$$\ell_2 + \ell_3 = -b$$
$$\ell_3 + \ell_4 = c$$
$$\ell_4 + \ell_1 = -K = P_{abc}, \tag{2.34}$$

where we use the notation $P_{ijk} = p_i + p_j + p_k$. On the cut, we solve for ℓ_2

$$\ell_1^2 = [\ell_2 \, a] \, \langle \ell_2 \, a \rangle = 0, \tag{2.35}$$
$$\ell_3^2 = [\ell_2 \, b] \, \langle b \, \ell_2 \rangle = 0, \tag{2.36}$$
$$\ell_2 = \alpha_{\ell_2} \tilde{\lambda}_b \lambda_a. \tag{2.37}$$

The conjugate of this is also valid but causes the subamplitudes on the cut to vanish, and so we will ignore them for now, although we must average over the two solutions for the final result. We solve α_{ℓ_2} using momentum conservation around two corners

$$\ell_4^2 = (P_{bc} + \ell_2)^2 = [\ell_2 | P_{bc} | \ell_2 \rangle + s_{bc} = 0,$$
$$\alpha_{\ell_2} = -\frac{\langle c \, b \rangle}{\langle c \, a \rangle},$$
$$\ell_2 = -\frac{\langle c \, b \rangle}{\langle c \, a \rangle} \tilde{\lambda}_b \lambda_a. \tag{2.38}$$

Similarly for ℓ_3

$$\ell_3 = -\frac{\langle a \, b \rangle}{\langle a \, c \rangle} \tilde{\lambda}_b \lambda_c \tag{2.39}$$

remembering we cannot have $\ell_3 \propto \tilde{\lambda}_c$ due to the $\overline{MHV}$ corner etc.

$$\ell_1 = \frac{\langle c \, a \rangle \, \tilde{\lambda}_a + \langle c \, b \rangle \, \tilde{\lambda}_b}{\langle c \, a \rangle} \lambda_a \,, \qquad \ell_4 = \frac{\langle c \, a \rangle \, \tilde{\lambda}_c + \langle b \, a \rangle \, \tilde{\lambda}_b}{\langle c \, a \rangle} \lambda_c. \tag{2.40}$$

41

Now that we have the solutions, remembering to average over the zero and non-zero solutions, we can write

$$A_3^{(0)}(a, \ell_2, \ell_1) A_3^{(0)}(b, \ell_3, \ell_2) A_3^{(0)}(c, \ell_4, \ell_3) A_{4:1}^{(1)}(\ell_4, d, e, \ell_1) \;=\; \frac{2 s_{ab} s_{bc}}{3} \times \frac{[d\,e]^2}{\langle a\,b \rangle \langle b\,c \rangle \langle c\,a \rangle} \tag{2.41}$$

$$= \frac{s_{ab} s_{bc}}{3} \times A_{5:3}(de; abc) \tag{2.42}$$

Consequently the different colour trace amplitudes will be of the form

$$F_5^{(2)} \sim \sum A_{5:3}(de; abc) \times F_{abc;de}^{1m} \tag{2.43}$$

where $F_{abc;de}^{1m} \equiv F^{1m}[s_{ab}, s_{bc}, s_{de}]$. We can determine the terms in the summation by evaluating $\mathcal{C}'$. Expanding $\mathcal{C}'$ and applying $\mathrm{U}(N_c)$ trace identities (1.88) we get

$$
\begin{aligned}
\mathcal{C}'_{(de;abc)} &= \sum_{m,n,p,q} \Big((\mathrm{Tr}[amn] - \mathrm{Tr}[man])(\mathrm{Tr}[bpn] - \mathrm{Tr}[pbn])(\mathrm{Tr}[pcq] - \mathrm{Tr}[pqc]) \Big) \\
&\quad \times \Big(N_c \, \mathrm{Tr}[mqed] + N_c \, \mathrm{Tr}[meqd]/2 + N_c \, \mathrm{Tr}[qemd]/2 + N_c \, \mathrm{Tr}[qmed] \\
&\qquad - 3\, \mathrm{Tr}[m]\, \mathrm{Tr}[qde] - 3\, \mathrm{Tr}[q]\, \mathrm{Tr}[mde] - 3\, \mathrm{Tr}[d]\, \mathrm{Tr}[emq] - 3\, \mathrm{Tr}[d]\, \mathrm{Tr}[eqm] \\
&\qquad + 3\, \mathrm{Tr}[de]\, \mathrm{Tr}[mq] + 3\, \mathrm{Tr}[dm]\, \mathrm{Tr}[eq] + 3\, \mathrm{Tr}[dq]\, \mathrm{Tr}[em] + \{d \leftrightarrow e\} \Big) \\
&= N_c^2 \Big(\mathrm{Tr}[deabc] + \mathrm{Tr}[edabc] - \mathrm{Tr}[badec] - \mathrm{Tr}[baedc] \Big) \\
&\quad + N_c \Big(-2\, \mathrm{Tr}[d](\mathrm{Tr}[eabc] - \mathrm{Tr}[baec]) - 2\, \mathrm{Tr}[e](\mathrm{Tr}[dabc] - \mathrm{Tr}[badc]) \\
&\qquad - \mathrm{Tr}[a](\mathrm{Tr}[debc] + \mathrm{Tr}[edbc] - \mathrm{Tr}[bdec] - \mathrm{Tr}[bedc]) \\
&\qquad - \mathrm{Tr}[b](\mathrm{Tr}[deac] + \mathrm{Tr}[edac] - \mathrm{Tr}[aedc] - \mathrm{Tr}[adec]) \\
&\qquad - \mathrm{Tr}[c](\mathrm{Tr}[deab] + \mathrm{Tr}[edab] - \mathrm{Tr}[adeb] - \mathrm{Tr}[aedb]) \\
&\qquad + 8\, \mathrm{Tr}[de](\mathrm{Tr}[abc] - \mathrm{Tr}[bac]) + \mathrm{Tr}[da](\mathrm{Tr}[bec] - \mathrm{Tr}[ebc]) \\
&\qquad + \mathrm{Tr}[db](\mathrm{Tr}[aec] - \mathrm{Tr}[eac]) + \mathrm{Tr}[dc](\mathrm{Tr}[aeb] - \mathrm{Tr}[eab]) \\
&\qquad - \mathrm{Tr}[ea](\mathrm{Tr}[dbc] - \mathrm{Tr}[bdc]) - \mathrm{Tr}[eb](\mathrm{Tr}[dac] - \mathrm{Tr}[adc]) - \mathrm{Tr}[ec](\mathrm{Tr}[dab] - \mathrm{Tr}[adb]) \Big) \\
&\quad + 3 \Big(-2\, \mathrm{Tr}[d]\, \mathrm{Tr}[e](\mathrm{Tr}[abc] - \mathrm{Tr}[bac]) + \mathrm{Tr}[d]\, \mathrm{Tr}[a](\mathrm{Tr}[ebc] - \mathrm{Tr}[bec]) \\
&\qquad + \mathrm{Tr}[d]\, \mathrm{Tr}[b](\mathrm{Tr}[eac] - \mathrm{Tr}[aec]) + \mathrm{Tr}[d]\, \mathrm{Tr}[c](\mathrm{Tr}[eab] - \mathrm{Tr}[aeb]) \\
&\qquad + \mathrm{Tr}[e]\, \mathrm{Tr}[a](\mathrm{Tr}[dbc] - \mathrm{Tr}[bdc]) + \mathrm{Tr}[e]\, \mathrm{Tr}[b](\mathrm{Tr}[dac] - \mathrm{Tr}[adc]) \\
&\qquad + \mathrm{Tr}[e]\, \mathrm{Tr}[c](\mathrm{Tr}[dab] - \mathrm{Tr}[adb]) \Big) \\
&\quad + 6 \Big(\mathrm{Tr}[deabc] - \mathrm{Tr}[dcbae] + \mathrm{Tr}[dcbea] - \mathrm{Tr}[daebc] + \mathrm{Tr}[dceba] - \mathrm{Tr}[dabec] + \mathrm{Tr}[dcaeb] - \mathrm{Tr}[dbeac] \\
&\qquad + \mathrm{Tr}[dbaec] - \mathrm{Tr}[dceab] + \mathrm{Tr}[dabce] - \mathrm{Tr}[decba] + \mathrm{Tr}[daecb] - \mathrm{Tr}[dbcea] + \mathrm{Tr}[dbeca] - \mathrm{Tr}[daceb] \Big).
\end{aligned}
$$

This is an expansion of the form

$$\mathcal{C}'_{(de;abc)} = \sum_\lambda a^\lambda_{(de;abc)} C^\lambda \tag{2.44}$$

where the C^λ are the different colour structures. Consequently the finite polylogarithmic part of the partial amplitudes is

$$F_{5:\lambda}^{(2)} = \sum_{(de;abc)} a^\lambda_{(de;abc)} A_{5:3}(d, e; a, b, c) \times \mathrm{F}_{abc;de}^{1m} \,. \tag{2.45}$$

Specifically we recover the previous results of [83] and [87],

$$F_{5:1}^{(2)}(a,b,c,d,e) = \sum_{\mathcal{P}_{5:1}} -A_{5:3}^{(1)}(d,e;a,b,c)\mathrm{F}_{abc;de}^{1m},$$

$$F_{5:3}^{(2)}(a,b:c,d,e) = \frac{4}{3}\sum_{\mathcal{P}_{5:3}}\Big(A_{5:3}^{(1)}(a,b;c,d,e)\,\mathrm{F}_{cde;ab}^{1m}$$
$$+\ \frac{1}{4}A_{5:3}^{(1)}(a,c;b,e,d)\,(\mathrm{F}_{bed;ac}^{1m} + \mathrm{F}_{bde;ac}^{1m} - \mathrm{F}_{dbe;ac}^{1m})\Big),\qquad(2.46)$$

where again the $\mathcal{P}$ sets follow the manifest symmetry of the $F_5^{(2)}$ arguments. We also determine directly the remaining $SU(N_c)$ partial amplitude,

$$F_{5:1B}^{(2)}(a,b,c,d,e) = 2\sum_{\mathcal{P}_{5:1}}\Big(A_{5:3}^{(1)}(a,b:c,d,e)\,\mathrm{F}_{cde;ab}^{1m}+$$
$$A_{5:3}^{(1)}(a,c;b,e,d)\,(\mathrm{F}_{bed;ac}^{1m} + \mathrm{F}_{bde;ac}^{1m} - \mathrm{F}_{dbe;ac}^{1m})\Big).\qquad(2.47)$$

This expression matches that obtained by using the results of (2.46) in (2.19).

The specifically $U(N_c)$ partial amplitudes may also be extracted directly:

$$F_{5:2}^{(2)}(a;b,c,d,e) = -\frac{2}{3}\sum_{\mathcal{P}_{5:2}}\Big(A_{5:3}^{(1)}(a,b;c,d,e)\,\mathrm{F}_{cde;ab}^{1m}$$
$$+\ \frac{1}{2}A_{5:3}^{(1)}(b,c;a,e,d)\,(\mathrm{F}_{ade;bc}^{1m} + \mathrm{F}_{dea;bc}^{1m} - \mathrm{F}_{dae;bc}^{1m})\Big)\qquad(2.48)$$

and

$$F_{5:1,1}^{(2)}(a;b;c,d,e) = -\sum_{\mathcal{P}_{5:1,1}}\Big(A_{5:3}^{(1)}(a,b;c,d,e)\,\mathrm{F}_{cde;ab}^{1m}$$
$$+\ A_{5:3}^{(1)}(a,c;b,e,d)\,(\mathrm{F}_{bed;ac}^{1m} + \mathrm{F}_{bde;ac}^{1m} - \mathrm{F}_{dbe;ac}^{1m})\Big).\qquad(2.49)$$

These satisfy the decoupling identities (2.17), providing a strong check on the results.

2.5 Recursion

The remaining part of the amplitude is the rational function $R_{n:c}^{(2)}$. This amplitude contains double poles and will therefore need augmented recursion to calculate. We outlined the fundamentals for a general calculation in Section 1.7, but we can now specialise to $R_{5:c}^{(2)}$.

We will use the Risager shift [23] which acts on three momenta, say p_a, p_b and p_c, to give

$$\lambda_a \to \lambda_{\hat{a}} = \lambda_a + z\,[b\,c]\,\lambda_\eta,$$
$$\lambda_b \to \lambda_{\hat{b}} = \lambda_b + z\,[c\,a]\,\lambda_\eta,\qquad(2.50)$$
$$\lambda_c \to \lambda_{\hat{c}} = \lambda_c + z\,[a\,b]\,\lambda_\eta,$$

where λ_η must satisfy $\langle a\,\eta\rangle \neq 0$ etc. but is otherwise unconstrained. For simplicity we choose it to be equal to q, the similarly unconstrained reference vector in (1.123). After applying the shift, the rational quantity of interest is a complex function parametrized by z i.e. $R(z)$.

If $R(z)$ vanishes at large $|z|$, then Cauchy's theorem applied to $R(z)/z$ over a contour at infinity implies

$$R = R(0) = -\sum_{z_j \neq 0} \text{Res}\Big[\frac{R(z)}{z}\Big]\Big|_{z_j} . \tag{2.51}$$

Employing the Risager shift (2.50) yields a shifted quantity with the desired asymptotic behaviour. This is difficult to tell a priori for two-loops but we can tell a posteriori. Both the Risager and BCFW shifts break the cyclic symmetry due to making a specific selection of legs, and the Risager shift depends on η. Cyclic symmetry is then restored in the final result when using the Risager shift, but not for the BCFW shift, and the result is independent on η. This implies the large z behaviour of the Risager shift is correct but is incorrect for the BCFW shift. This is not too surprising given the analysis that can be performed at tree level.

The effect of this shift is to excite poles belonging to various factorisation channels; the (one-loop)-(one-loop) and the (tree)-(two-loop) factorisations, where for the all-plus helicity we expect non-vanishing factorisations to look like,

$$R_5^{(1-1)} \sim A_3^{(1)} \times \frac{1}{K^2} \times A_4^{(1)} \tag{2.52}$$

$$R_5^{(0-2)} = A_3^{(0)} \times \frac{1}{K^2} \times A_4^{(2)} \tag{2.53}$$

such that the rational part of the amplitude can be written as

$$R_5^{(2)} = R_5^{(1-1)} + R_5^{(0-2)}. \tag{2.54}$$

Loop amplitudes in non-supersymmetric theories may have double poles in complex momenta. $R_5^{(1-1)}$ is written as similar to and not equal to since its leading singularity is a double pole which can be determined by factorisation theorems, however there is additional sub-leading information that is non-factorising in nature. Mathematically this is not a problem since, as has been discussed, we may use augmented recursion and the doubly off-shell current to perform a Laurent expansion. The required residue is then

$$\text{Res}\Big[\frac{R(z)}{z}\Big]\Big|_{z_j} = -\frac{c_{-2}}{z_j^2} + \frac{c_{-1}}{z_j} \tag{2.55}$$

and we can use Cauchy's theorem *provided* we know the value of both the leading and sub-leading poles. At this point, there are no general theorems determining the sub-leading pole and we need to determine it for each specific case.

We will start with the (tree)-(two-loop) piece. It only involves simple poles and their contributions are readily obtained from the rational parts of the four-point two-loop amplitude [79]:

$$R_{4:1}^{(2)}(K^+, c^+, d^+, e^+) = \frac{1}{3} A_{4:1}^{(1)}(k^+, c^+, d^+, e^+) \left(\frac{s_{ce}^2}{s_{cd}s_{de}} + 8\right),$$

$$R_{4:3}^{(2)}(K^+, c^+; d^+, e^+) = \frac{1}{9} A_{4:3}^{(1)}(k^+, c^+; d^+, e^+) \left(\frac{s_{cd}^2}{s_{ce}s_{de}} + \frac{s_{ce}^2}{s_{cd}s_{de}} + \frac{s_{de}^2}{s_{cd}s_{ce}} + 24\right). \tag{2.56}$$

This allows us to extend to full colour by writing the full colour decomposition of each side of the factorisation and using $U(N_c)$ trace identities. The specifically $U(1)$ amplitudes can

be related to the two rational amplitudes (2.56) via decoupling identities. Figure 2.6 gives the colour lines that contribute to the leading in colour planar amplitude but again we need to include the whole four-point, two-loop, amplitude (1.90).
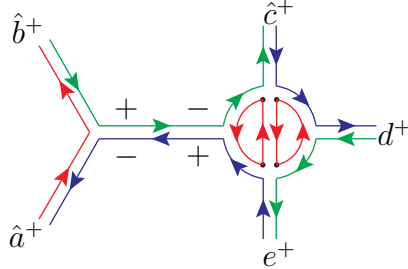
Figure 2.6: A ribbon graph representing the leading in colour contribution to a (tree)-(two-loop) channel. The external legs are dressed in a cyclic ordering to produce $Tr[abcde]$, while there are two closed internal colour lines belonging to the loops contributing a factor of N_c each.

The rational piece obtained from these factorisations is then obtained from standard recursion, performing the Risager shift, colour dressing all factorisations that have shifted legs on both sides, taking the residue and summing over all contributing diagrams.

We then look at the (one-loop)-(one-loop) factorisation. By considering a diagram of the form Figure 1.7 using an axial gauge formalism (1.123), we can determine the full pole structure of the rational piece, including the non-factorising simple poles.

The principal helicity assignment in Figure 1.7 gives

$$\int d\Lambda^{\text{colour}}(\alpha^+, a^+, b^+, \beta^-)\, \tau_n^{(1),\text{colour}}(\alpha^-, \beta^+, c^+, ..., n^+), \tag{2.57}$$

and we can apply the method to the full colour amplitude. The $U(N_c)$ color decomposition of $d\Lambda^{\text{colour}}$ contains a common kinematic factor so we have the colour decompositions

$$\tau_n^{(1),\text{colour}} = \sum_c C_c \tau_{n:c}^{(1)} \quad \text{and} \quad \int d\Lambda^{\text{colour}} = C_\Lambda \int d\Lambda_0\,, \tag{2.58}$$

where we can use axial gauge formalism to express three point off-shell tree amplitudes to write

$$\int d\Lambda_0(\alpha^+, a^+, b^+, \beta^-) = \frac{1}{(2\pi)^D} \int \frac{d^D\ell}{\ell^2 \alpha^2 \beta^2} \frac{[a|\ell|q\rangle [b|\ell|q\rangle}{\langle a\,q\rangle \langle b\,q\rangle} \frac{\langle \beta\,q\rangle^2}{\langle \alpha\,q\rangle^2}\,. \tag{2.59}$$

Hence the full color contribution is

$$\sum_c C_\Lambda C_c \int d\Lambda_0(\alpha^+, a^+, b^+, \beta^-)\, \tau_{n:c}^{(1)}(\alpha^-, \beta^+, c^+, \cdots n^+). \tag{2.60}$$

The various $\tau_{n:c}^{(1)}$ can be expressed as sums of the leading amplitudes $\tau_{n:1}^{(1)}$ via a series of $U(1)$ decoupling identities (2.3). We now focus on the five-point case, where the decoupling identities only make use of two distinct forms of the leading current,

$$\tau_{5:1}^{(1)}(\alpha^-, \beta^+, c^+, d^+, e^+) \quad \text{and} \quad \tau_{5:1}^{(1)}(\alpha^-, c^+, \beta^+, d^+, e^+)\,, \tag{2.61}$$

45

which we call the 'adjacent' and 'non-adjacent' leading currents respectively.

$\tau_{5:1}^{(1)}(\alpha^-, \beta^+, c^+, d^+, e^+)$ has been calculated previously for a specific choice of the axial gauge spinor $\lambda_q = \lambda_d$ [67]. Since we require currents for which all the legs have been permuted it is necessary to derive this current for arbitrary λ_q. The non-adjacent case has not previously been considered.

2.5.1 Obtaining the adjacent current

We do not need the full current, it just needs to satisfy the two conditions outlined in Section 1.7. Condition (C2) requires the current $\tau_{5:c}^{(1)}$ to reproduce the full partial amplitude $A_{5:c}^{(1)}$ in the $\alpha^2 \to 0$, $\beta^2 \to 0$ limit and so the current should have the same colour decomposition as the one-loop amplitude (1.89). We can use the decoupling identities (2.3) to relate any of the sub-leading currents to sums of the leading in colour currents $\tau_{5:1}^{(1)}$. The cyclic and flip symmetries inherited from $A_{5:1}^{(1)}$ mean that any of the $\tau_{5:c}^{(1)}$ can be related to $\tau_{5:1}^{(1)}(\alpha, \beta, c, d, e)$ and $\tau_{5:1}^{(1)}(\alpha, c, \beta, d, e)$ up to permutations of the legs $\{c, d, e\}$.

To build the current we start with the one-loop, five-point, single-minus partial amplitude

$$A_{5:1}^{(1)}(\alpha^-, \beta^+, c^+, d^+, e^+) = \sum_{j=i,ii,iii} A_{5:1j}^{(1)}\left(\alpha^-, \beta^+, c^+, d^+, e^+\right) \tag{2.62}$$

where

$$A_{5:1i}^{(1)}\left(\alpha^-, \beta^+, c^+, d^+, e^+\right) = \frac{1}{3}\frac{1}{\langle c\,d\rangle^2}\frac{\langle c\,e\rangle\,\langle\alpha\,d\rangle^3\,[d\,e]}{\langle\alpha\,\beta\rangle\,\langle d\,e\rangle^2\,\langle\beta\,c\rangle},$$

$$A_{5:1ii}^{(1)}\left(\alpha^-, \beta^+, c^+, d^+, e^+\right) = -\frac{1}{3}\frac{1}{\langle c\,d\rangle^2}\frac{[\beta\,e]^3}{[\alpha\,\beta]\,[e\,\alpha]}$$

and

$$A_{5:1iii}^{(1)}\left(\alpha^-, \beta^+, c^+, d^+, e^+\right) = \frac{1}{3}\frac{1}{\langle c\,d\rangle^2}\frac{\langle\alpha\,c\rangle^3\,\langle\beta\,d\rangle\,[\beta\,c]}{\langle d\,e\rangle\,\langle\alpha\,e\rangle\,\langle\beta\,c\rangle^2}.$$

Condition (C1) requires our approximation to the current to reproduce the correct leading singularities as $s_{\alpha\beta} \to 0$, the sources of these are depicted in Figure 2.7.
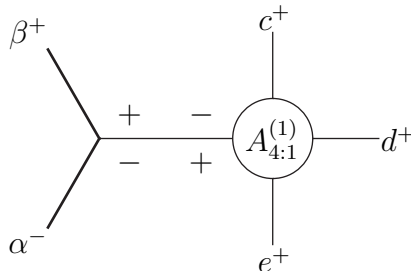
Figure 2.7: Factorisations of the current on the $s_{\alpha\beta} \to 0$ pole.

We determine these within the axial gauge formalism. The two channels give

$$\mathcal{F}_{dp}^{cde} \equiv \frac{[\beta\, k]\,\langle\alpha\, q\rangle^2}{\langle\beta\, q\rangle\,\langle k\, q\rangle}\frac{1}{s_{\alpha\beta}}A_{4:1}^{(1)}(k^-,c^+,d^+,e^+) = \frac{1}{3}\frac{\langle\alpha\, q\rangle^2}{\langle\beta\, q\rangle^2}\frac{\langle q|\alpha\beta|q\rangle}{s_{\alpha\beta}}\frac{\langle e\, c\rangle\,[c\, e]^3}{\langle c\, d\rangle\,\langle d\, e\rangle\,[e|P_{\alpha\beta}|q\rangle[c|P_{\alpha\beta}|q\rangle}$$

for the double pole, and

$$\mathcal{F}_{sb}^{cde} \equiv \frac{\langle\alpha\, k\rangle\,[\beta\, q]^2}{[\alpha\, q]\,[k\, q]}\frac{1}{s_{\alpha\beta}}A_{4:1}^{(1)}(k^+,c^+,d^+,e^+) = -\frac{1}{3}\frac{\langle\alpha\, k\rangle\,[\beta\, q]^2}{[\alpha\, q]\,[k\, q]}\frac{1}{s_{\alpha\beta}}\frac{[e\, k]^2}{\langle c\, d\rangle^2}\tag{2.63}$$

for the "square bracket pole", where $k = \alpha + \beta = -c - d - e$ which is null on the pole.

We start from $A_{5:1i}^{(1)}$ in terms of $\alpha^\flat$ and $\beta^\flat$ and take it off-shell using (1.123) and $s_{\alpha\beta} << 1$, aiming for $\mathcal{F}_{dp}^{cde}$. Using the identity

$$\frac{1}{\langle\alpha\,\beta\rangle\,\langle\beta\, c\rangle} = \frac{1}{\langle\alpha\, q\rangle\,\langle\beta\, q\rangle^2}\left(\frac{\langle q|\alpha\beta|q\rangle[q|P_{\alpha\beta}|q\rangle}{s_{\alpha\beta}[q|P_{\alpha\beta}|c\rangle} + \frac{\langle q\,\beta\rangle\,\langle q\, c\rangle\,[q|\alpha|q\rangle}{\langle\beta\, c\rangle\,[q|P_{\alpha\beta}|c\rangle}\right),\tag{2.64}$$

and the expansion

$$\frac{[\beta|P_{\alpha\beta}^\flat|d\rangle}{[\beta|P_{\alpha\beta}|q\rangle} = \frac{[q|P_{\alpha\beta}|d\rangle}{[q|P_{\alpha\beta}|q\rangle} + s_{\alpha\beta}\frac{\langle q\, d\rangle\,[\beta\, q]}{[\beta|P_{\alpha\beta}|q\rangle[q|P_{\alpha\beta}|q\rangle} + \mathcal{O}(s_{\alpha\beta}^2),\tag{2.65}$$

which simply makes use of a Schouten identity followed by taking $P_{\alpha\beta}$ off-shell, we find

$$A_{5:1i}^{(1)} = \mathcal{F}_{dp}^{cde}\left[1 + s_{\alpha\beta}\left(\frac{[q\, e]}{[c\, e]\,[q|P_{\alpha\beta}|c\rangle} + \frac{[c|q|d\rangle}{[q|P_{\alpha\beta}|q\rangle[c|e|d\rangle} + \frac{[e|q|d\rangle}{[q|P_{\alpha\beta}|q\rangle[e|c|d\rangle}\right) + \mathcal{O}(s_{\alpha\beta}^2)\right].\tag{2.66}$$

We see that $A_{5:1i}^{(1)}$ generates the correct singularity as $\langle\alpha\,\beta\rangle \to 0$. This terms generates the double pole when integrated and the form in (2.66) explicitly exposes the subleading contribution. We throw away terms of $\mathcal{O}(s_{\alpha\beta}^2)$ as this no longer contributes a pole, hence not requiring the complete current.

The $\mathcal{F}_{sb}^{cde}$ factorisation arises when $[\alpha\,\beta] \to 0$. This we obtain from $A_{5:1ii}^{(1)}$. Using,

$$k^\flat = k - \frac{k^2}{2k.q}q = \alpha^\flat + \beta^\flat + \delta q,\tag{2.67}$$

where

$$\delta = \frac{\alpha^2}{2\alpha.q} + \frac{\beta^2}{2\beta.q} - \frac{s_{\alpha\beta}}{2k.q},\tag{2.68}$$

we have

$$\mathcal{F}_{sb}^{cde} = \frac{1}{3}\frac{1}{s_{\alpha\beta}}\left[\frac{[e\,\beta]^2\,[\beta\, q]\,\langle\beta\,\alpha\rangle}{[\alpha\, q]\,\langle c\, d\rangle^2} + \delta[e|q|\alpha\rangle\frac{([e\,\beta]\,[\beta\, q]\,[k\, q] + [\beta\, q]^2\,[e\, k])}{[\alpha\, q]\,[k\, q]\,\langle c\, d\rangle^2}\right].\tag{2.69}$$

Now $A_{5:1ii}^{(1)}$ can be rewritten as

$$A_{5:1ii}^{(1)} = -\frac{1}{3}\frac{1}{\langle c\, d\rangle^2}\frac{[\beta\, e]^2\,[q\, e]}{[e\,\alpha]\,[\alpha\, q]} - \frac{1}{3}\frac{1}{\langle c\, d\rangle^2}\frac{[\beta\, e]^2\,[q\,\beta]}{[\alpha\,\beta]\,[\alpha\, q]}\tag{2.70}$$

and noting that

$$\frac{\langle \beta\,\alpha\rangle}{s_{\alpha\beta}} - \frac{1}{[\alpha\,\beta]} = \frac{\langle \beta\,\alpha\rangle\,[\alpha\,\beta] - s_{\alpha\beta}}{s_{\alpha\beta}\,[\alpha\,\beta]} = \frac{(\alpha^\flat + \beta^\flat)^2 - s_{\alpha\beta}}{s_{\alpha\beta}\,[\alpha\,\beta]} = -\left(\frac{\alpha^2}{2\alpha.q} + \frac{\beta^2}{2\beta.q}\right)\frac{2k.q}{s_{\alpha\beta}\,[\alpha\,\beta]}\,,$$

$$(2.71)$$

we see that $A^{(1)}_{5:1ii}$ has the form $\mathcal{F}^{cde}_{sb} + \Delta$ as $[\alpha\,\beta] \to 0$, where Δ contains terms of order α^2 and β^2. We therefore include a contribution to the current of the form $A^{(1)}_{5:1ii} - \Delta$ to satisfy condition (C1). As Δ vanishes when $\alpha^2 = \beta^2 = 0$, its inclusion does not compromise condition (C2).

The remaining piece of the one-loop amplitude, $A^{(1)}_{5:1iii}$, contains no poles as $\langle \alpha\,\beta\rangle \to 0$ or $[\alpha\,\beta] \to 0$ and we can simplify it using

$$\frac{\langle X\,\alpha\rangle}{\langle Y\,\alpha\rangle} = \frac{\langle X\,\alpha\rangle}{\langle Y\,\alpha\rangle}\frac{\langle Y\,a\rangle}{\langle Y\,a\rangle} = \frac{\langle X\,a\rangle}{\langle Y\,a\rangle} + \mathcal{O}(\langle \alpha\,a\rangle) \tag{2.72}$$

as terms of $\mathcal{O}(\langle \alpha\,a\rangle)$ do not ultimately contribute to the residue.

The adjacent leading current is then

$$\tau^{(1)}_{5:1}(\alpha^-,\beta^+,c^+,d^+,e^+) = \mathcal{F}^{cde}_{dp}\left[1 + s_{\alpha\beta}\left(\frac{[q\,e]}{[c\,e]\,[q|P_{\alpha\beta}|c\rangle} + \frac{[c|q|d\rangle}{[q|P_{\alpha\beta}|q\rangle[c|e|d\rangle} + \frac{[e|q|d\rangle}{[q|P_{\alpha\beta}|q\rangle[e|c|d\rangle}\right)\right]$$

$$+ \frac{i}{3\,\langle c\,d\rangle^2}\frac{\langle\alpha\,q\rangle^2}{\langle\beta\,q\rangle^2}\left[\frac{\langle a\,c\rangle\,[c|\beta|d\rangle}{\langle d\,e\rangle\,\langle e\,a\rangle} + \frac{\langle c\,e\rangle\,[d\,e]}{\langle d\,e\rangle^2}\left(\frac{[q|P_{\alpha\beta}|d\rangle^3}{[q|P_{\alpha\beta}|q\rangle^3}\frac{\langle q\,c\rangle\,\langle q\,a\rangle\,[q|\alpha|q\rangle}{\langle a\,c\rangle\,[q|P_{\alpha\beta}|c\rangle} - 3\frac{\langle q\,d\rangle\,[q|P_{\alpha\beta}|d\rangle^2[q|\beta|q\rangle}{[q|P_{\alpha\beta}|q\rangle^2[q|P_{\alpha\beta}|c\rangle}\right)\right]$$

$$+ \mathcal{F}^{cde}_{sb} + \frac{i}{3\,\langle c\,d\rangle^2}\left(-\frac{[\beta\,e]^2\,[q\,e]}{[e\,\alpha]\,[\alpha\,q]} + [e|q|\alpha\rangle\frac{([e\,\beta]\,[\beta\,q]\,[k\,q] + [\beta\,q]^2\,[e\,k])}{[\alpha\,q]\,[k\,q]\,2k.q}\right) + \mathcal{O}(s_{\alpha\beta})\,.$$

$$(2.73)$$

We then need the non-adjacent current $\tau^{(1)}_{5:1}(\alpha^-,c^+,\beta^+,d^+,e^+)$, which we again calculate by starting with the amplitude and taking off-shell. This is a non-planar current as demonstrated in Figure 2.8 and it is easy enough to guess that this will not contribute double poles due to the non-planar way in which a and b would need to go collinear. While this would imply you would only need to perform standard recursion as there are only simple poles, we see there are no factorisations that contribute to some of these colour structures. This is interesting as it implies the contributions from these types of currents are entirely non-factorising and we can still view the residue as in (2.55) but with $c_{-2} = 0$.
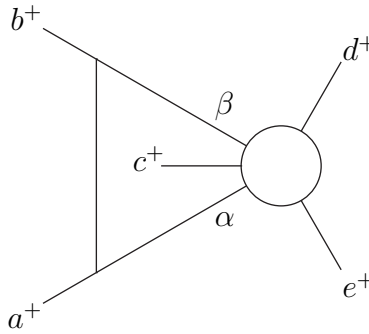
Figure 2.8: Diagram showing a non-planar current

The non-adjacent leading current is

$$\tau_{5:1}^{(1)}(\alpha^-, c^+, \beta^+, d^+, e^+) = \frac{1}{3} \frac{\langle \alpha\, q \rangle^2}{\langle \beta\, q \rangle^2} \left(\frac{\langle \alpha\, e \rangle\, [e\, c]}{\langle c\, \alpha \rangle\, \langle d\, e \rangle^2} - \frac{[e\, c]^3}{[e|\alpha|d][c|\alpha|d]} \right) + \mathcal{O}(\langle \alpha\, \beta \rangle). \qquad (2.74)$$

These currents must be integrated before extracting the rational pole. The non-adjacent case integrates to the simple form,

$$\int \frac{d^D \ell}{\ell^2 \alpha^2 \beta^2} \frac{1}{3} \frac{[a|\ell|q\rangle [b|\ell|q\rangle}{\langle a\, q \rangle\, \langle b\, q \rangle} \frac{\langle a\, e \rangle\, [e\, c]}{\langle c\, a \rangle\, \langle d\, e \rangle^2} \bigg|_{\mathbb{Q}} = \frac{1}{6} \frac{[e\, c]\, \langle a\, e \rangle\, [a\, b]}{\langle d\, e \rangle^2\, \langle c\, a \rangle\, \langle a\, b \rangle}, \qquad (2.75)$$

where the second term in eq. (2.74) has been dropped since it is a quadratic pentagon and does not contain any rational terms (this is because we need to at least reach scalar bubbles by integral reductions which cannot be done for a quadratic pentagon). The adjacent current needs a bit more work to integrate.

2.5.2 Integrating the Adjacent Current

Defining the helicity dependent integrated current as

$$C^{\lambda_\alpha, \lambda_\beta} = \int \mathrm{d}\Lambda_0(\alpha^{-\lambda_\alpha}, a^+, b^+, \beta^{-\lambda_\beta})\, \tau_{5:1}^{(1)}(\alpha^{\lambda_\alpha}, \beta^{\lambda_\beta}, c^+, d^+, e^+). \qquad (2.76)$$

we can split the it into five parts, picking for now the helicity configuration we have already discussed,

$$C^{-+} = C_{dp}^{-+} + C_{ap}^{-+} + C_{sf}^{-+} + C_{sl}^{-+} + C_{sk}^{-+} \qquad (2.77)$$

where C_{dp}^{-+} corresponds to integrating the $\mathcal{F}_{dp}$ part; C_{ap}^{-+} corresponds to integrating the "pole under the pole" piece from the double pole; C_{sf}^{-+} corresponds to integrating the $\mathcal{F}_{sb}$ piece and the C_{sl}^{-+} and C_{sk}^{-+} bits correspond to the last two terms in the current which come from the leftovers when deriving $\mathcal{F}_{sb}$ and the subtracted k^2 term when taking the current off-shell. We have defined this current for general q and so the C^{+-} is related by simple flip symmetries. The integrals are the same as in [67] except without the choice of $q \to b$ but we outline them here for completeness.

We will find that we can reduce all integrals to triangles. We make use of the identities for the general Feynman parametrisation

$$\frac{1}{D_1^{\nu_1} D_2^{\nu_2} \ldots D_n^{\nu_n}} = \frac{\Gamma[\sigma]}{\prod_{i=1}^n \Gamma(\nu_i)} \int_0^\infty \prod_{i=1}^n \mathrm{d}x_i x_i^{\nu_i - 1} \frac{\delta\left(1 - \sum_{j=1}^n x_j\right)}{[x_1 D_1 + x_2 D_2 + \ldots + x_n D_n]^\sigma} \qquad (2.78)$$

where $\sigma = \sum_{i=1}^n \nu_i$, and the loop momentum integral

$$\int \frac{\mathrm{d}^D \ell}{i \pi^{\frac{D}{2}}} \frac{\ell^{\mu_1} \ldots \ell^{\mu_{2m}}}{[\ell^2 - R^2 + i\delta]^\sigma} = (-1)^\sigma \left[(g^{\cdots})^{\otimes m}\right]^{\{\mu_1 \ldots \mu_{2m}\}} \left(-\frac{1}{2}\right)^m \frac{\Gamma[\sigma - m - \frac{D}{2}]}{\Gamma[\sigma]} (R^2 - i\delta)^{-\sigma + m + \frac{D}{2}}$$

$$(2.79)$$

where $\left[(g^{\cdots})^{\otimes m}\right]^{\{\mu_1 \ldots \mu_{2m}\}}$ means that μ_i are distributed over m copies of the metric tensor g in all possible ways. We have all cases of ℓ "capped" with a q, in other words $\ell|q\rangle$ and so the

only surviving integrals are scalar or ones with Feynman parameters in the numerator. This allows us to generalise the triangles, writing for the one-mass triangles

$$\mathcal{I}_{u,v}^{1\mathrm{m}} = \int_0^1 \mathrm{d}x_3 \int_0^{1-x_3} \mathrm{d}x_2 \frac{x_3^u x_2^v}{[x_2 x_3]^{1+\epsilon}} = \frac{1}{v-\epsilon} \int_0^1 \mathrm{d}x_3 x_3^{u-1-\epsilon}(1-x_3)^{v-\epsilon} = \frac{\Gamma[u-\epsilon]\Gamma[v-\epsilon]}{\Gamma[u+v+1-2\epsilon]}.$$

(2.80)

This is easy enough to expand and extract the rational contribution and similar results can be calculated for the two-mass triangles. The first piece is

$$\begin{aligned} C_{dp}^{-+} &= \int \frac{\mathrm{d}^D\ell}{\ell^2\alpha^2\beta^2} \frac{[a|\ell|q\rangle[b|\ell|q\rangle}{\langle a\,q\rangle\langle b\,q\rangle} \frac{1}{3} \frac{\langle q|\alpha\beta|q\rangle}{s_{\alpha\beta}} \frac{\langle e\,c\rangle[c\,e]^3}{\langle c\,d\rangle\langle d\,e\rangle[e|P_{\alpha\beta}|q\rangle[c|P_{\alpha\beta}|q\rangle} \\ &= -\frac{1}{18} \frac{[c\,e]^3\langle e\,c\rangle\langle q|ab|q\rangle}{\langle a\,b\rangle^2\langle c\,d\rangle\langle d\,e\rangle[e|P_{ab}|q\rangle[c|P_{ab}|q\rangle} \end{aligned}$$

(2.81)

and we see that both helicities have the same double pole contribution, giving

$$C_{dp}^{-+} + C_{dp}^{+-} = -\frac{1}{9} \frac{[c\,e]^3\langle e\,c\rangle\langle q|ab|q\rangle}{\langle a\,b\rangle^2\langle c\,d\rangle\langle d\,e\rangle[e|P_{ab}|q\rangle[c|P_{ab}|q\rangle}.$$

(2.82)

The second piece is

$$\begin{aligned} C_{ap}^{-+} = \int \frac{\mathrm{d}^D\ell}{\ell^2\alpha^2\beta^2} &\frac{[a|\ell|q\rangle[b|\ell|q\rangle}{\langle a\,q\rangle\langle b\,q\rangle\langle c\,d\rangle^2} \frac{1}{3} \\ &\times \left[\frac{\langle q|\alpha\beta|q\rangle\langle c\,d\rangle\langle e\,c\rangle[c\,e]^3}{\langle d\,e\rangle[e|P_{\alpha\beta}|q\rangle[c|P_{\alpha\beta}|q\rangle} \left(\frac{[q\,e]}{[c\,e][q|P_{\alpha\beta}|c\rangle} + \frac{[c|q|d\rangle}{[q|P_{\alpha\beta}|q\rangle[c|e|d\rangle} + \frac{[e|q|d\rangle}{[q|P_{\alpha\beta}|q\rangle[e|c|d\rangle} \right) \right. \\ &\left. + \frac{\langle a\,c\rangle[c|\beta|d\rangle}{\langle d\,e\rangle\langle e\,a\rangle} + \frac{\langle c\,e\rangle[d\,e]}{\langle d\,e\rangle^2} \left(\frac{[q|P_{\alpha\beta}|d\rangle^3}{[q|P_{\alpha\beta}|q\rangle^3} \frac{\langle q\,c\rangle\langle q\,a\rangle[q|\alpha|q\rangle}{\langle a\,c\rangle[q|P_{\alpha\beta}|c\rangle} - 3\frac{\langle q\,d\rangle[q|P_{\alpha\beta}|d\rangle^2[q|\beta|q\rangle}{[q|P_{\alpha\beta}|q\rangle^2[q|P_{\alpha\beta}|c\rangle} \right) \right] \end{aligned}$$

(2.83)

which are quartic and cubic triangles. All cases of loop momenta are contracted with the same axial gauge momentum q so only the scalar contributions of the Feynman parameter shifted integrals survive giving us

$$\begin{aligned} C_{ap}^{-+} = \frac{1}{18\langle c\,d\rangle^2} &\frac{[a\,b]}{\langle a\,b\rangle} \left[\frac{\langle q|ab|q\rangle\langle c\,d\rangle\langle e\,c\rangle[c\,e]^3}{\langle d\,e\rangle[e|P_{ab}|q\rangle[c|P_{ab}|q\rangle} \left(\frac{[q\,e]}{[c\,e][q|P_{ab}|c\rangle} + \frac{[c|q|d\rangle}{[q|P_{ab}|q\rangle[c|e|d\rangle} + \frac{[e|q|d\rangle}{[q|P_{ab}|q\rangle[e|c|d\rangle} \right) \right. \\ &\left. + \frac{\langle a\,c\rangle[c|a+2b|d\rangle}{\langle d\,e\rangle\langle e\,a\rangle} + \frac{\langle c\,e\rangle[d\,e]}{\langle d\,e\rangle^2} \left(\frac{[q|P_{ab}|d\rangle^3}{[q|P_{ab}|q\rangle^3} \frac{\langle q\,c\rangle\langle q\,a\rangle[q|2a+b|q\rangle}{\langle a\,c\rangle[q|P_{ab}|c\rangle} - 3\frac{\langle q\,d\rangle[q|P_{ab}|d\rangle^2[q|a+2b|q\rangle}{[q|P_{ab}|q\rangle^2[q|P_{ab}|c\rangle} \right) \right]. \end{aligned}$$

(2.84)

For the third piece we can make use of the factorisation to write the integral in terms of splitting functions. This is because if we write it as

$$\begin{aligned} C_{sf}^{-+} &= \int \frac{\mathrm{d}^D\ell}{\ell^2\alpha^2\beta^2} \frac{[a|\ell|q\rangle[b|\ell|q\rangle}{\langle a\,q\rangle\langle b\,q\rangle} \frac{\langle\beta\,q\rangle^2}{\langle\alpha\,q\rangle^2} \frac{\langle\alpha\,k\rangle[\beta\,q]^2}{[\alpha\,q][k\,q]} \frac{1}{s_{\alpha\beta}} A^{(1)}(k^+, c^+, d^+, e^+) \\ &= C_{tri}^{-+} \times \frac{1}{s_{\alpha\beta}} A^{(1)}(k^+, c^+, d^+, e^+), \end{aligned}$$

(2.85)

50

then the triangle integral

$$C_{tri}^{-+} = \int \frac{\mathrm{d}^D\ell}{\ell^2\alpha^2\beta^2} \frac{[a|\ell|q\rangle[b|\ell|q\rangle}{\langle a\,q\rangle\,\langle b\,q\rangle} \frac{\langle\beta\,q\rangle^2}{\langle\alpha\,q\rangle^2} \frac{\langle\alpha\,k\rangle\,[\beta\,q]^2}{[\alpha\,q]\,[k\,q]} \tag{2.86}$$

is closely related to the $(+,+,-)$ one-loop splitting function such that we find that

$$C_{sf}^{-+} + C_{sf}^{+-} = \frac{1}{3} \frac{[q\,a]\,[q\,b]\,[b\,a]}{[k\,q]^2} \times \frac{1}{s_{\alpha\beta}} A^{(1)}(k^+, c^+, d^+, e^+). \tag{2.87}$$

The fourth piece is

$$\begin{aligned}
C_{sl}^{-+} &= \int \frac{\mathrm{d}^D\ell}{\ell^2\alpha^2\beta^2} \frac{[a|\ell|q\rangle[b|\ell|q\rangle}{\langle a\,q\rangle\,\langle b\,q\rangle} \frac{\langle\beta\,q\rangle^2}{\langle\alpha\,q\rangle^2} \frac{1}{3} \frac{1}{\langle c\,d\rangle^2} \left(-\frac{[\beta\,e]^2\,[q\,e]}{[e\,\alpha]\,[\alpha\,q]} \right) \\
&= \frac{1}{3} \frac{1}{\langle c\,d\rangle^2} \frac{[q\,e]}{\langle a\,q\rangle\,\langle b\,q\rangle} \sum_{n=0,2} \int \frac{\mathrm{d}^D\ell}{\ell^2\alpha^2\beta^2} [a|\ell|q\rangle[b|\ell|q\rangle \frac{[e|\alpha|q\rangle^{1-n}[e|P_{ab}|q\rangle^n \kappa_n}{(\alpha+q)^2} + \mathcal{O}(\alpha^2)
\end{aligned} \tag{2.88}$$

where $\kappa_0 = \kappa_2 = 1$, $\kappa_1 = -2$ and we discard order α^2 terms that originate from promoting a term in the denominator to a propagator,

$$\frac{1}{2\alpha.q} - \frac{1}{(\alpha+q)^2} = \frac{\alpha^2}{2\alpha.q(\alpha+q)^2}, \tag{2.89}$$

because they do not contribute anything rational. The $n = 2$ contribution consists of a quadratic pentagon and so we can discard it. For the $n = 0, 1$ cases we can reduce the boxes to triangles using

$$[a|\ell|q\rangle[b|\ell|q\rangle = \frac{\alpha^2\langle q|b\ell|q\rangle + \beta^2\langle q|a\ell|q\rangle + \ell^2\langle .q|P_{ab}\beta|q\rangle}{\langle a\,b\rangle} \tag{2.90}$$

As before we only get contributions from the scalar part of the Feynman parameter shifted integrals, removing two of the triangles completely. The surviving triangle only gives rational pieces from the quadratic numerator leaving us with

$$C_{sl}^{-+} = -\frac{1}{6} \frac{[q\,e]\,[a\,b]}{\langle a\,b\rangle\,\langle c\,d\rangle^2} \frac{[e|b|q\rangle}{s_{bq}}. \tag{2.91}$$

Finally we have the C_{sk}^{-+} piece which uses the same leading order approximations as in previous cases to give

$$\begin{aligned}
C_{sk}^{-+} = \frac{1}{18} \frac{[a\,b]}{\langle a\,b\rangle} \frac{[e\,q]}{\langle c\,d\rangle^2\,2k.q} \Bigg(&\frac{1}{s_{bq}} (5[q|b|q\rangle[e|b|q\rangle + 3[q|a|q\rangle[e|b|q\rangle + [q|b|q\rangle[e|a|q\rangle) \\
&+ \frac{[e|P_{ab}|q\rangle}{2k.q} (5[q|b|q\rangle + 4[q|a|q\rangle) \Bigg).
\end{aligned} \tag{2.92}$$

At this stage we have not performed the Risager shift and so these results are quite general. We have been using (a, b, c, d, e) notation for the most part as these results can be coded up functionally and then summing over the contributions becomes a simple case of summing over arguments of these functions. The Risager shift then determines which diagrams we

need to sum over and we can then perform the shift and take the residue. The result has apparent q dependence with terms like s_{bq} present and once the full sum is done we can test the gauge independence by testing with different values of q and checking that we recover the manifest symmetries act as strong checks.

Having summed over all channels excited by the Risager shift, we obtain the full two-loop colour decomposition. The results are presented in the compact forms

$$R_{5:1}^{(2)}(a^+, b^+, c^+, d^+, e^+) = \frac{1}{9} \frac{1}{\langle a\,b\rangle \langle b\,c\rangle \langle c\,d\rangle \langle d\,e\rangle \langle e\,a\rangle} \sum_{\mathcal{P}_{5:1}} \left(\frac{\mathrm{tr}_+^2[deab]}{s_{de}s_{ab}} + 5s_{ab}s_{bc} + s_{ab}s_{cd} \right), \quad (2.93)$$

$$R_{5:3}^{(2)}(a^+, b^+; c^+, d^+, e^+) = \frac{2}{3} \frac{1}{\langle a\,b\rangle \langle b\,a\rangle \langle c\,d\rangle \langle d\,e\rangle \langle e\,c\rangle} \sum_{\mathcal{P}_{5:3}} \left(\frac{\mathrm{tr}_-[acde]\mathrm{tr}_-[ecba]}{s_{ae}s_{cd}} + \frac{3}{2}s_{ab}^2 \right) \quad (2.94)$$

and

$$\begin{aligned}
R_{5:1B}^{(2)}(a^+, b^+, c^+, d^+, e^+) = 2\epsilon\,(a, b, c, d)\Big(&\mathrm{C_{PT}}(b, c, a, d, e) \\
&+ \mathrm{C_{PT}}(a, b, e, c, d) + \mathrm{C_{PT}}(a, d, b, c, e) \\
&+ \mathrm{C_{PT}}(a, b, d, e, c) + \mathrm{C_{PT}}(a, c, d, b, e) \Big) \quad (2.95)
\end{aligned}$$

where

$$\mathrm{C_{PT}}(a, b, c, d, e) = \frac{1}{\langle a\,b\rangle \langle b\,c\rangle \langle c\,d\rangle \langle d\,e\rangle \langle e\,a\rangle}, \quad (2.96)$$

is the Parke-Taylor denominator for five gluons. These expressions are valid for both $U(N_c)$ and $SU(N_c)$ gauge groups and are remarkably compact. The first two results were originally presented in [87] but the result for $R_{5:1B}^{(2)}$ had previously been left to be calculated via (2.19). Clearly the result presented here is more efficient and indeed provided the first clue as to an n-point result for this colour structure but we will cover that in Chapter 4.

In this chapter, we have demonstrated how the full colour all-plus five-point amplitude may be computed in simple forms. We computed all the colour components directly and used colour relations between them as checks. While these results were already calculated, our methodology obtained these results without the need to determine two-loop non-planar integrals. This led to quick and compact forms of the polylogarithmic pieces and pushed the calculational bottleneck to augmented recursion, which compared to calculating two-loop non-planar integrals is a considerably more simple problem.

Augmented recursion produces relatively large analytic functions in the external momenta but also in the axial gauge vector q. The final result is independent of q and so one might imagine compact, analytic forms of the results exist, and indeed for the five-point amplitude we had the results of [87] to numerically compare with. The next chapter's results were new as of their publishing in [71], and so we needed to perform some functional reconstruction methods to find a compact analytic form. The following chapter therefore addresses this problem as we calculate the two-loop, six-point, full-colour, all-plus helicity amplitude.

Chapter 3

Colour Dressed Unitarity and Recursion: a Six Point Amplitude

3.1 Introduction

In the previous chapter we extended four-dimensional unitarity and augmented recursion to a full colour setting. We discussed n-point relations where appropriate but largely kept the discussion to five-point. With an eye on improved efficiency with higher multiplicity, we will start to introduce n-point discussions in this chapter but will continue to largely focus on a specific and new calculation, the six-point, full colour amplitude.

The six-point, two-loop colour decomposition is given by

$$
\begin{aligned}
\mathcal{A}_6^{(2)}(a,b,c,d,e,f) = N_c^2 & \sum_{S_6/\mathcal{P}_{6:1}} \text{Tr}[abcdef] A_{6:1}^{(2)}(a,b,c,d,e,f) + \\
& N_c \Bigg[\sum_{S_6/\mathcal{P}_{6:2}} \text{Tr}[a]\,\text{Tr}[bcdef] A_{6:2}^{(2)}(a;b,c,d,e,f) \\
& + \sum_{S_6/\mathcal{P}_{6:3}} \text{Tr}[ab]\,\text{Tr}[cdef] A_{6:3}^{(2)}(a,b;c,d,e,f) \\
& + \sum_{S_6/\mathcal{P}_{6:4}} \text{Tr}[abc]\,\text{Tr}[def] A_{6:4}^{(2)}(a,b,c;d,e,f) \Bigg] \\
& + \sum_{S_6/\mathcal{P}_{6:1}} \text{Tr}[abcdef] A_{6:1,B}^{(2)}(a,b,c,d,e,f) \\
& + \sum_{S_6/\mathcal{P}_{6:1,1}} \text{Tr}[a]\,\text{Tr}[b]\,\text{Tr}[cdef] A_{6:1,1}^{(2)}(a;b;c,d,e,f) \\
& + \sum_{S_6/\mathcal{P}_{6:1,2}} \text{Tr}[a]\,\text{Tr}[bc]\,\text{Tr}[def] A_{6:1,2}^{(2)}(a;b,c;d,e,f) \\
& + \sum_{S_6/\mathcal{P}_{6:2,2}} \text{Tr}[ab]\,\text{Tr}[cd]\,\text{Tr}[ef] A_{6:2,2}^{(2)}(a,b;c,d;e,f)
\end{aligned}
\tag{3.1}
$$

where we see new structures of $A_{6:4}^{(2)}$ and $A_{6:2,2}^{(2)}$, both of which are $\text{SU}(N_c)$ amplitudes. For the five-point amplitude we showed that $A_{5:1,2}^{(2)} = 0$ via a decoupling identity but this was

a five-point result that depended on the flip symmetry. We can derive n-point decoupling identities by setting one or more legs to being U(1), leaving us with

$$A_{n:2}^{(2)}(1; 2, 3, \cdots, n) + \sum_{\sigma_1} A_{n:1}^{(2)}(\sigma_1) = 0,$$

$$A_{n:3}^{(2)}(1, 2; 3, 4, \dots, n) + A_{n:1,1}^{(2)}(1; 2; 3, 4, \dots, n) - \sum_{\sigma \in COP\{2,1\}\{3,\dots,n\}} A_{n:1}^{(2)}(\sigma) = 0,$$

$$A_{n:1,s}^{(2)}(1; 2, 3, \dots, s+1; s+2, \dots, n) + \sum_{\sigma_2} A_{n:s+2}^{(2)}(\sigma_2; s+2, \dots, n) + \sum_{\sigma_3} A_{n:s+1}^{(2)}(2, \dots, s+1; \sigma_3) = 0,$$

(3.2)

where $\sigma_{1,2,3}$ are the sums over the different ways of inserting 1 into $\{2, 3, \dots, n\}$, $\{2, 3, \dots, s+1\}$ and $\{s+2, \dots, n\}$ respectively. We also have the tree-like (2.18) for the $A_{n:1B}^{(2)}$ as has already been discussed. These again provide checks on our results as colour dressing will recover the full colour decomposition and using U(N_c) trace identities will allow us to calculate the U(1) amplitudes and check the SU(N_c) amplitudes satisfy the decoupling relations with them. These are highly non-trivial but we will later take collinear limits as further checks.

3.2 Unitarity

In Chapter 2 we discussed the simplification of the two-loop problem to a pseudo one-loop calculation with one of the loop momentum already dealt with in the form of loop inserts. The validity of this approach was checked by performing triple cuts which isolated the genuine two-loop diagrams and we found these cuts to all vanish. This was an n-point check and so the methodology should continue to the six-point calculation.

We also presented new and compact forms of n-point, one-loop, subleading in colour amplitudes for the all-plus configuration. Indeed, for $A_{n:r}^{(1)}$ with $r > 2$ we see that this is remarkably only a single term. This makes full colour inserts into the scalar boxes, triangles and bubbles of (1.108) scale well with higher multiplicity.

The only added complication at six-point and higher is that of two-mass boxes. For four-dimensional unitarity we need alternating MHV and $\overline{\text{MHV}}$ trees as all other helicity configurations vanish on the cut. This eliminates any two-mass hard boxes and so we are left with two-mass easy boxes and one-mass boxes. We will now calculate the coefficients of the boxes in the finite polylogarithmic pieces $F_{6:c}^{(2)}$. As a reminder this is the finite, cut constructible piece after decomposing the amplitude into

$$A_{6:c}^{(2)} = U_{6:c}^{(2)} + F_{6:c}^{(2)} + R_{6:c}^{(2)},$$ (3.3)

where $U_{6:c}$ are the divergent terms given by (1.106) and $R_{6:c}^{(2)}$ are the purely rational terms which we recover via augmented recursion. The contributions to $F_{6:c}^{(2)}$ we will consider are given in Figure 3.1.
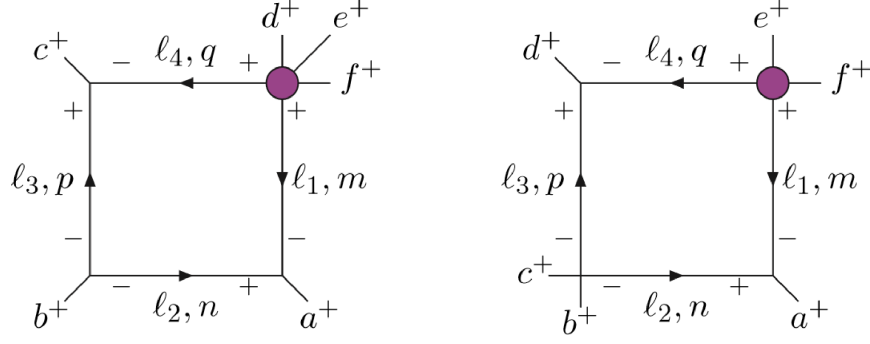
Figure 3.1: The labelling and internal helicities of the quadruple cut. The loop insert is given by the purple circle.

3.2.1 One-Mass Box Coefficients

Recalling that we know the n-point solution to the quadruple cuts on a one-mass box to be

$$\ell_2 = -\frac{\langle b\,a\rangle}{\langle c\,a\rangle}\bar{\lambda}_b\lambda_c, \qquad \ell_3 = -\frac{\langle b\,c\rangle}{\langle a\,c\rangle}\bar{\lambda}_b\lambda_a\,,$$

$$\ell_1 = \frac{\langle a\,c\rangle\,\bar{\lambda}_a + \langle b\,c\rangle\,\bar{\lambda}_b}{\langle a\,c\rangle}\lambda_a, \quad \ell_4 = \frac{\langle c\,a\rangle\,\bar{\lambda}_c + \langle b\,a\rangle\,\bar{\lambda}_b}{\langle c\,a\rangle}\lambda_c\,. \tag{3.4}$$

for the configuration in Figure 2.5, we can calculate the full colour coefficients of the one-mass boxes. We first need to find the independent solutions from the five-point one-loop corner. The tree corners combine to give

$$A_3^{(0)}(a^+, \ell_2^+, \ell_1^-)A_3^{(0)}(\ell_3^-, \ell_2^-, b^+)A_3^{(0)}(\ell_3^+, c^+, \ell_4^-)$$

$$= \frac{[\ell_2\,a]^3}{[\ell_1\,a]\,[\ell_2\,\ell_1]}\frac{[c\,\ell_3]^3}{[c\,\ell_4]\,[\ell_4\,\ell_3]}\frac{\langle\ell_3\,\ell_2\rangle^3}{\langle\ell_2\,b\rangle\,\langle b\,\ell_3\rangle}$$

$$= [b|ac|b] \tag{3.5}$$

which is antisymmetric in a and c so any two terms that are related by $\ell_1 \leftrightarrow \ell_4$ in the one-loop corner are simply related by $-\{a \leftrightarrow c\}$ in the full coefficient, recalling we are inserting the full colour, one-loop amplitude. This is not too surprising as this is just a relabelling of $\ell_1 \to \ell_4$ and $a \to c$ which is fine for the fully cross-symmetric all-plus helicity configuration.

We therefore only need

$$A_{5:1}^{(1)}(\ell_1^+, \ell_4^+, d, e, f)\,, \qquad A_{5:1}^{(1)}(\ell_1^+, d, \ell_4^+, e, f)\,, \quad A_{5:2}^{(1)}(d; \ell_1^+, \ell_4^+, e, f)\,, \qquad A_{5:2}^{(1)}(d; \ell_1^+, e, \ell_4^+, f)$$

$$A_{5:3}^{(1)}(\ell_1^+, \ell_4^+; d, e, f)\,, \qquad A_{5:3}^{(1)}(\ell_1^+, d; \ell_4^+, e, f)\,, \qquad A_{5:3}^{(1)}(d, e; \ell_1^+, \ell_4^+, f). \tag{3.6}$$

We would also expect $A_{5:2}^{(1)}(\ell_1^+; \ell_4^+, d, e, f)$ but these all cancel in the full colour sum due to the antisymmetry of the $A_{5:2}^{(1)}$ amplitude, but we would expect at seven-point to see these

contributing as the $A_{6:2}^{(1)}$ are symmetric. Pressing on we define seven functions

$$C_a^{1m}(a,b,c;d,e,f) = A_{5:1}^{(1)}(\ell_1^+,\ell_4^+,d,e,f)V(a^+,b^+,c^+)\mathrm{F}^{1m}(s_{ab},s_{bc},t_{def})$$
$$C_b^{1m}(a,b,c;d,e,f) = A_{5:1}^{(1)}(\ell_1^+,d,\ell_4^+,e,f)V(a^+,b^+,c^+)\mathrm{F}^{1m}(s_{ab},s_{bc},t_{def})$$
$$C_c^{1m}(a,b,c;d,e,f) = A_{5:2}^{(1)}(d;\ell_1^+,\ell_4^+,e,f)V(a^+,b^+,c^+)\mathrm{F}^{1m}(s_{ab},s_{bc},t_{def})$$
$$C_d^{1m}(a,b,c;d,e,f) = A_{5:2}^{(1)}(d;\ell_1^+,e,\ell_4^+,f)V(a^+,b^+,c^+)\mathrm{F}^{1m}(s_{ab},s_{bc},t_{def})$$
$$C_e^{1m}(a,b,c;d,e,f) = A_{5:3}^{(1)}(\ell_1^+,\ell_4^+;d,e,f)V(a^+,b^+,c^+)\mathrm{F}^{1m}(s_{ab},s_{bc},t_{def})$$
$$C_f^{1m}(a,b,c;d,e,f) = A_{5:3}^{(1)}(\ell_1^+,d;\ell_4^+,e,f)V(a^+,b^+,c^+)\mathrm{F}^{1m}(s_{ab},s_{bc},t_{def})$$
$$C_g^{1m}(a,b,c;d,e,f) = A_{5:3}^{(1)}(d,e;\ell_1^+,\ell_4^+,f)V(a^+,b^+,c^+)\mathrm{F}^{1m}(s_{ab},s_{bc},t_{def}).$$

with the tree combinations absorbing the dimensional part of the box function

$$V(a^+,b^+,c^+) = \frac{-2[b|ac|b]}{s_{ab}s_{bc}}. \tag{3.7}$$

and F^{1m} being the dimensionless contribution (2.29). The cut solutions can then be inserted to give the basis functions for the one-mass box contributions,

$$C_a^{1m}(a,b,c;d,e,f) = \frac{1}{3}\frac{t_{abc}\langle c|dP_{bc}|a\rangle + \langle c|defP_{de}|a\rangle + \langle a|fP_{de}|c\rangle s_{ef}}{\langle a\,b\rangle\,\langle b\,c\rangle\,\langle c\,a\rangle\,\langle c\,d\rangle\,\langle d\,e\rangle\,\langle e\,f\rangle\,\langle f\,a\rangle} \times \mathrm{F}^{1m}(s_{ab},s_{bc},t_{def})$$

$$C_b^{1m}(a,b,c;d,e,f) = \frac{1}{3}\frac{\langle a|dP_{ab}|c\rangle\langle c|dP_{bc}|a\rangle + \langle c\,a\rangle\,(s_{ef}\langle a|fP_{ab}|c\rangle - \langle a|P_{bc}\,efd|c\rangle)}{\langle a\,b\rangle\,\langle b\,c\rangle\,\langle c\,a\rangle\,\langle a\,d\rangle\,\langle d\,c\rangle\,\langle c\,e\rangle\,\langle e\,f\rangle\,\langle f\,a\rangle}$$
$$\times\,\mathrm{F}^{1m}(s_{ab},s_{bc},t_{def})$$

$$C_c^{1m}(a,b,c;d,e,f) = -\frac{\langle c\,a\rangle\,[d|ef|d] - [d|P_{abc}|c\rangle[d|P_{abc}|a\rangle}{\langle a\,b\rangle\,\langle b\,c\rangle\,\langle c\,a\rangle\,\langle c\,e\rangle\,\langle e\,f\rangle\,\langle f\,a\rangle}\times\mathrm{F}^{1m}(s_{ab},s_{bc},t_{def})$$

$$C_d^{1m}(a,b,c;d,e,f) = \frac{[d|P_{abc}|a\rangle[d|f|c\rangle - [d|P_{abc}|c\rangle[d|e|a\rangle}{\langle a\,b\rangle\,\langle b\,c\rangle\,\langle a\,e\rangle\,\langle e\,c\rangle\,\langle c\,f\rangle\,\langle f\,a\rangle}\times\mathrm{F}^{1m}(s_{ab},s_{bc},t_{def})$$

$$C_e^{1m}(a,b,c;d,e,f) = -2\frac{t_{abc}^2}{\langle a\,b\rangle\,\langle b\,c\rangle\,\langle c\,a\rangle\,\langle d\,e\rangle\,\langle e\,f\rangle\,\langle f\,d\rangle}\times\mathrm{F}^{1m}(s_{ab},s_{bc},t_{def})$$

$$C_f^{1m}(a,b,c;d,e,f) = -2\frac{[d|P_{abc}|c\rangle^2}{\langle a\,b\rangle\,\langle b\,c\rangle\,\langle c\,a\rangle\,\langle c\,e\rangle\,\langle e\,f\rangle\,\langle f\,c\rangle}\times\mathrm{F}^{1m}(s_{ab},s_{bc},t_{def})$$

$$C_g^{1m}(a,b,c;d,e,f) = -2\frac{[d\,e]^2\,\langle c\,a\rangle^2}{\langle a\,b\rangle\,\langle b\,c\rangle\,\langle c\,a\rangle\,\langle a\,c\rangle\,\langle c\,f\rangle\,\langle f\,a\rangle}\times\mathrm{F}^{1m}(s_{ab},s_{bc},t_{def}). \tag{3.8}$$

We next need the two-mass box coefficients.

3.2.2 Two-Mass Boxes Cut Solutions

The two-mass boxes have more complicated loop-momentum solutions. We will start with the specifically six point RHS diagram of Figure 3.1 before generalising to n-point. We have that

$$
\begin{aligned}
\ell_2 + \ell_1 &= a, \\
\ell_2 + \ell_3 &= -P_{bc}, \\
\ell_3 + \ell_4 &= d, \\
\ell_4 + \ell_1 &= -P_{ef}.
\end{aligned}
\tag{3.9}
$$

We first consider ℓ_2

$$
\begin{aligned}
\ell_2^2 &= [\ell_1\, a]\, \langle \ell_1\, a \rangle = 0, \\
\lambda_{\ell_1} &= \alpha_1 \lambda_a,
\end{aligned}
\tag{3.10}
$$

and then ℓ_4 to find α_1 in terms of $\tilde{\lambda}_{\ell_1}$,

$$
\begin{aligned}
\ell_4^2 &\to \alpha_1 [\ell_1 | P_{ef} | a \rangle = -s_{ef}, \\
\alpha_1 &= -\frac{s_{ef}}{[\ell_1 | P_{ef} | a \rangle},
\end{aligned}
\tag{3.11}
$$

which we use for ℓ_3^2,

$$
\ell_3^2 \to -s_{ef} [\ell_1 | P_{bc} | a \rangle = t_{abc} [\ell_1 | P_{ef} | a \rangle,
\tag{3.12}
$$

and then using momentum conservation and a Schouten identity

$$
\begin{aligned}
s_{ef} [\ell_1 | d | a \rangle &= (t_{def} - s_{ef})[\ell_1 | P_{ef} | a \rangle, \\
&= [d | P_{ef} | d \rangle [\ell_1 | P_{ef} | a \rangle = s_{ef} [\ell_1 | d | a \rangle + [d | P_{ef} | a \rangle [\ell_1 | P_{ef} | d \rangle, \\
&\to [d] | P_{ef} | a \rangle [\ell_1 | P_{ef} | d \rangle = 0, \\
&\to [\ell_1 | e | d \rangle + [\ell_1 | f | d \rangle = 0, \\
\tilde{\lambda}_{\ell_1} &= C_1 \left(\frac{\langle f\, d \rangle\, \tilde{\lambda}_f + \langle e\, d \rangle\, \tilde{\lambda}_e}{\langle e\, d \rangle\, \langle f\, d \rangle} \right),
\end{aligned}
\tag{3.13}
$$

where C_1 is some new scale factor that will contain helicity information. We can then write

$$
\begin{aligned}
\alpha_1 &= -\langle e\, d \rangle\, \langle f\, d \rangle\, \frac{s_{ef}}{C_1(\langle f\, d \rangle\, [f | e | a \rangle + \langle e\, d \rangle\, [e | f | a \rangle)} \\
&= \frac{\langle e\, d \rangle\, \langle f\, d \rangle}{C_1 \langle d\, a \rangle},
\end{aligned}
\tag{3.14}
$$

where we have used a Schouten identity in the denominator and we see that the scales will cancel in ℓ_1. Writing $\langle x\, y \rangle\, \tilde{\lambda}_x = |x|y\rangle$, we therefore have the solutions

$$
\ell_1 = \frac{|P_{ef}|d\rangle}{\langle d\, a \rangle} \lambda_a,
\tag{3.15}
$$

57

$$\ell_2 = \frac{|P_{bc}|d\rangle}{\langle d\,a\rangle}\lambda_a, \tag{3.16}$$

$$\ell_3 = \frac{|P_{bc}|a\rangle}{\langle a\,d\rangle}\lambda_d, \tag{3.17}$$

$$\ell_4 = \frac{|P_{ef}|a\rangle}{\langle a\,d\rangle}\lambda_d. \tag{3.18}$$

We can test these satisfy momentum conservation as a quick check

$$\ell_1 + \ell_2 = \frac{|P_{bcef}|d\rangle}{\langle d\,a\rangle}\lambda_a = -\frac{\langle a\,d\rangle}{\langle d\,a\rangle}\tilde{\lambda}_a\lambda_a = a \tag{3.19}$$

$$\ell_3 + \ell_4 = \frac{|P_{bcef}|a\rangle}{\langle a\,d\rangle}\lambda_d = -\frac{\langle d\,a\rangle}{\langle a\,d\rangle}\tilde{\lambda}_d\lambda_d = d \tag{3.20}$$

$$\ell_1 + \ell_4 = \tilde{\lambda}_f\left(\frac{\langle f\,d\rangle\,\lambda_a + \langle a\,f\rangle\,\lambda_d}{\langle d\,a\rangle}\right) + \tilde{\lambda}_e\left(\frac{\langle e\,d\rangle\,\lambda_a + \langle a\,e\rangle\,\lambda_d}{\langle d\,a\rangle}\right) = -P_{ef} \tag{3.21}$$

$$\ell_2 + \ell_3 = \tilde{\lambda}_b\left(\frac{\langle b\,d\rangle\,\lambda_a + \langle a\,b\rangle\,\lambda_d}{\langle d\,a\rangle}\right) + \tilde{\lambda}_c\left(\frac{\langle c\,d\rangle\,\lambda_a + \langle a\,c\rangle\,\lambda_d}{\langle d\,a\rangle}\right) = -P_{bc} \tag{3.22}$$

This generalises to an n-point box for the configuration in Figure 3.2,
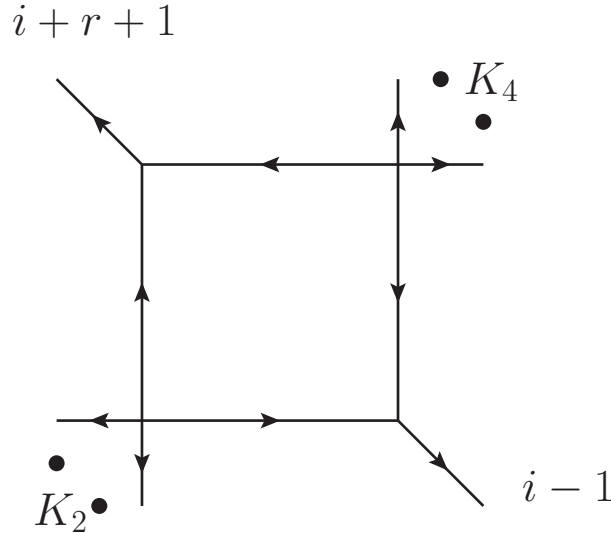
Figure 3.2: An n-point two-mass-easy box with $K_2 = p_i + \ldots + p_{i+r}$ and $K_4 = p_{i+r+2} + \ldots + p_{i-2}$ where the momentum labelling is modulo n.

$$\ell_1 = \frac{|K_4|i+r+1\rangle}{\langle (i+r+1)\,(i-1)\rangle}\lambda_{i-1},$$

$$\ell_2 = \frac{|K_2|i+r+1\rangle}{\langle (i+r+1)\,(i-1)\rangle}\lambda_{i-1},$$

$$\ell_3 = \frac{|K_2|i-1\rangle}{\langle (i-1)\,(i+r+1)\rangle}\lambda_{i+r+1},$$

$$\ell_4 = \frac{|K_4|i-1\rangle}{\langle (i-1)\,(i+r+1)\rangle}\lambda_{i+r+1}. \tag{3.23}$$

The two four-point tree amplitudes are related by

$$A_4^{(0)}(a^-,b^-,c^+,d^+) = \frac{s_{ac}}{s_{ab}}A_4^{(0)}(a^-,c^+,b^-,d^+) \tag{3.24}$$

and we therefore have the two box coefficients,

$$C_a^{2\mathrm{m}}(a;b,c;d;e,f) = \frac{1}{3}\frac{[e\,f]^2}{\langle a\,b\rangle\,\langle b\,c\rangle\,\langle c\,d\rangle\,\langle d\,a\rangle} \times \mathrm{F}^{2m}(t_{abc},t_{bcd},s_{bc},s_{ef})$$

$$C_b^{2\mathrm{m}}(a;b,c;d;e,f) = \frac{1}{3}\frac{[e\,f]^2}{\langle a\,b\rangle\,\langle b\,d\rangle\,\langle d\,c\rangle\,\langle c\,a\rangle} \times \mathrm{F}^{2m}(t_{abc},t_{bcd},s_{bc},s_{ef}). \tag{3.25}$$

The procedure is to then colour dress each corner, use $\mathrm{U}(N_c)$ trace identities to derive the trace structures for the external momentum, sum over all kinematically distinct diagrams where for full colour the order of the external legs on each corner does not matter as all permutations are captured in the colour decomposition. One can keep this in general form, tagging every trace structure with the associated amplitude label and arguments before substituting the results in. We can then look at the full colour decomposition and find the manifest symmetries by looking at the tags, bring the result into a manifestly symmetric sum of the above coefficients and finally substitute in the results of these coefficients. This allows us to then write the solution for the full colour finite polylogarithmic pieces as follows:

$$F_{6:1}^{(2)}(a,b,c,d,e,f) = \sum_{\mathcal{P}_{6:1}}\left(C_a^{1\mathrm{m}}(a,b,c;d,e,f) + C_a^{2\mathrm{m}}(a;b,c;d;e,f)\right), \tag{3.26}$$

$$F_{6:3}^{(2)}(a,b;c,d,e,f)$$

$$= \sum_{\mathcal{P}_{6:3}}\Bigg(C_a^{1\mathrm{m}}(a,b,c;d,e,f) + C_a^{1\mathrm{m}}(a,c,b;d,e,f) + C_a^{1\mathrm{m}}(c,a,b;d,e,f)$$

$$- C_b^{1\mathrm{m}}(a,c,d;b,e,f) - C_b^{1\mathrm{m}}(c,a,d;b,e,f) - C_b^{1\mathrm{m}}(c,d,a;b,e,f)$$

$$- C_b^{1\mathrm{m}}(d,e,f;c,a,b) + \frac{1}{2}C_g^{1\mathrm{m}}(d,e,f;a,b,c)$$

$$+ 4C_a^{2\mathrm{m}}(c;d,e;f;a,b) + C_a^{2\mathrm{m}}(b;e,f;a;c,d) + C_a^{2\mathrm{m}}(f;b,a;e;c,d)$$

$$- C_b^{2\mathrm{m}}(e;f,a;b;c,d) - C_b^{2\mathrm{m}}(f;e,b;a;c,d)$$

$$+ C_b^{2\mathrm{m}}(d;e,b;f;a,c) - C_a^{2\mathrm{m}}(b;d,e;f;a,c) - C_a^{2\mathrm{m}}(d;e,f;b;a,c)\Bigg), \tag{3.27}$$

$$F_{6:4}^{(2)}(a,b,c;d,e,f)$$

$$
\begin{aligned}
= \sum_{\mathcal{P}_{6:4}} \Bigg(& \frac{1}{3}C_e^{1\mathrm{m}}(a,b,c;d,e,f) - C_a^{1\mathrm{m}}(a,b,c;f,e,d) \\
& + C_b^{1\mathrm{m}}(d,b,a;c,e,f) + C_b^{1\mathrm{m}}(b,d,a;c,e,f) + C_b^{1\mathrm{m}}(b,a,d;c,e,f) \\
& + C_a^{2\mathrm{m}}(a;f,e;b;c,d) - \frac{1}{2}C_b^{2\mathrm{m}}(a;b,f;e;c,d) - \frac{1}{2}C_b^{2\mathrm{m}}(f;a,e;b;c,d) \\
& + C_b^{2\mathrm{m}}(a;b,d;c;e,f) - C_a^{2\mathrm{m}}(a;b,c;d;e,f) - C_a^{2\mathrm{m}}(d;a,b;c;e,f) \Bigg), \quad (3.28)
\end{aligned}
$$

$$F_{6:2,2}^{(2)}(a,b;c,d;e,f)$$

$$
\begin{aligned}
= \frac{1}{2} \sum_{\mathcal{P}_{6:2,2}} \Bigg(& C_g^{1\mathrm{m}}(a,b,c;e,f,d) + C_g^{1\mathrm{m}}(b,a,c;e,f,d) + C_g^{1\mathrm{m}}(b,c,a;e,f,d) \\
& + 6C_a^{2\mathrm{m}}(d;a,b;c;e,f) - 3C_b^{2\mathrm{m}}(a;b,c;d;e,f) - 3C_b^{2\mathrm{m}}(b;a,d;c;e,f) \Bigg),
\end{aligned}
$$
$$(3.29)$$

$$F_{6:1B}^{(2)}(a,b,c,d,e,f)$$

$$
\begin{aligned}
= \sum_{\mathcal{P}_{6:1}} \Bigg(& C_f^{1\mathrm{m}}(a,b,c;f,d,e) - C_f^{1\mathrm{m}}(c,b,a;d,e,f,) \\
& + C_f^{1\mathrm{m}}(b,f,e;a,c,d) + C_f^{1\mathrm{m}}(f,b,e;a,c,d) + C_f^{1\mathrm{m}}(f,e,b;a,c,d) \\
& - C_f^{1\mathrm{m}}(f,b,c;a,d,e) - C_f^{1\mathrm{m}}(b,f,c;a,d,e) - C_f^{1\mathrm{m}}(b,c,f;a,d,e) \\
& + 6C_b^{2\mathrm{m}}(f;b,e;d;a,c) - 6C_a^{2\mathrm{m}}(b;f,e;d;a,c) - 6C_a^{2\mathrm{m}}(f;e,d;b;a,c) \\
& + 6C_a^{2\mathrm{m}}(a;b,c;d;e,f) + 3C_a^{2\mathrm{m}}(f;b,c;e;a,d) + 3C_a^{2\mathrm{m}}(c;e,f;b;a,d) \\
& - 3C_b^{2\mathrm{m}}(b;c,f;e;a,d) - 3C_b^{2\mathrm{m}}(c;e,b;f;a,d) \Bigg). \quad (3.30)
\end{aligned}
$$

We also wish to test these results by ensuring they satisfy the decoupling identities (2.17). We therefore present the $U(N_c)$ pieces

$$F_{6:2}^{(2)}(a;b,c,d,e,f)$$

$$
\begin{aligned}
= \sum_{\mathcal{P}_{6:2}} \Bigg(& C_b^{1\mathrm{m}}(b,c,d;a,e,f) + C_c^{1\mathrm{m}}(b,c,d;a,e,f) - C_a^{1\mathrm{m}}(a,b,c;d,e,f) \\
& - C_a^{1\mathrm{m}}(b,a,c;d,e,f) - C_a^{1\mathrm{m}}(b,c,a;d,e,f) - 2C_a^{2\mathrm{m}}(b;c,d;e;f,a) \\
& + C_b^{2\mathrm{m}}(b;c,a;d;e,f) - C_a^{2\mathrm{m}}(a;b,c;d;e,f) - C_a^{2\mathrm{m}}(b;c,d;a;e,f) \Bigg), \quad (3.31)
\end{aligned}
$$

$$F_{6:1,1}^{(2)}(a;b;c,d,e,f)$$

$$= \sum_{\mathcal{P}_{6:1,1}} \Bigg(C_d^{\mathrm{1m}}(c,d,e;a,b,f) - 3C_a^{\mathrm{2m}}(c;d,e;f;a,b)$$

$$- C_c^{\mathrm{1m}}(b,c,d;a,e,f) - C_c^{\mathrm{1m}}(c,b,d;a,e,f) - C_c^{\mathrm{1m}}(c,d,b;a,e,f)$$

$$+ 3C_a^{\mathrm{2m}}(b;c,d;e;f,a) + 3C_a^{\mathrm{2m}}(c;d,e;b;f,a) - 3C_b^{\mathrm{2m}}(c;d,b;e;f,a) \Bigg),$$

$$(3.32)$$

and

$$F_{6:1,2}^{(2)}(a;b,c;d,e,f)$$

$$= \sum_{\mathcal{P}_{6:1,2}} \Bigg(\frac{1}{2}(C_c^{\mathrm{1m}}(c,b,d;a,e,f) + C_c^{\mathrm{1m}}(b,c,d;a,e,f) + C_c^{\mathrm{1m}}(b,d,c;a,e,f))$$

$$+ \frac{1}{2}(C_c^{\mathrm{1m}}(c,b,d;a,f,e) + C_c^{\mathrm{1m}}(b,c,d;a,f,e) + C_c^{\mathrm{1m}}(b,d,c;a,f,e))$$

$$- \frac{1}{2}(C_g^{\mathrm{1m}}(a,d,e;b,c,f) + C_g^{\mathrm{1m}}(d,a,e;b,c,f) + C_g^{\mathrm{1m}}(d,e,a;b,c,f))$$

$$- \frac{1}{2}C_g^{\mathrm{1m}}(d,e,f;b,c,a) - C_c^{\mathrm{1m}}(d,e,f;a,b,c)$$

$$- C_d^{\mathrm{1m}}(b,d,e;a,c,f) - C_d^{\mathrm{1m}}(d,b,e;a,c,f) - C_d^{\mathrm{1m}}(d,e,b;a,c,f)$$

$$+ 3C_b^{\mathrm{2m}}(c;b,f;e;a,d) + 3C_b^{\mathrm{2m}}(b;e,c;f;a,d)$$

$$- 3C_a^{\mathrm{2m}}(b;e,f;c;a,d) - 3C_a^{\mathrm{2m}}(e;b,c;f;a,d)$$

$$+ 3C_a^{\mathrm{2m}}(c;d,e;f;a,b) + 3C_a^{\mathrm{2m}}(d;e,f;c;a,b) - 3C_b^{\mathrm{2m}}(d;e,c;f;a,b)$$

$$- 3C_a^{\mathrm{2m}}(a;d,e;f;b,c) - 3C_a^{\mathrm{2m}}(d;e,f;a;b,c) + 3C_b^{\mathrm{2m}}(d;e,a;f;b,c) \Bigg)$$

$$(3.33)$$

and have confirmed that they do satisfy the identities. Given these results are new we wanted to check collinear limits explicitly. Interestingly, these six-point coefficients are conformally invariant: a feature noticed for the five-point all-plus amplitude in [93].

3.3   Collinear Limits

The IR and UV behaviour of this amplitude has been discussed and found to be (1.106). The divergent piece goes as

$$A_n^{(2)} = A_n^{(1)} I_n^{(1)} \tag{3.34}$$

where

$$I_n^{(1)} = \sum_{i=1}^{n} I_{i,i+1} \tag{3.35}$$

and

$$I_{i,i+1} = \left[-\frac{1}{\epsilon^2} \left(\frac{\mu^2}{s_{i,i+1}} \right)^{\epsilon} \right] \tag{3.36}$$

General forms of the full colour divergent piece are simple combinations of $A_{n:c}^{(1)}$ and sums of $I_{i,i+1}$ which we will denote by

$$U_{n:\lambda}^{(2)} = U_{n:\lambda}^{(1)} I_{n:\lambda}^{(1)} \tag{3.37}$$

We find the correct collinear limits numerically but it is interesting to view them analytically. We will use the $\text{Tr}(abc)\text{Tr}(def)$ term as an example.

$$
\begin{aligned}
U_{6:4}^{(2)}(a,b,c;d,e,f) &= U_{6:4}^{(1)}(a,b,c;d,e,f)I_{6:4}^{(1)}(a,b,c;d,e,f) \\
&= A_{6:4}^{(1)}(a,b,c;d,e,f)\Big(I_{a,b} + I_{b,c} + I_{c,a} + I_{d,e} + I_{e,f} + I_{f,d}\Big) \\
&+ A_{6:1}^{(1)}(a,b,c,d,e,f)\Big(I_{a,c} - I_{a,d} - I_{c,f} + I_{d,f}\Big) + A_{6:1}^{(1)}(c,a,b,d,e,f)\Big(I_{b,c} - I_{b,f} - I_{c,d} + I_{d,f}\Big) \\
&+ A_{6:1}^{(1)}(a,b,c,e,f,d)\Big(I_{a,c} - I_{a,e} - I_{c,d} + I_{d,e}\Big) + A_{6:1}^{(1)}(c,a,b,e,f,d)\Big(I_{b,c} - I_{b,d} - I_{c,e} + I_{d,e}\Big) \\
&+ A_{6:1}^{(1)}(a,b,c,f,d,e)(I_{a,c} - I_{a,f} - I_{c,e} + I_{e,f}) + A_{6:1}^{(1)}(c,a,b,f,d,e)\Big(I_{b,c} - I_{b,e} - I_{c,f} + I_{e,f}\Big) \\
&+ A_{6:1}^{(1)}(b,c,a,d,e,f)\Big(I_{a,b} - I_{a,f} - I_{b,d} + I_{d,f}\Big) + A_{6:1}^{(1)}(b,c,a,e,f,d)\Big(I_{a,b} - I_{a,d} - I_{b,e} + I_{d,e}\Big) \\
&+ A_{6:1}^{(1)}(b,c,a,f,d,e)\Big(I_{a,b} - I_{a,e} - I_{b,f} + I_{e,f}\Big).
\end{aligned} \tag{3.38}
$$

In the collinear limit, $k_a \to z \times K$ and $k_b \to (1-z) \times K = \bar{z} \times K$, and we expect

$$U_{6:4}^{(2)}(a,b,c;d,e,f)|_{a||b} \to S_-^{++,\text{tree}}U_{5:3}^{(2)}(k,c;d,e,f) + S_-^{++,(1)}A_{5:3}^{(1)}(k,c;d,e,f), \tag{3.39}$$

where

$$
\begin{aligned}
U_{5:3}^{(2)}(k,c;d,e,f) &= U_{5:3}^{(1)}(k,c;d,e,f)I_{5:3}^{(1)}(k,c;d,e,f) \\
&= A_{5:3}^{(1)}(k,c;d,e,f)\Big(I_{c,k} + I_{k,c} + I_{d,e} + I_{e,f} + I_{f,d}\Big) \\
&+ A_{5:1}^{(1)}(k,c,d,e,f)\Big(I_{d,f} - I_{c,f} + I_{k,c} - I_{k,d}\Big) + A_{5:1}^{(1)}(c,k,d,e,f)\Big(I_{c,k} - I_{c,d} + +I_{d,f} - I_{k,f}\Big) \\
&+ A_{5:1}^{(1)}(k,c,e,f,d)\Big(I_{d,e} - I_{c,d} + I_{k,c} - I_{k,e}\Big) + A_{5:1}^{(1)}(c,k,e,f,d)\Big(I_{c,k} - I_{c,e} + I_{d,e} - I_{k,d}\Big) \\
&+ A_{5:1}^{(1)}(k,c,f,d,e)\Big(I_{e,f} - I_{c,e} + I_{k,c} - I_{k,f}\Big) + A_{5:1}^{(1)}(c,k,f,d,e)\Big(I_{c,k} - I_{c,f} + I_{e,f} - I_{k,e}\Big),
\end{aligned} \tag{3.40}
$$

and $S_-^{++,(\ell)}$ are the splitting functions. We are not interested in the $S_+^{++,(1)}$ splitting function here as it is purely rational. From the leading case [67] we expect to find additional terms Δ coming from the $I_{i,j}$ and expect these to cancel with the finite polylogarithmic piece. We see that

$$
\begin{aligned}
A_{6:4}^{(1)}(a,b,c;d,e,f)|_{a||b} &\to S_-^{++,\text{tree}} \times A_{5:3}^{(1)}(K,c;d,e,f), \\
A_{6:1}^{(1)}(a,b,c,d,e,f)|_{a||b} &\to S_-^{++,\text{tree}} \times A_{5:1}^{(1)}(K,c;d,e,f),
\end{aligned}
$$

and

$$A_{6:1}^{(1)}(a,c,b,d,e,f)|_{a||b} \to 0 \tag{3.41}$$

as well as all other permutations of legs $\{c, d, e, f\}$. The last three terms in eq.(3.38) vanish in the collinear limit and the remaining terms clearly go to the correct limit. We have for $i \neq b$

$$
\begin{aligned}
I_{a,i} &\to \left(\frac{\mu^2}{z s_{ki}}\right)^{\epsilon} \approx 1 + \log\left(\frac{\mu^2}{z s_{ki}}\right)\epsilon + \frac{1}{2}\log\left(\frac{\mu^2}{z s_{ki}}\right)^2 \epsilon^2 \\
&= \left(\frac{\mu^2}{s_{ki}}\right)^{\epsilon} + \log\left(\frac{1}{z}\right)\epsilon + \frac{1}{2}\left[2\log\left(\frac{s_{ki}}{\mu^2}\right)\log\left(z\right) + \log\left(z\right)^2\right]\epsilon^2, \\
I_{a,b} &\to \left(\frac{\mu^2}{s_{ab}}\right)^{\epsilon} \approx 1 + \log\left(\frac{\mu^2}{s_{ab}}\right)\epsilon + \frac{1}{2}\log\left(\frac{\mu^2}{s_{ab}}\right)^2 \epsilon^2,
\end{aligned}
\tag{3.42}
$$

and

$$
\begin{aligned}
\left(\frac{1}{z\bar{z}s_{ab}}\right)^{\epsilon} &\approx 1 + \log\left(\frac{1}{z\bar{z}s_{ab}}\right)\epsilon + \frac{1}{2}\log\left(\frac{1}{z\bar{z}s_{ab}}\right)^2 \epsilon^2 \\
&= 1 + \log\left(\frac{1}{z}\right)\epsilon + \log\left(\frac{1}{\bar{z}}\right)\epsilon + \log\left(\frac{1}{s_{ab}}\right)\epsilon \\
&\quad + \frac{1}{2}\left[\log\left(\frac{1}{s_{ab}}\right)^2 + 2\log\left(s_{ab}\right)\log\left(z\bar{z}\right) + \log\left(z\bar{z}\right)^2\right]\epsilon^2.
\end{aligned}
\tag{3.43}
$$

Combinations $I_{ai} - I_{aj}$ or $I_{bi} - I_{bj}$ have cancelling $\frac{1}{\epsilon}$ terms and the combination $I_{ia} + I_{ab} + I_{bj}$ can recovers the correct r_-^{++} factors where the non-cancelling $\frac{1}{\epsilon}$ terms are combined to form the $\left(\frac{\mu^2}{z\bar{z}s_{ab}}\right)^{\epsilon}$ piece. We therefore find for the $I_{ai} - I_{aj}$ combination the undesired terms Δ^- are given by

$$
\begin{aligned}
\Delta_{ij}^{a-} &= -\log\left(\frac{s_{ai}}{s_{aj}}\right)\log\left(z\right), \\
\Delta_{ij}^{b-} &= -\log\left(\frac{s_{bi}}{s_{bj}}\right)\log\left(\bar{z}\right).
\end{aligned}
\tag{3.44}
$$

and from the first term in eq.(3.38) we have

$$
\Delta = \log\left(\frac{s_{ab}}{\mu^2}\right)\log(z\bar{z}) - \log\left(\frac{s_{ca}}{\mu^2}\right)\log(z) - \log\left(\frac{s_{bc}}{\mu^2}\right)\log(\bar{z}) - \log(z\bar{z}) - \frac{1}{3}z\bar{z} + \frac{\pi^2}{4}.
\tag{3.45}
$$

We therefore find in total

$$
\begin{aligned}
\Delta_{6:4} &= S_-^{++,\text{tree}} A_{5:3}^{(1)}(k, c; d, e, f)\Delta \\
&\quad + \sum_{Z_3(d,e,f)} \left(S_-^{++,\text{tree}} A_{5:1}^{(1)}(k, c, d, e, f)\Delta_{c,d}^{a-} + S_-^{++,\text{tree}} A_{5:1}^{(1)}(c, k, d, e, f)\Delta_{c,f}^{b-} \right)
\end{aligned}
\tag{3.46}
$$

We consequently require

$$
P_{6:4}^{(2)}(a, b, c; d, e, f) \to S_-^{++,\text{tree}} P_{5:3}^{(2)}(k, c; d, e, f) - \Delta_{6:4}'
\tag{3.47}
$$

where $\Delta_{6:4}'$ is the transcendental part of $\Delta_{6:4}$.

This piece is given by

$$P_{6:4}^{(2)}(a,b,c;d,e,f)$$

$$= \sum_{\mathcal{P}_{6:4}} \left(\frac{1}{3} C_{6:3i}^{1m}(a,b,c;d,e,f) - C_{6:1i}^{1m}(a,b,c;f,e,d) \right.$$

$$+ C_{6:1ii}^{1m}(d,b,a;c,e,f) + C_{6:1ii}^{1m}(b,d,a;c,e,f) + C_{6:1ii}^{1m}(b,a,d;c,e,f)$$

$$+ C_i^{2m}(a;f,e;b;c,d) - \frac{1}{2} C_{ii}^{2m}(a;b,f;e;c,d) - \frac{1}{2} C_{ii}^{2m}(f;a,e;b;c,d)$$

$$\left. + C_{ii}^{2m}(a;b,d;c;e,f) - C_i^{2m}(a;b,c;d;e,f) - C_i^{2m}(d;a,b;c;e,f) \right) \quad (3.48)$$

and we seek the correct collinear behaviour. The boxes vanish in the limit where the u-channel becomes collinear. We also have vanishing coefficients for any two-mass box with $a,b \in K_4$, as well as for when $a \in K_2, b \in K_4$ and vice versa eg. $C_{6:1ii}^{1m}(d,a,c;b,e,f)$

Using the identities

$$\mathrm{Li}_2(1-x) + \mathrm{Li}_2(1-\frac{1}{x}) = -\frac{1}{2}\log(x)^2 \quad (3.49)$$

and

$$\mathrm{Li}_2\left(1-\frac{1}{x}\right) - \mathrm{Li}_2(x) = \log(x)\log(1-x) - \frac{1}{2}\log(x)^2 \quad (3.50)$$

it can be shown that Δ' is given by the combination of boxes

$$F^{1m}(s_{ab}, s_{bc}, t_{abc}) + F^{1m}(s_{ca}, s_{bc}, t_{abc}) = -\Delta' \quad (3.51)$$

where Δ' is the irrational part of Δ. We see that in the first term

$$\frac{1}{3} \sum_{\mathcal{Z}_3(def)} \left(C_{6:3i}^{1m}(a,b,c;d,e,f) + C_{6:3i}^{1m}(c,a,b;d,e,f) \right) \rightarrow -S_-^{++,\mathrm{tree}} A_{5:3}^{(1)}(k,c;d,e,f)\Delta' \quad (3.52)$$

cancels the first part of $\Delta_{6:4}$'. For the second part we look at the combination of boxes

$$F^{1m}(s_{ba}, s_{ad}, t_{bad}) - F^{1m}(s_{ca}, s_{ab}, t_{cab}) = \Delta_{c,d}^{a-} \quad (3.53)$$

and find that the coefficients satisfy the correct collinear limits such that

$$\sum_{\mathcal{Z}_3(def)} \left(- C_{6:1i}^{1m}(c,a,b;f,e,d) + C_{6:1ii}^{1m}(b,a,d;c,e,f) \rightarrow -S_-^{++,\mathrm{tree}} A_{5:1}^{(1)}(k,c,d,e,f)\Delta_{c,d}^{a-} \right),$$

$$\sum_{\mathcal{Z}_3(def)} \left(- C_{6:1i}^{1m}(a,b,c;f,e,d) + C_{6:1ii}^{1m}(f,b,a;c,d,e) \rightarrow -S_-^{++,\mathrm{tree}} A_{5:1}^{(1)}(c,k,d,e,f)\Delta_{c,f}^{b-} \right)$$

$$(3.54)$$

which cancels the rest of $\Delta_{6:4}$.

Any remaining pieces cancel amongst themselves in the collinear limit. All remaining collinear limits were found to work numerically, remembering to take the logarithmic arguments off the real axis as prescribed by [94], such that

$$P_{i,j}^2 \rightarrow P_{i,j}^2 + i\delta. \quad (3.55)$$

This includes both planar collinear limits, non-planar collinear limits and limits between trace structures, for example taking the $a||b$ limit of $\mathrm{Tr}[ac]\mathrm{Tr}[bdef]$. With the cut-constructible piece calculated, we can move onto augmented recursion.

3.4 Recursion

The procedure is exactly the same as in the five-point case, albeit algebraically more complicated. We choose legs $\{a, b, c\}$ to undergo the Risager shift, breaking the symmetry and allowing us to sum over only the channels excited by this shift. We take the rational results of Chapter 2 for the (tree)-(two-loop) channels and must build off-shell currents as shown in Figure 1.7. After colour dressing all channels we can use decoupling identities to relate all currents to a basis set

$$\tau_{6:1}^{(1)}(\alpha^-, \beta^+, c^+, d^+, e^+, f^+) \;,\; \tau_{6:1}^{(1)}(\alpha^-, c^+, \beta^+, d^+, e^+) \text{ and } \tau_{6:1}^{(1)}(\alpha^-, c^+, d^+, \beta^+, e^+, f^+),$$
(3.56)

where due to the crossing symmetry we may relate all other currents to these three via relabellings and flips. The six-point single-minus one-loop amplitude is

$$\begin{aligned}
A_{6:1}^{(1)}(a^-, b^+, c^+, d^+, e^+, f^+) = \frac{1}{3}\Bigg(& \frac{[f|P_{bc}|a\rangle^3}{\langle a\,b\rangle \langle b\,c\rangle \langle d\,e\rangle^2 \, t_{abc}[f|P_{ab}|c\rangle} + \frac{[b|P_{cd}|a\rangle^3}{\langle c\,d\rangle^2 \langle e\,f\rangle \langle f\,a\rangle \, t_{bcd}[b|P_{cd}|e\rangle} \\
& + \frac{[b\,f]^3}{[a\,b][f\,a]\,t_{cde}} \left[\frac{[b\,c][c\,d]}{\langle d\,e\rangle [b|P_{cd}|e\rangle} - \frac{[d\,e][e\,f]}{\langle c\,d\rangle [f|P_{ab}|c\rangle} + \frac{[c\,e]}{\langle c\,d\rangle \langle d\,e\rangle} \right] \\
& - \frac{\langle a\,c\rangle^3 [b\,c] \langle b\,d\rangle}{\langle b\,c\rangle^2 \langle c\,d\rangle^2 \langle d\,e\rangle \langle e\,f\rangle \langle f\,a\rangle} + \frac{\langle a\,e\rangle^3 [e\,f] \langle d\,f\rangle}{\langle a\,b\rangle \langle b\,c\rangle \langle c\,d\rangle \langle d\,e\rangle^2 \langle e\,f\rangle^2} \\
& - \frac{\langle a\,d\rangle^3 \langle c\,e\rangle [d|P_{bc}|a\rangle}{\langle a\,b\rangle \langle b\,c\rangle \langle c\,d\rangle^2 \langle d\,e\rangle^2 \langle e\,f\rangle \langle f\,a\rangle} \Bigg)
\end{aligned}$$
(3.57)

and we want to build the three leading currents from this.

3.4.1 The Adjacent Current

We start with the on-shell amplitude

$$\begin{aligned}
& A_{6:1}^{(1)}(\alpha^-, \beta^+, c^+, d^+, e^+, f^+) \\
& = \frac{1}{3}\Bigg(\frac{[f|P_{\beta c}|\alpha\rangle^3}{\langle \alpha\,\beta\rangle \langle \beta\,c\rangle \langle d\,e\rangle^2 \, t_{\alpha\beta c}[f|P_{\alpha\beta}|c\rangle} + \frac{[\beta|P_{cd}|\alpha\rangle^3}{\langle c\,d\rangle^2 \langle e\,f\rangle \langle f\,\alpha\rangle \, t_{\beta cd}[\beta|P_{cd}|e\rangle} \\
& + \frac{[\beta\,f]^3}{[\alpha\,\beta][f\,\alpha]\,t_{cde}} \left[\frac{[\beta\,c][c\,d]}{\langle d\,e\rangle [\beta|P_{cd}|e\rangle} - \frac{[d\,e][e\,f]}{\langle c\,d\rangle [f|P_{\alpha\beta}|c\rangle} + \frac{[c\,e]}{\langle c\,d\rangle \langle d\,e\rangle} \right] \\
& - \frac{\langle \alpha\,d\rangle^3 \langle c\,e\rangle [d|P_{\beta c}|\alpha\rangle}{\langle \alpha\,\beta\rangle \langle \beta\,c\rangle \langle c\,d\rangle^2 \langle d\,e\rangle^2 \langle e\,f\rangle \langle f\,\alpha\rangle} \\
& - \frac{\langle \alpha\,c\rangle^3 [\beta\,c] \langle \beta\,d\rangle}{\langle \beta\,c\rangle^2 \langle c\,d\rangle^2 \langle d\,e\rangle \langle e\,f\rangle \langle f\,\alpha\rangle} + \frac{\langle \alpha\,e\rangle^3 [e\,f] \langle d\,f\rangle}{\langle \alpha\,\beta\rangle \langle \beta\,c\rangle \langle c\,d\rangle \langle d\,e\rangle^2 \langle e\,f\rangle^2} \Bigg)
\end{aligned}$$
(3.58)

Collecting $\mathcal{O}(s_{\alpha\beta}^n)$ singular terms

$$A_{6:1}^{(1)}(\alpha^-,\beta^+,c^+,d^+,e^+,f^+) =$$

$$\frac{1}{3}\left(\frac{1}{\langle\alpha\,\beta\rangle\langle\beta\,c\rangle\langle d\,e\rangle^2}\left[\frac{\langle d\,f\rangle\langle\alpha\,e\rangle^3\,[e\,f]}{\langle c\,d\rangle\langle e\,f\rangle^2} - \frac{\langle c\,e\rangle\langle\alpha\,d\rangle^3\,[d|c|\alpha\rangle}{\langle c\,d\rangle^2\langle e\,f\rangle\langle f\,\alpha\rangle} + \frac{[f|c|\alpha\rangle^3}{t_{\alpha\beta c}[f|k|c\rangle}\right]\right.$$

$$+ \frac{[\beta\,f]^3}{[f\,\alpha][\alpha\,\beta]\,t_{cde}}\left[\frac{[c\,e]}{\langle c\,d\rangle\langle d\,e\rangle} - \frac{[d\,e]\,[e\,f]}{\langle c\,d\rangle\,[f|k|c\rangle} + \frac{[\beta\,c]\,[c\,d]}{\langle d\,e\rangle\,[\beta|P_{cd}|e\rangle}\right]$$

$$+ \frac{1}{\langle d\,e\rangle^2\langle\beta\,c\rangle}\left[\frac{\langle c\,e\rangle\langle\alpha\,d\rangle^3\,[d\,\beta]}{\langle c\,d\rangle^2\langle e\,f\rangle\langle f\,\alpha\rangle} + 3\frac{[\beta\,f]\,[f|c|\alpha\rangle^2}{[f|k|c\rangle t_{\alpha\beta c}}\right]$$

$$+ \left.\frac{1}{\langle c\,d\rangle^2\langle e\,f\rangle\langle f\,\alpha\rangle}\left[\frac{\langle\alpha\,c\rangle^3\,[c|\beta|d\rangle}{\langle d\,e\rangle\langle\beta\,c\rangle^2} + \frac{[\beta|P_{cd}|\alpha\rangle^3}{[\beta|P_{cd}|e\rangle t_{\beta cd}}\right]\right) + \mathcal{O}(\langle\alpha\,\beta\rangle) \tag{3.59}$$

where $k = P_{\alpha\beta} = \alpha + \beta$. We want to build the current such that its leading singularities give the correct factorisations. The double pole piece comes from

$$\mathcal{F}_{dp} = \frac{[\beta\,q]\langle\alpha\,q\rangle^2}{\langle\beta\,q\rangle\langle k\,q\rangle s_{\alpha\beta}} A_{5:1}^{(1)}(k^-,c^+,d^+,e^+,f^+)$$

$$= \frac{1}{3}\frac{\langle\alpha\,q\rangle^2}{\langle\beta\,q\rangle^2}\frac{1}{s_{\alpha\beta}}\frac{\langle q|\alpha\beta|q\rangle}{\langle d\,e\rangle^2\,[q|k|q\rangle^2}\left(\frac{[c\,f]^3\,[q|k|q\rangle^2}{[f|k|q\rangle[c|k|q\rangle} + \frac{\langle c\,e\rangle\,[q|k|d\rangle^3\,[c\,d]}{\langle c\,d\rangle^2\langle e\,f\rangle\,[q|k|f\rangle}\right.$$

$$+ \left.\frac{\langle d\,f\rangle\,[q|k|e\rangle^3\,[e\,f]}{\langle c\,d\rangle\langle e\,f\rangle^2\,[q|k|c\rangle}\right). \tag{3.60}$$

We build this from the $\mathcal{O}(\langle\alpha\,\beta\rangle^{-1})$ piece so isolate this for now and calling it $A_{6:1,i}^{(1)}$

$$A_{6:1,i}^{(1)}(\alpha^-,\beta^+,c^+,d^+,e^+,f^+)$$

$$= \frac{1}{3}\frac{1}{\langle\alpha\,\beta\rangle\langle\beta\,c\rangle\langle d\,e\rangle^2}\left(\frac{\langle d\,f\rangle\langle\alpha\,e\rangle^3\,[e\,f]}{\langle c\,d\rangle\langle e\,f\rangle^2} - \frac{\langle c\,e\rangle\langle\alpha\,d\rangle^3\,[d|c|\alpha\rangle}{\langle c\,d\rangle^2\langle e\,f\rangle\langle f\,\alpha\rangle} + \frac{[f|c|\alpha\rangle^3}{t_{\alpha\beta c}[f|k|c\rangle}\right), \tag{3.61}$$

to which we apply

$$\frac{1}{\langle\alpha\,\beta\rangle\langle\beta\,c\rangle} = \frac{1}{\langle\alpha\,q\rangle\langle\beta\,q\rangle^2}\left(\frac{\langle q|\alpha\beta|q\rangle[q|k|q\rangle}{s_{\alpha\beta}[q|k|c\rangle} + \frac{\langle q\,\beta\rangle\langle q\,c\rangle\,[q|\alpha|q\rangle}{\langle\beta\,c\rangle\,[q|k|c\rangle}\right), \tag{3.62}$$

giving

$$A_{6:1,i}^{(1)}(\alpha^-,\beta^+,c^+,d^+,e^+,f^+) =$$

$$\frac{i}{3}\frac{1}{\langle\alpha\,q\rangle\langle\beta\,q\rangle^2\langle d\,e\rangle^2}\left(\frac{\langle q|\alpha\beta|q\rangle[q|k|q\rangle}{s_{\alpha\beta}[q|k|c\rangle} + \frac{\langle q\,\beta\rangle\langle q\,c\rangle\,[q|\alpha|q\rangle}{\langle\beta\,c\rangle\,[q|k|c\rangle}\right)$$

$$\times\left(\frac{\langle d\,f\rangle\langle\alpha\,e\rangle^3\,[e\,f]}{\langle c\,d\rangle\langle e\,f\rangle^2} - \frac{\langle c\,e\rangle\langle\alpha\,d\rangle^3\,[d|c|\alpha\rangle}{\langle c\,d\rangle^2\langle e\,f\rangle\langle f\,\alpha\rangle} + \frac{[f|c|\alpha\rangle^3}{t_{\alpha\beta c}[f|k|c\rangle}\right). \tag{3.63}$$

We collect the three terms

$$A_{6:1,i}^{(1)}(\alpha^-,\beta^+,c^+,d^+,e^+,f^+) =$$

$$\frac{1}{3}\frac{1}{\langle\alpha\,q\rangle\langle\beta\,q\rangle^2\langle d\,e\rangle^2}\frac{\langle q|\alpha\beta|q\rangle[q|k|q\rangle}{s_{\alpha\beta}[q|k|c\rangle}\left(\frac{\langle d\,f\rangle\langle\alpha\,e\rangle^3\,[e\,f]}{\langle c\,d\rangle\langle e\,f\rangle^2} - \frac{\langle c\,e\rangle\langle\alpha\,d\rangle^3\,[d|c|\alpha\rangle}{\langle c\,d\rangle^2\langle e\,f\rangle\langle f\,\alpha\rangle} + \frac{[f|c|\alpha\rangle^3}{t_{\alpha\beta c}[f|k|c\rangle}\right). \tag{3.64}$$

but we want to keep track of the finite terms as well so we will define $A_{6:1,i}^{(1),f}$ as a collection of these $\mathcal{O}(s_{\alpha\beta}^0)$ terms that we will keep adding to which originate from $A_{6:1,i}^{(1)}$,

$$
A_{6:1,i}^{(1),f}(\alpha^-,\beta^+,c^+,d^+,e^+,f^+) =
$$
$$
\frac{1}{3}\frac{1}{\langle \alpha\,q\rangle\,\langle\beta\,q\rangle^2\,\langle d\,e\rangle^2}\frac{\langle q\,\beta\rangle\,\langle q\,c\rangle\,[q|\alpha|q\rangle}{\langle\beta\,c\rangle\,[q|k|c\rangle}\left(\frac{\langle d\,f\rangle\,\langle\alpha\,e\rangle^3\,[e\,f]}{\langle c\,d\rangle\,\langle e\,f\rangle^2} - \frac{\langle c\,e\rangle\,\langle\alpha\,d\rangle^3\,[d|c|\alpha\rangle}{\langle c\,d\rangle^2\,\langle e\,f\rangle\,\langle f\,\alpha\rangle} + \frac{[f|c|\alpha\rangle^3}{t_{\alpha\beta c}[f|k|c\rangle}\right).
$$
$$
(3.65)
$$

We need to take α and β off shell using axial gauge equation (1.123) where we again choose the reference vectors from axial gauge and the Risager shift to be equal. Using

$$
\frac{[\beta|k|X\rangle}{[\beta|k|Y\rangle} = \frac{[q|k|X\rangle}{[q|k|Y\rangle}\left(1 + k^2\frac{[\beta\,q]\,\langle Y\,X\rangle}{[q|k|X\rangle[\beta|k|Y\rangle}\right) + \cdots \tag{3.66}
$$

and capping any $\langle \alpha\,X\rangle$ in the bracket with $[\beta\,\alpha]$ we slowly move toward the pole

$$
A_{6:1,i}^{(1)}(\alpha^-,\beta^+,c^+,d^+,e^+,f^+)
$$
$$
= \frac{1}{3}\frac{\langle\alpha\,q\rangle^2}{\langle\beta\,q\rangle^2\,\langle d\,e\rangle^2}\frac{\langle q|\alpha\beta|q\rangle}{s_{\alpha\beta}}\frac{[q|k|q\rangle}{[q|k|c\rangle}
$$
$$
\times\left[\frac{\langle d\,f\rangle\,[q|k|e\rangle^3\,[e\,f]}{\langle c\,d\rangle\,\langle e\,f\rangle^2\,[q|k|q\rangle^3}\left(1 + 3s_{\alpha\beta}\frac{[\beta|q|e\rangle}{[q|k|e\rangle[\beta|k|q\rangle}\right)\right.
$$
$$
- \frac{[f\,c]^3\,[q|k|c\rangle^3}{t_{\alpha\beta c}[f|k|c\rangle[q|k|q\rangle^3}\left(1 + 3s_{\alpha\beta}\frac{[\beta|q|c\rangle}{[q|k|c\rangle[\beta|k|q\rangle}\right)
$$
$$
\left.- \frac{\langle c\,e\rangle\,[q|k|d\rangle^3\,[d\,c]\,[q|k|c\rangle}{\langle c\,d\rangle^2\,\langle e\,f\rangle\,[q|k|f\rangle[q|k|q\rangle^3}\left(1 + 3s_{\alpha\beta}\frac{[\beta|q|d\rangle}{[q|k|d\rangle[\beta|k|q\rangle} + s_{\alpha\beta}\frac{[\beta\,q]\,\langle f\,c\rangle}{[q|k|c\rangle[\beta|k|f\rangle}\right)\right]
$$
$$
+ \cdots \tag{3.67}
$$

Here we have turned $\alpha^\flat + \beta^\flat \to k$ and so the ellipsis stands for $\mathcal{O}(\alpha^2,\beta^2)$ terms as they can simply be removed due to condition C2 without effecting condition C1. Note $k^\flat \neq \alpha^\flat + \beta^\flat$ which should be kept in mind as taking $k^\flat$ off-shell introduces $k^2 = s_{\alpha\beta}$ terms which cannot be thrown away and must be built into the current.

Gathering leading pole terms we have

$$
\tau_6^{dp} = \frac{1}{3}\frac{\langle\alpha\,q\rangle^2}{\langle\beta\,q\rangle^2\,\langle d\,e\rangle^2}\frac{\langle q|\alpha\beta|q\rangle}{s_{\alpha\beta}}\frac{[q|k|q\rangle}{[q|k|c\rangle}\left(\frac{\langle d\,f\rangle\,[q|k|e\rangle^3\,[e\,f]}{\langle c\,d\rangle\,\langle e\,f\rangle^2\,[q|k|q\rangle^3} - \frac{[f\,c]^3\,[q|k|c\rangle^3}{t_{\alpha\beta c}[f|k|c\rangle[q|k|q\rangle^3}\right.
$$
$$
\left.- \frac{\langle c\,e\rangle\,[q|k|d\rangle^3\,[d\,c]\,[q|k|c\rangle}{\langle c\,d\rangle^2\,\langle e\,f\rangle\,[q|k|f\rangle[q|k|q\rangle^3}\right) = \mathcal{F}_{dp} + \cdots \tag{3.68}
$$

and we give the same treatment to the $A_{6:1,i}^{(1),f}$ but now add the subleading pole terms that we

have just found to give

$$
A_{6:1,i}^{(1),f}(\alpha^-,\beta^+,c^+,d^+,e^+,f^+) =
$$

$$
\frac{1}{3}\frac{\langle \alpha\, q\rangle^2}{\langle \beta\, q\rangle^2 \langle d\, e\rangle^2}\left[\frac{\langle q\,\beta\rangle\, \langle q\, c\rangle\, [q|\alpha|q\rangle}{\langle \beta\, c\rangle\,[q|k|c\rangle}\left(\frac{\langle d\, f\rangle\,[e\, f]\,[q|k|e\rangle^3}{\langle c\, d\rangle\,\langle e\, f\rangle^2\,[q|k|q\rangle^3} - \frac{\langle c\, e\rangle\,[q|k|d\rangle^3\,[d\, c]\,[q|k|c\rangle}{\langle c\, d\rangle^2\,\langle e\, f\rangle\,[q|k|q\rangle^3[q|k|f\rangle}\right.\right.
$$

$$
\left.- \frac{[f\, c]^3\,[q|k|c\rangle^3}{t_{\alpha\beta c}[f|k|c\rangle\,[q|k|q\rangle^3}\right)
$$

$$
+ 3\frac{\langle q|\alpha\beta|q\rangle}{[q|k|c\rangle\,[q|k|q\rangle^2}\left(\frac{\langle d\, f\rangle\,[q|k|e\rangle^3\,[e\, f]}{\langle c\, d\rangle\,\langle e\, f\rangle^2}\frac{[\beta|q|e\rangle}{[q|k|e\rangle\,[\beta|k|q\rangle} - \frac{[f\, c]^3\,[q|k|c\rangle^3}{t_{\alpha\beta c}[f|k|c\rangle}\frac{[\beta|q|c\rangle}{[q|k|c\rangle\,[\beta|k|q\rangle}\right.
$$

$$
\left.\left.- \frac{\langle c\, e\rangle\,[q|k|d\rangle^3\,[d\, c]\,[q|k|c\rangle}{\langle c\, d\rangle^2\,\langle e\, f\rangle\,[q|k|f\rangle}\left[\frac{[\beta|q|d\rangle}{[q|k|d\rangle\,[\beta|k|q\rangle} + \frac{[\beta\, q]\,\langle f\, c\rangle}{3[q|k|c\rangle\,[\beta|k|f\rangle}\right]\right)\right]. \tag{3.69}
$$

We have now built the $\langle \alpha\,\beta\rangle \to 0$ factorisation into the current, next we seek to build the $[\alpha\,\beta] \to 0$ factorisation into the current. This is given by

$$
\mathcal{F}_{sb} = \frac{\langle \alpha\, k\rangle\,[\beta\, q]^2}{[\alpha\, q]\,[k\, q]\,s_{\alpha\beta}}A_{5:1}^{(1)}(k^+,c^+,d^+,e^+,f^+)
$$

$$
= -\frac{i}{3}\frac{\langle \alpha\, q\rangle^2}{\langle \beta\, q\rangle^2}\frac{[q|\beta|q\rangle^2}{[q|\alpha|q\rangle^2}\frac{[q|\alpha\beta|q]}{s_{\alpha\beta}[q|k|f\rangle[q|k|c\rangle\,\langle c\, d\rangle\,\langle d\, e\rangle\,\langle e\, f\rangle}\left(s_{cd}t_{\alpha\beta c} + s_{ef}t_{\alpha\beta f} - [c|def|c\rangle\right) \tag{3.70}
$$

The last line of (3.59) contains the $[\alpha\,\beta]^{-1}$ term so we call this $A_{6:1,ii}$

$$
A_{6:1,ii}(\alpha^-,\beta^+,c^+,d^+,e^+,f^+)
$$

$$
= \frac{1}{3}\frac{[\beta\, f]^3}{[f\, \alpha]\,[\alpha\, \beta]\,t_{cde}}\left[\frac{[c\, e]}{\langle c\, d\rangle\,\langle d\, e\rangle} - \frac{[d\, e]\,[e\, f]}{\langle c\, d\rangle\,[f|k|c\rangle} + \frac{[\beta\, c]\,[c\, d]}{\langle d\, e\rangle\,[\beta|P_{cd}|e\rangle}\right] \tag{3.71}
$$

and use the following rearrangements

$$
\frac{1}{[\alpha\, \beta]}\left(\frac{[\beta\, X]}{[\beta\, Y]} - \frac{[k^\flat\, X]}{[k^\flat\, Y]}\right) = \frac{1}{[\alpha\, \beta]}\frac{[\beta\, k^\flat]\,[X\, Y]}{[\beta\, Y]\,[k^\flat\, Y]} = -\frac{\langle q\, \alpha\rangle\,[X\, Y]}{[\beta\, Y]\,[Y|k|q\rangle}, \tag{3.72}
$$

$$
\frac{[\beta\, f]^3}{[\alpha\, \beta]\,[f\, \alpha]} = \frac{[\beta\, f]^2\,[q\, f]}{[\alpha\, q]\,[f\, \alpha]} - \frac{[\beta\, f]^2\,[\beta\, q]}{[\alpha\, \beta]\,[\alpha\, q]}, \tag{3.73}
$$

and

$$
\frac{[\beta\, f]^2\,[\beta\, q]\,\langle \beta\, \alpha\rangle}{[\alpha\, q]} = -\frac{\langle \alpha\, k^\flat\rangle\,[\beta\, q]^2}{[\alpha\, q]\,[k^\flat\, q]}\,[f\, k^\flat]^2 + s_{\alpha\beta}\frac{[f|q|\alpha\rangle}{[q|k|q\rangle}\frac{([f\, \beta]\,[\beta\, q]\,[k^\flat\, q] + [\beta\, q]^2\,[f\, k^\flat])}{[\alpha\, q]\,[k^\flat\, q]}. \tag{3.74}
$$

We therefore write

$$
A_{6:1,ii} = \frac{1}{3}\left(\frac{[\beta\, f]^2\,[q\, f]}{[f\, \alpha]\,[\alpha\, q]\,t_{cde}} + \frac{\langle \alpha\, k^\flat\rangle\,[\beta\, q]^2}{s_{\alpha\beta}\,[\alpha\, q]\,[k^\flat\, q]\,t_{cde}}\,[f\, k^\flat]^2 - \frac{[f|q|\alpha\rangle}{[q|k|q\rangle}\frac{([f\, \beta]\,[\beta\, q]\,[k^\flat\, q] + [\beta\, q]^2\,[f\, k^\flat])}{[\alpha\, q]\,[k^\flat\, q]\,t_{cde}}\right)
$$

$$
\times \left(\frac{[k^\flat\, c]\,[c\, d]}{\langle d\, e\rangle\,[k^\flat|P_{cd}|e\rangle} + \frac{[c\, e]}{\langle c\, d\rangle\,\langle d\, e\rangle} - \frac{[d\, e]\,[e\, f]}{\langle c\, d\rangle\,[f|k|c\rangle}\right) + \frac{\langle q\, \alpha\rangle\,[\beta\, f]^3\,[c\, d]\,[c|P_{cd}|e\rangle}{3\,[f\, \alpha]\,[\beta|P_{cd}|e\rangle\,\langle e|P_{cd}k|q\rangle\,\langle d\, e\rangle\,t_{cde}} \tag{3.75}
$$

68

which we separate into the leading factorising singularity and a finite piece

$$\tau_6^{sb} = -\frac{1}{3}\frac{\langle\alpha\,q\rangle^2}{\langle\beta\,q\rangle^2}\frac{[q|\beta|q\rangle^2}{[q|\alpha|q\rangle^2}\frac{[q|\alpha\beta|q]}{s_{\alpha\beta}[q|k|q\rangle^2}\frac{[f|k|q\rangle^2}{t_{cde}}\left(\frac{[c|k|q\rangle\,[c\,d]}{\langle d\,e\rangle\,\langle q|kP_{cd}|e\rangle}+\frac{[c\,e]}{\langle c\,d\rangle\,\langle d\,e\rangle}-\frac{[d\,e]\,[e\,f]}{\langle c\,d\rangle\,[f|k|c\rangle}\right),\tag{3.76}$$

$$A_{6:1,ii}^{(1),f}=\frac{1}{3}\left(\frac{[\beta\,f]^2\,[q\,f]}{[f\,\alpha]\,[\alpha\,q]\,t_{cde}}-\frac{[f|q|\alpha\rangle}{[q|k|q\rangle}\frac{([f\,\beta]\,[\beta\,q]\,[q|k|q\rangle-[\beta\,q]^2\,[f|k|q\rangle)}{[\alpha\,q]\,[q|k|q\rangle t_{cde}}\right)$$
$$\times\left(\frac{[c|k|q\rangle\,[c\,d]}{\langle d\,e\rangle\,\langle q|kP_{cd}|e\rangle}+\frac{[c\,e]}{\langle c\,d\rangle\,\langle d\,e\rangle}-\frac{[d\,e]\,[e\,f]}{\langle c\,d\rangle\,[f|k|c\rangle}\right)+\frac{\langle q\,\alpha\rangle\,[\beta\,f]^3\,[c\,d]\,[c|P_{cd}|e\rangle}{3\,[f\,\alpha]\,[\beta|P_{cd}|e\rangle\langle e|P_{cd}k|q\rangle\,\langle d\,e\rangle\,t_{cde}}.\tag{3.77}$$

We therefore have the two factorising terms and three non-factorising pieces

$$\tau_6^{dp}(\alpha^-,\beta^+,c^+,d^+,e^+,f^+)$$
$$=\frac{1}{3}\frac{\langle\alpha\,q\rangle^2}{\langle\beta\,q\rangle^2\,\langle d\,e\rangle^2}\frac{\langle q|\alpha\beta|q\rangle}{s_{\alpha\beta}}\frac{[q|k|q\rangle}{[q|k|c\rangle}\left(\frac{\langle d\,f\rangle\,[q|k|e\rangle^3\,[e\,f]}{\langle c\,d\rangle\,\langle e\,f\rangle^2\,[q|k|q\rangle^3}-\frac{[f\,c]^3\,[q|k|c\rangle^3}{t_{\alpha\beta c}[f|k|c\rangle[q|k|q\rangle^3}\right.$$
$$\left.-\frac{\langle c\,e\rangle\,[q|k|d\rangle^3\,[d\,c]\,[q|k|c\rangle}{\langle c\,d\rangle^2\,\langle e\,f\rangle\,[q|k|f\rangle[q|k|q\rangle^3}\right),\tag{3.78}$$

$$\tau_6^{sb}(\alpha^-,\beta^+,c^+,d^+,e^+,f^+)$$
$$=-\frac{1}{3}\frac{\langle\alpha\,q\rangle^2}{\langle\beta\,q\rangle^2}\frac{[q|\beta|q\rangle^2}{[q|\alpha|q\rangle^2}\frac{[q|\alpha\beta|q]}{s_{\alpha\beta}[q|k|q\rangle^2}\frac{[f|k|q\rangle^2}{t_{cde}}\left(\frac{[c|k|q\rangle\,[c\,d]}{\langle d\,e\rangle\,\langle q|kP_{cd}|e\rangle}+\frac{[c\,e]}{\langle c\,d\rangle\,\langle d\,e\rangle}-\frac{[d\,e]\,[e\,f]}{\langle c\,d\rangle\,[f|k|c\rangle}\right),\tag{3.79}$$

$$A_{6:1,i}^{(1),f}(\alpha^-,\beta^+,c^+,d^+,e^+,f^+)$$
$$=\frac{1}{3}\frac{\langle\alpha\,q\rangle^2}{\langle\beta\,q\rangle^2\,\langle d\,e\rangle^2}\left[\frac{\langle c\,q\rangle\,[q|\alpha|q\rangle}{[q|k|c\rangle^2[q|k|q\rangle^2}\left(\frac{\langle d\,f\rangle\,[e\,f]\,[q|k|e\rangle^3}{\langle c\,d\rangle\,\langle e\,f\rangle^2}-\frac{\langle c\,e\rangle\,[q|k|d\rangle^3\,[d\,c]\,[q|k|c\rangle}{\langle c\,d\rangle^2\,\langle e\,f\rangle\,[q|k|f\rangle}\right.\right.$$
$$\left.-\frac{[f\,c]^3\,[q|k|c\rangle^3}{t_{\alpha\beta c}[f|k|c\rangle}\right)$$
$$-3\frac{[q|\beta|q\rangle}{[q|k|c\rangle[q|k|q\rangle^2}\left(\frac{\langle d\,f\rangle\,[q|k|e\rangle^3[f|e|q\rangle}{[q|k|e\rangle\,\langle c\,d\rangle\,\langle e\,f\rangle^2}-\frac{[f\,c]^3\,[q|k|c\rangle^3}{t_{\alpha\beta c}[f|k|c\rangle}\frac{\langle q\,c\rangle}{[q|k|c\rangle}\right.$$
$$\left.\left.-\frac{\langle c\,e\rangle\,[q|k|d\rangle^3\,[d\,c]\,[q|k|c\rangle}{\langle c\,d\rangle^2\,\langle e\,f\rangle\,[q|k|f\rangle}\left[\frac{\langle q\,d\rangle}{[q|k|d\rangle}+\frac{[q|k|q\rangle\,\langle f\,c\rangle}{3[q|k|c\rangle[q|k|f\rangle}\right]\right)\right],\tag{3.80}$$

69

$$A_{6:1,ii}^{(1),f}(\alpha^-, \beta^+, c^+, d^+, e^+, f^+)$$

$$= \frac{1}{3}\frac{\langle \alpha\, q\rangle^2}{\langle \beta\, q\rangle^2}\left[\left(\frac{[f|\beta|q\rangle^2}{[f|\alpha|q\rangle[q|\alpha|q\rangle} + \frac{([f|\beta|q\rangle[q|\beta|q\rangle[q|k|q\rangle + [q|\beta|q\rangle^2[f|k|q\rangle)}{[q|\alpha|q\rangle[q|k|q\rangle^2}\right)\right.$$

$$\times \frac{[f\,q]}{t_{cde}}\left(\frac{[c|k|q\rangle\,[c\,d]}{\langle d\,e\rangle\,\langle q|kP_{cd}|e\rangle} + \frac{[c\,e]}{\langle c\,d\rangle\,\langle d\,e\rangle} - \frac{[d\,e]\,[e\,f]}{\langle c\,d\rangle\,[f|k|c\rangle}\right) - \left.\frac{[f|\beta|q\rangle^3\,[c\,d]\,[c|P_{cd}|e\rangle}{[f|\alpha|q\rangle\,\langle q|\beta P_{cd}|e\rangle\,\langle e|P_{cd}k|q\rangle\,\langle d\,e\rangle\,t_{cde}}\right],$$

$$\tag{3.81}$$

$$A_{6:1,iii}^{(1)}(\alpha^-, \beta^+, c^+, d^+, e^+, f^+) =$$

$$= \frac{1}{3}\frac{\langle \alpha\, q\rangle^2}{\langle \beta\, q\rangle^2}\left(-\frac{1}{\langle d\,e\rangle^2}\left[[d|\beta|q\rangle\frac{\langle c\,e\rangle\,[q|k|d\rangle^3}{\langle c\,d\rangle^2\,\langle e\,f\rangle\,[q|k|f\rangle[q|k|c\rangle[q|k|q\rangle} + 3[f|\beta|q\rangle\frac{[f\,c]^2\,[q|k|c\rangle}{[f|k|c\rangle t_{\alpha\beta c}[q|k|q\rangle}\right]\right.$$

$$\left.- \frac{1}{\langle c\,d\rangle^2\,\langle e\,f\rangle}\left[[c|\beta|d\rangle\frac{[q|k|c\rangle}{\langle d\,e\rangle\,[q|k|f\rangle} + \frac{\langle \beta\, q\rangle^3\,[\beta|P_{cd}|\alpha\rangle^3}{\langle q|\beta P_{cd}|e\rangle t_{\beta cd}\,\langle f\,\alpha\rangle\,\langle q\,\alpha\rangle^2}\right]\right).$$

$$\tag{3.82}$$

We have used simple rearrangements of the form

$$\frac{\langle q|\alpha\beta|q\rangle[\beta|q|X\rangle}{[\beta|k|q\rangle} = -[q|\beta|q\rangle\,\langle q\,X\rangle + \mathcal{O}(\beta^2) \tag{3.83}$$

etc. to write the finite pieces as above where many simplifications can be made due to this being the finite part of the current so any $\mathcal{O}(\alpha^2, \beta^2, s_{\alpha\beta})$ terms may be discarded. The two conditions are satisfied:

$$\tau_{6:1}^{(1)}(\alpha^-, \beta^+, c^+, d^+, e^+, f^+) = [\tau_6^{dp} + \tau_6^{sb} + A_{6:1,i}^{(1),f} + A_{6:1,ii}^{(1),f} + A_{6:1,iii}^{(1)}](\alpha^-, \beta^+, c^+, d^+, e^+, f^+)$$

$$= A_{6:1}^{(1)}(\alpha^-, \beta^+, c^+, d^+, e^+, f^+) + \mathcal{O}(s_{\alpha\beta}) + \mathcal{O}(\alpha^2) + \mathcal{O}(\beta^2) \tag{3.84}$$

where we have kept track of the $\mathcal{O}(s_{\alpha\beta})$ terms but ultimately they do not contribute to the residue so we do not need them explicitly, and

$$\lim_{s_{\alpha\beta}\to 0} \tau_{6:1}^{(1)}(\alpha^-, \beta^+, c^+, d^+, e^+, f^+) = \mathcal{F}_{dp} + \mathcal{F}_{sb}. \tag{3.85}$$

To aid integration we use

$$[c|\beta|d\rangle = \frac{[q|k|d\rangle}{[q|k|q\rangle}[c|\beta|q\rangle + \mathcal{O}(\alpha^2, \beta^2, s_{\alpha\beta}),$$

$$\frac{[q|\beta|q\rangle^2}{[q|\alpha|q\rangle} = [q|\alpha|q\rangle - 2[q|k|q\rangle + \frac{[q|k|q\rangle^2}{[q|\alpha|q\rangle},$$

$$\frac{[f|\beta|q\rangle[q|\beta|q\rangle}{[q|\alpha|q\rangle} = -[f|\beta|q\rangle - \frac{[f|\alpha|q\rangle[q|k|q\rangle}{[q|\alpha|q\rangle} + \frac{[f|k|q\rangle[q|k|q\rangle}{[q|\alpha|q\rangle},$$

$$\frac{[f|\beta|q\rangle^2}{[f|\alpha|q\rangle[q|\alpha|q\rangle} = \frac{[f|\alpha|q\rangle}{[q|\alpha|q\rangle} - 2\frac{[f|k|q\rangle}{[q|\alpha|q\rangle} + \frac{[f|k|q\rangle^2}{[f|\alpha|q\rangle[q|\alpha|q\rangle},$$

$$\frac{[f|\beta|q\rangle^3}{[f|\alpha|q\rangle\langle q|\beta P_{cd}|e\rangle} = -\frac{[f|\alpha|q\rangle^2}{\langle q|\beta P_{cd}|e\rangle} + 3\frac{[f|\alpha|q\rangle[f|k|q\rangle}{\langle q|\beta P_{cd}|e\rangle} - 3\frac{[f|k|q\rangle^2}{\langle q|\beta P_{cd}|e\rangle} + \frac{[f|k|q\rangle^3}{\langle q|\beta P_{cd}|e\rangle[f|\alpha|q\rangle},$$

$$\tag{3.86}$$

as well as

$$\frac{[\beta|P_{cd}|\alpha\rangle^3 \langle\beta\,q\rangle^3}{\langle f\,\alpha\rangle\,t_{\beta cd}\langle q|\beta P_{cd}|e\rangle\,\langle\alpha\,q\rangle^2} = -\frac{[q|k|q\rangle}{[q|k|f\rangle}\left(\frac{[\beta|P_{cd}|\beta\rangle^2}{\langle q|\beta P_{cd}|e\rangle} - \frac{[\beta|P_{cd}|\beta\rangle s_{cd}}{\langle q|\beta P_{cd}|e\rangle} + \frac{s_{cd}^2}{\langle q|\beta P_{cd}|e\rangle} - \frac{s_{cd}^3}{t_{\beta cd}\langle q|\beta P_{cd}|e\rangle}\right),$$

$$[\beta|P_{cd}|\beta\rangle = \frac{\langle\alpha|P_{cd}\alpha|q\rangle}{\langle q\,\alpha\rangle} + ([c|k|c\rangle + [d|k|d\rangle) + \mathcal{O}(s_{\alpha\beta}) \tag{3.87}$$

This reduces everything to either triangles which we can integrate, quadratic pentagons (or other such integrals which do not have rational pieces), and boxes which may be reduced to triangles via (2.90). This current was calculated for general q in [69] but there is a mistake in the paper for the integrated non-factorising current. Using the notation of that paper, the correct integrated current for the non-factorising piece is,

$$\mathcal{I}_{\text{n.f.}}^{\alpha-\beta+} \times \frac{18 \langle a\,b\rangle \langle d\,e\rangle^2 [q|P_{ab}|q\rangle^2}{[a\,b]} = \frac{\langle d\,e\rangle [c|a+2b|q\rangle[q|P_{ab}|c\rangle[q|P_{ab}|d\rangle[q|P_{ab}|q\rangle}{\langle c\,d\rangle^2 \langle e\,f\rangle [q|P_{ab}|f\rangle}$$

$$+ \frac{\langle d\,e\rangle^2 \langle a|P_{cd}a|q\rangle[q|P_{ab}|q\rangle^3\big(-3s_{cd}\langle q\,a\rangle \langle q|aP_{cd}|e\rangle + \langle a|P_{cd}a|q\rangle(5\langle q|aP_{cd}|e\rangle + 2\langle q|bP_{cd}|e\rangle)\big)}{\langle c\,d\rangle^2 \langle e\,f\rangle \langle q\,a\rangle^2 \langle q|aP_{cd}|e\rangle^2[q|P_{ab}|f\rangle}$$

$$+ \frac{2\langle d\,e\rangle^2 \langle a|P_{cd}a|q\rangle[q|P_{ab}|q\rangle^3\langle q|aP_{cd}|e\rangle\big(\langle a|P_{cd}b|q\rangle + 3\langle q\,a\rangle ([c|P_{ab}|c\rangle + [d|P_{ab}|d\rangle)\big)}{\langle c\,d\rangle^2 \langle e\,f\rangle \langle q\,a\rangle^2 \langle q|aP_{cd}|e\rangle^2[q|P_{ab}|f\rangle}$$

$$+ \frac{\langle d\,f\rangle [q|P_{ab}|e\rangle^2\Big(-\langle c\,q\rangle [e\,f][q|P_{ab}|e\rangle[q|2a+b|q\rangle + 3[f|e|q\rangle[q|P_{ab}|c\rangle[q|a+2b|q\rangle\Big)}{\langle c\,d\rangle \langle e\,f\rangle^2 [q|P_{ab}|c\rangle^2}$$

$$+ \frac{\langle c\,e\rangle [q|P_{ab}|d\rangle^2[d|a+2b|q\rangle[q|P_{ab}|d\rangle[q|P_{ab}|f\rangle[q|P_{ab}|q\rangle}{\langle c\,d\rangle^2 \langle e\,f\rangle [q|P_{ab}|c\rangle[q|P_{ab}|f\rangle^2}$$

$$+ \frac{\langle c\,e\rangle [q|P_{ab}|d\rangle^2 [d\,c]\langle c\,q\rangle [q|P_{ab}|d\rangle[q|P_{ab}|f\rangle[q|2a+b|q\rangle}{\langle c\,d\rangle^2 \langle e\,f\rangle [q|P_{ab}|c\rangle[q|P_{ab}|f\rangle^2}$$

$$- \frac{\langle c\,e\rangle [q|P_{ab}|d\rangle^2 [d\,c][q|a+2b|q\rangle\big(3\langle q\,d\rangle [q|P_{ab}|c\rangle[q|P_{ab}|f\rangle + \langle f\,c\rangle [q|P_{ab}|d\rangle[q|P_{ab}|q\rangle\big)}{\langle c\,d\rangle^2 \langle e\,f\rangle [q|P_{ab}|c\rangle[q|P_{ab}|f\rangle^2}$$

$$+ \frac{[f\,c]^2 [q|P_{ab}|c\rangle\big(3[f|a+2b|q\rangle[q|P_{ab}|q\rangle + [f\,c]\left(\langle c\,q\rangle [q|2a+b|q\rangle - 3\langle q\,c\rangle [q|a+2b|q\rangle\right)\big)}{[f|P_{ab}|c\rangle t_{abc}}$$

$$+ \frac{\langle d\,e\rangle [c\,d]}{t_{cde}}\left(\frac{[f\,q][c|P_{ab}|q\rangle\Big([f|a+2b|q\rangle[q|P_{ab}|q\rangle + [f|P_{ab}|q\rangle\big(6[q|P_{ab}|q\rangle - [q|2a+b|q\rangle\big)\Big)}{\langle q|P_{ab}P_{cd}|e\rangle}\right.$$

$$\left. + \frac{[c|d|e\rangle[f|a|q\rangle[q|P_{ab}|q\rangle^2\Big(2\langle q|bP_{cd}|q\rangle[f|a|q\rangle + \langle q|aP_{cd}|q\rangle\big(5[f|a|q\rangle + 2[f|b|q\rangle - 9[f|P_{ab}|q\rangle\big)\Big)}{\langle e|P_{cd}P_{ab}|q\rangle\langle q|aP_{cd}|e\rangle\langle q|aP_{cd}|q\rangle}\right)$$

$$+ \frac{\langle d\,e\rangle [c\,e][f\,q]\Big([f|a+2b|q\rangle[q|P_{ab}|q\rangle + [f|P_{ab}|q\rangle(6[q|P_{ab}|q\rangle - [q|2a+b|q\rangle)\Big)}{\langle c\,d\rangle t_{cde}}$$

$$+ \frac{\langle d\,e\rangle^2 [d\,e][e\,f][f\,q]\Big(-[f|a+2b|q\rangle[q|P_{ab}|q\rangle + [f|P_{ab}|q\rangle(-6[q|P_{ab}|q\rangle + [q|2a+b|q\rangle)\Big)}{\langle c\,d\rangle [f|P_{ab}|c\rangle t_{cde}},$$

$$(3.88)$$

where $t_{ijk} = (p_i + p_j + p_k)^2$ and note the difference in convention of factorising a factor of i out in (1.3). The remaining integrals from [69] are correct and so will not be presented here. To be clear, it is only in the appendix of [69] that this mistake exists; the final results

presented in [69] are correct. The remaining two currents are given by

$$
\tau_{6:1}^{(1)}(\alpha^-, c^+, \beta^+, d^+, e^+, f^+)
$$

$$
= \frac{1}{3}\left(\frac{\langle d\,f\rangle\,\langle\alpha\,e\rangle^3\,[e\,f]}{\langle c\,\beta\rangle\,\langle d\,e\rangle^2\,\langle e\,f\rangle^2\,\langle\alpha\,c\rangle\,\langle\beta\,d\rangle} - \frac{\langle\alpha\,d\rangle^3\,\langle\beta\,e\rangle\,[d|c|\alpha\rangle}{\langle c\,\beta\rangle\,\langle d\,e\rangle^2\,\langle e\,f\rangle\,\langle f\,\alpha\rangle\,\langle\alpha\,c\rangle\,\langle\beta\,d\rangle^2} \right.
$$

$$
+ \frac{[c|d|\alpha\rangle^3}{\langle e\,f\rangle\,\langle f\,\alpha\rangle\,\langle\beta\,d\rangle^2\,[c|P_{\beta d}|e\rangle\,t_{c\beta d}} + \frac{[f|c|\alpha\rangle^3}{\langle c\,\beta\rangle\,\langle d\,e\rangle^2\,\langle\alpha\,c\rangle\,[f|c|\beta\rangle[c|P_{\alpha\beta}|c\rangle}
$$

$$
\left. + \frac{[c\,f]^3}{[f\,\alpha]\,[\alpha\,c]\,t_{\beta de}} \times \left[\frac{[\beta\,e]}{\langle d\,e\rangle\,\langle\beta\,d\rangle} + \frac{[c\,\beta]\,[\beta\,d]}{\langle d\,e\rangle\,[c|P_{\beta d}|e\rangle} - \frac{[d\,e]\,[e\,f]}{\langle\beta\,d\rangle\,[f|c|\beta\rangle} \right] \right) + \mathcal{O}(s_{\alpha\beta}) \qquad (3.89)
$$

and

$$
\tau_{6:1}^{(1)}(\alpha^-, c^+, d^+, \beta^+, e^+, f^+)
$$

$$
= \frac{1}{3}\left(-\frac{\langle c\,\beta\rangle\,\langle\alpha\,d\rangle^3\,[c\,d]}{\langle c\,d\rangle^2\,\langle d\,\beta\rangle^2\,\langle e\,f\rangle\,\langle f\,\alpha\rangle\,\langle\beta\,e\rangle} + \frac{\langle\alpha\,e\rangle^3\,\langle\beta\,f\rangle\,[e\,f]}{\langle c\,d\rangle\,\langle d\,\beta\rangle\,\langle e\,f\rangle^2\,\langle\alpha\,c\rangle\,\langle\beta\,e\rangle^2} \right.
$$

$$
+ \frac{[c|d|\alpha\rangle^3}{\langle d\,\beta\rangle^2\,\langle e\,f\rangle\,\langle f\,\alpha\rangle\,[c|P_{d\beta}|e\rangle\,t_{cd\beta}} + \frac{[f|P_{cd}|\alpha\rangle^3}{\langle c\,d\rangle\,\langle\alpha\,c\rangle\,\langle\beta\,e\rangle^2\,[f|P_{\alpha c}|d\rangle\,t_{\alpha cd}}
$$

$$
\left. + \frac{[c\,f]^3}{[f\,\alpha]\,[\alpha\,c]\,t_{d\beta e}} \times \left[\frac{[d\,e]}{\langle d\,\beta\rangle\,\langle\beta\,e\rangle} + \frac{[c\,d]\,[d\,\beta]}{\langle\beta\,e\rangle\,[c|P_{d\beta}|e\rangle} - \frac{[e\,f]\,[\beta\,e]}{\langle d\,\beta\rangle\,[f|P_{\alpha c}|d\rangle} \right] \right) + \mathcal{O}(s_{\alpha\beta}). \qquad (3.90)
$$

Many of the terms in the non-adjacent currents do not give rationals upon integration. We are thus left with

$$
\int \frac{d^D\ell}{\ell^2\alpha^2\beta^2}\frac{i}{(2\pi)^D}\frac{[a|\ell|q\rangle[b|\ell|q\rangle}{\langle a\,q\rangle\,\langle b\,q\rangle}\tau_{6:1}^{(1)}(\alpha^-, c^+, \beta^+, d^+, e^+, f^+)|_{\mathbb{Q}}
$$

$$
= \frac{1}{6}\frac{[a\,b]}{\langle a\,b\rangle}\left(\frac{\langle d\,f\rangle\,\langle a\,e\rangle^3\,[e\,f]\,\langle b\,q\rangle^2}{\langle c\,b\rangle\,\langle d\,e\rangle^2\,\langle e\,f\rangle^2\,\langle a\,c\rangle\,\langle b\,d\rangle\,\langle a\,q\rangle^2} - \frac{\langle a\,d\rangle^3\,\langle b\,e\rangle\,[d|c|a\rangle\,\langle b\,q\rangle^2}{\langle c\,b\rangle\,\langle d\,e\rangle^2\,\langle e\,f\rangle\,\langle f\,a\rangle\,\langle a\,c\rangle\,\langle b\,d\rangle^2\,\langle a\,q\rangle^2} \right.
$$

$$
\left. + \frac{[f|c|a\rangle^3\,\langle b\,q\rangle^2}{\langle c\,b\rangle\,\langle d\,e\rangle^2\,\langle a\,c\rangle\,\langle a\,q\rangle^2\,[f|c|b\rangle[c|P_{ab}|c\rangle} \right) \qquad (3.91)
$$

and

$$
\int \frac{d^D\ell}{\ell^2\alpha^2\beta^2}\frac{i}{(2\pi)^D}\frac{[a|\ell|q\rangle[b|\ell|q\rangle}{\langle a\,q\rangle\,\langle b\,q\rangle}\tau_{6:1}^{(1)}(\alpha^-, c^+, d^+, \beta^+, e^+, f^+)|_{\mathbb{Q}}
$$

$$
= \frac{1}{6}\frac{[a\,b]}{\langle a\,b\rangle}\left(\frac{\langle a\,e\rangle^3\,\langle b\,f\rangle\,\langle b\,q\rangle^2\,[e\,f]}{\langle c\,d\rangle\,\langle d\,b\rangle\,\langle e\,f\rangle^2\,\langle a\,c\rangle\,\langle a\,q\rangle^2\,\langle b\,e\rangle^2} - \frac{\langle c\,b\rangle\,\langle b\,q\rangle^2\,\langle a\,d\rangle^3\,[c\,d]}{\langle c\,d\rangle^2\,\langle d\,b\rangle^2\,\langle e\,f\rangle\,\langle f\,a\rangle\,\langle a\,q\rangle^2\,\langle b\,e\rangle} \right). \qquad (3.92)
$$

Summing over all the channels excited by the Risager shift and all helicities we recover the full colour two-loop amplitude. The results obey the correct collinear limits and decoupling identities. As with the five-point calculation, the results in their present form are large and have q's scattered throughout, clearly involving massive redundancies. The next section will discuss functional reconstruction using numerical fitting and ansatz building, rewriting the answers in much more compact analytic form.

3.5 Rational Results - Fitting a Function

For the leading in colour amplitude we expect the Parke-Taylor denominator (2.96) to be able to be factorised out. With double poles we then expect to be able to fit functions that might look like

$$\frac{1}{\langle a\,b\rangle\,\langle b\,c\rangle\,\langle c\,d\rangle\,\langle d\,e\rangle\,\langle e\,f\rangle\,\langle f\,a\rangle}\left(\frac{\mathcal{N}_{\text{dp}}}{\langle i\,i+1\rangle}+\frac{\mathcal{N}_{\text{overlap}}}{\langle i\,i+1\rangle\,\langle i+1\,i+2\rangle}+\mathcal{N}_{\text{sp}}\right),\qquad(3.93)$$

where we expect $\mathcal{N}_{\text{dp}}$ and $\mathcal{N}_{\text{overlap}}$ to be obtained from factorisation theorems, the overlap part being double poles that contribute to multiple channels and so we need to be careful about overcounting terms. We can then fit $\mathcal{N}_{\text{sp}}$ by building an ansatz with no spinor weight/helicity scaling and has momentum weight $m=4$ such that

$$\langle a\,b\rangle\,\langle b\,c\rangle\,\langle c\,d\rangle\,\langle d\,e\rangle\,\langle e\,f\rangle\,\langle f\,a\rangle\,R_{6:1}^{(2)}-\sum_i\left(\frac{\mathcal{N}_{\text{dp}}}{\langle i\,i+1\rangle}+\frac{\mathcal{N}_{\text{overlap}}}{\langle i\,i+1\rangle\,\langle i+1\,i+2\rangle}\right)=\mathcal{N}_{\text{sp}},\quad(3.94)$$

where $R_{6:1}^{(2)}$ is the rational result that we will have calculated in terms of q in the previous section. While this is not necessarily an easy process for leading in colour, it is a bit simpler than at subleading colour orders. This is because the amplitude is maximally planar and so we only have poles between adjacent gluons meaning the Parke Taylor denominator is clearly able to be factorised out. For subleading in colour amplitudes, one might expect the denominator to be a global Parke-Taylor-like one but for whichever manifest symmetry is present such as with the all plus $A_{n:r}^{(1)}$

$$A_{n:r}^{(1)}(1^+,2^+,3^+,\cdots,r-1;r\cdots n^+)=\quad-2\frac{(P_{1,r-1}^2)^2}{(\langle 1\,2\rangle\,\langle 2\,3\rangle\cdots\langle(r-1)\,1\rangle)(\langle r\,(r+1)\rangle\cdots\langle n\,r\rangle)},$$

but we find this to not be the case. We must subtract double and multiparticle poles and then numerically sit near simple poles and test which types are present. This allows us to build a picture of what kinds of structures we expect to see, allowing us to identify possible spurious simple poles from the factorisations. Once the factorisations are identified, the author used the singular structure from the factorisations to guess what kind of rational functions we could expect. This will be more clear with an example.

We will go over some examples now to explain how we generated compact results for subleading in colour.

3.5.1 $R_{6:2,2}$

We first consider the $\text{Tr}(ab)\text{Tr}(cd)\text{Tr}(ef)$ structure. This contains only multiparticle poles. Colour dressing the factorisations and summing over diagrams gives us the following contribution to the multiparticle pole

$$R_{6:2,2}^m=\frac{1}{4}\sum_{\mathcal{P}_{6:2,2}}A_{4:3}^{(1)}(k^-,c^+;a^+,b^+)\frac{-1}{t_{abc}}A_{4:3}^{(1)}(k^+,d^+;e^+,f^+)=\frac{1}{4}\sum_{\mathcal{P}_{6:2,2}}R_{6:2,2}^{m,b}.\qquad(3.95)$$

The other factorisations have no contribution to this amplitude. Looking at one term and using the freedom to cycle legs according to the sum this gives

$$R_{6:2,2}^{m,b}=4\frac{[d|P_{def}|b\rangle\,[d|P_{def}|c\rangle\,[b\,c]}{\langle a\,b\rangle\,\langle b\,c\rangle\,\langle c\,a\rangle\,\langle e\,f\rangle^2\,t_{abc}}.\qquad(3.96)$$

$R_{6:2,2}$ has no double poles so $\langle e\,f \rangle^2$ is unphysical and needs to be removed. Multiplying by $\frac{\langle d\,e \rangle}{\langle d\,e \rangle}$ and using

$$[d|P_{def}|b\rangle\,\langle d\,e\rangle = [d|P_{def}|d\rangle\,\langle b\,e\rangle + [d|P_{def}|e\rangle\,\langle d\,b\rangle = -[d|P_{abc}|d\rangle\,\langle b\,e\rangle + [d|f|e\rangle\,\langle d\,b\rangle$$
$$= (t_{abc} - s_{ef})\,\langle b\,e\rangle + [f|d|b\rangle\,\langle e\,f\rangle\,, \tag{3.97}$$

cancels the physical t_{abc} pole in one term which no longer contributes to the residue, and cancels the double poles in the other two terms, leaving us with

$$R_{6:2,2}^{m,b} = 4\frac{[f|P_{de}|b\rangle[d|P_{def}|c\rangle\,[b\,c]}{\langle a\,b\rangle\,\langle b\,c\rangle\,\langle c\,a\rangle\,\langle d\,e\rangle\,\langle e\,f\rangle\,t_{abc}} + \mathcal{O}(t^0_{abc}). \tag{3.98}$$

We therefore have isolated the multiparticle pole contributions to the amplitude and can fit the simple pole function. This looks close to an $r = 4$ Parke-Taylor like denominator and so we rewrite it as

$$R_{6:2,2}^{m,b} = \frac{4}{\langle a\,b\rangle\,\langle b\,c\rangle\,\langle c\,a\rangle\,\langle d\,e\rangle\,\langle e\,f\rangle\,\langle f\,d\rangle}\frac{\langle b|kfdk|c\rangle\,[b\,c]}{t_{abc}}$$
$$= \frac{1}{\langle a\,b\rangle\,\langle b\,c\rangle\,\langle c\,a\rangle\,\langle d\,e\rangle\,\langle e\,f\rangle\,\langle f\,d\rangle}G_{6:2,2}^{[1]}, \tag{3.99}$$

as this might indicate a form for the simple pole structure. With this in mind we build the ansatz,

$$R_{6:2,2}^{(2)} = \sum_{\mathcal{P}_{6:2,2}}\left[\frac{1}{\langle a\,b\rangle\,\langle b\,c\rangle\,\langle c\,a\rangle\,\langle d\,e\rangle\,\langle e\,f\rangle\,\langle f\,d\rangle}\left(G_{6:2,2}^{[1]} + \mathcal{N}_{6:2,2}\right)\right]. \tag{3.100}$$

Note the denominator partially breaks the $\mathcal{P}_{6:2,2}$ symmetry and so we cannot factorise it out of the manifest symmetry sum. However there is an antisymmetry in $Z_2(a,b)$ and $Z_2(e,f)$ and a symmetry in $Z_2(\{ab\},\{ef\}) \times Z_2(c,d)$. The ansatz for $\mathcal{N}_{6:2,2}$ can be built to have this partially broken symmetry and we finally get,

$$R_{6:2,2}^{(2)} = \sum_{\mathcal{P}_{6:2,2}}\left[\frac{1}{\langle a\,b\rangle\,\langle b\,c\rangle\,\langle c\,a\rangle\,\langle d\,e\rangle\,\langle e\,f\rangle\,\langle f\,d\rangle}\left(G_{6:2,2}^1(a,b,c,d,e,f) + G_{6:2,2}^2(a,b,c,d,e,f)\right)\right].$$
$$G_{6:2,2}^{[1]}(a,b,c,d,e,f) = \frac{\langle b|P_{abc}fdP_{abc}|c\rangle\,[b\,c]}{t_{abc}},$$
$$G_{6:2,2}^{[2]}(a,b,c,d,e,f) = s_{ad}[e|P_{bc}|e\rangle - s_{ac}[e|P_{fa}|e\rangle - s_{af}s_{ae} - s_{ae}s_{cd}. \tag{3.101}$$

3.5.2 $\mathbf{R_{6:4}}$

This colour structure has both double poles and multiparticle poles. Consider the $\mathrm{Tr}(abc)\mathrm{Tr}(def)$ structure. colour dressing the multiparticle and double pole factorisations gives

$$R_{6:4} = \frac{1}{9}\sum_{\mathcal{P}_{6:4}}\sum_{\lambda=\pm}\left[A_{4:1}^{(1)}(k^\lambda, a^+, b^+, c^+)A_{4:2}^{(1)}(k^{-\lambda}; d^+, e^+, f^+) + 3A_3^{(1)}(a^+, b^+, k^+)A_{5:3}^{(1)}(k^-, c^+; d^+, e^+, f^+)\right].$$
$$\tag{3.102}$$

First we may note that under the $Z_3(abc)$ symmetry within the $\mathcal{P}_{6:4}$ sum, we can cycle legs freely to write

$$\sum_{Z_3(abc)} A_{4:2}^{(1)}(k^+; a^+, b^+, c^+) = -\sum_{Z_3(abc)} \left(A_{4:1}^{(1)}(k^+, a^+, b^+, c^+) + A_{4:1}^{(1)}(k^+, b^+, c^+, a^+) + A_{4:1}^{(1)}(k^+, c^+, a^+, b^+) \right)$$

$$= -3 \sum_{Z_3(abc)} A_{4:1}^{(1)}(k^+, a^+, b^+, c^+) \tag{3.103}$$

which reduces the rational piece to

$$R_{6:4}$$

$$= \frac{1}{3} \sum_{\mathcal{P}_{6:4}} \left[A_{4:1}^{(1)}(k^-, a^+, b^+, c^+) A_{4:2}^{(1)}(k^+; d^+, e^+, f^+) + A_3^{(1)}(a^+, b^+, k^+) A_{5:3}^{(1)}(k^-, c^+; d^+, e^+, f^+) \right]. \tag{3.104}$$

Next we consider the double pole factorisation. We have presented the form for this one-loop single-minus at n-point in Chapter 2, and noting that again that with the freedom to exchange legs according to the $\mathcal{P}_{6:4}$ symmetry, we may write

$$\sum_{\mathcal{P}_{6:4}} A_{5:3}^{(1)}(k^-, c; d, e, f) = \sum_{\mathcal{P}_{6:4}} \sum_{Z_3(def)} \frac{\sum_{c \leq i < j \leq f} \langle k|ij|k \rangle}{\langle c\,d \rangle \langle d\,e \rangle \langle e\,f \rangle \langle f\,c \rangle} = 3 \sum_{\mathcal{P}_{6:4}} \frac{\sum_{c \leq i < j \leq f} \langle k|ij|k \rangle}{\langle c\,d \rangle \langle d\,e \rangle \langle e\,f \rangle \langle f\,c \rangle} \tag{3.105}$$

where the numerator is

$$\langle k|c(d+e+f)|k \rangle \langle k|d(e+f)|k \rangle + \langle k|ef|k \rangle = \langle k|cd|k \rangle + \langle k|ef|k \rangle \tag{3.106}$$

and we use the one-loop vertex (2.7) to write this factorisation as

$$R_{6:4}^{dp} = -\frac{1}{3} \frac{[a\,b]}{\langle a\,b \rangle^2} \frac{\langle a|cd|b \rangle + \langle a|ef|b \rangle}{\langle c\,d \rangle \langle d\,e \rangle \langle e\,f \rangle \langle f\,c \rangle}. \tag{3.107}$$

Next considering the multiparticle pole we have

$$A_{4:2}(k^-; d, e, f) = -\frac{\langle k|de|k \rangle}{\langle d\,e \rangle \langle e\,f \rangle \langle f\,d \rangle},$$

$$A_{4:1}(k^+, a, b, c) = -\frac{1}{3} \frac{[k\,a]^2}{\langle b\,c \rangle^2} \tag{3.108}$$

which gives

$$R_{6:4}^m = -\frac{1}{9} \frac{[a|P_{bc}|d\rangle [a|P_{bc}|e\rangle [d\,e]}{\langle b\,c \rangle^2 \langle d\,e \rangle \langle e\,f \rangle \langle f\,d \rangle t_{abc}} \tag{3.109}$$

which contains a spurious double pole in $\langle b\,c \rangle$. We again make use of a Schouten identity to write

$$R_{6:4}^m = -\frac{1}{9} \frac{[b|P_{abc}|d\rangle [a|P_{abc}|e\rangle [d\,e]}{\langle c\,a \rangle \langle b\,c \rangle \langle d\,e \rangle \langle e\,f \rangle \langle f\,d \rangle t_{abc}} + \mathcal{O}(t_{abc}^0). \tag{3.110}$$

This hints to an ansatz of the form

$$R_{6:4} = \frac{1}{9} \sum_{\mathcal{P}_{6:4}} \left[\frac{1}{\langle a\,b \rangle \langle b\,c \rangle \langle c\,a \rangle \langle d\,e \rangle \langle e\,f \rangle \langle f\,d \rangle} \left(G_{6:4}^m + \mathcal{N}_{6:4}^m \right) \right.$$
$$\left. + \frac{[a\,b]}{\langle a\,b \rangle \langle c\,d \rangle \langle d\,e \rangle \langle e\,f \rangle \langle f\,c \rangle} \left(G_{6:4}^{dp} + \mathcal{N}_{6:4}^{dp} \right) \right]. \tag{3.111}$$

We find

$$A_{6:4}^{(2)}(a,b,c;d,e,f)|_{\mathbb{Q}} =$$
$$R_{6:4}(a,b,c,d,e,f) = \frac{1}{36} \sum_{\mathcal{P}_{6:4}} \left[\frac{1}{\langle a\,b \rangle \langle b\,c \rangle \langle c\,a \rangle \langle d\,e \rangle \langle e\,f \rangle \langle f\,d \rangle} \left(G_{6:4}^1(a,b,c,d,e,f) + G_{6:4}^2(a,b,c,d,e,f) \right) \right.$$
$$\left. + \frac{12}{\langle a\,b \rangle \langle c\,d \rangle \langle d\,e \rangle \langle e\,f \rangle \langle f\,c \rangle} \left(G_{6:4}^3(a,b,c,d,e,f) + G_{6:4}^4(a,b,c,d,e,f) \right) \right],$$
$$G_{6:4}^1(a,b,c,d,e,f) = \frac{4 \langle e|P_{abc}a|b \rangle [e|dP_{abc}|b]}{t_{abc}},$$
$$G_{6:4}^2(a,b,c,d,e,f) = s_{ad}^2 + 106\, s_{ab} s_{ad} + 102\, [a|bcd|a \rangle - 4\, [a|bde|a \rangle - 4\, [a|dbe|a \rangle$$
$$G_{6:4}^3(a,b,c,d,e,f) = -\frac{[a\,b]}{\langle a\,b \rangle} \left(\langle a|cd|b \rangle + \langle a|ef|b \rangle \right)$$
$$G_{6:4}^4(a,b,c,d,e,f) = [a|cd|b] + [a|ef|b] \tag{3.112}$$

3.5.3 $R_{6:3}$

This colour amplitude has overlapping double poles and multiparticle poles. If we consider the factorisations given in Figure 3.3 and Figure 3.4
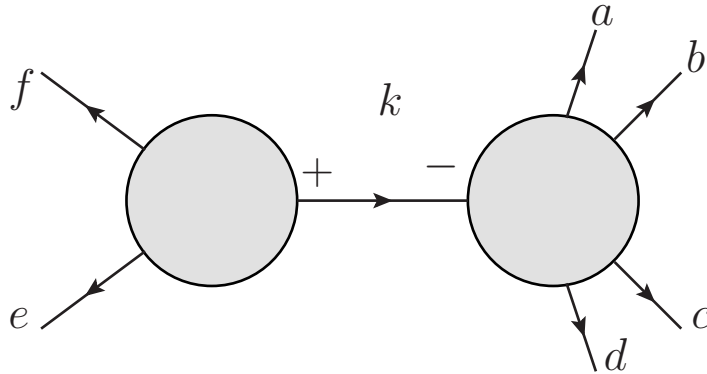
Figure 3.3: Double pole factorisation contributing to the $\langle e\,f \rangle^2$ double pole.
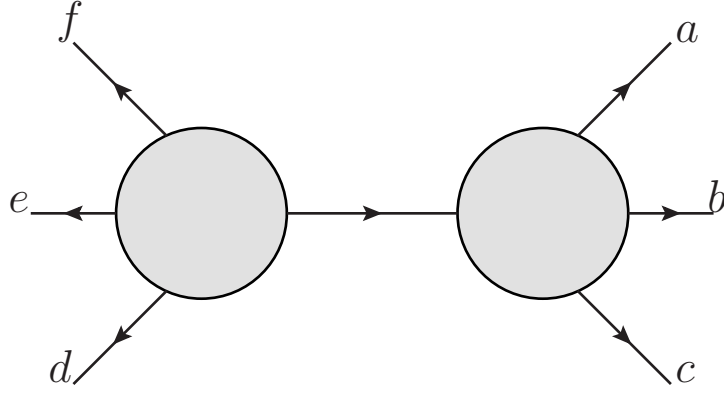
Figure 3.4: The t_{def} multiparticle factorisation. Both helicities are accounted for.

then we find something that looks like

$$\sum_{\mathcal{P}_{6:3}} \frac{\mathcal{N}_{dp}(a,b,c,d,e,f)}{\langle a\,b\rangle\,\langle b\,c\rangle\,\langle c\,d\rangle\,\langle d\,e\rangle\,\langle e\,f\rangle^2\,\langle f\,a\rangle\,t_{def}}, \tag{3.113}$$

from the double pole factorisation and

$$\sum_{\mathcal{P}_{6:3}} \frac{\mathcal{N}_{t}(a,b,c,d,e,f)}{\langle a\,b\rangle\,\langle b\,c\rangle\,\langle c\,d\rangle\,\langle d\,e\rangle\,\langle e\,f\rangle^2\,\langle f\,a\rangle\,t_{def}}, \tag{3.114}$$

from the multiparticle factorisation. The double pole and multiparticle poles are not spurious and each factorisation gives contributions to both. There is clearly an overlap and therefore an overcounting issue if we simply leave it like this. The goal is then to be able to rewrite each factorisation as

$$\sum_{\mathcal{P}_{6:3}} \frac{\mathcal{N}_{dp}(a,b,c,d,e,f)}{\langle a\,b\rangle\,\langle b\,c\rangle\,\langle c\,d\rangle\,\langle d\,e\rangle\,\langle e\,f\rangle^2\,\langle f\,a\rangle\,t_{def}}$$
$$= \sum_{\mathcal{P}_{6:3}} \frac{\mathcal{N}'_{dp}(a,b,c,d,e,f)}{\langle a\,b\rangle\,\langle b\,c\rangle\,\langle c\,d\rangle\,\langle d\,e\rangle\,\langle e\,f\rangle^2\,\langle f\,a\rangle} + \frac{\mathcal{N}_{tdp}(a,b,c,d,e,f)}{\langle a\,b\rangle\,\langle b\,c\rangle\,\langle c\,d\rangle\,\langle d\,e\rangle\,\langle e\,f\rangle^2\,\langle f\,a\rangle\,t_{def}} + \mathcal{O}(\langle e\,f\rangle^{-1}), \tag{3.115}$$

for the double pole factorisation where $\mathcal{O}(\langle e\,f\rangle^{-1})$ implies that there are no double poles in $\langle e\,f\rangle$ but says nothing about the multiparticle poles, and

$$\sum_{\mathcal{P}_{6:3}} \frac{\mathcal{N}_{t}(a,b,c,d,e,f)}{\langle a\,b\rangle\,\langle b\,c\rangle\,\langle c\,d\rangle\,\langle d\,e\rangle\,\langle e\,f\rangle^2\,\langle f\,a\rangle\,t_{def}}$$
$$= \sum_{\mathcal{P}_{6:3}} \frac{\mathcal{N}'_{t}(a,b,c,d,e,f)}{\langle a\,b\rangle\,\langle b\,c\rangle\,\langle c\,d\rangle\,\langle d\,e\rangle\,\langle e\,f\rangle\,\langle f\,a\rangle\,t_{def}} + \sum_{\mathcal{P}_{6:3}} \frac{\mathcal{N}_{tdp}(a,b,c,d,e,f)}{\langle a\,b\rangle\,\langle b\,c\rangle\,\langle c\,d\rangle\,\langle d\,e\rangle\,\langle e\,f\rangle^2\,\langle f\,a\rangle\,t_{def}} + \mathcal{O}(t^0_{def}). \tag{3.116}$$

$\mathcal{N}'_{dp}$ and $\mathcal{N}'_{t}$ here are numerators for the function which only contains the double pole and multiparticle pole respectively and we need to get $\mathcal{N}_{tdp}$ to be the same contribution from

both channels, where we can then include a symmetry factor to account for the overcounting (or equivalently throw one of them away). This can be done algebraically or we can try to build an ansatz for this. For this amplitude we needed the following result

$$A_{5:3}^{(1)}(a^+, b^+; c^-, d^+, e^+) = A_{5:3b}^{(1)}(a^+, b^+; c^-, d^+, e^+) + A_{5:3b}^{(1)}(b^+, a^+; c^-, d^+, e^+)$$
$$- A_{5:3b}^{(1)}(a^+, b^+; c^-, e^+, d^+) - A_{5:3b}^{(1)}(b^+, a^+; c^-, e^+, d^+)$$

where

$$A_{5:3b}^{(1)}(a^+, b^+; c^-, d^+, e^+) = -i \left(\frac{\langle c\,e \rangle \, \langle c|be|c \rangle}{\langle a\,b \rangle \, \langle a\,e \rangle \, \langle b\,e \rangle \, \langle c\,d \rangle \, \langle d\,e \rangle} + \frac{[d\,e] \, (s_{cd}\,[b\,e] - [b|da|e])}{\langle a\,b \rangle \, \langle a\,d \rangle \, \langle d\,e \rangle \, [c\,d] \, [c\,e]} \right). \tag{3.117}$$

which we fit numerically as it was easier to algebraically manipulate than using the decoupling identity. We used this to find $\mathcal{N}'_{dp}$, $\mathcal{N}'_t$ and $\mathcal{N}_{tdp}$ which we will see in the results section.

This covers the tricks used for numerical fitting and spurious pole cleaning that was performed at six-point. As an aside, it seems going to seven-point also introduces overlapping multiparticle poles. This does not cause issues, for example the $R_{7:2,2}(a, b; c, d; e, f, g)$ has contributions to the t_{abe} poles,

$$\frac{\mathcal{N}_1(a, b; c, d; e, f, g)}{t_{abe}t_{cdf}} + \frac{\mathcal{N}_2(a, b; c, d; e, f, g)}{t_{abe}t_{cdg}} \tag{3.118}$$

then we can manipulate the factors multiplying the t poles such that $\mathcal{N}_1(a, b; c, d; e, f, g) = \mathcal{N}_2(c, d; a, b; f, g, e) + \mathcal{O}(t_{abe})$ and we can then halve this to account for the symmetry factor when summing over the full $\mathcal{P}_{7:2,2}$ ($\frac{1}{2}$ because one of the two terms gets contributions from the t_{cdg} factorisation and the other term gets contributions from the t_{cdf} channel). $\mathcal{N}$ is a rational function not just a numerator. This implies the t_{abe} contribution from this channel would be

$$\frac{1}{2} \frac{\mathcal{N}_1(a, b; c, d; e, f, g)}{t_{abe}t_{cdf}} + \frac{1}{2} \frac{\mathcal{N}_1(c, d; a, b; f, g, e)}{t_{abe}t_{cdg}} + \mathcal{O}(t_{abe}^0), \tag{3.119}$$

although going to seven-point clearly becomes algebraically/numerically more complicated.

Back to six-point, we find the following results.

3.6 $R_{6:c}$

We below present the rational parts of each of the colour amplitudes in the two-loop colour decomposition.

3.6.1 $R_{6:1}^{(2)}$

$$R_{6:1}^{(2)}(a, b, c, d, e, f) = \frac{1}{9} \sum_{\mathcal{P}_{6:1}} \frac{G_{6:1}^1 + G_{6:1}^2 + G_{6:1}^3 + G_{6:1}^4 + G_{6:1}^5}{\langle a\,b \rangle \, \langle b\,c \rangle \, \langle c\,d \rangle \, \langle d\,e \rangle \, \langle e\,f \rangle \, \langle f\,a \rangle} \tag{3.120}$$

where

$$G^1_{6:1}(a,b,c,d,e,f) = \frac{s_{cd}s_{df}\langle f|a\,P_{abc}|e]}{\langle f\,e\rangle\,t_{abc}} + \frac{s_{ac}s_{cd}\langle a|f\,P_{def}|b]}{\langle a\,b\rangle\,t_{def}},$$

$$G^2_{6:1}(a,b,c,d,e,f) = \frac{[a\,b]\,[e\,f]}{\langle a\,b\rangle\,\langle e\,f\rangle}\,\langle a\,e\rangle^2\,\langle b\,f\rangle^2 + \frac{1}{2}\frac{[f\,a]\,[c\,d]}{\langle f\,a\rangle\,\langle c\,d\rangle}\,\langle a\,c\rangle^2\,\langle d\,f\rangle^2,$$

$$G^3_{6:1}(a,b,c,d,e,f) = \frac{s_{df}\,\langle f\,a\rangle\,\langle c\,d\rangle\,[a\,c]\,[d\,f]}{t_{abc}},$$

$$G^4_{6:1}(a,b,c,d,e,f) = \frac{\langle a|be|f\rangle t_{abc}}{\langle a\,f\rangle} \tag{3.121}$$

and

$$G^5_{6:1}(a,b,c,d,e,f) = s_{fa}s_{bc} + s_{ac}s_{be} + \frac{5}{2}s_{af}s_{cd} - 8[a|bcf|a\rangle - 8[a|cde|a\rangle - \frac{1}{2}[a|cdf|a\rangle - \frac{11}{2}[b|cef|b\rangle \tag{3.122}$$

This was first calculated in [68] and later presented in a alternate form [69]. It was susequently confirmed by Badger et al in [95].

3.6.2 $\quad R^{(2)}_{6:3}$

$$R^{(2)}_{6:3}(a,b;c,d,e,f) = \sum_{\mathcal{P}_{6:3}} \Bigg[\frac{1}{3}\Big(H^1_{6:3}(a,b,c,d,e,f) - H^1_{6:3}(a,b,c,d,f,e) \Big)$$

$$+ \frac{1}{3} \frac{\Big(G^2_{6:3}(a,b,c,d,e,f) + G^3_{6:3}(a,b,c,d,e,f) + G^4_{6:3}(a,b,c,d,e,f) \Big)}{\langle a\,b\rangle\,\langle b\,c\rangle\,\langle c\,a\rangle\,\langle d\,e\rangle\,\langle e\,f\rangle\,\langle f\,d\rangle}$$

$$+ \frac{1}{12} \frac{G^5_{6:3}(a,b,c,d,e,f)}{\langle a\,b\rangle\,\langle b\,c\rangle\,\langle c\,d\rangle\,\langle d\,e\rangle\,\langle e\,f\rangle\,\langle f\,a\rangle} \Bigg] \tag{3.123}$$

where

$$H^1_{6:3}(a,b,c,d,e,f) = \frac{G^1_{6:3}(a,b,c,d,e,f)}{\langle a\,b\rangle\,\langle b\,c\rangle\,\langle c\,d\rangle^2\,\langle d\,e\rangle\,\langle e\,f\rangle\,\langle f\,a\rangle} + \frac{[c\,d]}{\langle c\,d\rangle^2}\frac{\langle c\,f\rangle\,\langle d\,b\rangle\,[b|f|d\rangle}{\langle a\,b\rangle\,\langle a\,f\rangle\,\langle b\,f\rangle\,\langle d\,e\rangle\,\langle e\,f\rangle}$$

$$G^1_{6:3}(a,b,c,d,e,f) = s_{ce}\langle c|bf|d\rangle - s_{cf}\langle c|be|d\rangle$$

$$G^2_{6:3}(a,b,c,d,e,f) = \frac{[d|P_{def}b|a]\langle d|fP_{def}|a\rangle + s_{de}[f|cbd|f\rangle + [b|df|e]\langle b|cP_{abc}|e\rangle}{t_{def}}$$

$$G^3_{6:3}(a,b,c,d,e,f) = -\frac{s_{df}\langle d|fb|c\rangle[c|P_{ab}|e\rangle}{\langle d\,e\rangle\,t_{def}} - \frac{s_{de}\langle f|db|c\rangle[c|d|e\rangle}{\langle e\,f\rangle\,t_{def}}$$

$$G^4_{6:3}(a,b,c,d,e,f) = -s_{bd}s_{de} - [a|bde|a\rangle + [b|cde|b\rangle - [a|bdf|a\rangle$$
$$+ [b|cdf|b\rangle + [b|cef|b\rangle - [b|def|b\rangle$$

$$G^5_{6:3}(a,b,c,d,e,f) = -4s^2_{ac} + 2s_{ab}s_{ad} - 2s_{ac}s_{ad} + 2s_{ab}s_{ae} - 2s_{ac}s_{ae} + 2s^2_{bd} - 2s^2_{be} + 2s^2_{bf}$$
$$- 8s_{ac}s_{cd} + 4s_{bc}s_{cd} + 12s_{bd}s_{cd} + 6s^2_{cd} - 8s_{ac}s_{ce} + 12s_{bc}s_{ce} + 16s_{bd}s_{ce}$$
$$+ 4s_{be}s_{ce} + 8s_{cd}s_{ce} + 2s^2_{ce} + 2s^2_{cf} - 8s_{ac}s_{de} - 4s_{ad}s_{de} - 4s_{bc}s_{de} + 4s_{cd}s_{de}$$
$$+ 4s_{ce}s_{de} - 8[a|bce|a\rangle - 39[a|bcf|a\rangle - 18[a|bdf|a\rangle + 2[a|bef|a\rangle$$
$$- 10[a|cdf|a\rangle - 2[a|cef|a\rangle - 4[a|def|a\rangle + 8[b|cde|b\rangle - 4[b|cdf|b\rangle$$
$$- 4[b|cef|b\rangle - 4[b|def|b\rangle - 4[c|def|c\rangle \tag{3.124}$$

80

We chose to organise the results to follow the form of $A_{5:3}(a^+, b^+; k^-, c^+, d^+)$ here but we could have organised it by pole structures as we do for the other amplitudes.

3.6.3 $\mathbf{R}_{6:4}^{(2)}$

$$R_{6:4}^{(2)}(a, b, c, d, e, f) = \frac{1}{36} \sum_{\mathcal{P}_{6:4}} \left[\frac{\left(G_{6:4}^1(a, b, c, d, e, f) + G_{6:4}^2(a, b, c, d, e, f) \right)}{\langle a\,b \rangle \langle b\,c \rangle \langle c\,a \rangle \langle d\,e \rangle \langle e\,f \rangle \langle f\,d \rangle} \right.$$
$$\left. + 12 \frac{\left(G_{6:4}^3(a, b, c, d, e, f) + G_{6:4}^4(a, b, c, d, e, f) \right)}{\langle a\,b \rangle \langle c\,d \rangle \langle d\,e \rangle \langle e\,f \rangle \langle f\,c \rangle} \right], \qquad (3.125)$$

where

$$G_{6:4}^1(a, b, c, d, e, f) = \frac{4 \langle e|P_{abc}a|b \rangle [e|dP_{abc}|b]}{t_{abc}},$$
$$G_{6:4}^2(a, b, c, d, e, f) = s_{ad}^2 + 106\, s_{ab}s_{ad} + 102\, [a|bcd|a\rangle - 4\, [a|bde|a\rangle - 4\, [a|dbe|a\rangle,$$
$$G_{6:4}^3(a, b, c, d, e, f) = -\frac{[a\,b]}{\langle a\,b \rangle} \Big(\langle a|cd|b\rangle + \langle a|ef|b\rangle \Big),$$
$$G_{6:4}^4(a, b, c, d, e, f) = [a|cd|b] + [a|ef|b]. \qquad (3.126)$$

3.6.4 $\mathbf{R}_{6:2,2}^{(2)}$

$$R_{6:2,2}^{(2)}(a, b; c, d; e, f) = \sum_{\mathcal{P}_{6:2,2}} \frac{G_{6:2,2}^1(a, b, c, d, e, f) + G_{6:2,2}^2(a, b, c, d, e, f)}{\langle a\,b \rangle \langle b\,c \rangle \langle c\,a \rangle \langle d\,e \rangle \langle e\,f \rangle \langle f\,d \rangle}, \qquad (3.127)$$

where

$$G_{6:2,2}^1(a, b, c, d, e, f) = \frac{\langle b|P_{abc}f|d \rangle [b|cP_{abc}|d]}{t_{abc}},$$
$$G_{6:2,2}^2(a, b, c, d, e, f) = s_{ad}[e|P_{bc}|e\rangle - s_{ac}[e|P_{fa}|e\rangle - s_{af}s_{ae} - s_{ae}s_{cd}. \qquad (3.128)$$

3.6.5 $\mathbf{R}_{6:1B}^{(2)}$

We will conjecture an n-point formula for this amplitude in Chapter 4 for which we find full agreement here.

$$R_{6:1B}^{(2)}(a, b, c, d, e, f) = R_{6:1B_1}^{(2)}(a, b, c, d, e, f) + R_{6:1B_2}^{(2)}(a, b, c, d, e, f) \qquad (3.129)$$

where

$$R_{6:1B_1}^{(2)}(a, b, c, d, e, f) = \frac{-2}{\mathrm{C_y}(a, b, c, d, e, f)} \times \sum_{a \leq i < j < k < l \leq f} \epsilon(i, j, k, l) \qquad (3.130)$$

81

and

$$R^{(2)}_{6:1B_2}(a,b,c,d,e,f) = 4\Big(\frac{\epsilon(c,d,e,f)}{\mathrm{C_y}(a,b,d,e,c,f)} + \frac{\epsilon(c,d,e,f)}{\mathrm{C_y}(a,b,e,c,d,f)} + \frac{\epsilon(c,d,e,f)}{\mathrm{C_y}(a,b,e,d,c,f)}$$

$$+\frac{\epsilon(a,b,c,d)}{\mathrm{C_y}(a,c,d,b,e,f)} - \frac{\epsilon(a,b,c,f)}{\mathrm{C_y}(a,c,d,e,b,f)} + \frac{\epsilon(a,b,c,d)}{\mathrm{C_y}(a,d,b,c,e,f)} - \frac{\epsilon(a,c,d,f)}{\mathrm{C_y}(a,d,b,e,c,f)}$$

$$+\frac{\epsilon(a,b,c,d)}{\mathrm{C_y}(a,d,c,b,e,f)} + \frac{\epsilon(a,b,d,f)}{\mathrm{C_y}(a,d,c,e,b,f)} - \frac{\epsilon(a,c,d,f)}{\mathrm{C_y}(a,d,e,b,c,f)} + \frac{\epsilon(a,b,d,f)}{\mathrm{C_y}(a,d,e,c,b,f)}$$

$$-\frac{\epsilon(a,d,e,f)}{\mathrm{C_y}(a,e,b,c,d,f)} + \frac{\epsilon(a,c,e,f)}{\mathrm{C_y}(a,e,b,d,c,f)} + \frac{\epsilon(a,c,e,f)}{\mathrm{C_y}(a,e,d,b,c,f)} - \frac{\epsilon(a,b,e,f)}{\mathrm{C_y}(a,e,d,c,b,f)}\Big) \quad (3.131)$$

where $\mathrm{C_y}(a_1,a_2,a_3,a_4,a_5,a_6)$ is the cyclic Parke-Taylor denominator for six gluons,

$$\mathrm{C_y}(a,b,c,d,e,f) = \langle a\,b\rangle \langle b\,c\rangle \langle c\,d\rangle \langle d\,e\rangle \langle e\,f\rangle \langle f\,a\rangle. \quad (3.132)$$

3.6.6 $\mathbf{R^{(2)}_{6:1,1}}$

We also calculate the $U(N_c)$ amplitudes

$$R^{(2)}_{6:1,1}(a;b;c,d,e,f) = \sum_{\mathcal{P}_{6:1,1}} \Bigg(\frac{G^1_{6:1,1}(a,b,c,d,e,f) + G^2_{6:1,1}(a,b,c,d,e,f)}{\langle b\,c\rangle \langle c\,d\rangle \langle d\,b\rangle \langle a\,e\rangle \langle e\,f\rangle \langle f\,a\rangle}$$

$$+ \frac{G^3_{6:1,1}(a,b,c,d,e,f)}{\langle a\,c\rangle \langle c\,d\rangle \langle d\,b\rangle \langle b\,e\rangle \langle e\,f\rangle \langle f\,a\rangle} \Bigg) \quad (3.133)$$

where

$$G^1_{6:1,1}(a,b,c,d,e,f) = \frac{[c|P_{bcd}\,ef\,P_{bcd}\,b|c\rangle}{t_{bcd}},$$

$$G^2_{6:1,1}(a,b,c,d,e,f) = 2s_{ab}s_{cd} - s_{ac}s_{ae} + s_{ac}s_{cd} + s_{ad}s_{cd} - s^2_{cd} - s_{cd}s_{ce} - s_{cd}s_{cf} - s_{cd}s_{df}$$

$$- [a|cde|a\rangle + \frac{1}{2}[c|def|c\rangle$$

and

$$G^3_{6:1,1}(a,b,c,d,e,f) = 2s_{ab}s_{ac} + 2s^2_{ac} + 2s_{ac}s_{ad} + 2s_{ac}s_{ae} + 2s_{ac}s_{bc} - s_{ae}s_{bc} + s_{ab}s_{cd} + s_{ac}s_{cd}$$

$$+ s_{ad}s_{cd} - 2s_{ae}s_{cd} + 2s_{ad}s_{ce} - 2s_{ae}s_{ce} - s_{cd}s_{ce} - s^2_{ce} - s_{cd}s_{cf} + s_{ce}s_{df}$$

$$- \frac{1}{2}s_{cd}s_{ef} + 2[a|cbd|a\rangle + 2[a|cbe|a\rangle + 4[a|cde|a\rangle - [c|def|c\rangle. \quad (3.134)$$

3.6.7 $\mathbf{R^{(2)}_{6:1,2}}$

$$R^{(2)}_{6:1,2}(a;b,c;d,e,f) = \sum_{\mathcal{P}_{6:2,1}} \frac{\Big(G^1_{6:1,2}(a,b,c,d,e,f) + G^2_{6:1,2}(a,b,c,d,e,f)\Big)}{\langle e\,f\rangle \langle f\,a\rangle \langle a\,e\rangle \langle b\,c\rangle \langle c\,d\rangle \langle d\,b\rangle} \quad (3.135)$$

where

$$G^1_{6:1,2}(a,b,c,d,e,f) = -\frac{[e|f P_{bc}\,db\,P_{cd}|e\rangle + [e|P_{cd}\,bc\,P_{bd}\,a|e\rangle}{t_{bcd}},$$

$$G^2_{6:1,2}(a,b,c,d,e,f) = [a|bce|a\rangle - 2[b|dce|b\rangle + [b|def|b\rangle \quad (3.136)$$

3.6.8 $\mathbf{R^{(2)}_{6:2}}$

It is compactly written by its decoupling identity which was checked numerically.

$$R^{(2)}_{6:2}(a; b, c, d, e, f) = -\sum_{\mathcal{P}_{6:2}} R^{(2)}_{6:1}(a, b, c, d, e, f) \qquad (3.137)$$

where the sum is over legs $Z_5(b, c, d, e, f)$. These expressions are valid for both $U(N_c)$ and $SU(N_c)$ gauge groups and are remarkably compact. We have confirmed that they satisfy the constraints arising from the decoupling identities. The $SU(N_c)$ amplitudes have the correct collinear limits: all non-adjacent and inter-trace limits vanish and adjacent limits within a single trace factorise correctly. All of the partial amplitudes have the correct symmetries. Again, recursion involves choosing specific legs to shift, breaking the symmetry of the amplitude. Restoration of this symmetry is a powerful check of the validity of our results. We have checked that none of the $R^{(2)}_{6:c}$ are annihilated by the conformal operator.

This was the first full-colour, six-point, two-loop amplitude to be calculated. Going to seven-point, we should not see any more types of currents needed and the leading, adjacent current has already been calculated in [69]. Indeed, the seven-point, full-colour, two-loop, all-plus helicity amplitude has been fully calculated and we now have compact forms, although this publication is presently being prepared. Of course, n-point expressions are highly desirable and we move now onto an n-point calculation and conjecture.

Chapter 4

n-point QCD Two-Loop Amplitudes

4.1 Introduction

We have thus far looked at how the study of scattering amplitudes has evolved over the years, from Feynman diagrams to the techniques of today. In this discussion we have covered the use of four-dimensional unitarity and augmented recursion to simplify calculation, and in doing so have calculated the full-colour, two-loop amplitudes for the all-plus helicity configuration for five- and six-points. We briefly mention how the seven-point version of this amplitude has also been calculated but we await the publication of compact results for the rational part of it. These calculations become more complicated with added legs, although we argue that with these techniques, higher multiplicity does not pose anything more complicated than larger ansatz and numerical files to fit against in the functional reconstruction step. Nevertheless, an n-point formula for amplitudes is clearly highly desirable.

In this chapter, we continue the all-plus helicity discussion and we will present a conjecture for a very specific colour partial two-loop amplitude which is valid for an arbitrary number of legs. We have already discussed this amplitude as being the "maximally non-planar" amplitude $A_{n:1B}^{(2)}$ from (1.90). From a very different viewpoint, this partial amplitude arises in open string theory from the non-planar, two loop orientable surface. Although it is very specific this hopefully will provide a useful multi-leg two loop expression from which to study the structure and properties of amplitudes.

We will also explicitly calculate the n-point, full-colour, cut-constructible part of the two-loop, all-plus helicity amplitude (cut-constructible from a four-dimensional unitarity perspective). While this is not the full amplitude as we do not get the rational piece, it serves as a good check for future calculations.

4.2 A String Theory Interlude

We assume here that the reader has already read the details of two-loop colour structures from previous chapters. As a summary, there are no decoupling identities that relate $A_{n:1B}^{(2)}$ to other partial amplitudes but they do exhibit a tree-like decoupling identity (2.18). Further group theory relations exist [39] which do give relations between $A_{n:1B}^{(2)}$ and other $\mathrm{SU}(N_c)$ amplitudes but do not fully constrain this amplitude beyond five-points. The origin of this partial amplitude is easier to understand from a string theory perspective, although we do not go into the details of string theory in this thesis.

String theory contains massless gauge bosons as part of its spectrum of states and much can be gleaned from the string theory organisation of the scattering amplitudes. An open string has endpoints with the quantum numbers of quarks and anti-quarks (Chan-Paton factors). A string amplitude is obtained by summing over all world sheets linking the external states. A simple example is shown in Figure 4.1.
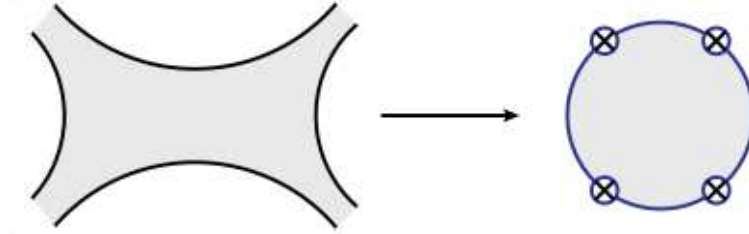
Figure 4.1: In open string theory, the surface linking external open string states may be mapped to a disc where the external states are vertex operators lying on the boundary.

The surface linking the external states can be conformally mapped to the surface shown with vertex operators attached to the boundary. Each vertex operator contains an adjoint colour matrix T^a. Tracing over the colour indices naturally gives an expansion of the amplitude in terms of colour traces

$$A = \sum (\text{colour traces}) \times A(\alpha)$$

where α is the string tension. The string theory amplitude contains contributions from an infinite number of states however in the infinite string tension limit the amplitude reduces to that of field theory. The colour structure survives this limit.
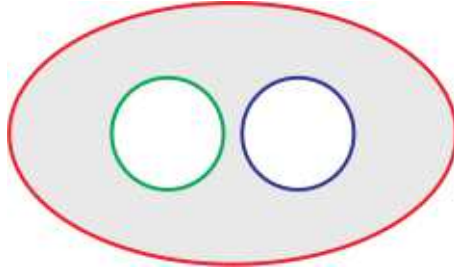
Figure 4.2: A typical surface with three boundaries. Vertex operators can be attached to any of the boundaries.

A typical surface contributing at two-loop is shown in Figure 4.2. This has three boundaries to which gauge boson vertex operators may be attached. If any edge is free of gauge bosons, a factor of N_c is generated by summing over the colours the boundary may have. Populating this surface by vertex operators generates the expansion of (1.90) *except* for the single trace term $A^{(2)}_{n:1B}$. This arises from a different category of surface. If we consider the surface shown in Figure 4.3 with the edges identified as shown then the surface is a two-loop surface which is non-planar, but nonetheless is oriented and has a single boundary. Attaching gauge bosons to the edge gives the single trace term and is, in string theory, the source of $A^{(2)}_{n:1B}$.
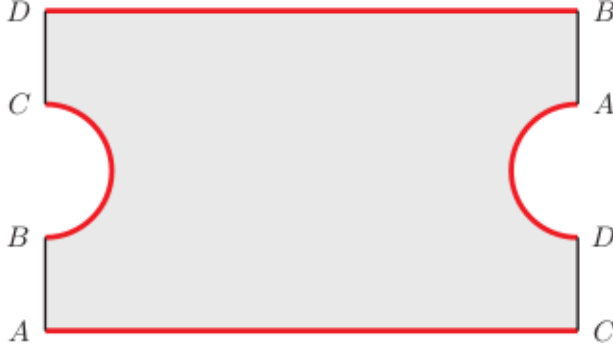
Figure 4.3: This surface with edges $A - B$ and $C - D$ identified is an oriented surface with a single edge. In string theory attaching vector bosons to the edge of this surface generates the sub-sub-leading single trace colour term.

4.3 The All-plus Amplitudes

We are now in a position to look at the specific amplitude where all gluons have the same helicity. Again we will assume the reader has seen the details of this amplitude in the previous chapter so we will only summarise here. The tree-level amplitude vanishes for this helicity configuration. Consequently, the one-loop amplitude is rational (to order ϵ^0 in the dimensional regularisation parameter) and the two-loop amplitudes will have a simpler singular structure in ϵ.

The leading in colour one-loop partial amplitude has an all-n expression [63]

$$A_{n:1}^{(1)}(1^+, 2^+, \ldots, n^+) = -\frac{1}{3} \frac{1}{\langle 1\,2 \rangle \langle 2\,3 \rangle \cdots \langle n\,1 \rangle} \sum_{1 \le i < j < k < l \le n} \mathrm{tr}_-[ijkl] + O(\epsilon). \qquad (4.1)$$

This expression is order ϵ^0 but all-ϵ expressions exist for the first few amplitudes in this series [46]. In this expression,

$$\mathrm{tr}_-[ijkl] \equiv \mathrm{tr}(\frac{(1-\gamma_5)}{2} \slashed{k}_i \slashed{k}_j \slashed{k}_k \slashed{k}_l) = \frac{1}{2}\mathrm{tr}(\slashed{k}_i \slashed{k}_j \slashed{k}_k \slashed{k}_l) - \frac{1}{2}\varepsilon(i,j,k,l) = \langle i\,j \rangle [j\,k] \langle k\,l \rangle [l\,i], \quad (4.2)$$

and $\varepsilon(i,j,k,l) = \mathrm{tr}_+[ijkl] - \mathrm{tr}_-[ijkl]$. $\mathrm{tr}_+[ijkl]$ is similarly $\mathrm{tr}(\frac{1+\gamma_5}{2} \slashed{k}_i \slashed{k}_j \slashed{k}_k \slashed{k}_l)$. This amplitude has the same denominator as the Parke-Taylor amplitude. This combination will reappear in many places so we define

$$\mathrm{C_{PT}}(a_1, a_2, a_3, \cdots, a_n) \equiv \frac{1}{\langle a_1\,a_2 \rangle \langle a_2\,a_3 \rangle \cdots \langle a_n\,a_1 \rangle} \equiv \frac{1}{\mathrm{C_y}(a_1, a_2, a_3, \cdots, a_n)}. \qquad (4.3)$$

Interestingly, the numerator of (4.1) can be split into trace terms and ε pieces (originally called E_n and O_n in ref [63]). Specifically for the five point amplitude,

$$A_{5:1}^{(1)}(1^+, 2^+, 3^+, 4^+, 5^+) = -\frac{1}{3} \frac{s_{12}s_{23} + s_{23}s_{34} + s_{34}s_{45} + s_{45}s_{51} + s_{51}s_{12} + \varepsilon(1,2,3,4)}{\langle 1\,2 \rangle \langle 2\,3 \rangle \langle 3\,4 \rangle \langle 4\,5 \rangle \langle 5\,1 \rangle} + O(\epsilon).$$
$$(4.4)$$

The expression (4.1) was first conjectured by studying collinear limits starting with $n = 5$ and later proven correct using off-shell recursion [96]. This division into E_n and O_n and collinear limit viewpoint is important as we will shortly conjecture an n-point expression using only

collinear limits and inspired by this division. In fact, we will see that O_n appears again in the two-loop amplitude.

Continuing with the all-plus summary, in [70] and Chapter 2, we presented compact expressions for the subleading terms

$$A_{n:2}^{(1)}(1^+; 2^+, 3^+, \cdots, n^+) = -\frac{1}{\langle 2\,3\rangle \langle 3\,4\rangle \cdots \langle n\,2\rangle} \sum_{2 \leq i < j \leq n} [1\,i]\,\langle i\,j\rangle\,[j\,1]$$

$$= -\frac{\sum_{2 \leq i < j \leq n} [1\,i]\,\langle i\,j\rangle\,[j\,1]}{\mathrm{C_y}(2, 3, \cdots, n)}$$

and for $r \geq 3$

$$A_{n:r}^{(1)}(1^+, 2^+, \cdots, r-1^+; r^+, \cdots, n^+) = -2\frac{(K_{1 \cdots r-1}^2)^2}{(\langle 1\,2\rangle \langle 2\,3\rangle \cdots \langle (r-1)\,1\rangle)(\langle r\,(r+1)\rangle \cdots \langle n\,r\rangle)}$$

$$= -2\frac{(K_{1 \cdots r-1}^2)^2}{\mathrm{C_y}(1, 2, \cdots, r-1)\mathrm{C_y}(r, r+1, \cdots, n)}.$$

These expressions are remarkably simple given the number of terms arising in the naive application of (2.3). They will also be useful in calculating the n-point cut-constructible piece.

At two-loop, the all-plus amplitude has been computed for four, five and six-points, its relative simplicity making it the first target in computations. We have already covered the five and six-point calculation in this thesis and we previously separated the amplitude into a cut-constructible piece and a rational piece,

$$A_{n:c}^{(2)} = P_{n:c}^{(2)} + R_{n:c}^{(2)}.$$

Here, by cut-constructible piece we mean singular pieces and polylogarithmic pieces, four-dimensional unitarity might recover some rational pieces but it will not capture the whole contribution and so we discard anything rational and finite, using augmented recursion to obtain the entire rational piece as a separate calculation.

The IR singular structure of a colour partial amplitude is determined by general theorems [33]. Consequently we can split the cut-constructible amplitude into a term containing both the IR and UV divergences, $U_{n:c}^{(2)}$, and finite terms $F_{n:c}^{(2)}$,

$$P_{n:c}^{(2)} = U_{n:c}^{(2)} + F_{n:c}^{(2)} + \mathcal{O}(\epsilon) \tag{4.5}$$

where $F_{n:c}^{(2)}$ is the "infrared finite hard" function of reference [87].

We have seen that for this helicity configuration, both the UV divergences and collinear IR divergences are proportional to n and cancel leaving only the soft IR singular terms [32]. We have also seen that $U_{n:c}^{(2)}$ is known via general theorems [33] and that it is given for $c = 1B$ in (1.106).

Given the general expressions for $U_{n:c}^{(2)}$, the challenge is to compute the finite parts of the amplitude: $F_{n:c}^{(2)}$ and $R_{n:c}^{(2)}$. We calculate the polylogarithmic piece using four-dimensional unitarity and for this partial amplitude we can calculate the rational term using only the factorisation properties of the amplitude, which we will discuss in the following section.

4.4 Factorisation Properties of $A_{n:1B}^{(2)}$

In this section we make some comments regarding the singularity structure of the sub-sub leading amplitudes: $A_{n:1B}^{(2)}$ and $A_{n:s,t}^{(2)}$. In general amplitudes have:

1. Multiparticle Poles

2. Double Complex Poles

3. Complex Poles

4. Collinear Poles

We will demonstrate that $A_{n:1B}$ is lacking the first two and that only the last is determined by general theorems. Fortunately this will be sufficient to generate a form for the rational functions.

As the all-plus amplitude vanishes at tree level, multiparticle poles can only arise if the amplitude factorises into two one-loop factors,

$$\mathcal{A}^{1-loop}(\cdots, K_i^\lambda) \times \frac{1}{K^2} \times \mathcal{A}^{1-loop}(\cdots, -K_i^{-\lambda}).\tag{4.6}$$

This is non-zero with one amplitude being the single minus one-loop amplitude and the other the all-plus. Both of these are rational. Only the subleading amplitudes from each of the one-loop factors will contribute to the N_c^0 term and the colour terms must be of the form

$$\sim \text{Tr}(iS_1)\,\text{Tr}(S_2) \times \text{Tr}(iS_3)\,\text{Tr}(S_4)\tag{4.7}$$

where we sum over the colour matrix T^i and we have suppressed the explicit colour matrices for the lists of legs S_i. The S_1 and S_3 may be null and if both are null, we obtain a factor of N_c. Otherwise we obtain

$$\text{Tr}(S_1S_3)\,\text{Tr}(S_2)\,\text{Tr}(S_4).\tag{4.8}$$

So there are (one-loop)-(one-loop) factorisations in $A_{n:s,t}^{(2)}$ but not in $A_{n:1B}^{(2)}$. Therefore $A_{n:1B}^{(2)}$ has no $1/K^2$ terms for K being made up of more than two particles. The presence of the single minus amplitude within the factorisation makes all-n expressions difficult to find because there is no compact n-point expression for the one-loop single-minus amplitude.

Amplitudes also contain double poles in complex momentum. These arise from diagrams such as shown in Figure 4.4 where one factor arises from the explicit pole and the other from the loop integral.
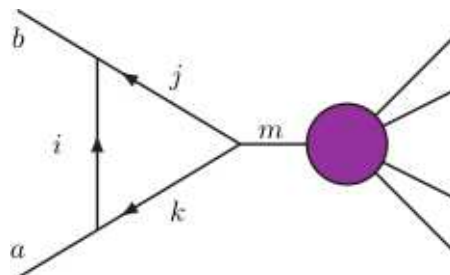
Figure 4.4: Contributions to amplitudes giving a double pole with color indices shown.

The colour structure of the double pole diagram therefore contains

$$f^{aik} f^{bij} f^{kjm} A(m, \cdots).$$ (4.9)

We can turn this into colour traces and evaluate:

$$\left(\text{Tr}[aki] - \text{Tr}[kai] \right) \left(\text{Tr}[bji] - \text{Tr}[jbi] \right) \left(\text{Tr}[kjm] - \text{Tr}[kmj] \right)$$
$$= N_c \text{Tr}[bam] - N_c \text{Tr}[abm].$$

Hence there is no N_c^0 contribution and so both $A_{n:1B}^{(2)}$ and $A_{n:s,t}^{(2)}$ are free of double poles.

Unfortunately, the single poles are not as simple as one might imagine. For example, at five point the potential factorisation

$$A_{5:1B}^{(2)} \longrightarrow A_3^{(0)}(a^+, b^+, K^-) \times \frac{1}{s_{ab}} \times A_{4:1B}^{(2)}(K^+, \cdots)$$ (4.10)

vanishes since $A_{4:1B}^{(2)}(1^+, 2^+, 3^+, 4^+) = 0$, nonetheless $A_{5:1B}^{(2)}$ has poles in $\langle a\, b \rangle$. These single poles arise from non-factorising terms as computed in [70, 71] where the double and single poles are determined for the $n = 5$ and $n = 6$ cases. These may be seen as "pole under the pole" parts of double poles as seen with other colour structures, but with the coefficient of the double pole piece being zero.

Finally we consider collinear limits. If adjacent legs a and b become collinear with $k_a = zK$ and $k_b = (1 - z)K$, then we expect

$$A_{n:1B}^{(2)}(\cdots, a^+, b^+, \cdots) \longrightarrow S_-^{++}(a, b, K) A_{n-1:1B}^{(2)}(\cdots, K^+, \cdots)$$ (4.11)

where

$$S_-^{++}(a, b, K) = \frac{1}{\sqrt{z(1-z)} \, \langle a\, b \rangle} \, .$$ (4.12)

The amplitude has no collinear singularity if a and b are not adjacent. Demanding the correct collinear behaviour was sufficient to generate the conjecture for the one-loop all plus amplitude, and we will now generate a conjecture for the rational part of $A_{n:1B}^{(2)}$ using collinear limits. This will be proceeded by an explicit calculation of the finite polylogarithmic part of the full all-plus amplitude at n-points.

4.5   Explicit Formula of $R_{n:1B}^{(2)}$

The four point amplitude $R_{4:1B}^{(2)}$ has been calculated in [78, 79] as part of the full four point computation and found to vanish:

$$R_{4:1B}^{(2)}(1^+, 2^+, 3^+, 4^+) = 0 \, .$$ (4.13)

The five point amplitude has been computed. In [87] , five point amplitudes $A_{5:1}^{(2)}$ and $A_{5:3}^{(2)}$ were computed explicitly. Using the results of [39] this implies a form of $A_{5:1B}^{(2)}$. In [70] the $A_{5:r}^{(2)}$ were recomputed using augmented recursion [64, 69] and four dimensional unitarity and

$A^{(2)}_{5:1B}$ was computed directly in a simple form. The explicit form is

$$R^{(2)}_{5:1B}(1^+, 2^+, 3^+, 4^+, 5^+) = 2\varepsilon\,(1,2,3,4) \sum_{Z_5(1,2,3,4,5)} \mathrm{C_{PT}}(1,2,5,3,4)$$

$$= 2\varepsilon\,(1,2,3,4) \left(\mathrm{C_{PT}}(1,2,5,3,4) + \mathrm{C_{PT}}(2,3,1,4,5) + \mathrm{C_{PT}}(3,4,2,5,1) \right.$$

$$\left. + \mathrm{C_{PT}}(4,5,3,1,2) + \mathrm{C_{PT}}(5,1,4,2,3) \right)$$

Since the summation is over the five cyclic permutations of the legs $(1,2,3,4,5)$ this expression is manifestly cyclically symmetric. However it is far from unique since the Parke-Taylor factors $\mathrm{C_{PT}}$ are not all linearly independent. Since they are manifestly cyclic symmetric there are clearly $(n-1)!$ terms. They also satisfy identities identical to the decoupling identity for tree amplitudes which can be used to reduce these to a basis of $(n-2)!$ independent terms. Specifically we can rewrite

$$\sum_{(a_2,a_3,\cdot,a_n)\in P(2,3,\cdots,n)} \alpha_i \mathrm{C_{PT}}(1,a_2,a_3,\cdots,a_n) = \sum_{(a_2,a_3,\cdot,a_{n-1})\in P(2,3,\cdots,n-1)} \alpha'_i \mathrm{C_{PT}}(1,a_2,a_3,\cdots,a_{n-1},n)$$

$$(4.14)$$

If we choose to rewrite $R^{(2)}_{n:1B}$ in terms of this reduced set, cyclic symmetry will not be manifest but there is the advantage of working with a basis rather than a spanning set. For the five point amplitude we then have

$$R^{(2)}_{5:1B}(1^+, 2^+, 3^+, 4^+, 5^+) \quad = 2\varepsilon\,(1,2,3,4) \left(-\mathrm{C_{PT}}(1,2,3,4,5) \right. \qquad (4.15)$$

$$\left. + 2\Big(\mathrm{C_{PT}}(1,3,4,2,5) + \mathrm{C_{PT}}(1,4,3,2,5) + \mathrm{C_{PT}}(1,4,2,3,5) \Big) \right)$$

This can be split into two parts

$$R^{(2)}_{5:1B}(1^+, 2^+, 3^+, 4^+, 5^+) \quad = R^{(2)}_{5:1B_1}(1^+, 2^+, 3^+, 4^+, 5^+) + R^{(2)}_{5:1B_2}(1^+, 2^+, 3^+, 4^+, 5^+) \quad (4.16)$$

where

$$R^{(2)}_{5:1B_1}(1^+, 2^+, 3^+, 4^+, 5^+) \;=\; -2\varepsilon\,(1,2,3,4)\,\mathrm{C_{PT}}(1,2,3,4,5) \qquad (4.17)$$

$$R^{(2)}_{5:1B_2}(1^+, 2^+, 3^+, 4^+, 5^+) \;=\; 4\varepsilon\,(1,2,3,4)\,(\mathrm{C_{PT}}(1,3,4,2,5) + \mathrm{C_{PT}}(1,4,3,2,5) + \mathrm{C_{PT}}(1,4,2,3,5))$$

The term $R^{(2)}_{5:1B_1}$ is reminiscent of the one loop expression which allows us to propose the n-point expression

$$R^{(2)}_{n:1B_1}(1^+, 2^+, \cdots, n^+) = -2\,\mathrm{C_{PT}}(1,2,\cdots,n-1,n) \times \sum_{1\leq i<j<k<l\leq n} \varepsilon(i,j,k,l) \qquad (4.18)$$

90

The expression for $R^{(2)}_{6:1B_2}$ has fourteen terms,

$$
\begin{aligned}
R^{(2)}_{6:1B_2}(1^+, 2^+, 3^+, 4^+, 5^+, 6^+) = 4i\Big(& \frac{\varepsilon(3,4,5,6)}{C_y(1,2,4,5,3,6)} + \frac{\varepsilon(3,4,5,6)}{C_y(1,2,5,3,4,6)} + \frac{\varepsilon(3,4,5,6)}{C_y(1,2,5,4,3,6)} \\
& + \frac{\varepsilon(1,2,3,4)}{C_y(1,3,4,2,5,6)} - \frac{\varepsilon(1,2,3,6)}{C_y(1,3,4,5,2,6)} + \frac{\varepsilon(1,2,3,4)}{C_y(1,4,2,3,5,6)} - \frac{\varepsilon(1,3,4,6)}{C_y(1,4,2,5,3,6)} \\
& + \frac{\varepsilon(1,2,3,4)}{C_y(1,4,3,2,5,6)} + \frac{\varepsilon(1,2,4,6)}{C_y(1,4,3,5,2,6)} - \frac{\varepsilon(1,3,4,6)}{C_y(1,4,5,2,3,6)} + \frac{\varepsilon(1,2,4,6)}{C_y(1,4,5,3,2,6)} \\
& - \frac{\varepsilon(1,4,5,6)}{C_y(1,5,2,3,4,6)} + \frac{\varepsilon(1,3,5,6)}{C_y(1,5,2,4,3,6)} + \frac{\varepsilon(1,3,5,6)}{C_y(1,5,4,2,3,6)} - \frac{\varepsilon(1,2,5,6)}{C_y(1,5,4,3,2,6)} \Big) .
\end{aligned}
\tag{4.19}
$$

This expression was first constructed by demanding it satisfy the correct collinear limits and subsequently verified using augmented recursion techniques as we saw in Chapter 3.

While this is the minimal expression, it is not the best for generalising. Defining

$$
\varepsilon(\{a_1, a_2, \cdots, a_m\}, b, c, \{d_1, d_2, \cdots, d_p\}) \equiv \sum_{i=1}^{m} \sum_{j=1}^{p} \varepsilon(a_i, b, c, d_j) ,
\tag{4.20}
$$

we can replace $\varepsilon(3,4,5,6)$ by $\varepsilon(\{1,2\},4,3,6)$ etc. which makes the following pattern clearer [97].

Then by demanding the correct collinear limits we are led to the expression

$$
R^{(2)}_{n:1B_2}(1^+, 2^+, \cdots, n^+) = 4 \sum_{r=1}^{n-4} \sum_{s=r+4}^{n}
$$

$$
\sum_{i=r+1}^{s-2} \sum_{j=i+1}^{s-1} \varepsilon(\{1,\cdots,r\}, j, i, \{s,\cdots,n\})(-1)^{i-j+1} \times \sum_{\alpha \in S_{r,s,i,j}} C_{PT}(\{\alpha_{S_{r,s,i,j}}\}) . \tag{4.21}
$$

To define $S_{r,s,i,j}$ we divide the list of indices,

$$
\begin{aligned}
\{1,2,3,\cdots,n\} &= \{1,\cdots,r; r+1,\cdots,i-1; i; i+1,\cdots,j-1; j; j+1,\cdots,s-1; s,\cdots,n\} \\
&\equiv \{1,\cdots r,\} \oplus S_1 \oplus \{i\} \oplus S_2 \oplus \{j\} \oplus S_3 \oplus \{s,\cdots,n\}
\end{aligned}
\tag{4.22}
$$

with

$$
S_1 = \{r+1,\cdots,i-1\}, \quad S_2 = \{i+1,\cdots,j-1\}, \quad S_3 = \{j+1,\cdots,s-1\} .
\tag{4.23}
$$

The sets S_i may be null. Then

$$
S_{r,s,i,j} = Mer(S_1, \bar{S}_2, S_3)
\tag{4.24}
$$

where $\bar{S}_2$ is the reverse of S_2 and $Mer(S_1, \bar{S}_2, S_3)$ is the set of all mergers of the three sets which respect the ordering within the S_i and

$$
\alpha_{S_{r,s,i,j}} = \{1,\cdots,r\} \oplus \{j\} \oplus \alpha \oplus \{i\} \oplus \{s,\cdots,n\} .
\tag{4.25}
$$

The expression for $R^{(2)}_{n:1B_2}$ presumably has other realisations, however within the chosen basis the coefficients of the C_{PT} are uniquely given. The expression has the correct collinear limit of legs $n-1$ and n but does not have manifest cyclic symmetry, however we have checked

to a large number of external legs (up to 14) that the expression is cyclically symmetric, that it has all the correct collinear limits and it has the correct flip properties. The $R_{n:1B_1}^{(2)}$ and $R_{n:1B_2}^{(2)}$ do not individually satisfy the decoupling identity however the combination $R_{n:1B_1}^{(2)} + R_{n:1B_2}^{(2)}$ does, another strong check satisfied.

The term $R_{n:1B_1}^{(2)}$ can be rewritten in a form which looks more similar to $R_{n:1B_2}^{(2)}$ by manipulating the tensors

$$R_{n:1B_1}^{(2)}(1^+, 2^+, \cdots, n^+) = -2\,\mathrm{C_{PT}}(1, 2, \cdots, n) \times \sum_{1 \le i < j < k < l \le n} \varepsilon(i, j, k, l) \qquad (4.26)$$

$$= -2\,\mathrm{C_{PT}}(1, 2, \cdots, n) \times \sum_{r=1}^{n-4} \sum_{s=r+4}^{n} \varepsilon(\{1, 2, \cdots, r\}, r+1, s-1, \{s, s+1, \cdots, n\})\,.$$

This result, while only conjectured, satisfies several highly non-trivial properties and is the first n-point rational amplitude at two-loops for QCD. $A_{n:1B}$ will in fact be the first two-loop QCD amplitude for arbitrary numbers of legs after we calculate the finite polylogarithmic piece. We will now calculate this piece and will do so for the full all-plus amplitude.

4.6 Polylogarithmic Terms

We will now calculate the finite polylogarithmic piece of the all-plus amplitude $F_{n:c}^{(2)}$. This will give future calculations a formula to test against. It also gives $F_{n:1B}^{(2)}$ which along with $R_{n:1B}^{(2)}$ and the known IR divergent piece, will give the full n-point partial amplitude.
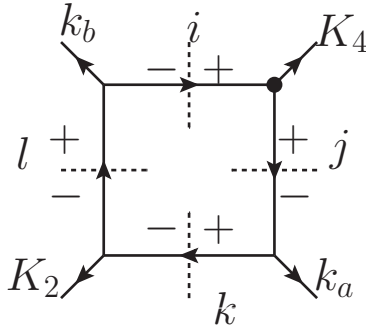
Figure 4.5: Four dimensional cuts of the two-loop all-plus amplitude involving an all-plus one-loop vertex (indicated by ●). K_2 may be null but K_4 must contain at least two external legs. k_a and k_b are single legs and all external legs are positive helicity.

We will again assume you have read the details of previous chapters but will summarise what is needed for the calculation here. The expression for the $F_{n:c}^{(2)}$ for the all-plus colour amplitudes is [92] of the form

$$F_{n:c}^{(2)} = \sum_i c_i \mathrm{F}_i^{2m}$$

where summation variable i refers to summing over different configuration of scalar boxes, c_i

are rational coefficients of these boxes, and

$$
\begin{aligned}
\mathrm{F^{2m}}[S, T, K_2^2, K_4^2] &= \operatorname{Li}_2\left(1 - \frac{K_2^2}{s}\right) + \operatorname{Li}_2\left(1 - \frac{K_2^2}{t}\right) + \operatorname{Li}_2\left(1 - \frac{K_4^2}{s}\right) + \operatorname{Li}_2\left(1 - \frac{K_4^2}{t}\right) \\
&\quad - \operatorname{Li}_2\left(1 - \frac{K_2^2 K_4^2}{st}\right) + \frac{1}{2}\log^2\left(\frac{s}{t}\right) .
\end{aligned}
$$

The $\mathrm{F^{2m}}$ are the combination of polylogs which appear in the two-mass box with the orientation of Figure 4.5 with $s = (K_2 + k_a)^2$ and $t = (K_2 + k_b)^2$. In the specific case where $K_2^2 = 0$,

$$
\mathrm{F^{2m}}[s, t, 0, K_4^2] = \operatorname{Li}_2\left(1 - \frac{K_4^2}{s}\right) + \operatorname{Li}_2\left(1 - \frac{K_4^2}{t}\right) + \frac{1}{2}\log^2\left(\frac{s}{t}\right) + \frac{\pi^2}{6} .
$$

The key features needed for the calculation are as follows: the ability to reduce the two-loop problem to a pseudo one-loop problem which we argued for in Chapter 2; quadruple cuts then completely constrain the loop momentum and we can solve the box coefficients in (1.108); compact, analytic forms of the subleading in colour, one-loop all-plus helicity amplitudes which are presented again in Chapter 2 and presented below,

$$
\begin{aligned}
A_{n:1}^{(1)}(1^+, 2^+, 3^+, \cdots, n^+) &= -\frac{1}{3}\frac{\sum_{i<j<k<l}\operatorname{Tr}_-(ijkl)}{\langle 1\,2\rangle\langle 2\,3\rangle\cdots\langle n\,1\rangle} \\
A_{n:2}^{(1)}(1^+; 2^+, 3^+, \cdots, n^+) &= -\frac{\sum_{i<j}[1|ij|1]}{\langle 2\,3\rangle\langle 3\,4\rangle\cdots\langle n\,2\rangle} \\
A_{n:3}^{(1)}(1^+, 2^+; 3^+, \cdots, n^+) &= 2\frac{[1\,2]^2}{\langle 3\,4\rangle\langle 4\,5\rangle\cdots\langle n\,3\rangle} \\
A_{n:r}^{(1)}(1^+, 2^+, 3^+, \cdots, r-1; r\cdots n^+) &= -2\frac{(P_{1\ldots r-1}^2)^2}{(\langle 1\,2\rangle\langle 2\,3\rangle\cdots\langle(r-1)\,1\rangle)(\langle r\,(r+1)\rangle\cdots\langle n\,r\rangle)}.
\end{aligned}
$$

Looking to an n-point calculation we change to set-based notation, allowing us to write things in terms of sets of arbitrary numbers of legs. We start by defining the dimensionless two-mass box function where the massive corners are described by the sets of legs A_1 and A_2,

$$
F(a, b; A_1; A_2) = F^{2m}[K_{aA_1}^2, K_{A_1 b}^2, K_{A_1}^2, K_{A_2}^2],
$$

and

$$
F(a, b; \{\}, A_2) = F(a, b; A_1, \{\}) = 0. \tag{4.27}
$$

We then need to consider all of the possible partial amplitudes that might appear on each corner. We therefore define the following kinematic coefficients with associated box function,

starting with the leading in colour amplitude where T_1 or T_2 might be empty,

$$
\begin{aligned}
&C_1(a, b, S_1, S_2, T_1, T_2) \\
&= A_{\mathcal{S}}^{(0)}(k^-, S_1, l^-, S_2) A_3^{(0)}(a^+, k^+, j^-) A_3^{(0)}(l^+, b^+, i^-) A_{\mathcal{T}:1}^{(1)}(i^+, T_1, j^+, T_2) \\
&= \frac{1}{3} \langle a\, b \rangle^2\, C_{PT}(a, S_1, b, S_2) C_{PT}(b, T_1, a, T_2) \\
&\quad \times \left(\frac{\langle b|T_1 T_2|b \rangle \langle a|T_1 T_2|a \rangle}{\langle a\, b \rangle^2} + \sum_{u<v<w<x \in K_4} \mathrm{tr}_-[uvwx] + \sum_{u<v \in T_1} \frac{K_4^2 \langle b|uv|a \rangle + \langle a|T_2 uv K_4|b \rangle}{\langle b\, a \rangle} \right. \\
&\quad + \sum_{u<v \in T_2} \frac{\langle b|K_4 uv T_2|a \rangle}{\langle b\, a \rangle} + \sum_{u<v<w \in K_4} \frac{\langle b|uvw K_4|a \rangle}{\langle a\, b \rangle} + \sum_{u<v<w \in T_1} \frac{\langle b|K_4 uvw|a \rangle}{\langle a\, b \rangle} \\
&\quad \left. + \sum_{u<v<w \in T_2} \frac{\langle a|uvw K_4|b \rangle}{\langle b\, a \rangle} \right) \times F(a, b; K_2 = S_1 \oplus S_2; K_4 = T_1 \oplus T_2), \quad (4.28)
\end{aligned}
$$

where $\mathcal{S} = |S_1 \oplus S_2| + 2$ and $\mathcal{T} = |T_1 \oplus T_2| + 2$ etc. For $A_{n:r}^{(1)}$ with $r - 1 > 1$ there are two cases,

$$
\begin{aligned}
&C_2(a, b, S_1, S_2, T_1, T_2, T_3) \\
&= A_{\mathcal{S}}^{(0)}(k^-, S_1, l^-, S_2) A_3^{(0)}(a^+, k^+, j^-) A_3^{(0)}(l^+, b^+, i^-) A_{\mathcal{T}:r}^{(1)}(i^+, T_1, j^+, T_2; T_3) \\
&= 2 \langle a\, b \rangle^2\, C_{PT}(b, T_1, a, T_2)\, C_{PT}(T_3) C_{PT}(a, S_1, b, S_2) \times \left(K_{T_3}^2 \right)^2 \\
&\quad \times F(a, b; S_1 \oplus S_2; T_1 \oplus T_2 \oplus T_3) \quad (4.29)
\end{aligned}
$$

where $r - 1 = |T_3|$ and

$$
\begin{aligned}
&C_3(a, b, S_1, S_2, T_1, T_2) \\
&\equiv A_{\mathcal{S}}^{(0)}(k^-, S_1, l^-, S_2) A_3^{(0)}(a^+, k^+, j^-) A_3^{(0)}(l^+, b^+, i^-) A_{\mathcal{T}:r}^{(1)}(i^+, T_1; j^+, T_2) \\
&= 2\langle a|K_{T_2} K_{T_1}|b \rangle^2 C_{PT}(a S_1 b S_2) C_{PT}(b T_1) C_{PT}(T_2 a). \\
&\quad \times F(a, b; S_1 \oplus S_2; T_1 \oplus T_2) \quad (4.30)
\end{aligned}
$$

where $r - 1 = |T_2| + 1$. For the $U(1)$ corners we have two coefficients

$$
\begin{aligned}
&C_4(a, b, S_1, S_2, T_1, T_2, t_3) \\
&\equiv A_{\mathcal{S}}^{(0)}(k^-, S_1, l^-, S_2) A_3^{(0)}(a^+, k^+, j^-) A_3^{(0)}(l^+, b^+, i^-) A_{\mathcal{T}:2}^{(1)}(t_3; i^+, T_1, j^+, T_2) \\
&= \langle a\, b \rangle^2\, C_{PT}(a, S_1, b, S_2) C_{PT}(b, T_1, a, T_2) \\
&\quad \times \left(\frac{[t_3|K_4|a \rangle [t_3|(K_{T_1} - K_{T_2})|b \rangle}{\langle a\, b \rangle} + 2[t_3|T_2 T_1|t_3] + \sum_{v<w \in K_4} [t_3|vw|t_3] \right) \\
&\quad \times F(a, b; S_1 \oplus S_2; T_1 \oplus T_2 \oplus t_3) \quad (4.31)
\end{aligned}
$$

where t_3 is a single leg within K_4 so $K_4 = K_{T_1} + K_{T_2} + k_3 = -i - j$ and

$$
\begin{aligned}
&C_5(a, b, S_1, S_2, T_1) \\
&= A_{\mathcal{S}}^{(0)}(k^-, S_1, l^-, S_2) A_3^{(0)}(a^+, k^+, j^-) A_3^{(0)}(l^+, b^+, i^-) A_{\mathcal{T}:2}^{(1)}(i^+; j^+, T_1) \\
&= - C_{PT}(a, T_1)\, C_{PT}(a, S_1, b, S_2) \times \left(K_4^2 \langle a|T_1 K_4|a \rangle + \sum_{u<v \in T_1} \langle a|K_4 uv K_4|a \rangle \right) \\
&\quad \times F(a, b; S_1 \oplus S_2; T_1). \quad (4.32)
\end{aligned}
$$

This fifth coefficient will never contribute to the boxes when fully colour dressed due to the ever present colour contribution

$$(\text{Tr}[bil] - \text{Tr}[bli])\text{Tr}[i] = \text{Tr}[bl] - \text{Tr}[bl] = 0, \tag{4.33}$$

where b, i and l are the momentum around the tree corner indicated in Figure 4.5. Colour dressing the two-mass boxes we extract the contribution to each trace structure in the following section.

4.6.1 Leading

Defining the sets

$$U_{ab} = \{a+1, a+2, \cdots, b-1\} \text{ and } V_{ab} = \{b+1, \cdots, a-1\} \tag{4.34}$$

ie split the list $\{1, 2, \cdots, n\}$ into $\{a, U_{ab}, b, V_{ab}\}$ where a is cycled to the front we have

$$F_{n:1}^{(2)}(1^+, 2^+, \cdots, n^+) = \sum_{a<b} \left(C_1(a, b, U_{ab}, 0, V_{ab}, 0) + C_1(a, b, 0, V_{ab}, 0, U_{ab}). \right) \tag{4.35}$$

This is another way of writing the previously obtained n-point result [69].

4.6.2 SU(N_c) N_c Double Trace Terms

Considering terms like $\text{Tr}[X]\text{Tr}[Y] = \text{Tr}[x_1, x_2, \cdots, x_{r-1}]\text{Tr}[y_1, y_2, \cdots, y_{n+1-r}]$, if a and b are within the same trace we define U_{ab} and V_{ab} as before with respect to the elements of this trace, and define new lists $X_i, Y_j = X/\{i\}$ and $Y/\{j\}$ respectively. The ordering of these sets matters, for example X_i is defined to start with the $(i+1)$th element such that,

$$X = \{1, 2, \cdots, r\} \rightarrow \{i, i+1, \cdots, i-1\} \rightarrow X_i = \{i+1, i+2, \cdots, i-1\}. \tag{4.36}$$

We also need to define Spl_2 as the set of splits of a list into two lists maintaining list order. So if $U = \{u_1, u_2, \cdots, u_r\}$

$$Spl_2(U) = \{U^i\} = (\{u_1, u_2, \cdots, u_i\}, \{u_{i+1}, \cdots, u_r\}). \tag{4.37}$$

This includes splits involving the empty set $(\{\}, U)$ and $(U, \{\})$ and counts them separately. For later convenience we will define the sum over $Spl_2(U_a)$ as the sum over the sets $\{(A_1^i, A_2^i)\} \in Spl_2(U_a)$ and similarly for leg b, $\{(B_1^i, B_2^i)\} \in Spl_2(U_b)$, where legs a and b are the legs on the massless corners of the two-mass box.

Finally it will also be useful to define the following double sum

$$\sum_{CSpl_2(U)} \equiv \sum_{V \in Z(U)} \sum_{Spl_2(V)}, \tag{4.38}$$

which is a sum over the splits of all cycles of the set U. We can now write the amplitude as

$$F_{n:r}^{(2)}(1^+, 2^+, \cdots (r-1)^+; r^+, \cdots, n^+) = F_{n:r}^{(2)}(X; Y)$$

$$= -\sum_{a \in X} \sum_{b \in Y} \sum_{Spl_2(X_a)} \sum_{Spl_2(Y_b)} \left[C_1(a, b, B_2^j, A_2^i, B_1^j, A_1^i) + C_1(a, b, A_1^i, B_1^j, A_2^i, B_2^j) \right]$$

$$+ \sum_{Z_2(X,Y)} \sum_{a<b \in X} \left(\left[C_2(a, b, 0, V_{ab}, 0, U_{ab}, Y) + C_2(a, b, U_{ab}, 0, V_{ab}, 0, Y) \right] \right.$$

$$\left. + \sum_{(A_1^i, A_2^i) \in CSpl_2(Y)} \left[C_1(a, b, U_{ab}, A_1^i, V_{ab}, A_2^i) + C_1(a, b, A_1^i, V_{ab}, A_2^i, U_{ab}) \right] \right), \qquad (4.39)$$

where we have suppressed notation such as the sum over Z_2 meaning swapping X and Y within that sum and $a < b \in X$ being in terms of the ordering of X. This expression works for $r = 2$ with the suitable $U(1)$ modification. For example when $|Y| = 1$ we replace $C_2(a, b, 0, V_{ab}, 0, U_{ab}, Y)$ with $C_4(a, b, 0, V_{ab}, 0, U_{ab}, Y)$ and many of the above sums become trivial.

4.6.3 $SU(N_c)$ Triple Trace Terms

We now consider terms like $\text{Tr}[X]\text{Tr}[Y]\text{Tr}[Z]$ with obvious generalisations of previously defined sets.

$$F_{n:s,t}^{(2)}(1^+, \cdots, s^+; (s+1)^+, \cdots, (s+t)^+; (s+t+1)^+, \cdots, n^+) = F_{n:s,t}^{(2)}(X; Y; Z)$$

$$= \sum_{Z_3(X,Y,Z)} \left(\sum_{Z_2(X,Y)} \sum_{a<b \in X} \sum_{(A_1^i, A_2^i) \in CSpl_2(Y)} \left[C_2(a, b, U_{ab}, A_1^i, V_{ab}, A_2^i, Z) + C_2(a, b, A_1^i, V_{ab}, A_2^i, U_{ab}, Z) \right] \right.$$

$$\left. - \sum_{a \in X} \sum_{b \in Y} \sum_{Spl_2(X_a)} \sum_{Spl_2(Y_b)} \left[C_2(a, b, B_2^j, A_2^i, B_1^j, A_1^i, Z) + C_2(a, b, A_1^i, B_1^j, A_2^i, B_2^j, Z) \right] \right). \qquad (4.40)$$

Again if $s = 1$ or $s = t = 1$ we simply replace C_2 with C_4 in the sum where appropriate.

4.6.4 N_c-independent Single Trace Term

Finally, completing the $A_{n:1B}^{(2)}$ all-plus amplitude, we have

$$F_{n:1B}^{(2)}(1^+, 2^+, 3^+, \cdots, n^+) =$$

$$\sum_{a<b} \left(- \sum_{(U_1^i:U_2^i) \in Spl_2(U_{ab})} \sum_{(V_1^i:V_2^i) \in Spl_2(V_{ab})} \left[C_3(a, b, U_2^i, V_2^i, V_1^i, U_1^i) + C_3(a, b, U_1^i, V_1^i, U_2^i, V_2^i) \right] \right.$$

$$\left. + \sum_{(V_1^i, V_2^i, V_3^i) \in Spl_3(V_{ab})} C_3(a, b, U_{ab}, V_2^i, V_1^i, V_3^i) + \sum_{(U_1^i, U_2^i, U_3^i) \in Spl_3(U_{ab})} C_3(a, b, U_2^i, V_{ab}, U_3^i, U_1^i) \right). \qquad (4.41)$$

These results are easy enough to encode and have been shown to satisfy the decoupling identities (3.2) for up to $n = 7$. This is the last piece of the colour decomposition and so we now have the full $F_n^{(2)}$ finite-polylogarithmic piece.

4.7 Conclusions

We have presented an ansatz for a very specific colour amplitude at two loops which is valid for an arbitrary number of external legs. Although we are short of a proof of the ansatz it satisfies consistency conditions and factorisations which suggest it is correct. We have explicitly calculated the all-n finite cut-constructible piece of the all-plus helicity amplitude. All-n formulae provide a very useful laboratory for testing conjectures and behaviour. For example, it was recently shown in ref. [93] that the one-loop all-plus amplitude is conformally invariant: however the all-n expression allows us to check that $R^{(2)}_{n:1B}$ is *not* conformally invariant although the coefficients C_3 are. The all-plus amplitude at one-loop is very special and has relations to amplitudes in other theories. In particular the $N = 4$ MHV amplitude is related to it by a dimension shift of integral functions [46] and also the one-loop amplitude coincides with that of self-dual Yang-Mills [98, 99]. It would be very interesting to see if any of these or similar properties extend to two-loop and beyond.

We have so far discussed full colour, all-plus helicity amplitudes. They have proven to be remarkably simple using four-dimensional unitarity, with the main bottleneck being the need for augmented recursion and functional reconstruction for the rational piece. We will now turn to the leading in colour amplitude for a different helicity configuration, the single-minus, two-loop amplitude.

Chapter 5

Five-point, Two-Loop, Single-Minus Amplitude

5.1 Preliminaries

We wish to calculate the leading in colour amplitude $A_{5:1}^{(2)}(a^-, b^+, c^+, d^+, e^+)$. We will again assume knowledge of certain details from previous chapters but we will review necessary details here. We can split the amplitude into two pieces

$$A_{5:1}^{(2)}(a^-, b^+, c^+, d^+, e^+) = P_{5:1}^{(2)}(a^-, b^+, c^+, d^+, e^+) + R_{5:1}^{(2)}(a^-, b^+, c^+, d^+, e^+), \qquad (5.1)$$

where P refers to cut constructible pieces and R refers to the rational contribution. R will not be fully captured with four-dimensional unitarity and therefore needs augmented recursion. This chapter will focus on calculating $P_{5:1}^{(2)}(a^-, b^+, c^+, d^+, e^+)$. $P_{5:1}$ can be further split into two pieces

$$P_{5:1}^{(2)}(a^-, b^+, c^+, d^+, e^+) = U_{5:1}^{(2)}(a^-, b^+, c^+, d^+, e^+) + F_{5:1}^{(2)}(a^-, b^+, c^+, d^+, e^+), \qquad (5.2)$$

where $U^{(2)}$ is the diverging piece and $F^{(2)}$ is the finite remainder. As with the all-plus case, the tree amplitude of this helicity configuration vanishes and so, for reasons given in Chapter 1, we will deal with unrenormalised amplitudes. We know that the infrared diverging piece takes the simple form [33],

$$U_{5:1}^{(2)}(a^-, b^+, c^+, d^+, e^+) = A_{5:1}^{(1)}(a^-, b^+, c^+, d^+, e^+) \times I_5[a, b, c, d, e] \qquad (5.3)$$

where I_5 is given by (1.101). We again use four-dimensional unitarity to calculate $P_{5:1}^{(2)}$ and we can use $U_{5:1}^{(2)}$ as a good check that the calculation is correct. This amplitude is already known and has been calculated in [2]. We develop this technique with an eye on automation, once it has been finalised it should scale well to higher multiplicities. We will discuss $R_{5:1}^{(2)}$ at the end but we believe it should be at worst algebraically more difficult than the all-plus case and should not present any further issues.

Moving on to the calculation; in the previous chapters we were able to make use of properties of the all-plus amplitudes to reduce a two-loop problem to a pseudo one-loop problem. A good indication that this was viable was looking at three-point, one-loop all-plus insertions on a scalar box. For the single-minus case we may perform similar tests but discover an issue. Using the configuration in Figure 5.1 as an example, we now need $\ell_2 = \alpha_{\ell_2} \tilde{\lambda}_a \lambda_b$

98

for $A^{(0)}(l_2^+, a^-, l_3^-)$ to be finite but this causes (2.6) to diverge. The other cut solution causes the tree corner to diverge which tells us the problem cannot be reduced to a pseudo one-loop problem. We must therefore approach this as an explicit two-loop calculation.
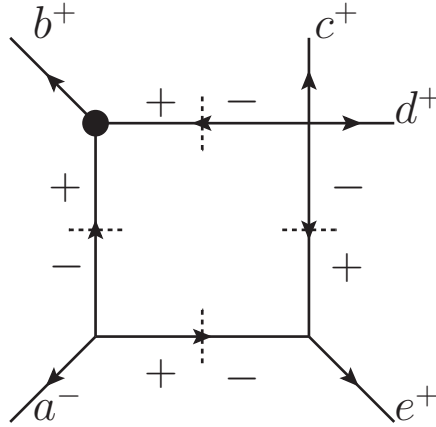
Figure 5.1: An insert which diverges on a quadruple cut. The small black circle indicates the one-loop insert.

We generate numerators for a given diagram using four-dimensional unitarity. We discussed in Chapter 2 that we classify two types of diagrams; genuine two loop diagrams such as the tricorner box where you must cut (in a topological sense) more than one internal line to reduce the diagram to two separate diagrams, and $(\text{one} - \text{loop})^2$ diagrams which are reducible by a single topological cut. Our strategy is to then look at all of the continuous triple unitarity cuts that contribute to a product of tree amplitudes, fully constraining the numerators of the genuine two loop diagrams. All $(\text{one} - \text{loop})^2$ diagrams vanish on such cuts. We discussed this for the all-plus helicity configuration, in which case there were not enough negative helicity legs to make a non-zero product of trees on a triple cut. The single minus has no such problem.
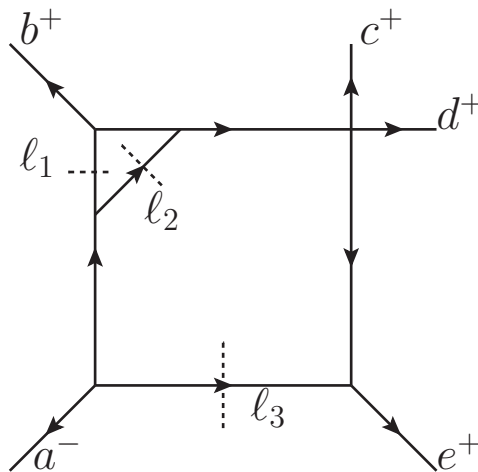
Figure 5.2: An example of a triple cut on a tricorner box. This contributes to $A^{(0)}(a^-, \ell_1^{\lambda_1}, \ell_2^{\lambda_2}, \ell_3^{\lambda_3}) \times A^{(0)}(-\ell_3^{-\lambda_3}, -\ell_2^{-\lambda_2}, -\ell_1^{-\lambda_1}, b^+, c^+, d^+, e^+)$ where $\{\lambda_1, \lambda_2, \lambda_3\} \in \{-, +, +\}$.

The technique was to look at all of the cuts and try to form numerators that could be generalised and mostly blind to helicity. For example we might look at the cut,

$$\sum_{\lambda_1,\lambda_2,\lambda_3} A^{(0)}(a^-, \ell_1^{\lambda_1}, \ell_2^{\lambda_2}, \ell_3^{\lambda_3}) \times A^{(0)}(-\ell_3^{-\lambda_3}, -\ell_2^{-\lambda_2}, -\ell_1^{-\lambda_1}, b^+, c^+, d^+, e^+) \tag{5.4}$$

where the sum over λ_i's is the sum over all helicity configurations for the cut loop momenta, many of which will vanish but all must be accounted for. We would expect the cut in Figure 5.2 to contribute to (5.4), and so we can manipulate this equation in a way that would provide a numerator for the remaining set of uncut propagators of this diagram. If one then accounts for all remaining cuts that can be achieved in Figure 5.2, we can look for a numerator that is common to all cuts for that diagram, and this numerator is then the starting point for integration.

This needs to be done for all possible cuts of the amplitude, and we do it in a way that manages to achieve a general set of numerators, $\mathcal{N}_\eta(a, k, \bar{a}, i, j, \omega)$. Here η indicates which diagram the numerator is for, a is the single negative-helicity leg and the remaining arguments refer to the external legs indicated on Figure 5.3 etc. Any of these remaining arguments may be a, but $\bar{a}$ is labelled as such to indicate that all numerators vanish for $a = \bar{a}$. We will shortly discuss how these numerators get pieced together, but for now the numerators and associated diagram are given as follows [100]:

$$\mathcal{N}_{tbx} = \langle a\,\bar{a} \rangle\, [\bar{a}|(-L_3)|a\rangle \langle \omega|QL_2|a\rangle [\omega|L_1PL_2|a\rangle, \tag{5.5}$$
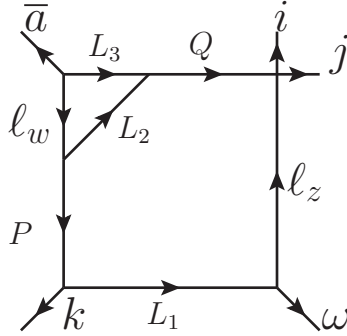
Figure 5.3: Tricorner box. $\eta = tbx$

$$\mathcal{N}_{fbbx} = \langle a\,\bar{a} \rangle\, [\bar{a}|\ell_\omega|\omega\rangle \langle a|L_A L_B|a\rangle [\omega|\ell_z\ell_\omega L_A|a\rangle. \tag{5.6}$$
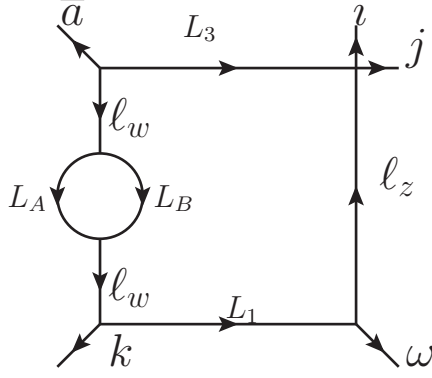
Figure 5.4: Bubble in box between two null corners. $\eta = nfbbx$.

The remaining numerators for diagrams with all-plus bubbles will be left to Appendix A. It will later be shown that while they are needed for the cuts they all vanish upon integration as they contain $\langle a|L_A L_B|a\rangle$. The remaining all-plus triangle diagrams are as follows:

$$
\begin{aligned}
\mathcal{N}_{stt} = {} & - \langle a\,\bar{a}\rangle\, [\bar{a}|(-L_3)|a\rangle\langle a|L_2 Q|k\rangle[k|L_2|a\rangle \\
& + \delta_a^j\, \langle a\,\bar{a}\rangle\, [\bar{a}|(-L_3)|a\rangle\, \langle a\,k\rangle\, [k|L_1 Q(-L_3)|a\rangle,
\end{aligned}
\tag{5.7}
$$
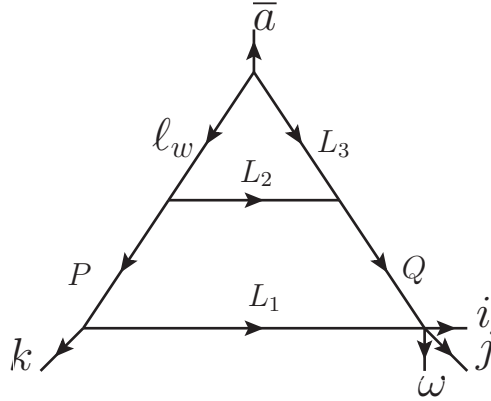
Figure 5.5: Triangle in triangle, $\eta = stt$. There is an extra term when the negative helicity leg is in the middle of the massive corner $a = j$.

where here δ_a^j indicates an additional term only present when $a = j$ is in the middle of massive corner. Pressing on we have

$$
\begin{aligned}
\mathcal{N}_{K21} = {} & \langle a\,\bar{a}\rangle\, [\bar{a}|\ell_w|a\rangle\, \langle a\,k\rangle\, [k|P|a\rangle \\
& + \delta_a^j\, \langle a\,\bar{a}\rangle\, [\bar{a}|P|a\rangle\, \langle a\,k\rangle\, [k|P|a\rangle \\
& + \delta_a^j\, \langle a\,\bar{a}\rangle\, [\bar{a}|\ell_w|a\rangle\, \langle a\,k\rangle\, [k|\ell_w|a\rangle,
\end{aligned}
\tag{5.8}
$$

Figure 5.6: Kite diagram with two null corners and one massive corner, with $\eta = K21$. There are extra terms when the negative helicity leg is in the middle of the massive corner $a = j$.

$$\mathcal{N}_{K31} = \langle a\,\bar{a}\rangle\,[\bar{a}|\ell_w|a\rangle\,\langle a\,\omega\rangle\,[\omega|L_1|a\rangle, \tag{5.9}$$

Figure 5.7: Kite diagram with three null corners and one massive corner, with $\eta = K31$.

$$\mathcal{N}_{K12} = \langle a\,\bar{a}\rangle\,[\bar{a}|(-L_3)|a\rangle\,\langle a|L_2(-L_3)|a\rangle, \tag{5.10}$$

Figure 5.8: Kite diagram with one null corner and two massive corners, with $\eta = K12$.

and finally,

$$\mathcal{N}_{K1Q} = \frac{1}{2} \langle a | \bar{a} L_3 | a \rangle \langle a | \bar{a} Q | a \rangle. \tag{5.11}$$
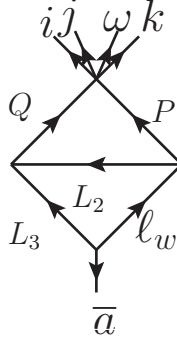
Figure 5.9: Kite diagram with one null corner and one massive corner, with $\eta = K1Q$.

Note that the numerators are written in a way that is valid for on-shell or off-shell loop momenta. The flips of these diagrams were also built into the numerators, where the flips of the diagrams are demonstrated in Figure 5.10. Using the same normalisation as in the all-plus cases, the numerators were built such that in total we need

$$\mathcal{I}^{(2)}(a^-, b^+, c^+, d^+, e^+) =$$

$$= \frac{2}{\langle a\,b \rangle \langle b\,c \rangle \langle c\,d \rangle \langle d\,e \rangle \langle e\,a \rangle} \sum_{\{k, \bar{a}, i, j, w\}} \sum_{\eta} \left(\frac{\mathcal{N}_\eta(a, k, \bar{a}, i, j, \omega)}{\mathcal{P}_\eta(a, k, \bar{a}, i, j, \omega)} + \frac{\mathcal{N}_\eta(a, k, \omega, j, i, \bar{a})}{\mathcal{P}_\eta(a, k, \omega, j, i, \bar{a})} \right) \tag{5.12}$$

where the sum over $\{k, \bar{a}, i, j, w\}$ is over $Z_5(a, b, c, d, e)$, $\mathcal{P}_\eta$ are the propagators for the diagram, and $\mathcal{I}^{(2)}$ is the object that needs to be integrated. One must not forget any relevant symmetry factors for diagrams such as $K21$ whose flips are not distinct diagrams. Noting that all of the $t < 7$ diagrams with all-plus triangles may be related to the tricorner box with various propagators pinched, the task is then to integrate these numerators, first using the two-mass triangle parametrisation of the all-plus triangle in $\eta = tbx$. For the second integral, one could either separate them out into box, triangle and bubble integrals but, as we will see, we elected to treat the second integral as a box parametrisation across all structures.
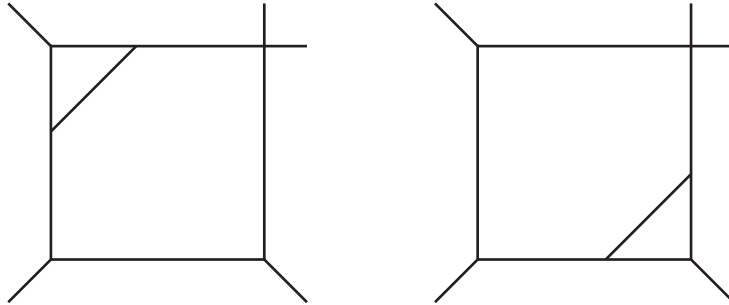
Figure 5.10: Two distinct diagrams but whose numerators will be related by a flip.

Before we integrate, it behoves us to address the $(\text{one} - \text{loop})^2$ diagrams. We can view these diagrams as pseudo one-loop diagrams with loop inserts in a similar way to the all-plus

103

case. The difference here is that a quadruple cut will not simply give us a product of tree amplitudes and we need to calculate the numerators for each insert. This is done by looking at double cuts on the already constrained numerators such as the one in Figure 5.11 which contributes to the following amplitude cut,

$$\mathcal{C}_{abl} = \frac{1}{32\pi^2} \sum_{\lambda_1, \lambda_2} A^{(1)}(a^-, b^+, \ell_1^{\lambda_1}, \ell_2^{\lambda_2}) \times A^{(0)}(-\ell_2^{-\lambda_2}, -\ell_1^{-\lambda_1}, c^+, d^+, e^+). \quad (5.13)$$
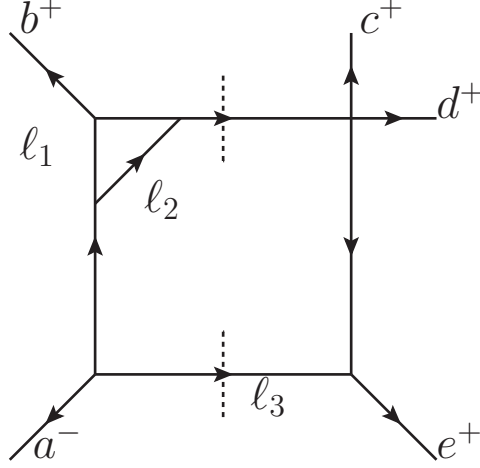
Figure 5.11: An example of a double cut on a tricorner box. The cut will act on the numerator $\mathcal{N}_{tbx}(a, a, b, c, d, e)$ in this case.

We then find the inserts via

$$\mathcal{I}_{ab\ell}^{(1,1)}(a^-, b^+, c^+, d^+, e^+) = \mathcal{C}_{ab\ell} - \frac{\mu^{4-D}}{i\pi^{\frac{D}{2}} e^{-\epsilon\gamma}} \int \mathrm{d}^D \ell \, \mathcal{I}^{(2)}(a^-, b^+, c^+, d^+, e^+)|_{ab\ell} \quad (5.14)$$

where $\mathcal{I}_{ab\ell}^{(1,1)}$ is referring to the pseudo one-loop insert pieces that will need to be integrated, $ab\ell$ is referring to cuts which constrain legs a and b to the one-loop side of the cut. We take $\epsilon \to 0$ once the first integral of the genuine two loop pieces $\mathcal{I}^{(2)}$ is done as it is a cut in four dimensions.

It is important to remember that a given insert might contribute to multiple cuts and we therefore need to find the overlaps between cuts to ensure we have the correct numerator. For example, in Figure 5.12, if we have b^+ on the loop corner as with Figure 5.11, then the left diagram contributes to $A^{(1)}(a^-, b^+, \ell_1^{\lambda_{\ell_1}}, \ell_2^{\ell_{\lambda_2}}) \times A^{(0)}(-\ell_2^{-\ell_{\lambda_2}}, -\ell_1^{-\ell_{\lambda_1}}, c^+, d^+, e^+)$ while the right diagram contributes to $A^{(1)}(\ell_1^{\ell_{\lambda_1}}, \ell_2^{\ell_{\lambda_2}}, b^+, c^+, d^+) \times A^{(0)}(e^+, a^-, -\ell_2^{-\lambda_{\ell_2}}, -\ell_1^{-\ell_{\lambda_1}})$. We therefore need to look at both of these cuts of the amplitude and find a common numerator to each with the associated uncut box propagators. We do this for every cut and look for every diagram that contributes to multiple cuts. Once this is done, the remainder will then be inserts into one-mass triangles and massive bubbles which only contribute to one cut (and as we will see are the source of the IR piece for this amplitude).
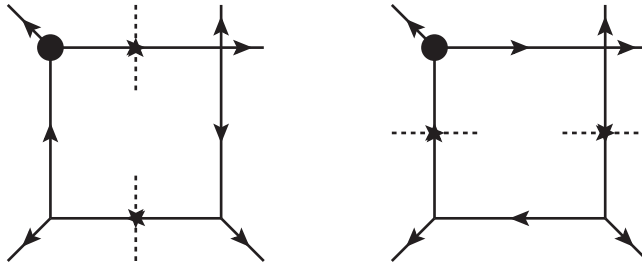
Figure 5.12: A loop insert that contributes to multiple double cuts, with the loop given by the black circle. We find the numerator that is associated with each box of this type such that it correctly contributes to each cut.

These inserts are given in Appendix A [100]. We can use standard one-loop techniques such as generalised unitarity to isolate scalar box, triangle and bubble coefficients. We will therefore begin by integrating the inserts as this simply uses techniques discussed in the all-plus configuration.

5.2 Inserts

We now have a set of genuine two-loop numerators which gives us the correct triple-cuts into tree-tree pieces. We also have a set of inserts in one-mass boxes, two-mass triangles, one-mass triangles and bubbles that, along with the two-loop numerators, give us the correct double cuts into (one-loop)-tree and tree-(one-loop) pieces. The inserts already have one loop momentum accounted for, and so we can use generalised unitarity to calculate the remaining loop integral. This will involve performing quadruple cuts, triple cuts and double cuts in a way that isolates the coefficients of the scalar box, triangle and bubble integrals.

5.2.1 Quadruple cuts

We will begin with the quadruple cuts. As previously discussed, we perform four cuts which can fully constrain the loop momentum. The previous calculation of the quadruple cuts were for the specific case of factorising the all-plus amplitudes into a product of three tree amplitudes and a one-loop amplitude, where one solution caused the trees to vanish and the remaining solution gave the entire coefficient. Here we are cutting a box with an already specified numerator so we will need both solutions. Keeping the general external momentum labels as in Figure 5.3 we have

$$
\begin{aligned}
\ell_1 - \ell_2 &= \omega \\
\ell_2 - \ell_3 &= k \\
\ell_3 + \ell_4 &= \overline{a} \\
\ell_4 + \ell_1 &= P_{ij}.
\end{aligned}
\tag{5.15}
$$

105

Solving for ℓ_2

$$\ell_1^2 = [\ell_2\,\omega]\,\langle\ell_2\,\omega\rangle = 0, \tag{5.16}$$

$$\ell_3^2 = [\ell_2\,k]\,\langle k\,\ell_2\rangle = 0, \tag{5.17}$$

$$\ell_2^{(1)} = \alpha_{\ell_2}^{(1)}\,\tilde{\lambda}_k\lambda_\omega, \tag{5.18}$$

$$\ell_2^{(2)} = \alpha_{\ell_2}^{(2)}\,\tilde{\lambda}_\omega\lambda_k. \tag{5.19}$$

We solve α_{ℓ_2} using momentum conservation around two corners

$$\ell_4^2 = (P_{k\bar{a}} - \ell_2)^2 = -[\ell_2|P_{k\bar{a}}|\ell_2\rangle + s_{k\bar{a}} = 0,$$

$$\alpha_{\ell_2}^{(1)} = \frac{\langle k\,\bar{a}\rangle}{\langle\omega\,\bar{a}\rangle},$$

$$\alpha_{\ell_2}^{(2)} = \frac{[k\,\bar{a}]}{[\omega\,\bar{a}]},$$

$$\ell_1^{(1)} = \frac{\langle\omega\,\bar{a}\rangle\,\tilde{\lambda}_\omega + \langle k\,\bar{a}\rangle\,\tilde{\lambda}_k}{\langle\omega\,\bar{a}\rangle}\lambda_\omega\,, \qquad \ell_1^{(2)} = \frac{[\omega\,\bar{a}]\,\lambda_\omega + [k\,\bar{a}]\,\lambda_k}{[\omega\,\bar{a}]}\tilde{\lambda}_\omega. \tag{5.20}$$

We then average over both solutions after simply substituting them into the insert numerators.

5.2.2 Triple Cuts

As discussed in previous chapters, the triple cuts will leave one variable unconstrained and also picks up contributions from the scalar boxes. There are simple enough ways of approaching this problem, for example one way of extracting this coefficient is given in [101] but one has to be careful of the Jacobian when performing these cuts on box structures. This practically translates to there being a vanishing solution and non-vanishing solution depending on which propagator you start your parametrisation with, and then you must average over these two solutions. This takes some extra work to ensure you have the correct solution and so we develop a new parametrisation for triangles with at least one massless corner.

We start with the general condition that cut momentum ℓ_0 flows away from a massless corner and towards a massive corner, as shown in Figure 5.13. The number of legs in the massive corner is irrelevant and the following is blind to what the mass is on the third corner. We have the three δ-functions:

$$\delta\big(\ell_0^2\big) \qquad \delta\big((\ell_0 - P)^2\big) \qquad \delta\big((\ell_0 + e)^2\big) \tag{5.21}$$

and we can write P as a sum of two null momenta as we have done previously

$$P = P^\flat + \frac{P^2}{[\eta|P|\eta\rangle}\eta = P^\flat + P^\sharp. \tag{5.22}$$
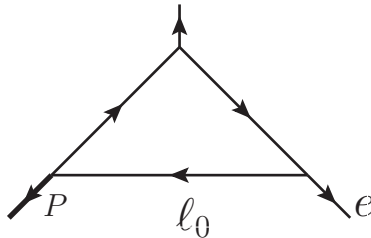
Figure 5.13: Triple cut configuration, with ℓ_0 flowing from null leg $e^2 = 0$ and towards $P^2 \neq 0$.

We may use the null momenta in (5.22) to construct an orthogonal basis for ℓ_0. We choose

$$\ell_0 = A(P^\flat + P^\sharp) + B(P^\flat - P^\sharp) + C\left(f\frac{\langle q\,P^\flat\rangle}{\langle q\,P^\sharp\rangle}\tilde{\lambda}_{P^\flat}\lambda_{P^\sharp} + f\frac{[q\,P^\flat]}{[q\,P^\sharp]}\tilde{\lambda}_{P^\sharp}\lambda_{P^\flat}\right)$$

$$+ iD\left(f\frac{\langle q\,P^\flat\rangle}{\langle q\,P^\sharp\rangle}\tilde{\lambda}_{P^\flat}\lambda_{P^\sharp} - f\frac{[q\,P^\flat]}{[q\,P^\sharp]}\tilde{\lambda}_{P^\sharp}\lambda_{P^\flat}\right). \tag{5.23}$$

Here f is an arbitrary scalar and q an arbitrary null vector. To keep ℓ_0 real we impose that $A, B, C, D, f, P^\sharp, P^\flat$ and q are all real. This is clear when writing

$$\ell_0^2 = P^2\left(A^2 - B^2 + f^2\frac{[q|P^\flat|q\rangle}{[q|P^\sharp|q\rangle}(C^2 + D^2)\right)$$

$$= P^2\left(A^2 - B^2 + C^2 + D^2\right) \tag{5.24}$$

where we have made an obvious choice of f^2 for the last line. We also make the choice in (5.22) that $\eta = e$, so that $\langle P^\sharp\,e\rangle = [P^\sharp\,e] = 0$ and we can write

$$(\ell_0 - P)^2 = P^2\left((A-1)^2 - B^2 + C^2 + D^2\right)$$

$$(\ell_0 + e)^2 = P^2\left(A^2 - B^2 + C^2 + D^2\right) + 2(A+B)e\cdot P^\flat. \tag{5.25}$$

Making the change of variables to $\{A, B, C, D\}$

$$\int \mathrm{d}^4\ell_0 \to (P^2)^2\int \mathrm{d}A\mathrm{d}B\mathrm{d}C\mathrm{d}D, \tag{5.26}$$

and recalling that

$$\delta|g(x)| = \sum_i \frac{\delta(x - x_i)}{|\frac{\mathrm{d}}{\mathrm{d}x}g(x)|_{x=x_i}} = \sum_i \frac{\delta(x - x_i)}{|\delta_i'|}, \tag{5.27}$$

where x_i are the roots of $g(x)$, we do the B integration using $\delta_1 = \delta(\ell_0^2)$

$$B^2 = A^2 + C^2 + D^2 \qquad \text{and} \qquad \frac{1}{|\delta'|} = \frac{1}{|2\sqrt{A^2 + C^2 + D^2}P^2|}. \tag{5.28}$$

Next we can do the A integration using $\delta_2 = \delta\left((\ell_0 - P)^2\right) = \delta\left(P^2[(A-1)^2 - A^2]\right)$, finding

$$A = \frac{1}{2} \qquad \text{and} \qquad \frac{1}{|\delta'|} = \frac{1}{|2P^2|}. \tag{5.29}$$

The last constraint is $\delta_3 = \delta\left((\ell_0 + e)^2\right) = \delta\left([1 \pm \sqrt{1 + 4C^2 + 4D^2}]e\cdot P^\flat\right)$ which leads to (performing the C integration)

$$\frac{1}{|\delta'|} = \frac{\sqrt{1 + 4C^2 + 4D^2}}{|4e\cdot P^\flat C|}. \tag{5.30}$$

There is an issue here that the only real solution to the constraint is that $C^2 + D^2 = 0 \to C = D = 0$ and the integral diverges. Luckily this is just a coordinate singularity and we can switch to polar coordinates for the remaining integrals

$$C = \rho\cos(\theta) \qquad D = \rho\sin(\theta) \qquad \int \mathrm{d}C\mathrm{d}D \to \int \rho\,\mathrm{d}\rho\,\mathrm{d}\theta, \tag{5.31}$$

and so

$$\int \mathrm{d}C\delta\left([1\pm\sqrt{1+4C^2+4D^2}]e\cdot P^\flat\right)\to\int\mathrm{d}\rho\frac{\rho\sqrt{1+4\rho^2}\delta|\rho|}{\rho|4e\cdot P^\flat|},\qquad(5.32)$$

where we see the ρ in the Jacobian cancels the ρ from the δ function and we can constrain $\rho=0$. There may be cases where this integrand being naively finite might cause issues but it would be easy enough to put in a small mass for e which would keep ρ small but finite, and then set e massless later. However, this might be overcautious as everything here is algebraic and we find that this parametrisation matches the parametrisation in [101] with the suitable corrections already discussed in place. The remaining integral is just an angular integral and we see that cutting a box, with uncut propagator $\mathcal{P}(\ell_0)$ and numerator $\mathcal{N}(\ell_0)$, schematically gives us

$$\int\mathrm{d}^4\ell_0\delta_1\delta_2\delta_3\frac{\mathcal{N}(\ell_0)}{\mathcal{P}(\ell_0)}=\int\mathrm{d}^4\ell_0\delta_1\delta_2\delta_3\left(\frac{c_\mathrm{box}}{\mathcal{P}(\ell_0)}+c_\mathrm{tri}\right),\qquad(5.33)$$

where c_box is the coefficient from the quadruple cuts and c_tri is the scalar triangle coefficient associated with this cut. We then simply have

$$c_\mathrm{tri}=\frac{\mathcal{N}(\ell_0)-c_\mathrm{box}}{\mathcal{P}(\ell_0)}\Big|_{\ell_0=P^\sharp}.\qquad(5.34)$$

One then just has to be careful that nothing diverges at $\ell_0=P^\sharp=\frac{P^2}{[e|P|e\rangle}e$, but otherwise (5.34) is a very simple way of extracting the triangle coefficients. There are some interesting patterns in the results thus far that may be worth further investigation. The box and two-mass triangle inserts were organised so we could identify which pieces would contribute to different double cuts. We then had the one-mass triangle and bubble inserts which only contributed to one double cut. We find that for every box and two-mass triangle insert, $\mathcal{N}(P^\sharp)=0$. This means that all of the c_{tri} for these inserts go as $-\frac{c_{box}}{\mathcal{P}(P^\sharp)}$, and so the IR contributions of the box cuts cancel exactly with the triangle cuts on these inserts. We are then left with the one-mass triangle and bubble inserts. Triangle cuts on the bubble inserts vanish. Interestingly we found that for every one-mass triangle insert,

$$c_{tri}^{i,i+1}I_3^{1m}(s_{i,i+1})=\frac{1}{\epsilon^2}\frac{\mathcal{N}^{i,i+1}(P^\sharp)}{s_{i,i+1}}(-s_{i,i+1})^{-\epsilon}=-\frac{1}{\epsilon^2}A_5^{(1)}(a^-,b^+,c^+,d^+,e^+)(-s_{i,i+1})^{-\epsilon}$$

$$=A_5^{(1)}(a^-,b^+,c^+,d^+,e^+)\times I_{i,i+1}^{(2)},\qquad(5.35)$$

where $\mathcal{N}^{i,i+1}$ is referring to the insert in the one-mass triangle with mass $P_{i,i+1}^2$, and $I_{i,i+1}^{(2)}$ is the IR divergent structure (1.97). This is true of all of these inserts and so summing over all of the triangles gives the entire IR piece. Perhaps there is some deeper reason for this but this was surprising to me as it means we should expect an overall zero coefficient for the $\frac{1}{\epsilon^2}$ pieces from the (tree)-(tree) genuine two-loop side, and that any remaining $\frac{1}{\epsilon}$ pieces from bubble cuts should cancel with all $\frac{1}{\epsilon}$ pieces from the genuine two-loop side. The inserts themselves do not resemble each other apart from ones that can be related by flips so it was also a surprise that they all reduced to the one-loop single-minus amplitude. Closer inspection of the inserts may be warranted as there may be lessons learned from seeing which pieces cancel with each other. Can we reduce calculation further if we know a priori where the redundancies occur? These are questions that the author did not have time to study further unfortunately.

5.2.3 Double Cuts

We use the canonical basis approach [91] to extract the scalar bubble coefficients. This involves rewriting numerators on specific cuts into a canonical form where the coefficient of the respective scalar bubble integral may be extracted. The canonical bases can be organised into terms with uncut "massless" propagators of the form $(\ell_1 \pm k)^2$ where $k^2 = 0$ and ℓ_1 is one of the cut loop momenta, or "massive" propagators where $k^2 \neq 0$. Of course they are all massless in the sense that there is no internal mass but we will hereby refer to massless and massive to indicate the value of k^2, similarly to how we refer to massive triangles etc.

Looking to higher multiplicities there were some interesting features that simplified the form of the massive propagator results, independently of the number of legs.
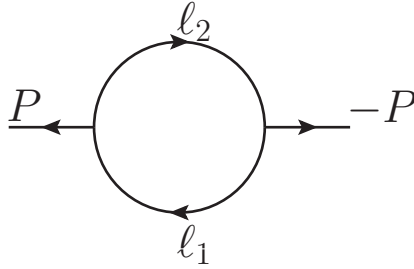
Figure 5.14: The bubble considered in the double cuts.

First lets review some results of [91] for completeness. In the following ℓ_1 and ℓ_2 refer to the cut momenta flowing in the directions indicated by Figure 5.14. Note that this differs from how we have defined them in the double cut, $A^{(1)} \times A^{(0)}$, where $\ell_1 \to -\ell_1$. Starting with an example, a piece of an insert may be written in a canonical form with a massless propagator

$$\mathcal{H}_1(A; B; \ell_1) = \frac{\langle \ell_1 \, B \rangle}{\langle \ell_1 \, A \rangle} = -\frac{[A|\ell_1|B\rangle}{(\ell_1 - k_A)^2} \tag{5.36}$$

where $k_A^2 = 0$ and k_A is taken to be real. This was then evaluated as a covariant, linear triangle integral shown in Figure 5.15 and then the coefficient of $-\log(-P^2)$ was extracted to give

$$H_1(a; B; P) = \frac{[A|P|B\rangle}{[A|P|A\rangle}. \tag{5.37}$$
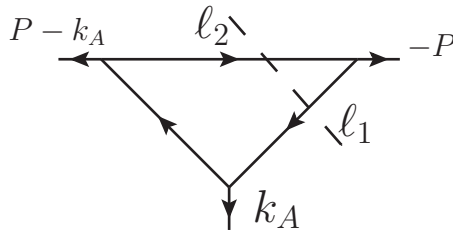
Figure 5.15: Double cut on a triangle. Configuration used for H_1 calculation.

This is all easy enough to automate in Mathematica, where one has to rewrite the inserts into canonical form but then can simply replace the canonincal forms with the results. The

massive propagator cases take a bit more work to automate. Starting with the example

$$\mathcal{G}_0(B; D; Q; \ell_1) = \frac{[D|\ell_1|B\rangle}{(\ell_1 + Q)^2}, \qquad (5.38)$$

one can define null linear combinations of P and Q,

$$\hat{P}^\mu = \frac{1}{2\sqrt{\Delta_3}}\left(P^2 Q^\mu - \left(P \cdot Q - \frac{\sqrt{\Delta_3}}{2}\right)P^\mu\right), \quad \hat{Q}^\mu = \frac{1}{2\sqrt{\Delta_3}}\left(-P^2 Q^\mu + \left(P \cdot Q + \frac{\sqrt{\Delta_3}}{2}\right)P^\mu\right),$$
$$(5.39)$$

where $\Delta_3 = 4(P \cdot Q)^2 - 4P^2 Q^2$ is the Gram determinant of the triangle integral that has legs of momenta P, Q and $-P - Q$. This linear combination (5.39) is of course valid for any momenta P and Q. The scalar bubble coefficient associated with (5.38) can then be separated into two $\mathcal{H}_1$ pieces which are rational conjugates of each other, and then combined to give the totally rational,

$$G_0(B; D; Q; P) = \frac{[D|P(QP - PQ)|B\rangle}{\Delta_3} = \frac{[D|P[Q, P]|B\rangle}{\Delta_3}. \qquad (5.40)$$

This again is easily generalised for a given configuration, needing only P and Q to be specifically entered as arguments and with B and D being determined by code similar to the massless cases. Going to $\mathcal{O}(\ell)$ and higher, naively plugging the results from [91] gets messy but there are features of double cutting two-mass easy boxes that simplify the form of the results, and we can reduce the redundancies a bit earlier rather than at the end. This will be done in a way that scales to any number of legs and can be automated.

Higher order, massive propagator terms can be reduced to $\mathcal{G}_1^2$ and $\mathcal{G}_1^1$ forms, where

$$\mathcal{G}_1^n = f^n(\ell)\frac{[D\,\ell]\langle C\,\ell\rangle\langle B\,\ell\rangle}{[\ell|\mathcal{Q}|\ell\rangle\langle A\,\ell\rangle}, \qquad (5.41)$$

with $f^n(\ell)$ being a polynomial of degree n in ℓ, and we have used the fact that $(\ell - P)^2 = 0$ to rewrite the massive propagator

$$(\ell + Q)^2 = Q^2 + [\ell|Q|\ell\rangle = [\ell|Q + \frac{Q^2}{P^2}P|\ell\rangle = [\ell|\mathcal{Q}|\ell\rangle. \qquad (5.42)$$

We can rewrite (5.41) as

$$\mathcal{G}_1^n\langle A|P\mathcal{Q}|A\rangle$$
$$= \frac{P^2 f^n(\ell)\langle B\,\ell\rangle}{[\ell|\mathcal{Q}|\ell\rangle}\left(\frac{[D|\mathcal{Q}|A\rangle\langle C\,A\rangle}{\langle A\,\ell\rangle} + \frac{4}{P^2}\left(\frac{[D|\mathcal{Q}|\hat{P}\rangle\langle C|\hat{P}\hat{\mathcal{Q}}|A\rangle}{\langle\ell\,\hat{P}\rangle} + \frac{[D|\mathcal{Q}|\hat{\mathcal{Q}}\rangle\langle C|\hat{\mathcal{Q}}\hat{P}|A\rangle}{\langle\ell\,\hat{\mathcal{Q}}\rangle}\right)\right)$$
$$- f^n(\ell)\langle B\,\ell\rangle\left(\frac{[D|P|A\rangle\langle C\,A\rangle}{\langle A\,\ell\rangle} + \frac{4}{P^2}\left(\frac{[D|P|\hat{P}\rangle\langle C|\hat{P}\hat{\mathcal{Q}}|A\rangle}{\langle\ell\,\hat{P}\rangle} + \frac{[D|P|\hat{\mathcal{Q}}\rangle\langle C|\hat{\mathcal{Q}}\hat{P}|A\rangle}{\langle\ell\,\hat{\mathcal{Q}}\rangle}\right)\right).$$
$$(5.43)$$

Here the $\hat{P}$ and $\hat{\mathcal{Q}}$ are the null linear combination (5.39) but with $Q \to \mathcal{Q}$. This splits $\mathcal{G}_1^n$ into pieces with either only massless propagators, or terms with the massive propagator but

of lower order in ℓ. This can be iteratively applied until everything is in a canonical form. The remaining terms of interest are then

$$\mathcal{G}_1^{\hat{\mathcal{Q}}} = \frac{[D\,\ell]\,\langle C\,\ell\rangle\,\langle B\,\ell\rangle}{[\ell|\mathcal{Q}|\ell\rangle\,\langle\hat{\mathcal{Q}}\,\ell\rangle}, \tag{5.44}$$

$$G_1^{\hat{\mathcal{Q}}} = 2\frac{[D|[\mathcal{Q},P]P|C\rangle[\hat{\mathcal{Q}}|P|B\rangle + \left(P^2[D|\mathcal{Q}|B\rangle - (P\cdot\mathcal{Q} + \sqrt{\Delta_3}/2)\right)[D|P|B\rangle)[\hat{\mathcal{Q}}|P|C\rangle}{P^2\Delta_3}, \tag{5.45}$$

and a similar result at $\mathcal{O}(\ell)$, again all given in [91]. $G_1^{\hat{P}}$ is simply related to (5.45) via rational conjugation.

These results generalise to any multiplicity but quickly become unwieldy and we would like to reduce the size of our results for faster numerical evaluation, especially in future calculations when numerical fitting will be required. Naively applying these results for this case leads to a lot of redundancies which can be dealt with analytically without losing much generality, the only constraint being that the cuts are on "two-mass-easy" boxes, including the one-mass box limit of this as we see in the five-point case. This constraint is fine for single-minus calculations as we do not expect to see "two-mass-hard" boxes or higher mass boxes [100].
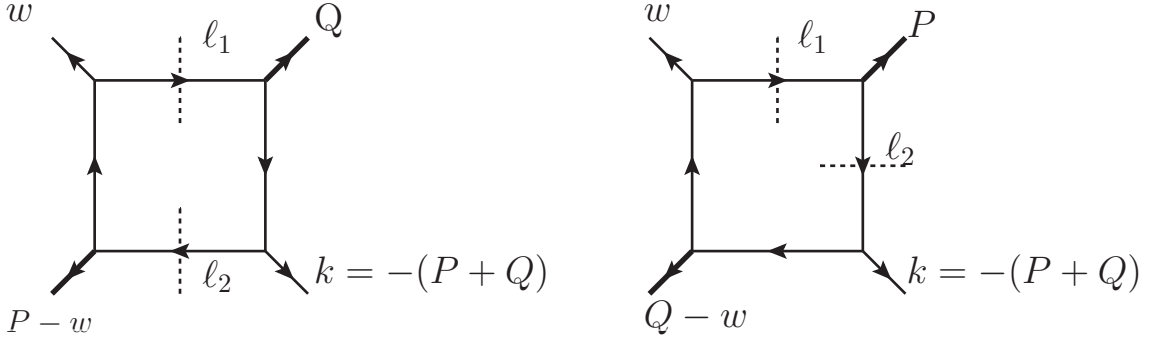
Figure 5.16: The two independent double cuts that contribute to the non-zero scalar bubble coefficients. Here $k^2 = (P+Q)^2 = 0$.

The simplification comes from making a suitable choice of ℓ_1 such that $(P+Q)^2 = 0$. This can always be achieved for the two-mass-easy boxes, as shown in Figure 5.16. Of course it may be easier, depending on the numerator, to write the uncut propagators as both being massless but with different cut momenta ℓ_1 and ℓ_2, but this often leads to canonical forms that require more work. From here we see that

$$\mathcal{Q}^2 = Q^2 + \frac{Q^4}{P^2} + 2\frac{Q^2}{P^2}P\cdot Q = \frac{Q^2}{P^2}(P+Q)^2 = 0. \tag{5.46}$$

This is useful as if we write $\hat{P}$ and $\hat{\mathcal{Q}}$ as nullified combinations of each other the corresponding Gram determinant simplifies to $\Delta_3 = 4\,(P\cdot\mathcal{Q})^2$ and so $\sqrt{\Delta_3}$ is rational. Keeping the labelling from Figure 5.16 such that $P + Q = -k$, it is easy to show that further simplifications can

be made such as

$$2P \cdot \mathcal{Q} = 2P \cdot \left(Q + \frac{Q^2}{P^2}P\right) = [k|P|k\rangle,$$

$$\hat{P}^\mu = \frac{P^2}{4P \cdot \mathcal{Q}}\mathcal{Q}^\mu,$$

$$\hat{\mathcal{Q}}^\mu = \frac{1}{4P \cdot \mathcal{Q}}, \left(-P^2\mathcal{Q}^\mu + 2P \cdot \mathcal{Q}P^\mu\right) = \frac{P^2}{2[k|P|k\rangle}k^\mu,$$

$$\langle X|P\mathcal{Q}|Y\rangle = \langle X|kP|Y\rangle,$$

$$\langle X|k\mathcal{Q}|Y\rangle = \frac{[k|P|k\rangle}{P^2}\langle X|kP|y\rangle,$$

$$\Delta(P,Q) = 4(P \cdot Q)^2 - 4P^2Q^2$$

$$= \left((P+Q)^2 - P^2 - Q^2\right)^2 - 4P^2Q^2 = (P^2 - Q^2)^2 = [k|P|k\rangle^2. \qquad (5.47)$$

$\mathcal{Q}$ being null only relies on the massive propagator being $(\ell_1 + Q)^2$ with $(\ell_1 - P)^2 = 0$ such that $(P+Q)^2 = 0$, or equivalently with $\ell_1 \to -\ell_1$. The uncut propagators simply specify P and Q. All of the above allows us to write the reduction (5.43) in a more useful form

$$\frac{[D|\ell|C\rangle\langle B\,\ell\rangle}{[\ell|\mathcal{Q}|\ell\rangle\langle A\,\ell\rangle} = \frac{\langle B\,\ell\rangle}{\langle A|Pk|A\rangle}\left(\frac{P^2}{[\ell|\mathcal{Q}|\ell\rangle}\left(\frac{[D|\mathcal{Q}|A\rangle\langle C\,A\rangle}{\langle A\,\ell\rangle} + \frac{P^2[D|\mathcal{Q}|\hat{\mathcal{Q}}\rangle\langle C|k\mathcal{Q}|A\rangle}{[k|P|k\rangle^2\left\langle \ell\,\hat{\mathcal{Q}}\right\rangle}\right)\right.$$

$$\left. - \left(\frac{[D|P|A\rangle\langle C\,A\rangle}{\langle A\,\ell\rangle} + \frac{P^2}{[k|P|k\rangle^2}\left(\frac{[D|P|\hat{P}\rangle\langle C|\mathcal{Q}k|A\rangle}{\left\langle \ell\,\hat{P}\right\rangle} + \frac{[D|P|\hat{\mathcal{Q}}\rangle\langle C|k\mathcal{Q}|A\rangle}{\left\langle \ell\,\hat{\mathcal{Q}}\right\rangle}\right)\right)\right), \qquad (5.48)$$

as well as

$$G_1^{\hat{\mathcal{Q}}} = 2\frac{[D|[Q,P]P|C\rangle[\hat{\mathcal{Q}}|P|B\rangle - P^2[D|k|B\rangle[\hat{\mathcal{Q}}|P|C\rangle}{P^2[k|P|k\rangle^2},$$

$$G_1^{\hat{P}} = 2\frac{[D|[Q,P]P|C\rangle[\hat{P}|P|B\rangle + \left(P^2[D|Q|B\rangle + Q^2[D|P|B\rangle\right)[\hat{P}|P|C\rangle}{P^2[k|P|k\rangle^2}. \qquad (5.49)$$

At two-loop we only see cubic terms so this only needs to be performed once per cubic term as the results for all of the special cases are known up to quadratic order. All of these results are easily coded up with only P and Q needing to be specified. The results here work for any two-mass easy box with any number of legs so this should all scale well going to higher multiplicity and reduce computational requirements.

One final thing, the inserts required a new canonical form to be calculated of the form

$$\mathcal{H}_0^3(D_1, D_2, D_3, B_1, B_2, B_3) = [D_1|\ell|B_1\rangle[D_2|\ell|B_2\rangle[D_3|\ell|B_3\rangle. \qquad (5.50)$$

A new parametrisation is proposed here where we again define $P = P^\flat + P^\sharp$ for $\ell^2 = (\ell - P)^2 = 0$:

$$\ell = (P^\flat + P^\sharp)A + (P^\flat - P^\sharp)B + \lambda_{P^\flat}\tilde{\lambda}_{P^\sharp}C + \lambda_{P^\sharp}\tilde{\lambda}_{P^\flat}C^* \qquad (5.51)$$

and we want to change to spherical polar coordinates. To do this we need to be careful that $P_0^\flat > 0$ and $P_0^\sharp > 0$. This is because the magnitudes of the basis vectors are P^2, $-P^2$, $-P^2$

and $-P^2$, and for the mostly minus metric we want $P^2 > 0$ to have the correct spherical integration region. Having changed to spherical polar coordinates and imposing the cuts, we have left over

$$
\begin{aligned}
\ell &= \frac{P^\flat + P^\sharp}{2} + \cos(\theta)\frac{P^\flat - P^\sharp}{2} + \sin(\theta)e^{i\phi}\frac{\lambda_{P^\flat}\tilde{\lambda}_{P^\sharp}}{2} + \sin(\theta)e^{-i\phi}\frac{\lambda_{P^\sharp}\tilde{\lambda}_{P^\flat}}{2} \\
&= \cos^2\left(\frac{\theta}{2}\right)P^\flat + \sin^2\left(\frac{\theta}{2}\right)P^\sharp + \sin\left(\frac{\theta}{2}\right)\cos\left(\frac{\theta}{2}\right)e^{i\phi}\lambda_{P^\flat}\tilde{\lambda}_{P^\sharp} + \sin\left(\frac{\theta}{2}\right)\cos\left(\frac{\theta}{2}\right)e^{-i\phi}\lambda_{P^\sharp}\tilde{\lambda}_{P^\flat},
\end{aligned}
\tag{5.52}
$$

and we can read off that

$$
\lambda_\ell = \cos\left(\frac{\theta}{2}\right)\lambda_{P^\flat} + \sin\left(\frac{\theta}{2}\right)e^{-i\phi}\lambda_{P^\sharp}, \quad \tilde{\lambda}_\ell = \cos\left(\frac{\theta}{2}\right)\tilde{\lambda}_{P^\flat} + \sin\left(\frac{\theta}{2}\right)e^{i\phi}\tilde{\lambda}_{P^\sharp}.
\tag{5.53}
$$

We may then define

$$
z = e^{-i\phi},
\tag{5.54}
$$

include a normalisation measure of

$$
-\frac{\sin(\theta)}{2(2\pi i)z},
\tag{5.55}
$$

and then perform the θ integral and the z integral via Cauchy's Theorem to obtain (after a little tidying)

$$
\begin{aligned}
&H_0^3(D_1, D_2, D_3, B_1, B_2, B_3, P) \\
&= \frac{1}{4}[D_1|P|B_1\rangle[D_2|P|B_2\rangle[D_3|P|B_3\rangle - \frac{P^2}{12}[D_2\,D_3]\langle B_2\,B_3\rangle[D_1|P|B_1\rangle \\
&\quad - \frac{P^2}{12}[D_3\,D_1]\langle B_3\,B_1\rangle[D_2|P|B_2\rangle - \frac{P^2}{12}[D_1\,D_2]\langle B_1\,B_2\rangle[D_3|P|B_3\rangle \\
&= \frac{1}{12}\sum_{i\in Z_3(1,2,3)}\Big([D_i|P|B_i\rangle[D_{i+1}|P|B_{i+1}\rangle[D_{i+2}|P|B_{i+2}\rangle - P^2[D_i\,D_{i+1}]\langle B_i\,B_{i+1}\rangle[D_{i+2}|P|B_{i+2}\rangle\Big).
\end{aligned}
\tag{5.56}
$$

We therefore have target canonical forms, an automated piece of code which takes them and gives the coefficient of the scalar bubble, and a way of reducing the algebraic complexity of massive propagator pieces on two-mass easy boxes. This is all written to scale to higher multiplicities.

Some preliminary tests that we can perform include checking the correct flip symmetries of the results. We expect the insert numerators to have the same flip symmetries as the amplitude, and indeed the numerators have been built to accommodate these flip symmetries. We therefore expect the cuts and integrated results to also have the same flip symmetries, as indicated by the example given in Figure 5.17.
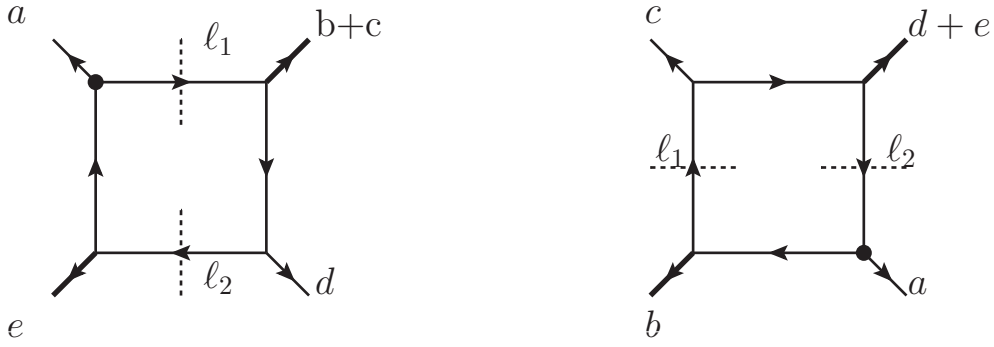
Figure 5.17: Two insert structures related by flips. The integrated result of the left diagram with $\{a, b, c, d, e\} = \{1, 2, 3, 4, 5\}$ is equal to that of the right diagram with $\{a, b, c, d, e\} = \{1, 5, 4, 3, 2\}$.

With that said we now have all of the inserts integrated and can move on to the genuine two-loop structures.

5.3 Two-Loop Pieces

We have so far only needed to deal with pseudo one-loop calculations but it now behoves us to look at explicit two-loop integrals. We can look at the structures and expect at worst a two-mass triangle integral followed by a box integral. These integrals will have varying powers on the propagators and Feynman parameters in the numerators. Every numerator associated with a diagram that contains a bubble within an internal propagator looks schematically like

$$\frac{(L_A|a\rangle)^n \langle a|L_A \ell_w|a\rangle}{L_A^2 (L_A - \ell_w)^2} \rightarrow \frac{(L_A|a\rangle)^n \langle a|L_A \ell_w|a\rangle}{\left((L_A - x\ell_w)^2 + x(1-x)\ell_w^2\right)^2} \rightarrow \frac{((L_A + x\ell_w)|a\rangle)^n \langle a|L_A \ell_w|a\rangle}{\left(L_A^2 + x(1-x)\ell_w^2\right)^2}$$
(5.57)

where we have suppressed integral notation, $(L_A|a\rangle)^n$ indicates that any other factors of L_A are capped with leg a, and x is the Feynman shift variable. We are then left with tensor integrals that integrate to 0 either because they are odd powers of L_A as there is always at least one power, or because the result contains $\langle a\, a \rangle$.

We therefore only have contributions from diagrams with triangle insertions. We see some of the numerators go up to as much as $(L_3)^4$ and so expect at worst quartic powers in the Feynman parameters. We can solve these integrals using some well established techniques such as dimension shifting the integrals and making use of generalised scalar box integrals. We will briefly review these two techniques but then calculate a new version of the generalised box result which is much more compact and easier to perform ϵ-expansions on.

5.3.1 Dimension Shifting

We make use of the identities for the general Feynman parametrisation

$$\frac{1}{D_1^{\nu_1} D_2^{\nu_2} \dots D_n^{\nu_n}} = \frac{\Gamma[\sigma]}{\prod_{i=1}^n \Gamma(\nu_i)} \int_0^\infty \prod_{i=1}^n \mathrm{d}x_i x_i^{\nu_i - 1} \frac{\delta\left(1 - \sum_{j=1}^n x_j\right)}{[x_1 D_1 + x_2 D_2 + \dots + x_n D_n]^\sigma}, \qquad (5.58)$$

where $\sigma = \sum_{i=1}^{n} \nu_i$, and the loop momentum integral

$$\int \frac{\mathrm{d}^D \ell}{i\pi^{\frac{D}{2}}} \frac{\ell^{\mu_1} \dots \ell^{\mu_{2m}}}{[\ell^2 - R^2 + i\delta]^\sigma} = (-1)^\sigma \left[(g^{\dots})^{\otimes m}\right]^{\{\mu_1 \dots \mu_{2m}\}} \left(-\frac{1}{2}\right)^m \frac{\Gamma[\sigma - m - \frac{D}{2}]}{\Gamma[\sigma]} (R^2 - i\delta)^{-\sigma + m + \frac{D}{2}}, \tag{5.59}$$

where $\left[(g^{\dots})^{\otimes m}\right]^{\{\mu_1 \dots \mu_{2m}\}}$ means that μ_i are distributed over m copies of g in all possible ways. Given $\sum_i x_i = 1$ we complete the square to write

$$x_1 D_1 + \cdots x_n D_n \to \ell^2 - R^2 + i\delta, \tag{5.60}$$

and so we can combine (5.58) and (5.59) to give a scalar integral

$$\mathcal{I}_s^D(\nu_1, \dots, \nu_n) := \int \frac{\mathrm{d}^D \ell}{D_1^{\nu_1} \dots D_n^{\nu_n}} = (-1)^\sigma \frac{\Gamma(\sigma - \frac{D}{2})}{\prod_{i=1}^{n} \Gamma(\nu_i)} \int_0^\infty \prod_{i=1}^{n} \mathrm{d}x_i x_i^{\nu_i - 1} \frac{i\pi^{\frac{D}{2}} \delta(1 - \sum_{j=1}^{n} x_j)}{[R^2 - i\delta]^{\sigma - \frac{D}{2}}}, \tag{5.61}$$

where D is the dimension and does not have to be $4 - 2\epsilon$. We also need to consider tensor integrals with possible extra powers of the Feynman parameters $\delta\nu_i$,

$$\mathcal{I}_t^D(\nu_1, \delta\nu_1, \nu_2, \delta\nu_2, \cdots, \nu_n, \delta\nu_n)$$

$$= p_{1\mu_1} \dots p_{2m\mu_{2m}} \frac{\Gamma(\sigma)}{\prod_{i=1}^{n} \Gamma(\nu_i)} \int \mathrm{d}^D \ell \int_0^\infty \prod_{i=1}^{n} \mathrm{d}x_i x_i^{\nu_i - 1} \frac{\prod_{j=1}^{n} x_j^{\delta\nu_j} \ell^{\mu_1} \dots \ell^{\mu_{2m}} \delta(1 - \sum_{k=1}^{n} x_k)}{[x_1 D_1 + x_2 D_2 + \dots + x_n D_n]^\sigma}$$

$$= p_{1\mu_1} \dots p_{2m\mu_{2m}} \left[(g^{\dots})^{\otimes m}\right]^{\{\mu_1 \dots \mu_{2m}\}} \left(-\frac{1}{2}\right)^m \frac{\Gamma(\sigma - m - \frac{D}{2})}{\prod_{i=1}^{n} \Gamma(\nu_i)}$$

$$\times \int_0^\infty \prod_{i=1}^{n} \mathrm{d}x_i x_i^{\nu_i + \delta x_i - 1} \frac{i\pi^{\frac{D}{2}} \delta(1 - \sum_{j=1}^{1} x_j)(-1)^\sigma}{[R^2 - i\delta]^{\sigma + \delta\sigma - [\frac{D}{2} + m + \delta\sigma]}}$$

$$= p_{1\mu_1} \dots p_{2m\mu_{2m}} \left[(g^{\dots})^{\otimes m}\right]^{\{\mu_1 \dots \mu_{2m}\}} \left(-\frac{1}{2}\right)^m$$

$$\times \prod_{i=1}^{n} \frac{\Gamma(\nu_i + \delta\nu_i)}{\Gamma(\nu_i)} \pi^{\frac{D}{2} - \frac{\tilde{D}}{2}} (-1)^{\delta\sigma} \mathcal{I}_s^{\tilde{D}}(\nu_1 + \delta\nu_1, \cdots, \nu_n + \delta\nu_n), \tag{5.62}$$

where $\delta\sigma = \sum_{i=1}^{n} \delta\nu_i$ and the shifted dimension is

$$\tilde{D} = D + 2m + 2\delta\sigma. \tag{5.63}$$

This allows us to relate any tensor integrals with bonus powers of Feynman parameters in the numerator to be related to scalar integrals with shifted powers on the propagators and shifted dimensions. Again, we expect at worst a two-mass triangle integral followed by a one-mass box integral with quartic power of loop momentum. We therefore would like to consider a general form of a scalar one-mass box integral with arbitrary dimension or powers of propagators. This has been previously calculated but we will push it further and provide a much more compact form.

5.3.2 Generalised scalar one-mass box integral
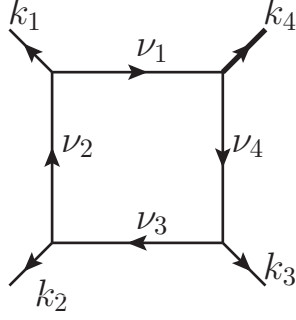
Figure 5.18: A generalised one-mass box with $k_4^2 = M^2$ and all other $k_i^2 = 0$. The internal propagators $\{A_1, A_2, A_3, A_4\}$ have arbitrary powers $\{\nu_1, \nu_2, \nu_3, \nu_4\}$.

Our starting point was the result from [1] which used a derivation in [102] which we will summarise here. Starting with the labels in Figure 5.18, the generic scalar one-mass box integral is given by

$$I_4^D(\nu_1, \nu_2, \nu_3, \nu_4; s, t, M^2) = \int \frac{\mathrm{d}^D \ell}{i\pi^{\frac{D}{2}}} \frac{1}{A_1^{\nu_1} A_2^{\nu_2} A_3^{\nu_3} A_4^{\nu_4}} \tag{5.64}$$

where more generally the $\{s, t, M^2\} = \{Q_i^2\}$ are all external kinematic scales for a given setup. We use incoming external momentum k_i for this derivation so we can write the propagators as

$$A_1 = \ell^2 + i\delta, \qquad A_i = (\ell + \sum_{j=1}^{i-1} k_j)^2 + i\delta, \quad i \neq 1, \tag{5.65}$$

where for the one-mass box we consider $k_4^2 = M^2$. This ordering of ν_i will be used for the rest of this paper. We rewrite (5.64) using Schwinger parameters x_i,

$$I_4^D(\nu_1, \nu_2, \nu_3, \nu_4; \{Q_i^2\}) = (-1)^\sigma \prod_{i=1}^{4} \frac{1}{\Gamma(\nu_i)} \int_0^\infty \mathrm{d}x_i \, x_i^{\nu_i - 1} \int \frac{\mathrm{d}^D \ell}{i\pi^{\frac{D}{2}}} e^{\sum_{i=1}^{4} x_i A_i}$$

$$= \int \mathcal{D}x \int \frac{\mathrm{d}^D \ell}{i\pi^{\frac{D}{2}}} e^{\sum_{i=1}^{4} x_i A_i}, \tag{5.66}$$

and then perform the Gaussian integral to give

$$I_4^D(\nu_1, \nu_2, \nu_3, \nu_4; \{Q_i^2\}) = \int \mathcal{D}x \frac{1}{\mathcal{P}^{\frac{D}{2}}} e^{\mathcal{Q}/\mathcal{P}}, \tag{5.67}$$

where

$$\mathcal{P} = x_1 + x_2 + x_3 + x_4, \tag{5.68}$$

and

$$\mathcal{Q} = x_1 x_3 s + x_2 x_4 t + x_1 x_4 M^2. \tag{5.69}$$

116

This is then evaluated using the suggestions found in [103–105], where we treat the dimension D as a negative, even integer for (5.66) and (5.67). This allows us to write (5.66) and $\frac{1}{\mathcal{P}^{\frac{D}{2}}}$ in (5.67) as a multinomial expansion. This expansion can be written as

$$
\begin{aligned}
&I_4^D(\nu_1, \nu_2, \nu_3, \nu_4; s, t, M^2) \\
&= \int \mathcal{D}x \sum_{n_1, n_2, n_3, n_4 \geq 0} \int \frac{\mathrm{d}^D \ell}{i\pi^{\frac{D}{2}}} \frac{(x_1 A_1)^{n_1}}{n_1!} \frac{(x_2 A_2)^{n_2}}{n_2!} \frac{(x_3 A_3)^{n_3}}{n_3!} \frac{(x_4 A_4)^{n_4}}{n_4!} \\
&= \int \mathcal{D}x \sum_{\mathcal{S} \geq 0} \frac{(x_1 x_3 s)^{q_1} (x_2 x_4 t)^{q_2} (x_1 x_4 M^2)^{q_3}}{q_1! q_2! q_3!} \frac{x_1^{p_1} x_2^{p_2} x_3^{p_3} x_4^{p_4}}{p_1! p_2! p_3! p_4!} \times (p_1 + p_2 + p_3 + p_4)!, \quad (5.70)
\end{aligned}
$$

$\mathcal{S} = \{q_1, q_2, q_3, p_1, p_2, p_3, p_4\}$ and with the constraint

$$
q_1 + q_2 + q_3 + p_1 + p_2 + p_3 + p_4 = -\frac{D}{2}, \quad (5.71)
$$

which ensures the powers of $\mathcal{P}$ and $\mathcal{Q}$ are correct. This equality in (5.70) comes from expanding (5.66) and (5.67), and given that the x_i are independent variables the integrands themselves must be equal. Calling $\nu_i = -n_i$, we can take the $x_i^{-\nu_i}$ coefficients and compare these with the other side of the equality, extracting the Schwinger integrand to give

$$
\begin{aligned}
I_4^D(\nu_1, \nu_2, \nu_3, \nu_4; s, t, M^2) = \sum_{\mathcal{S} \geq 0} & \frac{\Gamma[1 + p_1 + p_2 + p_3 + p_4]}{\Gamma[1 + q_1]\Gamma[1 + q_2]\Gamma[1 + q_3]} \\
& \times \left(\prod_{i=1}^{4} \frac{\Gamma[1 - \nu_i]}{\Gamma[1 + p_i]} \right) s^{q_1} t^{q_2} (M^2)^{q_3}, \quad (5.72)
\end{aligned}
$$

where we can read off the constraints

$$
\begin{aligned}
q_1 + q_3 + p_1 &= -\nu_1, \\
q_2 + p_2 &= -\nu_2, \\
q_1 + p_3 &= -\nu_3, \\
q_2 + q_3 + p_4 &= -\nu_4, \\
q_1 + q_2 + q_3 + p_1 + p_2 + p_3 + p_4 &= -\frac{D}{2}. \quad (5.73)
\end{aligned}
$$

We are left with a system of five constraints on seven summation variable, meaning two variables will always be unconstrained and so we have fifteen possible pairings (twenty-one total pairings but six have no solutions). We have also assumed here that both D and ν_i are negative integers and need to analytically continue the solutions to forms that converge for positive and possibly non-integer D and ν_i. The procedure for presenting these solutions in a sensible closed form is to first convert any Γ-functions into Pochhammer symbols

$$
(z)_n = \frac{\Gamma[z + n]}{\Gamma[z]}, \quad (5.74)
$$

as this is the most suitable way of presenting generalised hypergeometric functions. Following the example in [1] and solving for variables q_1 and q_2, we have the solution (labelled $I^{\{q_1, q_2\}}$

for obvious reasons)

$$I^{\{q_1,q_2\}} = (M^2)^{\frac{D}{2}-\sigma} \frac{\Gamma[1-\nu_1]\Gamma[1-\nu_4]\Gamma[1+\sigma-D]}{\Gamma\left[1+\frac{D}{2}-\sigma\right]\Gamma\left[1+\nu_{123}-\frac{D}{2}\right]\Gamma\left[1+\nu_{234}-\frac{D}{2}\right]}$$

$$\times \sum_{q_1,q_2 \geq 0} \frac{\left(\sigma-\frac{D}{2}\right)_{q_1+q_2}(\nu_3)_{q_1}(\nu_2)_{q_2}}{\left(1+\nu_{123}-\frac{D}{2}\right)_{q_1}\left(1+\nu_{234}-\frac{D}{2}\right)_{q_2}} \frac{\left(\frac{s}{M^2}\right)^{q_1}}{q_1!} \frac{\left(\frac{t}{M^2}\right)^{q_2}}{q_2!}$$

$$= (-1)^{\frac{D}{2}}(M^2)^{\frac{D}{2}-\sigma} \frac{\Gamma\left[\sigma-\frac{D}{2}\right]\Gamma\left[\frac{D}{2}-\nu_{123}\right]\Gamma\left[\frac{D}{2}-\nu_{234}\right]}{\Gamma[\nu_1]\Gamma[\nu_4]\Gamma[D-\sigma]}$$

$$\times F_2\left[\sigma-\frac{D}{2};\nu_3,\nu_2;1+\nu_{123}-\frac{D}{2},1+\nu_{234}-\frac{D}{2};S,T\right], \quad (5.75)$$

where $S = \frac{s}{M^2}$, $T = \frac{t}{M^2}$, $\nu_{ij} = \nu_i + \nu_j$, $\nu_{ijk} = \nu_i + \nu_j + \nu_k$, F_2 is a generalised hypergeometric function, in this case the Appell function

$$F_2[a;b,b';c,c';x,y] := \sum_{m,n \geq 0} \frac{(a)_{m+n}(b)_m(b')_n}{(c)_m(c')_n} \frac{x^m}{m!} \frac{y^n}{n!}, \quad (5.76)$$

and we have used the identity

$$\prod_{i=1}^{3} \frac{\Gamma[\alpha_i]}{\Gamma[\beta_i]} = (-1)^{\sum_{i=1}^{3}(\beta_i-\alpha_i)} \prod_{i=1}^{3} \frac{\Gamma[1-\beta_i]}{\Gamma[1-\alpha_i]}, \quad (5.77)$$

with $\sum_{i=1}^{3}(\beta_i - \alpha_i) = \frac{D}{2}$ and we assume $\frac{D}{2}$ is an integer. This assumption has already been made when performing the multinomial expansion. This final result is analytic in D and ν_i for D being non-integer and ν_i being positive integers. It is also analytic for non-integer ν_i, which is something we will have to consider. A similar process may be followed for the remaining fourteen solutions. In all cases we can write the solutions as some prefactor multiplying a generalised hypergeometric function, a total list of the relevant functions is given in [102].

These generalised hypergeometric functions have different convergence regions. These regions are fully detailed in [102] but as an example, for F_2 we require $|x| + |y| < 1$ whereas for the Horn function H_2 has convergence for $-|x| + \frac{1}{|y|} > 1$, $|x| < 1$, $|y| < 1$. We can divide the kinematic regions indicated in Figure 5.19 which is provided in [1], and as follows:
region I
$|s| + |t| < M^2$;
region II(a)
$|t| > M^2 + |s|$ and $M^2 > |s|$;
region II(b)
$|t| > M^2 + |s|$ and $M^2 < |s|$;
region III(a)
$|s| > M^2 + |t|$ and $M^2 > |t|$;
and finally region III(b)
$|s| > M^2 + |t|$ and $M^2 < |t|$.
In any one region there will be solutions to the system that converge and solutions that do not converge. The generalised scalar box integral is then the sum of all of the convergent functions in any given region. Some of the solutions will appear in multiple kinematic regions and there are certain values of ν_i that would appear to cause individual solutions to diverge but they can be regularised and seen to cancel in the full sum. It is also possible to relate

the functions to each others via analytic continuation. This is the main result of [1] but we would like to take it further.
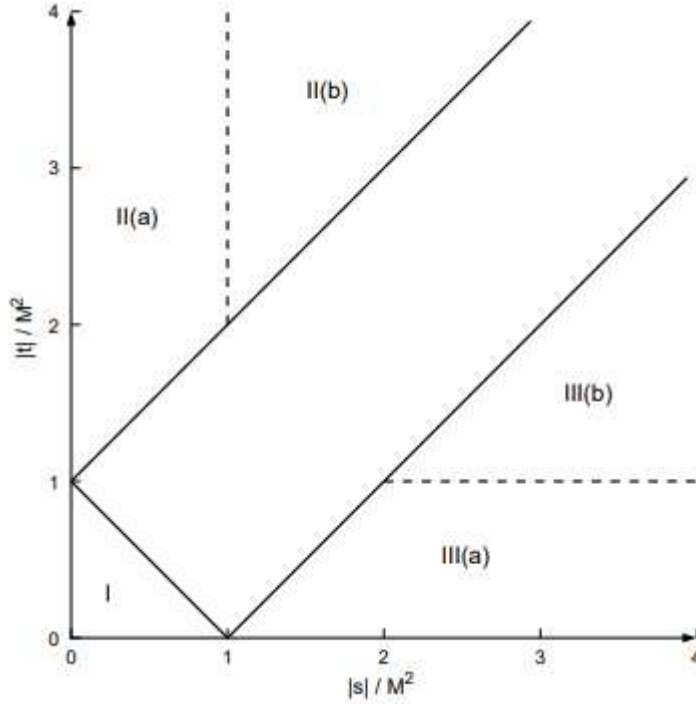
Figure 5.19: The kinematic regions for the one-loop box with one off-shell leg as shown in [1]. The solid line shows the phase-space boundary $|s| + |t| = M^2$, together with the reflections $|s| = |t| + M^2$ and $|t| = |s| + M^2$. The reflections are relevant for the convergence properties of the hypergeometric functions which only involve the absolute values of ratios of the scales. The dashed lines show the boundaries $|s| = M^2$ and $|t| = M^2$.

We will only consider working in the fundamental region (region I) as this helps when we need to perform a Mellin-Barnes expansion. In this region the general one-mass scalar box integral has the form

$$I_4^D(\nu_1, \nu_2, \nu_3, \nu_4; s, t, M^2) = I^{\{q_1, q_2\}} + I^{\{p_1, q_1\}} + I^{\{p_1, p_4\}} + I^{\{p_4, q_2\}} \tag{5.78}$$

where it is to be understood that the functions on the right hand side of the equality have the same arguments as on the left hand side. We have already seen $I^{\{q_1, q_2\}}$, the remaining three are

$$I^{\{p_1, q_1\}} = (-1)^{\frac{D}{2}} T^{\frac{D}{2} - \nu_{234}} (M^2)^{\frac{D}{2} - \sigma} \frac{\Gamma[\nu_{234} - \frac{D}{2}]\Gamma[\frac{D}{2} - \nu_{123}]\Gamma[\frac{D}{2} - \nu_{34}]}{\Gamma[\nu_2]\Gamma[\nu_4]\Gamma[D - \sigma]}$$

$$\times F_2 \left[\nu_1; \nu_3, \frac{D}{2} - \nu_{34}; 1 + \nu_{123} - \frac{D}{2}, 1 + \frac{D}{2} - \nu_{234}; S, T \right], \tag{5.79}$$

119

$$I^{\{p_1,p_4\}} = (-1)^{\frac{D}{2}} S^{\frac{D}{2}-\nu_{123}} T^{\frac{D}{2}-\nu_{234}} (M^2)^{\frac{D}{2}-\sigma}$$

$$\times \frac{\Gamma[\nu_{123}-\frac{D}{2}]\Gamma[\nu_{234}-\frac{D}{2}]\Gamma[\frac{D}{2}-\nu_{12}]\Gamma[\frac{D}{2}-\nu_{23}]\Gamma[\frac{D}{2}-\nu_{34}]}{\Gamma[\nu_1]\Gamma[\nu_2]\Gamma[\nu_3]\Gamma[\nu_4]\Gamma[D-\sigma]}$$

$$\times F_2\left[\frac{D}{2}-\nu_{23};\frac{D}{2}-\nu_{12},\frac{D}{2}-\nu_{34};1+\frac{D}{2}-\nu_{123},1+\frac{D}{2}-\nu_{234};S,T\right], \qquad (5.80)$$

and

$$I^{\{p_4,q_2\}} = (-1)^{\frac{D}{2}} S^{\frac{D}{2}-\nu_{123}} (M^2)^{\frac{D}{2}-\sigma} \frac{\Gamma[\nu_{123}-\frac{D}{2}]\Gamma[\frac{D}{2}-\nu_{12}]\Gamma[\frac{D}{2}-\nu_{234}]}{\Gamma[\nu_1]\Gamma[\nu_3]\Gamma[D-\sigma]}$$

$$\times F_2\left[\nu_4;\frac{D}{2}-\nu_{12},\nu_2;1+\frac{D}{2}-\nu_{123},1+\nu_{234}-\frac{D}{2};S,T\right]. \qquad (5.81)$$

These are results that we pick up from. Looking ahead to the second integration, we expect to see boxes that have undergone a Mellin-Barnes identity which we will see functionally adds a further infinite sum to these boxes. We expect to see many different types of boxes and would like to eventually ϵ-expand them all which we can already see will be an unwieldy endeavour.

5.3.3   A New Compact Form of the Scalar One-Mass Box

We would like to push these results to a more manageable form. We will be making use of hypergeometric identities which can be found in many places such as [106].

First note that these have a common structure

$$\frac{(-1)^{\frac{D}{2}}(M^2)^{\frac{D}{2}-\sigma}f(S,T)}{\Gamma[\nu_1]\Gamma[\nu_2]\Gamma[\nu_3]\Gamma[\nu_4]\Gamma[D-\sigma]}\Gamma[a]\Gamma[b]\Gamma[b']\Gamma[1-c]\Gamma[1-c']F_2[a;b,b';c,c';S,T], \qquad (5.82)$$

where $f(S,T)$ are combinations of $S^{\frac{D}{2}-\nu_{123}}$ and $T^{\frac{D}{2}-\nu_{234}}$. $I^{\{q_1,q_2\}}$ and $I^{\{p_4,q_2\}}$ have b' and c' in common so we will add them together for now

$$I^{\{q_1,q_2\}} + I^{\{p_4,q_2\}}$$

$$= (-1)^{\frac{D}{2}}(M^2)^{\frac{D}{2}-\sigma}\frac{\Gamma[\frac{D}{2}-\nu_{234}]}{\Gamma[\nu_1]\Gamma[D-\sigma]}$$

$$\times \left(\frac{\Gamma[\sigma-\frac{D}{2}]\Gamma[\frac{D}{2}-\nu_{123}]}{\Gamma[\nu_4]}F_2\left[\sigma-\frac{D}{2};\nu_3,\nu_2;1+\nu_{123}-\frac{D}{2},1+\nu_{234}-\frac{D}{2};S,T\right]\right.$$

$$\left.+ S^{\frac{D}{2}-\nu_{123}}\frac{\Gamma[\nu_{123}-\frac{D}{2}]\Gamma[\frac{D}{2}-\nu_{12}]}{\Gamma[\nu_3]} + F_2\left[\nu_4;\frac{D}{2}-\nu_{12},\nu_2,1+\frac{D}{2}-\nu_{123},1+\nu_{234}-\frac{D}{2};S,T\right]\right)$$

$$= (-1)^{\frac{D}{2}}(M^2)^{\frac{D}{2}-\sigma}\frac{\Gamma[\frac{D}{2}-\nu_{234}]}{\Gamma[\nu_1]\Gamma[D-\sigma]}\sum_{n\geq0}\frac{(\nu_2)_n}{(1+\nu_{234}-\frac{D}{2})_n}\frac{T^n}{n!}$$

$$\times \left(\frac{\Gamma[\sigma-\frac{D}{2}]\Gamma[\frac{D}{2}-\nu_{123}](\sigma-\frac{D}{2})_n}{\Gamma[\nu_4]}\,_2F_1\left[\sigma-\frac{D}{2}+n,\nu_3;1+\nu_{123}-\frac{D}{2};S\right]\right.$$

$$\left.+ S^{\frac{D}{2}-\nu_{123}}\frac{\Gamma[\nu_{123}-\frac{D}{2}]\Gamma[\frac{D}{2}-\nu_{12}](\nu_4)_n}{\Gamma[\nu_3]}\,_2F_1\left[\nu_4+n,\frac{D}{2}-\nu_{12};1+\frac{D}{2}-\nu_{123};S\right]\right), \qquad (5.83)$$

120

where we have used the fact that

$$F_2[a; b, b'; c, c'; x, y] = \sum_{n \geq 0} \frac{(a)_n (b')_n}{(c')_n} \frac{y^n}{n!} \, _2F_1(a + n, b; c; x).$$
(5.84)

This begins to look like the identity

$$_2F_1(a, b, c; z) = \frac{\Gamma[c]\Gamma[b-a]}{\Gamma[b]\Gamma[c-a]} (1 - z)^{-a} \, _2F_1 \left[a, c - b; a - b + 1; \frac{1}{1-z} \right]$$
$$+ \frac{\Gamma[c]\Gamma[a-b]}{\Gamma[a]\Gamma[c-b]} (1 - z)^{-b} \, _2F_1 \left[b, c - a; b - a + 1; \frac{1}{1-z} \right],$$
(5.85)

if we set $a = \sigma - \frac{D}{2} + n$, $b = \nu_4 + n$, $c = \nu_{34} + n$. This leads us to

$$I^{\{q_1, q_2\}} + I^{\{p_4, q_2\}}$$

$$= (-1)^{\frac{D}{2}} (M^2)^{\frac{D}{2} - \sigma} \frac{\Gamma[\frac{D}{2} - \nu_{234}]}{\Gamma[\nu_1]\Gamma[\nu_4]\Gamma[D - \sigma]} \sum_{n \geq 0} \frac{(\nu_2)_n}{(1 + \nu_{234} - \frac{D}{2})_n} \frac{T^n}{n!} \frac{\Gamma[a]\Gamma[b]\Gamma[c-a]}{\Gamma[c]} S^{-a}$$

$$\times \left(S^a \frac{\Gamma[c]\Gamma[b-a]}{\Gamma[b]\Gamma[c-a]} \, _2F_1[a, c - b; a - b + 1; S] + S^b \frac{\Gamma[c]\Gamma[a-b]}{\Gamma[a]\Gamma[c-b]} \, _2F_1[b, c - a; b - a + 1; S] \right)$$

$$= (-1)^{\frac{D}{2}} S^{\frac{D}{2} - \sigma} (M^2)^{\frac{D}{2} - \sigma} \frac{\Gamma[\frac{D}{2} - \nu_{234}]\Gamma[\frac{D}{2} - \nu_{12}]}{\Gamma[\nu_1]\Gamma[\nu_4]\Gamma[D - \sigma]} \sum_{n \geq 0} \frac{(\nu_2)_n}{(1 + \nu_{234} - \frac{D}{2})_n} \frac{(\frac{T}{S})^n}{n!}$$

$$\times \frac{\Gamma[\sigma - \frac{D}{2} + n]\Gamma[\nu_4 + n]}{\Gamma[\nu_{34} + n]} \, _2F_1 \left[\sigma - \frac{D}{2} + n, \nu_4 + n; \nu_{34} + n; \frac{S - 1}{S} \right],$$
(5.86)

where we have set $S = \frac{1}{1-z}$. Similarly for the other pair

$$I^{\{p_1, q_1\}} + I^{\{p_1, p_4\}}$$

$$= (-1)^{\frac{D}{2}} T^{\frac{D}{2} - \nu_{234}} (M^2)^{\frac{D}{2} - \sigma} \frac{\Gamma[\nu_{234} - \frac{D}{2}]\Gamma[\frac{D}{2} - \nu_{34}]}{\Gamma[\nu_2]\Gamma[\nu_4]\Gamma[D - \sigma]} \sum_{n \geq 0} \frac{(\frac{D}{2} - \nu_{34})_n}{(1 + \frac{D}{2} - \nu_{234})_n} \frac{T^n}{n!}$$

$$\times \left(\Gamma \left[\frac{D}{2} - \nu_{123} \right] (\nu_1)_n \, _2F_1 \left[\nu_1 + n, \nu_3; 1 + \nu_{123} - \frac{D}{2}; S \right] \right.$$

$$+ S^{\frac{D}{2} - \nu_{123}} \frac{\Gamma[\nu_{123}] - \frac{D}{2}]\Gamma[\frac{D}{2} - \nu_{12}]\Gamma[\frac{D}{2} - \nu_{23}](\frac{D}{2} - \nu_{23})_n}{\Gamma[\nu_1]\Gamma[\nu_3]}$$

$$\times \left. _2F_1 \left[\frac{D}{2} - \nu_{23} + n, \frac{D}{2} - \nu_{12}; 1 + \frac{D}{2} - \nu_{123}; S \right] \right)$$
(5.87)

where we now set $a = \nu_1 + n$, $b = \frac{D}{2} - \nu_{23} + n$, $c = \frac{D}{2} - \nu_2 + n$ and rewrite

$$I^{\{p_1,q_1\}} + I^{\{p_1,p_4\}}$$

$$= (-1)^{\frac{D}{2}} T^{\frac{D}{2}-\nu_{234}} (M^2)^{\frac{D}{2}-\sigma} \frac{\Gamma[\nu_{234} - \frac{D}{2}]\Gamma[\frac{D}{2} - \nu_{34}]}{\Gamma[\nu_1]\Gamma[\nu_2]\Gamma[\nu_4]\Gamma[D-\sigma]} \sum_{n\geq 0} \frac{(\frac{D}{2} - \nu_{34})_n}{(1 + \frac{D}{2} - \nu_{234})_n} \frac{T^n}{n!} \frac{\Gamma[a]\Gamma[b]\Gamma[c-a]}{\Gamma[c]} S^{-a}$$

$$\times \left(S^a \frac{\Gamma[c]\Gamma[b-a]}{\Gamma[b]\Gamma[c-a]} {}_2F_1[a, c-b; a-b+1; S] + S^b \frac{\Gamma[c]\Gamma[a-b]}{\Gamma[a]\Gamma[c-b]} {}_2F_1[b, c-a; b-a+1; S] \right)$$

$$= (-1)^{\frac{D}{2}} S^{-\nu_1} T^{\frac{D}{2}-\nu_{234}} (M^2)^{\frac{D}{2}-\sigma} \frac{\Gamma[\nu_{234} - \frac{D}{2}]\Gamma[\frac{D}{2} - \nu_{12}]\Gamma[\frac{D}{2} - \nu_{34}]}{\Gamma[\nu_1]\Gamma[\nu_2]\Gamma[\nu_4]\Gamma[D-\sigma]} \sum_{n\geq 0} \frac{(\frac{D}{2} - \nu_{34})_n}{(1 + \frac{D}{2} - \nu_{234})_n} \frac{(\frac{T}{S})^n}{n!}$$

$$\times \frac{\Gamma[\nu_1 + n]\Gamma[\frac{D}{2} - \nu_{23} + n]}{\Gamma[\frac{D}{2} - \nu_2 + n]} {}_2F_1\left[\nu_1 + n, \frac{D}{2} - \nu_{23} + n; \frac{D}{2} - \nu_2 + n; \frac{S-1}{S}\right]. \tag{5.88}$$

We can push these expressions further by using a Pfaff transformation [107],

$$_2F_1[a, b; c; z] = (1-z)^{-a} \, {}_2F_1\left[a, c-b; c; \frac{z}{z-1}\right] \tag{5.89}$$

and then writing the hypergeometric function in integral representation

$$I^{\{q_1,q_2\}} + I^{\{p_4,q_2\}}$$

$$= (-1)^{\frac{D}{2}} S^{\frac{D}{2}-\sigma} (M^2)^{\frac{D}{2}-\sigma} \frac{\Gamma[\frac{D}{2} - \nu_{234}]\Gamma[\frac{D}{2} - \nu_{12}]}{\Gamma[\nu_1]\Gamma[\nu_4]\Gamma[D-\sigma]} \sum_{n\geq 0} \frac{(\nu_2)_n}{(1 + \nu_{234} - \frac{D}{2})_n} \frac{(\frac{T}{S})^n}{n!}$$

$$\times \frac{\Gamma[\sigma - \frac{D}{2} + n]\Gamma[\nu_4 + n]}{\Gamma[\nu_{34} + n]} {}_2F_1\left[\sigma - \frac{D}{2} + n, \nu_4 + n; \nu_{34} + n; \frac{S-1}{S}\right]$$

$$= (-1)^{\frac{D}{2}} S^{\frac{D}{2}-\nu_{123}} (M^2)^{\frac{D}{2}-\sigma} \frac{\Gamma[\sigma - \frac{D}{2}]\Gamma[\frac{D}{2} - \nu_{234}]\Gamma[\frac{D}{2} - \nu_{12}]}{\Gamma[\nu_1]\Gamma[\nu_4]\Gamma[D-\sigma]}$$

$$\times \sum_{n\geq 0} \frac{(\nu_2)_n}{(1 + \nu_{234} - \frac{D}{2})_n} \frac{T^n}{n!} \frac{(\sigma - \frac{D}{2})_n \Gamma[\nu_4 + n]}{\Gamma[\nu_{34} + n]} {}_2F_1\left[\frac{D}{2} - \nu_{12}, \nu_4 + n; \nu_{34} + n; 1 - S\right]$$

$$= (-1)^{\frac{D}{2}} S^{\frac{D}{2}-\nu_{123}} (M^2)^{\frac{D}{2}-\sigma} \frac{\Gamma[\sigma - \frac{D}{2}]\Gamma[\frac{D}{2} - \nu_{234}]\Gamma[\frac{D}{2} - \nu_{12}]}{\Gamma[\nu_1]\Gamma[\nu_4]\Gamma[D-\sigma]}$$

$$\times \int_0^1 du (1 - u(1-S))^{\nu_{12}-\frac{D}{2}} u^{\nu_4-1}(1-u)^{\nu_3-1} \sum_{n\geq 0} \frac{(\sigma - \frac{D}{2})_n (\nu_2)_n}{(1 + \nu_{234} - \frac{D}{2})_n} \frac{(uT)^n}{n!} \tag{5.90}$$

and following the same steps

$$I^{\{p_1,q_1\}} + I^{\{p_1,p_4\}}$$

$$= (-1)^{\frac{D}{2}} S^{\frac{D}{2}-\nu_{123}} T^{\frac{D}{2}-\nu_{234}} (M^2)^{\frac{D}{2}-\sigma} \frac{\Gamma[\nu_{234} - \frac{D}{2}]\Gamma[\frac{D}{2} - \nu_{12}]\Gamma[\frac{D}{2} - \nu_{34}]}{\Gamma[\nu_2]\Gamma[\nu_3]\Gamma[\nu_4]\Gamma[D-\sigma]}$$

$$\times \int_0^1 du \, u^{\frac{D}{2}-\nu_{23}-1}(1-u)^{\nu_3-1}(1 - u(1-S))^{\nu_{12}-\frac{D}{2}} \sum_{n\geq 0} \frac{(\frac{D}{2} - \nu_{34})_n (\nu_1)_n}{(1 + \frac{D}{2} - \nu_{234})_n} \frac{(uT)^n}{n!}. \tag{5.91}$$

Strictly speaking, (5.89) is only valid for $z \notin \{1, \infty\}$ which is not true for $\frac{S-1}{S}$ in some parts of the fundamental region. We will see in Section 5.5.4 that it actually benefits us to be a bit

loose with which region we are in for intermediate steps, and worry about which Riemann sheet we are on later. Having said that, it is still good to keep these assumptions in mind as we never know what complications might arise for higher multiplicities.

We can then combine all four terms, pushing towards (5.85) with $a = \nu_2$, $b = \frac{D}{2} - \nu_{34}$, $c = \nu_{12}$ and $uT = \frac{1}{1-z}$ to give

$$I_4^D(\nu_1, \nu_2, \nu_3, \nu_4; s, t, M^2) = I^{\{q_1, q_2\}} + I^{\{p_4, q_2\}} + I^{\{p_1, q_1\}} + I^{\{p_1, p_4\}}$$

$$= (-1)^{\frac{D}{2}} S^{\frac{D}{2} - \nu_{123}} (M^2)^{\frac{D}{2} - \sigma} \frac{\Gamma[\sigma - \frac{D}{2}]\Gamma[\frac{D}{2} - \nu_{12}]\Gamma[\frac{D}{2} - \nu_{34}]}{\Gamma[\nu_3]\Gamma[\nu_4]\Gamma[\nu_{12}]\Gamma[D - \sigma]}$$

$$\times \int_0^1 du \sum_{n \geq 0} (1 - u(1 - S))^{\nu_{12} - \frac{D}{2}} u^{\nu_4 - 1} (1 - u)^{\nu_3 - 1}$$

$$\times \left[(uT)^{\nu_2} \frac{\Gamma[\nu_{12}]\Gamma[\frac{D}{2} - \nu_{234}]}{\Gamma[\frac{D}{2} - \nu_{34}]\Gamma[\nu_1]} \frac{(\nu_2)_n (\sigma - \frac{D}{2})_n}{(1 + \nu_{234} - \frac{D}{2})_n} \frac{(uT)^n}{n!} \right.$$

$$\left. + (uT)^{\frac{D}{2} - \nu_{34}} \frac{\Gamma[\nu_{12}]\Gamma[\nu_{234} - \frac{D}{2}]}{\Gamma[\nu_2]\Gamma[\sigma - \frac{D}{2}]} \frac{(\frac{D}{2} - \nu_{34})_n (\nu_1)_n}{(1 + \frac{D}{2} - \nu_{234})_n} \frac{(uT)^n}{n!} \right] (uT)^{-\nu_2}$$

$$= (-1)^{\frac{D}{2}} S^{\frac{D}{2} - \nu_{123}} (M^2)^{\frac{D}{2} - \sigma} \frac{\Gamma[\sigma - \frac{D}{2}]\Gamma[\frac{D}{2} - \nu_{12}]\Gamma[\frac{D}{2} - \nu_{34}]}{\Gamma[\nu_3]\Gamma[\nu_4]\Gamma[\nu_{12}]\Gamma[D - \sigma]}$$

$$\times \int_0^1 du \sum_{n \geq 0} (1 - u(1 - S))^{\nu_{12} - \frac{D}{2}} u^{\nu_4 - 1} (1 - u)^{\nu_3 - 1} \left[\frac{(\nu_2)_n (\frac{D}{2} - \nu_{34})_n}{(\nu_{12})_n} \frac{(\frac{uT-1}{uT})^n}{n!} \right] (uT)^{-\nu_2}$$

$$= (-1)^{\frac{D}{2}} S^{\frac{D}{2} - \nu_{123}} (M^2)^{\frac{D}{2} - \sigma} \frac{\Gamma[\sigma - \frac{D}{2}]\Gamma[\frac{D}{2} - \nu_{12}]\Gamma[\frac{D}{2} - \nu_{34}]}{\Gamma[\nu_3]\Gamma[\nu_4]\Gamma[\nu_{12}]\Gamma[D - \sigma]}$$

$$\times \int_0^1 du \sum_{n \geq 0} (1 - u(1 - S))^{\nu_{12} - \frac{D}{2}} u^{\nu_4 - 1} (1 - u)^{\nu_3 - 1} \left[\frac{(\nu_2)_n (\sigma - \frac{D}{2})_n}{(\nu_{12})_n} \frac{(1 - uT)^n}{n!} \right] \quad (5.92)$$

where the last line comes from performing a Pfaff transformation followed by an Euler transformation

$$_2F_1[a, b; c; z] = (1 - z)^{c-a-b} \, _2F_1[c - a, c - b; c; z]. \quad (5.93)$$

We arrive at a compact form of a general one-mass scalar box function. It is an integral involving a hypergeometric function, or as we will see, an infinite sum of Appell F_1 functions but we will see later it is quite simple to $\epsilon-$expand and usually simplifies greatly for specific cases. We will also see later that with a bit of work we can simplify the Mellin-Barnes sum of the general box that we will need for the tricorner box.

With the triangle integral in mind, we can use this result to derive an expression for a general two-mass triangle by setting $\nu_3 \to 0$. We use Picard's integral representation of the F_1 function,

$$F_1[a; b_1, b_2; c; x, y] = \frac{\Gamma[c]}{\Gamma[a]\Gamma[c - a]} \int_0^1 du \, u^{a-1} (1 - u)^{c-a-1} (1 - ux)^{-b_1} (1 - uy)^{-b_2} \quad (5.94)$$

for $\mathrm{Re}(a) > 0$ and $\mathrm{Re}(c - a) > 0$, as well as

$$F_1[a; b_1, b_2; a; x, y] = (1 - x)^{-b_1} (1 - y)^{-b_2} \quad (5.95)$$

123

to express (5.92) as

$$
I_3^{D,2m}(\nu_1, \nu_2, \nu_4; t, M^2) = I_4^D(\nu_1, \nu_2, \nu_3 \to 0, \nu_4; s, t, M^2)
$$

$$
= (-1)^{\frac{D}{2}}(M^2)^{\frac{D}{2}-\sigma} S^{\frac{D}{2}-\nu_{123}} \frac{\Gamma[\frac{D}{2}-\nu_{12}]\Gamma[\sigma-\frac{D}{2}]\Gamma[\frac{D}{2}-\nu_{34}]}{\Gamma[\nu_3]\Gamma[\nu_4]\Gamma[\nu_{12}]\Gamma[D-\sigma]}
$$

$$
\times \sum_{m \geq 0} \frac{(\sigma-\frac{D}{2})_m (\nu_2)_m}{(\nu_{12})_m m!} \int_0^1 \mathrm{d}u\, u^{\nu_4-1}(1-u)^{\nu_3-1}(1-u(1-S))^{\nu_{12}-\frac{D}{2}}(1-uT)^m \Big|_{\nu_3 \to 0}
$$

$$
= (-1)^{\frac{D}{2}}(M^2)^{\frac{D}{2}-\sigma} S^{\frac{D}{2}-\nu_{123}} \frac{\Gamma[\frac{D}{2}-\nu_{12}]\Gamma[\sigma-\frac{D}{2}]\Gamma[\frac{D}{2}-\nu_{34}]}{\Gamma[\nu_3]\Gamma[\nu_4]\Gamma[\nu_{12}]\Gamma[D-\sigma]}
$$

$$
\times \sum_{m \geq 0} \frac{(\sigma-\frac{D}{2})_m (\nu_2)_m}{(\nu_{12})_m m!} \frac{\Gamma[\nu_3]\Gamma[\nu_4]}{\Gamma[\nu_{34}]} F_1\left(\nu_4; \frac{D}{2}-\nu_{12}, -m; \nu_{34}; 1-S, T\right)\Big|_{\nu_3 \to 0}
$$

$$
= (-1)^{\frac{D}{2}}(M^2)^{\frac{D}{2}-\sigma} \frac{\Gamma[\frac{D}{2}-\nu_{12}]\Gamma[\sigma-\frac{D}{2}]\Gamma[\frac{D}{2}-\nu_4]}{\Gamma[\nu_4]\Gamma[\nu_{12}]\Gamma[D-\sigma]}
$$

$$
\times \sum_{m \geq 0} \frac{(\sigma-\frac{D}{2})_m (\nu_2)_m (1-T)^m}{(\nu_{12})_m m!}
$$

$$
= (-1)^{\frac{D}{2}}(M^2)^{\frac{D}{2}-\sigma} \frac{\Gamma[\frac{D}{2}-\nu_{12}]\Gamma[\sigma-\frac{D}{2}]\Gamma[\frac{D}{2}-\nu_4]}{\Gamma[\nu_4]\Gamma[\nu_{12}]\Gamma[D-\sigma]} {}_2F_1\left(\sigma-\frac{D}{2}, \nu_2; \nu_{12}; 1-T\right). \tag{5.96}
$$

This agrees with previous calculation although it is more compact than the form presented in [102]. We can do the exact same procedure for one-mass triangles by setting $\nu_4 \to 0$ to get

$$
I_3^{D,1m}(\nu_1, \nu_2, \nu_3; s) = I_4^D(\nu_1, \nu_2, \nu_3, \nu_4 \to 0; s, t, M^2)
$$

$$
= (-1)^{\frac{D}{2}} s^{\frac{D}{2}-\nu_{123}} \frac{\Gamma[\frac{D}{2}-\nu_{12}]\Gamma[\sigma-\frac{D}{2}]\Gamma[\frac{D}{2}-\nu_{23}]}{\Gamma[\nu_3]\Gamma[\nu_1]\Gamma[D-\sigma]}, \tag{5.97}
$$

agreeing with the already well established result. These results were checked numerically for several configurations. A quick check of the standard scalar triangles shows us

$$
I_3^{D,2m}(1,1,1; p_1^2, p_2^2) = (-1)^{2-\epsilon}(p_2^2)^{-1-\epsilon} \frac{\Gamma[-\epsilon]\Gamma[1+\epsilon]\Gamma[1-\epsilon]}{\Gamma[1-2\epsilon]} {}_2F_1\left[1+\epsilon, 1; 2; 1-\frac{p_1^2}{p_2^2}\right]
$$

$$
= \frac{(-1)^{-\epsilon} r_\Gamma}{\epsilon^2}(p_2^2)^{-1-\epsilon}\left[\frac{(p_2^2)^{1+\epsilon}((p_1^2)^{-\epsilon}-(p_2^2)^{-\epsilon})}{p_1^2-p_2^2}\right] = \frac{r_\Gamma\left[(-p_1^2)^{-\epsilon}-(-p_2^2)^{-\epsilon}\right]}{\epsilon^2(p_1^2-p_2^2)}
$$

$$
I_3^{D,1m}(1,1,1; s) = (-1)^{2-\epsilon} s^{-1-\epsilon} \frac{\Gamma[-\epsilon]^2\Gamma[1+\epsilon]}{\Gamma[1-2\epsilon]} = r_\Gamma \frac{(-s)^{-\epsilon}}{\epsilon^2 s}
$$

as we would expect.

5.3.4 Integrating the Numerators
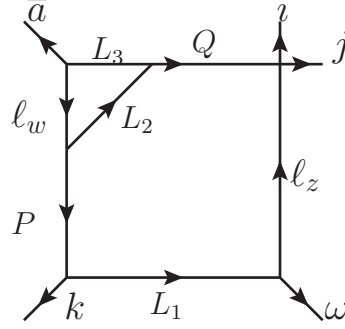
We are now prepared to perform the first integration. Using the labels in Figure 5.3 and above, we choose L_3 as the loop momentum to integrate and so rewrite

$$L_2 = Q - L_3 \qquad l_w = -L_3 - \overline{a} \qquad . \tag{5.98}$$

Using the tricorner box numerator as an example

$$
\begin{aligned}
\mathcal{N} &= \langle a|\overline{a}(-L_3)|a\rangle\langle a|L_2 P L_1 w Q L_2|a\rangle \\
&= \langle a|\overline{a}(-L_3)|a\rangle\langle a|(Q - L_3)P L_1 w Q(Q - L_3)|a\rangle \\
&= \langle a|\overline{a}(-L_3)|a\rangle\langle a|QP L_1 w Q(-L_3)|a\rangle + \langle a|\overline{a}(-L_3)|a\rangle\langle a|(-L_3)P L_1 w Q(-L_3)|a\rangle + \dots
\end{aligned}
\tag{5.99}
$$

where the ellipsis means a propagator was cancelled creating lower order diagrams (which we still keep track of). Next we Feynman parametrise

$$
\begin{aligned}
L_2^2 L_3^2 l_w^2 &\to \left((1 - x_2 - x_3)L_3^2 + x_3(Q - L_3)^2 + x_2(-L_3 - \overline{a})^2\right)^3 \\
&= \left(L_3^2 + 2L_3 \cdot (x_2\overline{a} - x_2 Q) + x_3 Q^2\right)^3 \\
&= \left((L_3 + x_2\overline{a} - x_3 Q)^2 + x_3(1 - x_3)Q^2 + x_2 x_3[\overline{a}|Q|\overline{a}\rangle\right). \\
L_3 &\to L_3 + x_3 Q - x_2\overline{a}.
\end{aligned}
\tag{5.100}
$$

Note here that every L_3 in the numerator appears as $\dots L_3|a\rangle$ so any tensor integral involving the L_3 would be proportional to $\langle a\, a\rangle = 0$. This is all easily automated in a way that performs the substitutions and counts the powers of the Feynman parameters. This can then easily be generalised by combining (5.62) and (5.96) to give

$$
\begin{aligned}
&\int \frac{\mathrm{d}^D \ell}{i\pi^{\frac{D}{2}}} \frac{x_2^m x_3^n}{(L_3^2)^{\nu_1}((L_3 + \overline{a})^2)^{\nu_2}((L_3 - Q)^2)^{\nu_4}} \\
&= \frac{\Gamma[\nu_2 + m]\Gamma[\nu_4 + n]}{\Gamma[\nu_2]\Gamma[\nu_4]}(-1)^{m+n} I_3^{D=4+2m+2n-2\epsilon,2m}(\nu_1, \nu_2 + m, \nu_4 + n; P^2, Q^2),
\end{aligned}
\tag{5.101}
$$

where given it is the first integral $\nu_1 = \nu_2 = \nu_4 = 1$ here. These integrals had previously been calculated using Feynman integration and provided to me but (5.101) served as a good check.

We can inspect the results here to find they each provide bonus powers of the remaining loop integral propagators,

$$\frac{(Q^2)^{m-\epsilon}}{(P^2-Q^2)^{1+m}}, \qquad \frac{(P^2)^{m-\epsilon}}{(P^2-Q^2)^{1+m}}. \tag{5.102}$$

where $m = \{0, 1, 2\}$, as well as various Γ functions and powers of ϵ which are kept track of. These are the bonus powers of propagators that come from the first triangle integrals. We will eventually need to expand the $(P^2 - Q^2)$ in the denominator using a Mellin-Barnes expansion but there are some simplifications we can do first. We use the following replacements

$$[\omega|L_1 P|\bar{a}] \to L_1^2 [\omega\,\bar{a}] + [\omega|L_1 k|\bar{a}], \qquad [\omega|L_1 P Q|a\rangle \to L_1^2 [\omega|Q|a\rangle + [\omega|L_1 k Q|a\rangle,$$
$$[k|L_1 Q|\bar{a}] \to -P^2 [k\,\bar{a}], \quad [\omega|L_1 Q|\bar{a}] \to -P^2 [\omega\,\bar{a}] - [\omega|kQ|\bar{a}],$$
$$[\bar{a}|P|a\rangle \to -[\bar{a}|Q|a\rangle, \quad [k|L_1|a\rangle \to -[k|\bar{a}|a\rangle - [k|Q|a\rangle,$$
$$[\omega|L_1|a\rangle \to -[\omega|P_{k\bar{a}}|a\rangle - [\omega|Q|a\rangle, \quad [k|P|a\rangle \to -[k|\bar{a}|a\rangle - [k|Q|a\rangle \tag{5.103}$$

followed by further replacements

$$[\bar{a}|Q|a\rangle \to \frac{[\bar{a}|Q|k\rangle\,\langle a\,\bar{a}\rangle + [\bar{a}|Q|\bar{a}\rangle\,\langle k\,a\rangle}{\langle k\,\bar{a}\rangle}$$

$$[\omega|Q|a\rangle \to \frac{1}{\langle k\,\omega\rangle}\left(\frac{L_1^2 [\bar{a}|P_{\omega k}|a\rangle}{[k\,\bar{a}]} + \ell_z^2\,\langle k\,a\rangle - \frac{P^2 [\bar{a}|\omega|a\rangle}{[k\,\bar{a}]} - [\omega|P_{k\bar{a}}|a\rangle\,\langle k\,\omega\rangle + \frac{[\bar{a}|Q|k\rangle[k|\omega|a\rangle}{[\bar{a}\,k]}\right)$$

$$[k|Q|a\rangle \to \frac{1}{[\omega\,\bar{a}]}\left(\frac{L_1^2 [\bar{a}|P_{\omega k}|a\rangle}{\langle k\,\omega\rangle} + \frac{\ell_z^2\,\langle k\,a\rangle\,[k\,\bar{a}]}{\langle k\,\omega\rangle} - \frac{P^2 [\omega\,\bar{a}]\,\langle a\,\omega\rangle}{\langle k\,\omega\rangle} - [\omega|P_{k\bar{a}}|a\rangle\,[k\,\bar{a}] \right.$$
$$\left. + \frac{[\bar{a}|Q|k\rangle\,[k\,\omega]\,\langle a\,k\rangle\,\langle\omega\,\bar{a}\rangle}{\langle k\,\bar{a}\rangle\,\langle k\,\omega\rangle} + \frac{[\bar{a}|Q|\bar{a}\rangle[\omega|k|a\rangle}{\langle k\,\bar{a}\rangle}\right)$$

$$[\bar{a}|Q|\omega\rangle \to \frac{1}{\langle k\,\bar{a}\rangle}\left([\bar{a}|Q|k\rangle\,\langle\omega\,\bar{a}\rangle + [\bar{a}|Q|\bar{a}\rangle\,\langle k\,\omega\rangle\right)$$

$$[\omega|L_1|k\rangle \to \to \frac{1}{[k\,\bar{a}]}\left(P^2 [\omega\,\bar{a}] - L_1^2 [\omega\,\bar{a}] - [\bar{a}|Q|k\rangle\,[k\,\omega]\right)$$

$$[\omega|L_1|\bar{a}] \to \frac{1}{\langle\omega\,k\rangle}\left(\frac{L_1^2 [\bar{a}|P_{k\omega}|\bar{a}\rangle}{[k\,\bar{a}]} - \ell_z^2\,\langle\bar{a}\,k\rangle + \frac{P^2 [\omega\,\bar{a}]\,\langle\omega\,\bar{a}\rangle}{[k\,\bar{a}]} - \frac{[\bar{a}|Q|k\rangle\,[k\,\omega]\,\langle\omega\,\bar{a}\rangle}{[k\,\bar{a}]}\right). \tag{5.104}$$

with the goal of having all the loop momentum contributions being in the form of either an inverse propagator, $[\bar{a}|Q|\bar{a}\rangle = P^2 - Q^2$ to reduce the Mellin-Barnes denominator, or $[k|Q|\bar{a}\rangle$. This means our second integral either has cancelled propagators or only an x_4 Feynman parameter being contributed. This means $\nu_3 \leq 1$ for all terms which makes the later expansions more simple.

Something to note here is that a triangle with an $\ell_z^2 \times [k|Q|\bar{a}\rangle$ will pick up a tensor integral if the second integration is Feynman parametrised as a triangle. This can either be dealt with by explicitly performing this tensor integral but we found it to be easier to automate by simply treating this as a box with $\nu_4 = -1$. It is easy to show these methods are equal,

126

for example

$$
\begin{aligned}
\int \frac{\mathrm{d}P}{i\pi^{\frac{D}{2}}} \frac{\ell_z^2 [k|P|\overline{a}\rangle}{P^2(P+\overline{a})^2(P-k)^2} &= \int \frac{\mathrm{d}P}{i\pi^{\frac{D}{2}}} \frac{(P-k-\omega)^2 [k|P|\overline{a}\rangle}{P^2(P+\overline{a})^2(P-k)^2} \\
&= \int \frac{\mathrm{d}p}{i\pi^{\frac{D}{2}}} \int \mathrm{d}x_2 \mathrm{d}x_3 \frac{(p^2 - x_2 x_3 s_{k\overline{a}} + s_{k\omega} - [\omega|p - x_2\overline{a} + x_3 k|\omega\rangle - [k|p - x_2\overline{a}|k\rangle)[k|p|\overline{a}\rangle}{\left[p^2 - R^2 + i\delta\right]^3} \\
&= 0 - \int \frac{\mathrm{d}p}{i\pi^{\frac{D}{2}}} \int \mathrm{d}x_2 \mathrm{d}x_3 \frac{[\omega|p|\omega\rangle [k|p|\overline{a}\rangle}{\left[p^2 - R^2 + i\delta\right]^3} \\
&= -\int \frac{\mathrm{d}p}{i\pi^{\frac{D}{2}}} \int \mathrm{d}x_2 \mathrm{d}x_3 \frac{(2\omega \cdot p)(2\lambda_{\overline{a}} \tilde{\lambda}_k \cdot p)}{\left[p^2 - R^2 + i\delta\right]^3} = \frac{1}{2}(4\omega \cdot \lambda_{\overline{a}} \tilde{\lambda}_k) \times \mathcal{I}_s^{6-2\epsilon}(1,1,1,0) \\
&= [k|\omega|\overline{a}\rangle \times \mathcal{I}_s^{6-2\epsilon}(1,1,1,0)
\end{aligned}
\tag{5.105}
$$

where here we have used (5.62) to perform the tensor integral after a triangle Feynman parametrisation. Opting instead for the box parametrisation

$$
P \to p - x_2\overline{a} + x_3 k + x_4 P_{k\omega},
\tag{5.106}
$$

we see schematically, again using (5.62),

$$
\begin{aligned}
\int \frac{\mathrm{d}P}{i\pi^{\frac{D}{2}}} \frac{[k|P|\overline{a}\rangle}{P^2 Q^2 L_1^2 (\ell_z^2)^{-1}} &\to \int \frac{\mathrm{d}p}{i\pi^{\frac{D}{2}}} \frac{x_4 [k|\omega|\overline{a}\rangle}{P^2 Q^2 L_1^2 (\ell_z^2)^{-1}} \\
&= [k|\omega|\overline{a}\rangle \frac{\Gamma[0]}{\Gamma[-1]}(-1)\mathcal{I}_s^{6-2\epsilon}(1,1,1,-1+1) = [k|\omega|\overline{a}\rangle \times \mathcal{I}_s^{6-2\epsilon}(1,1,1,0)
\end{aligned}
\tag{5.107}
$$

and so we see (5.105) and (5.107) are equal. All cases of tensors being treated as scalar pseudo-boxes have been checked by hand and numerically. Having now rewritten the numerators to simplify the second integral and choosing to use a box Feynman parametrisation for everything to avoid the need for tensor integrals and to aid in automation, we must now consider the Mellin-Barnes expansion.

5.4 Mellin-Barnes Expansion

We now have a set of integrated structures which can be sorted into boxes, two-mass triangles, one-mass triangles and massless bubbles. We have written the numerators of these structures to contain only propagators, $[\overline{a}|Q|\overline{a}\rangle$ and $[k|Q|\overline{a}\rangle$ so we expect only scalar integrals. We also have $(P^2 - Q^2)$ terms in the denominator which need to be expanded via a Mellin-Barnes expansion

$$
\frac{1}{[\overline{a}|Q|\overline{a}\rangle^{1+\kappa}} = \frac{1}{2\pi i} \frac{1}{\Gamma[1+\kappa]} \int_{c-i\infty}^{c+i\infty} \mathrm{d}z \frac{\Gamma[-z]\Gamma[1+\kappa+z]}{(P^2)^{-z}(-Q^2)^{z+1+\kappa}}.
\tag{5.108}
$$

The Γ function is never zero so we can use Cauchy's Residue Theorem by closing the contour either to capture the poles in $\Gamma[-z]$ or $\Gamma[1+\kappa+z]$ to solve the z integral depending on the relative size of the Feynman parameters associated with P and Q. This can be seen with a

simple example

$$\frac{1}{(Q^2)^{\nu_1}(P^2)^{\nu_2}L_1^2\ell_z^2[\bar{a}|Q|\bar{a}\rangle^{1+\kappa}}$$

$$=\frac{1}{2\pi i}\frac{1}{\Gamma[1+\kappa]}\int_{c-i\infty}^{c+i\infty}dz\,\Gamma[-z]\Gamma[1+\kappa+z](-1)^{1+\kappa+z}\frac{\Gamma[2+\alpha_0+\beta_0]}{\Gamma[\alpha_0+z]\Gamma[\beta_0-z]}$$

$$\times\int dx_1\int dx_2\int dx_3\int dx_4\frac{(x_1)^{\alpha_0+z-1}(x_2)^{\beta_0-z-1}\delta(1-x_1-x_2-x_3-x_4)}{\left[p^2-R^2+i\delta\right]^{\alpha_0+\beta_0+2}}$$

$$=\frac{1}{2\pi i}\frac{1}{\Gamma[1+\kappa]}\int_{c-i\infty}^{c+i\infty}dz\,\Gamma[-z]\Gamma[1+\kappa+z](-1)^{1+\kappa+z}\frac{\Gamma[2+\alpha_0+\beta_0]}{\Gamma[\alpha_0+z]\Gamma[\beta_0-z]}$$

$$\times\int dx_1\int dx_2\int dx_3\int dx_4\frac{(x_1)^{\alpha_0-1}(x_2)^{\beta_0-1}\delta(1-x_1-x_2-x_3-x_4)}{\left[p^2-R^2+i\delta\right]^{\alpha_0+\beta_0+2}}\left(\frac{x_1}{x_2}\right)^z. \quad (5.109)$$

where any cases of ν_1 before the Mellin-Barnes expansion will pick up $1+\kappa+z$ and ν_2 picks up $-z$. We have denoted this as $\nu_1=\alpha_0-1-\kappa$ and $\nu_2=\beta_0$. After the expansion any cases of $\nu_1+\nu_2$ will have cancelling z and will not contribute to the contour integral. Closing the contour on left side of the complex plane, the residue at $\Gamma[-N]$ is $\frac{(-1)^N}{\Gamma[1+N]}=\frac{(-1)^N}{N!}$ which happens for all integer $N\geq 0$ and so we can write the contour integral as

$$\sum_{N\geq 0}\frac{(-1)^{2N}}{N!}\frac{\Gamma[1+\kappa+N]}{\Gamma[\alpha_0+N]\Gamma[\beta_0-N]}\left(\frac{x_1}{x_2}\right)^N. \quad (5.110)$$

x_1 is always smaller than x_2 and so this summation converges, allowing us to interchange the integral and summation representation. This all translates to us being able to simply rewrite our functions as

$$f(\nu_{\hat{1}},\nu_2,\nu_3,\nu_4)\to\sum_{N\geq 0}(-1)^{1+\kappa}\frac{(1+\kappa)_N}{N!}f(\nu_1+N,\nu_2-N,\nu_3,\nu_4) \quad (5.111)$$

where we define $\nu_{\hat{1}}=\nu_1-1-\kappa$. We can now go back to our simplified general box function (5.92) and look at a Mellin-Barnes expansion, where the reason for choosing the fundamental region can now be made clear. If we want to perform a loop integral on objects of the form (5.111) then we would ideally like to commute the dz and $d\ell$ integrals. However, in doing so we might introduce new poles if the loop integral result has gamma functions of the form $\Gamma[\nu_1]$ etc, and there is an ambiguity about whether to include these poles in the contour integral. Looking at (5.92), we see that all gamma functions are either free of ν_1 and ν_2, come with the combination $\nu_1+\nu_2$ where the z cancels, or do not contain poles within our chosen contour.

Pressing on, we can rewrite (5.92) using an Euler transformation,

$$(-1)^{\frac{D}{2}}(M^2)^{\frac{D}{2}-\sigma}(S)^{\frac{D}{2}-\nu_{123}}\frac{\Gamma[\frac{D}{2}-\nu_{12}]\Gamma[\sigma-\frac{D}{2}]\Gamma[\frac{D}{2}-\nu_{34}]}{\Gamma[\nu_3]\Gamma[\nu_4]\Gamma[\nu_{12}]\Gamma[D-\sigma]}$$

$$\times\int_0^1 du\sum_{n\geq 0}(1-u(1-S))^{\nu_{12}-\sigma}u^{\nu_4-1}(1-u)^{\nu_3-1}\left[\frac{(\nu_1)_n(\frac{D}{2}-\nu_{34})_n}{(\nu_{12})_n}\frac{(1-uT)^n}{n!}(uT)^{\frac{D}{2}-\nu_{234}}\right]$$

$$(5.112)$$

where we can see that the bit that the Mellin-Barnes expansion effects is

$$
\begin{aligned}
\mathcal{S}_n &= (-1)^{1+\kappa} \sum_{N \geq 0} \sum_{n \geq 0} \frac{(\nu_1 + N)_n (\frac{D}{2} - \nu_{34})_n}{(\nu_{12})_n} \frac{(1 - uT)^n}{n!} (1 + \kappa)_N \frac{(uT)^{\frac{D}{2} + N - \nu_{234}}}{N!} \\
&= (-1)^{1+\kappa} \sum_{N \geq 0} \sum_{n \geq 0} \frac{(\nu_1)_{N+n} (\frac{D}{2} - \nu_{34})_n (1 + \kappa)_N}{(\nu_{12})_n (\nu_1)_N} \frac{(1 - uT)^n}{n!} \frac{(uT)^{\frac{D}{2} + N - \nu_{234}}}{N!} \\
&= (-1)^{1+\kappa} (uT)^{\frac{D}{2} - \nu_{234}} F_2 \left[\nu_1; \frac{D}{2} - \nu_{34}, 1 + \kappa; \nu_{12}, \nu_1; 1 - uT, uT \right] \\
&= (-1)^{1+\kappa} (uT)^{\frac{D}{2} - \nu_{234}} (1 - uT)^{-1-\kappa} F_1 \left[\frac{D}{2} - \nu_{34}; \nu_{\hat{1}}, 1 + \kappa; \nu_{12}; 1 - uT, 1 \right] \\
&= (-1)^{1+\kappa} (uT)^{\frac{D}{2} - \nu_{234}} (1 - uT)^{-1-\kappa} \frac{\Gamma[\nu_{12}] \Gamma[\hat{\sigma} - \frac{D}{2}]}{\Gamma[\nu_{\hat{1}2}] \Gamma[\sigma - \frac{D}{2}]} {}_2F_1 \left[\frac{D}{2} - \nu_{34}, \nu_{\hat{1}}; \nu_{\hat{1}2}; 1 - uT \right] \\
&= (-1)^{1+\kappa} (1 - uT)^{-1-\kappa} \frac{\Gamma[\nu_{12}] \Gamma[\hat{\sigma} - \frac{D}{2}]}{\Gamma[\nu_{\hat{1}2}] \Gamma[\sigma - \frac{D}{2}]} {}_2F_1 \left[\hat{\sigma} - \frac{D}{2}, \nu_2; \nu_{\hat{1}2}; 1 - uT \right], \quad (5.113)
\end{aligned}
$$

where we have used the identity

$$
F_2[a; b, b'; c, a; x, y] = (1 - y)^{-b'} F_1 \left[b; a - b', b'; c; x, \frac{x}{1 - y} \right], \quad (5.114)
$$

and the fact that

$$
F_1[a; b_1, b_2; c; z, 1] = {}_2F_1[a, b_2; c; 1] \, {}_2F_1[a, b_1; c - b_2; z], \quad (5.115)
$$

which further reduces via

$$
{}_2F_1[a, b; c; 1] = \frac{\Gamma[c] \Gamma[c - a - b]}{\Gamma[c - a] \Gamma[c - b]}. \quad (5.116)
$$

This last reduction has the condition that $c - a - b > 0$ so we have assumed $\hat{\sigma} - \frac{D}{2} > 0$ with $\hat{\sigma} = \sigma - 1 - \kappa$. This condition is not satisfied for all of the boxes, but it always contains ϵ so we can analytically continue the ϵ into a range that keeps this condition satisfied, then bring it back for the expansion. $\mathcal{S}_n$ has now been reduced from a double infinite sum back down to a single infinite sum and can now be replaced in (5.112) to give

$$
\begin{aligned}
&I_4^{D,MB}(\nu_1, \nu_2, \nu_3, \nu_4; s, t, M^2) \\
&= (-1)^{\frac{D}{2} + 1 + \kappa} (M^2)^{\frac{D}{2} - \sigma} S^{\frac{D}{2} - \nu_{123}} \frac{\Gamma[\frac{D}{2} - \nu_{12}] \Gamma[\hat{\sigma} - \frac{D}{2}] \Gamma[\frac{D}{2} - \nu_{34}]}{\Gamma[\nu_3] \Gamma[\nu_4] \Gamma[\nu_{\hat{1}2}] \Gamma[D - \sigma]} \\
&\quad \times \int_0^1 du (1 - u(1 - S))^{\nu_{12} - \frac{D}{2}} (1 - uT)^{-1-\kappa} u^{\nu_4 - 1} (1 - u)^{\nu_3 - 1} {}_2F_1 \left[\hat{\sigma} - \frac{D}{2}, \nu_2; \nu_{\hat{1}2}; 1 - uT \right] \\
&\hspace{11cm} (5.117)
\end{aligned}
$$

which trivially simplifies to (5.92) for $\kappa = -1$. With these results, we took our numerators and performed the first integral, then took the box Feynman shift, counted the extra x_4 powers and performed the necessary dimension shifting. It is easy enough to store the values of $\{\nu_1 = \nu_{\hat{1}} + 1 + \kappa, \nu_2, \nu_3, \nu_4, \delta x_4, \kappa, \tilde{D}\}$, strip the coefficients from the relevant terms and compile a list of all of the boxes to be ϵ-expanded. While we treat everything as a box in

terms of the Feynman shift it is convenient to separate the terms into boxes, triangles and bubbles for a few reasons: it made it easier to track down bugs, we only expect to see certain initial structures as a triangle followed by a triangle etc, one-mass triangles reduced to Γ functions so we could just use Mathematica's built in Series function to ϵ-expand them and we can discard massless bubbles straight away as they have no kinematic scale (although this was of course checked in the debugging stage to be sure). Regardless we will hereby refer to all structures as "boxes" for simplicity as they have all been treated as such with respect to the Feynman parametrisation.

It should be noted here that this procedure has been so-far automated in a way that is blind to the number of legs in the massive corner of the box. Our numerators are written entirely in terms of $\bar{a}$, k, ω and loop momenta so this, along with the inserts code which has all been written to scale with multiplicity, should be simple enough to translate to higher multiplicities. The only additional structures we expect to see would be two-mass-easy boxes which would need the same treatment as (5.117).

5.5 ϵ-Expansions

There are several ways we can expand these boxes. An easily automated method is the nested sums approach which we will review later as there was a small number of cases where this approach was straightforward and bypassed issues of diverging integration spaces. The form of (5.117) however suggests we should expand this in an integral form. Schematically this involved taking a piece like $(1 - uZ)^{a+b\epsilon}$ and expanding it as

$$\int_0^1 \mathrm{d}u f(u)(1 - uZ)^{a+b\epsilon} = \int_0^1 \mathrm{d}u\, f(u)(1 - uZ)^a \left(1 + b\epsilon \log[1 - uZ] + \frac{b^2\epsilon^2}{2}\log[1 - uZ]^2 \right)$$

(5.118)

and integrating the result. In some cases the integral diverges near the limits but it was mostly enough to integrate with respect to u and take the series expansion of $u = 1 - \delta$ and $u = \delta$, seeing that the divergences cancelled explicitly. In a few cases this was not enough and some extra work was needed which will be outlined shortly. Indeed, these integrations are being done using Mathematica which has its own built in Riemann sheet and branch cuts which we will ignore for now. Once we have covered the ϵ-expansion in a bit more detail we will outline how we fixed the correct Riemann sheet but suffice to say that the worst problem this approach seemed to cause was somewhat large and unwieldy intermediate expressions, although still no larger than ≈ 10kb in size per box.

Using this method we found 55 boxes ($\nu_3 = 1$ and $\nu_4 \geq 1$), 27 two-mass triangles ($\nu_3 = 0$ and $\nu_4 \geq 1$) and 22 non-vanishing one-mass triangles ($\nu_3 = 1$ and $\nu_4 \leq 0$). The vanishing referred to here is specifically due to parametrising the triangles as a pseudo-box, where in some cases this leads to the triangle gaining ℓ_z^2 powers due to x_4 shifts, promoting it from a one-mass triangle to a box again. In any such cases, the coefficient trivially vanishes due to the $\frac{\Gamma[\nu_4 + \delta\nu_4]}{\Gamma[\nu_4]}$ factor. These cases can be identified and discarded, reducing the number of terms needed (again, in the debugging stage these were checked to make sure there was no diverging box which might multiply this zero to give something finite). Within the 22 one-mass triangles, a few of the triangles integrate to zero so are also vanishing. The rest were all massless bubbles ($\nu_3 = 0$ and $\nu_4 \leq 0$) which integrate to zero. Any cases of $\kappa < -1$ simply had their $[\bar{a}|Q|\bar{a}\rangle$ expanded in the numerator as $P^2 - Q^2$.

It is possible for both loop integrals to provide $\frac{1}{\epsilon^2}$ terms although we expect cancellations. The boxes and triangles generally come in pairs of

$$I_4(\nu_1 = m + \epsilon, \nu_2 = n) - I_4(\nu_1 = m, \nu_2 = n + \epsilon) \tag{5.119}$$

where m and n are integers and whose leading order in ϵ terms cancel. When we perform the Feynman shift and collect the full coefficients of each box for the second integrations, we see that some boxes do not have a pair (more accurately they have a pairing box with vanishing coefficient). These unpaired boxes were at worst $\mathcal{O}(\epsilon^{-3})$, which meant overall we see at worst $\frac{1}{\epsilon^3}$ terms at leading order, so our $\frac{1}{\epsilon^4}$ coefficient is correctly vanishing. Perhaps some closer inspection into the nature of these cancellations would be enlightening, for example it seems that the leading nature of the $(P^2)^{-\epsilon}$ term differing from the $(Q^2)^{-\epsilon}$ term has some dependence on whether P leads to a null corner and Q leads to a non-null corner.

On the subject of future investigations, it is worth noting that when going to higher multiplicities we expect to see a lot of overlap of these one-mass boxes and triangles. The numerators should not get any higher in powers of loop momenta and so we expect to see a lot of the one-mass boxes have already been expanded here.

5.5.1 Boxes

We will now review some techniques we used to aid in the ϵ-expansions. First it is useful to highlight cases of (5.117) where the hypergeometric function collapses. In cases of $\nu_2 = 0$ and $\nu_2 = -1$ we can rewrite (5.117) as

$$
\begin{aligned}
I_{4,\nu_2=0}^{D,MB} &= (-1)^{\frac{D}{2}+1+\kappa}(M^2)^{\frac{D}{2}-\sigma}S^{\frac{D}{2}-\nu_{123}}\frac{\Gamma[\frac{D}{2}-\nu_{12}]\Gamma[\hat{\sigma}-\frac{D}{2}]\Gamma[\frac{D}{2}-\nu_{34}]}{\Gamma[\nu_3]\Gamma[\nu_4]\Gamma[\nu_{\hat{1}2}]\Gamma[D-\sigma]} \\
&\quad \times \int_0^1 du(1-u(1-S))^{\nu_{12}-\frac{D}{2}}u^{\nu_4-1}(1-u)^{\nu_3-1}(1-uT)^{-1-\kappa} \\
&= (-1)^{\frac{D}{2}+1+\kappa}(M^2)^{\frac{D}{2}-\sigma}S^{\frac{D}{2}-\nu_{123}}\frac{\Gamma[\frac{D}{2}-\nu_{12}]\Gamma[\hat{\sigma}-\frac{D}{2}]\Gamma[\frac{D}{2}-\nu_{34}]}{\Gamma[\nu_{34}]\Gamma[\nu_{\hat{1}2}]\Gamma[D-\sigma]} \\
&\quad \times F_1\left[\nu_4; \frac{D}{2}-\nu_{12}, 1+\kappa; \nu_{34}; 1-S, T\right]
\end{aligned} \tag{5.120}
$$

and

$$
\begin{aligned}
I_{4,\nu_2=-1}^{D,MB} &= (-1)^{\frac{D}{2}+1+\kappa}(M^2)^{\frac{D}{2}-\sigma}S^{\frac{D}{2}-\nu_{123}}\frac{\Gamma[\frac{D}{2}-\nu_{12}]\Gamma[\hat{\sigma}-\frac{D}{2}]\Gamma[\frac{D}{2}-\nu_{34}]}{\Gamma[\nu_{34}]\Gamma[\nu_{\hat{1}2}]\Gamma[D-\sigma]} \\
&\quad \times \left(F_1\left[\nu_4; \frac{D}{2}-\nu_{12}, 1+\kappa; \nu_{34}; 1-S, T\right] - \frac{\hat{\sigma}-\frac{D}{2}}{\nu_{\hat{1}2}}F_1\left[\nu_4; \frac{D}{2}-\nu_{12}, \kappa; \nu_{34}; 1-S, T\right]\right).
\end{aligned} \tag{5.121}
$$

For the $\nu_2 = 1$ cases, we have the freedom to push the hypergeometric sum forward without changing the factorial in the denominator. This is not always needed but in some cases $\hat{\sigma} - \frac{D}{2}$ was causing divergences when expanding so it helped to make this argument bigger. It also allows us to rewrite the Mellin-Barnes expanded boxes in ways that relate to the

pre-expanded boxes

$$I_{4,\nu_2=1}^{D,MB} = (-1)^{\frac{D}{2}+1+\kappa}(M^2)^{\frac{D}{2}-\sigma}S^{\frac{D}{2}-\nu_{123}}\frac{\Gamma[\frac{D}{2}-\nu_{12}]\Gamma[\hat{\sigma}-\frac{D}{2}]\Gamma[\frac{D}{2}-\nu_{34}]}{\Gamma[\nu_3]\Gamma[4]\Gamma[\nu_{\hat{1}2}]\Gamma[D-\sigma]}$$

$$\times \int_0^1 du(1-u(1-S))^{\nu_{12}-\frac{D}{2}}u^{\nu_4-1}(1-u)^{\nu_3-1}(1-uT)^{-1-\kappa}$$

$$\times \left[\sum_{p=0}^{\kappa}\frac{(\hat{\sigma}-\frac{D}{2})_p}{(\nu_{\hat{1}2})_p}(1-uT)^p + \sum_{q=p-\kappa-1=0}^{\infty}\frac{(\hat{\sigma}-\frac{D}{2})_{q+\kappa+1}}{(\nu_{\hat{1}2})_{q+\kappa+1}}(1-uT)^{q+\kappa+1}\right]$$

$$= (-1)^{\frac{D}{2}+1+\kappa}(M^2)^{\frac{D}{2}-\sigma}S^{\frac{D}{2}-\nu_{123}}\frac{\Gamma[\frac{D}{2}-\nu_{12}]\Gamma[\frac{D}{2}-\nu_{34}]}{\Gamma[\nu_3]\Gamma[\nu_4]\Gamma[D-\sigma]}$$

$$\left[\sum_{p=0}^{\kappa}\frac{\Gamma[\hat{\sigma}-\frac{D}{2}+p]\Gamma[\nu_3]\Gamma[\nu_4]}{\Gamma[\nu_{\hat{1}2}+p]\Gamma[\nu_{34}]}F_1\left[\nu_4;\frac{D}{2}-\nu_{12},1+\kappa-p;\nu_{34};1-S,T\right]\right.$$

$$\left.+\frac{\Gamma[\sigma-\frac{D}{2}]}{\Gamma[\nu_{12}]}\int_0^1 du(1-u(1-S))^{\nu_{12}-\frac{D}{2}}u^{\nu_4-1}(1-u)^{\nu_3-1}\,_2F_1\left[\sigma-\frac{D}{2},1;\nu_{12};1-uT\right]\right],$$
(5.122)

which is a sum of Appell F_1 functions followed by the pre-Mellin Barnes expanded box up to a factor of $(-1)^{1+\kappa}$. For the $(P^2)^{-\epsilon}$ cases we perform a Pfaff transformation to give

$$I_4^{D,MB} = (-1)^{\frac{D}{2}+1+\kappa}(M^2)^{\frac{D}{2}-\sigma}S^{\frac{D}{2}-\nu_{123}}\frac{\Gamma[\frac{D}{2}-\nu_{12}]\Gamma[\hat{\sigma}-\frac{D}{2}]\Gamma[\frac{D}{2}-\nu_{34}]}{\Gamma[\nu_3]\Gamma[\nu_4]\Gamma[\nu_{\hat{1}2}]\Gamma[D-\sigma]}T^{\frac{D}{2}-\hat{\sigma}}$$

$$\times \int_0^1 du(1-u(1-S))^{\nu_{12}-\frac{D}{2}}u^{\frac{D}{2}-\nu_{\hat{1}23}-1}(1-u)^{\nu_3-1}(1-uT)^{-1-\kappa}$$

$$\times \,_2F_1\left[\hat{\sigma}-\frac{D}{2},\nu_{\hat{1}};\nu_{\hat{1}2};\frac{uT-1}{uT}\right].$$
(5.123)

and can similarly look at collapsing $\nu_{\hat{1}}=-1$ and $\nu_{\hat{1}}=0$ cases. This time we may use the identity

$$F_1[a;b_1,b_2;b_1+b_2;x,y] = (1-x)^{-a}\,_2F_1\left[a,b_2;b_1+b_2;\frac{y-x}{1-y}\right]$$
(5.124)

132

to reduce one of the summations and give

$$I^{D,MB}_{4,\nu_{\hat{1}}=0}$$

$$= (-1)^{\frac{D}{2}+1+\kappa}(M^2)^{\frac{D}{2}-\sigma}S^{\frac{D}{2}-\nu_{123}}\frac{\Gamma[\frac{D}{2}-\nu_{12}]\Gamma[\hat{\sigma}-\frac{D}{2}]\Gamma[\frac{D}{2}-\nu_{34}]}{\Gamma[\nu_3]\Gamma[\nu_4]\Gamma[\nu_{\hat{1}2}]\Gamma[D-\sigma]}T^{\frac{D}{2}-\hat{\sigma}}$$

$$\times \int_0^1 du(1-u(1-S))^{\nu_{12}-\frac{D}{2}}u^{\frac{D}{2}-\nu_{\hat{1}23}-1}(1-u)^{\nu_3-1}(1-uT)^{-1-\kappa}$$

$$= (-1)^{\frac{D}{2}+1+\kappa}(M^2)^{\frac{D}{2}-\sigma}S^{\frac{D}{2}-\nu_{123}}\frac{\Gamma[\frac{D}{2}-\nu_{12}]\Gamma[\hat{\sigma}-\frac{D}{2}]\Gamma[\frac{D}{2}-\nu_{34}]\Gamma[\frac{D}{2}-\nu_{\hat{1}23}]}{\Gamma[\frac{D}{2}-\nu_{\hat{1}2}]\Gamma[\nu_4]\Gamma[\nu_{\hat{1}2}]\Gamma[D-\sigma]}T^{\frac{D}{2}-\hat{\sigma}}$$

$$\times F_1\left[\frac{D}{2}-\nu_{\hat{1}23};\frac{D}{2}-\nu_{12},1+\kappa;\frac{D}{2}-\nu_{\hat{1}2};1-S,T\right]$$

$$= (-1)^{\frac{D}{2}+1+\kappa}(M^2)^{\frac{D}{2}-\sigma}S^{\frac{D}{2}-\nu_{123}}\frac{\Gamma[\frac{D}{2}-\nu_{12}]\Gamma[\hat{\sigma}-\frac{D}{2}]\Gamma[\frac{D}{2}-\nu_{34}]\Gamma[\frac{D}{2}-\nu_{\hat{1}23}]}{\Gamma[\frac{D}{2}-\nu_{\hat{1}2}]\Gamma[\nu_4]\Gamma[\nu_{\hat{1}2}]\Gamma[D-\sigma]}T^{\frac{D}{2}-\hat{\sigma}}$$

$$\times S^{\nu_{\hat{1}23}-\frac{D}{2}}\,_2F_1\left[\frac{D}{2}-\nu_{\hat{1}23},1+\kappa;\frac{D}{2}-\nu_{\hat{1}2};\frac{S+T-1}{S}\right] \tag{5.125}$$

and

$$I^{D,MB}_{4,\nu_{\hat{1}}=-1}$$

$$= (-1)^{\frac{D}{2}+1+\kappa}(M^2)^{\frac{D}{2}-\sigma}S^{\frac{D}{2}-\nu_{123}}\frac{\Gamma[\frac{D}{2}-\nu_{12}]\Gamma[\hat{\sigma}-\frac{D}{2}]\Gamma[\frac{D}{2}-\nu_{34}]}{\Gamma[\nu_4]\Gamma[\nu_{\hat{1}2}]\Gamma[D-\sigma]}T^{\frac{D}{2}-\hat{\sigma}}$$

$$\times \left[\frac{\Gamma[\frac{D}{2}-\nu_{\hat{1}23}]}{\Gamma[\frac{D}{2}-\nu_{\hat{1}2}]}S^{\nu_{\hat{1}23}-\frac{D}{2}}\,_2F_1\left[\frac{D}{2}-\nu_{\hat{1}23},1+\kappa;\frac{D}{2}-\nu_{\hat{1}2};\frac{S+T-1}{S}\right]\right.$$

$$\left.+\frac{\hat{\sigma}-\frac{D}{2}}{\nu_{\hat{1}2}}\frac{\Gamma[\frac{D}{2}-\nu_{\hat{1}23}-1]}{\Gamma[\frac{D}{2}-\nu_{\hat{1}2}-1]}S^{1+\nu_{\hat{1}23}-\frac{D}{2}}\,_2F_1\left[\frac{D}{2}-\nu_{\hat{1}23}-1,\kappa;\frac{D}{2}-\nu_{\hat{1}2}-1;\frac{S+T-1}{S}\right]\right]. \tag{5.126}$$

We can peel off the κ's again for $\nu_{\hat{1}}=1$ cases to give

$$I^{D,MB}_{4,\nu_{\hat{1}}=1}$$

$$= (-1)^{\frac{D}{2}+1+\kappa}(M^2)^{\frac{D}{2}-\sigma}S^{\frac{D}{2}-\nu_{123}}\frac{\Gamma[\frac{D}{2}-\nu_{12}]\Gamma[\frac{D}{2}-\nu_{34}]}{\Gamma[\nu_3]\Gamma[\nu_4]\Gamma[D-\sigma]}$$

$$\times \left[\sum_{p=0}^{\kappa}(-1)^p\frac{\Gamma[\hat{\sigma}-\frac{D}{2}+p]\Gamma[\nu_3]\Gamma[\frac{D}{2}-\nu_{\hat{1}23}-p]}{\Gamma[\nu_{\hat{1}2}+p]\Gamma[\frac{D}{2}-\nu_{\hat{1}2}-p]}T^{\frac{D}{2}-\hat{\sigma}-p}S^{p+\nu_{\hat{1}23}-\frac{D}{2}}\right.$$

$$\times \,_2F_1\left[\frac{D}{2}-\nu_{\hat{1}23}-p,1+\kappa-p;\frac{D}{2}-\nu_{\hat{1}2}-p;\frac{S+T-1}{S}\right]$$

$$+(-1)^{1+\kappa}\frac{\Gamma[\sigma-\frac{D}{2}]}{\Gamma[\nu_{12}]}T^{\frac{D}{2}-\sigma}\int_0^1 du(1-u(1-S))^{\nu_{12}-\frac{D}{2}}u^{\frac{D}{2}-\nu_{123}-1}(1-u)^{\nu_3-1}$$

$$\left.\times \,_2F_1\left[\sigma-\frac{D}{2},1;\nu_{12};\frac{uT-1}{uT}\right]\right]. \tag{5.127}$$

This is a sum of hypergeometrics but unlike the $\nu_2=1$ case the last term is not exactly the pre-Mellin Barnes expanded box as we have the $\nu_{\hat{1}}=1$ argument in the hypergeometric. We

133

may define $\nu_{\hat{2}} = \nu_2 + 1 + \kappa$ and then the final term looks like the pre-Mellin Barnes expanded box but with $\nu_{\hat{1}}$ and $\nu_{\hat{2}}$ as arguments instead of ν_1 and ν_2.

From here, most of the expansions could be done using the integral representations and then using (5.118) as a schematic way of expanding as we have previously discussed. However in some cases the integration region near the limits would diverge in a way that would not allow this simple method. We can find ways around this by deriving some identities using Appell functions and summations. For example, we often consider the $F_1[a; b, b'; c; x, y]$ with $a = \nu_4$ and $c = \nu_{34}$ in $F_1[a; b, b'; c; x, y]$ and for all of our boxes/triangles we have $\nu_3 \leq 1$ which gives commonly occuring special cases of $c = 1 + a$. Taking the $\nu_3 = 1$ boxes, we will take the general case of expanding in some small variable δ, rewriting the logarithms in (5.118) as their summation representation

$$
\begin{aligned}
F_1[a; \delta, b'; 1 + a; x, y] &= \frac{\Gamma[1 + a]}{\Gamma[a]} \int_0^1 \mathrm{d}u \, u^{a-1} (1 - ux)^{-\delta} (1 - uy)^{-b'} \\
&= {}_2F_1[a, b'; 1 + a; y] + \delta \frac{\Gamma[1 + a]}{\Gamma[a]} \sum_{k=1}^{\infty} \frac{x^k}{k} \int_0^1 \mathrm{d}u \, u^{a+k-1} (1 - uy)^{-b'} + \ldots \\
&= {}_2F_1[a, b'; 1 + a; y] + \delta \sum_{k=1}^{\infty} \frac{x^k}{k} \frac{(a)_k}{(1 + a)_k} \, {}_2F_1[a + k, b'; 1 + a + k; y] + \ldots .
\end{aligned}
$$
(5.128)

We can relate F_1 to an infinite sum of ${}_2F_1$'s via

$$
F_1[a; b, b'; c; x, y] = \sum_{k=0}^{\infty} \frac{(b)_k (a)_k}{(c)_k} \frac{x^k}{\Gamma[1 + k]} \, {}_2F_1[a + k, b'; c + k; y]
$$
(5.129)

and then remove the k from the logarithm and relabel the summation variable

$$
\begin{aligned}
&\frac{\partial}{\partial x} \sum_{k=1}^{\infty} \frac{x^k}{k} \frac{(a)_k}{(1 + a)_k} \, {}_2F_1[a + k, b'; 1 + a + k; y] \\
&= \frac{\Gamma[a]}{\Gamma[2 + a]} \sum_{q=0}^{\infty} \frac{x^q}{\Gamma[1 + q]} \frac{(1)_q (1 + a)_q}{(2 + a)_q} \, {}_2F_1[1 + a + q, b'; 2 + a + q; y] \\
&= \frac{1}{a(1 + a)} F_1[1 + a; 1, b'; 2 + a; x, y].
\end{aligned}
$$
(5.130)

We would then like to integrate this with respect to x but first lets derive a useful result for this. Using

$$
\sum_{m,n \geq 0} f(m + n, m - n) \rightarrow \sum_{s=m+n \geq 0} \sum_{\Delta=0}^{s} f(s, 2\Delta - s)
$$
(5.131)

we can resum an F_1 function as

$$F_1[a; 1, 1; 1 + a; x, y] = \sum_{m,n \geq 0} \frac{(a)_{m+n}}{(1 + a)_{m+n}} x^m y^n$$

$$= \sum_{m,n \geq 0} \frac{(a)_{m+n}}{(1 + a)_{m+n}} x^{([m+n]+[m-n])/2} y^{([m+n]-[m-n])/2}$$

$$= \sum_{s \geq 0} \sum_{\Delta = 0}^{s} \frac{(a)_s}{(1 + a)_s} x^\Delta y^{s-\Delta}$$

$$= \sum_{s \geq 0} \frac{(a)_s}{(1 + a)_s} \left(\frac{x^{s+1} - y^{s+1}}{x - y} \right) = \frac{x\, _2F_1[a, 1; 1 + a, x] - y\, _2F_1[a, 1; 1 + a; y]}{x - y}.$$

$$(5.132)$$

We can then take the special case of (5.130) with $a = b' = 1$

$$\frac{\partial}{\partial x} \sum_{k=1}^{\infty} \frac{x^k}{k} \frac{(1)_k}{(2)_k} \, _2F_1[1 + k, 1; 2 + k; y]$$

$$= \frac{1}{2} F_1[2; 1, 1; 3; x, y] = \frac{x\, _2F_1[1, 2; 3; x] - y\, _2F_1[1, 2; 3; y]}{x - y}$$

$$= \frac{x\log[1 - y] - y\log[1 - x]}{(x - y)xy} \qquad (5.133)$$

which we can integrate between boundaries $\{0, x\}$ to give us

$$F_1[1; \delta, 1; 2; x, y] = -\frac{\log[1 - y]}{y}$$

$$+ \delta \frac{\log[\frac{1-y}{1-x}]\log[\frac{y-x}{y-1}] - \text{Li}_2[x] - \text{Li}_2[\frac{x-1}{y-1}] - \log[1 - y]\log[\frac{y}{y-1}] + \text{Li}_2[\frac{1}{1-y}]}{y}$$

$$(5.134)$$

and similarly

$$F_1[1; \delta_1, 1; 2 + \delta_2; x, y] = -\frac{\log[1 - y]}{y}$$

$$+ \delta_1 \frac{\log[\frac{1-y}{1-x}]\log[\frac{y-x}{y-1}] - \text{Li}_2[x] - \text{Li}_2[\frac{x-1}{y-1}] - \log[1 - y]\log[\frac{y}{y-1}] + \text{Li}_2[\frac{1}{1-y}]}{y}$$

$$+ \delta_2 \frac{-\log[1 - y] + \frac{\pi^2}{6} + \log[1 - y]\log[\frac{y}{y-1}] + \text{Li}_2[\frac{1}{1-y}]}{y}. \qquad (5.135)$$

We can then perform exactly the same tricks multiple times, differentiating to deal with the $\frac{1}{k}$ from the logs, collapsing F_1's to $_2F_1$'s then resumming these back into to F_1's which can

again collapse, then integrating. This allows us to find

$$F_1[1; 1+\delta, 1; 2; x, y] = \frac{1}{y-x} \log \left[\frac{1-x}{1-y} \right]$$

$$+ \frac{2\delta}{y-x} \left[\log \left[\frac{1-y}{1-x} \right] \log \left[\frac{y-x}{y-1} \right] - \text{Li}_2 \left[\frac{x-1}{y-1} \right] - \log[1-y] \log \left[\frac{y}{y-1} \right] \right.$$

$$+ \left. \text{Li}_2 \left[\frac{1}{1-y} \right] + \log[1-x] \log \left[\frac{x}{x-1} \right] - \text{Li}_2 \left[\frac{1}{1-x} \right] + \frac{\pi^2}{6} \right] + \dots \quad (5.136)$$

If we need to go to higher orders in δ, these again usually can be expanded and then integrated without too much issue using Mathematica. If not we can use the same tricks to get general expansions of F_1's. For example the second order term for the above expansion involves

$$\sum_{k \geq 1} \sum_{k' \geq 1} \frac{x^k}{k} \frac{x^{k'}}{k'} \frac{(a)_{k+k'}}{(1+a)_{k+k'}} F_1[a+k+k'; 1, 1; 1+a+k+k'; x, y]$$

$$= \sum_{k, k' \geq 1} \frac{x^k x^{k'}}{kk'} \frac{(a)_{k+k'}}{(1+a)_{k+k'}} \frac{x \, _2F_1[1, a+k+k'; 1+a+k+k'; x] - y \, _2F_1[1, a+k+k'; 1+a+k+k'; y]}{x-y}$$

$$(5.137)$$

and we can again deal with the $\frac{1}{kk'}$ by differentiating as

$$\frac{\partial}{\partial w} \frac{\partial}{\partial w'} \sum_{k, k' \geq 1} \frac{w^k}{k} \frac{(w')^{k'}}{k'} \frac{(a)_{k+k'}}{(1+a)_{k+k'}} \, _2F_1[1, a+k+k'; 1+a+k+k'; Z]$$

$$= \frac{\Gamma[1+a]\Gamma[2+a]}{\Gamma[a]\Gamma[3+a]} \sum_{q, q', m \geq 0} w^q (w')^{q'} Z^m \frac{(2+a)_{q+q'+m}}{(3+a)_{q+q'+m}}$$

$$= \sum_{q \geq 0} \frac{\Gamma[1+a]\Gamma[2+a+q]}{\Gamma[a]\Gamma[3+a+q]} F_1[2+a+q; 1, 1; 3+a+q; w', Z]$$

$$= \sum_{q \geq 0} \frac{\Gamma[1+a]\Gamma[2+a+q]}{\Gamma[a]\Gamma[3+a+q]} \frac{w' \, _2F_1[1, 2+a+q; 3+a+q; w'] - Z \, _2F_1[1, 2+a+q; 3+a+q; Z]}{w' - Z},$$

$$(5.138)$$

where we we need to consider the $Z = x$ and $Z = y$ cases. In both of these cases we integrate w and w' between boundaries $[0, x]$. This is easy enough to do in Mathematica and gives us $F_1[1; 1+\delta, 1; 2; x, y]$ to second order in δ. The same game can be played for expansions on other arguments in F_1.

This procedure can be generalised to cases with $c \neq 1 + a$. We can look at the box with arguments $\{\nu_1 = 2, \nu_2 = 1 + \epsilon, \nu_3 = 1, \nu_4 = 5, D = 12 - 2\epsilon, \kappa = 0\}$ as an example and go into

some detail to give an example of tricks used.

$$I^{D,MB}_{4,\nu_{\bar{1}}=1}[2, 1+\epsilon, 1, 5, 12-2\epsilon, 0]$$

$$= \frac{(-1)^{-\epsilon}(M^2)^{-3-2\epsilon}S^{2-2\epsilon}T^{-3-2\epsilon}\Gamma[3-2\epsilon]\Gamma[-\epsilon]}{(24\Gamma[3-3\epsilon]\Gamma[2+\epsilon]\Gamma[3+\epsilon])}$$

$$\times \left(-T\,\Gamma[3+\epsilon]\Gamma[2+2\epsilon] \int_0^1 du\, u^{2-2\epsilon}(1-u(1-S))^{-3+2\epsilon}(1-uT)^{-1} \right.$$

$$\left. + \Gamma[2+\epsilon]\Gamma[3+2\epsilon] \int_0^1 du(u^{1-2\epsilon}(1-u(1-S))^{-3+2\epsilon} \,{}_2F_1\left[3+2\epsilon, 1, 3+\epsilon, \frac{uT-1}{uT}\right] \right)$$

$$= pre(c_a I_a + c_b I_b) \tag{5.139}$$

where pre is the prefactor in the second line and we take c_i to be the kinematic coefficient of the integral I_i on the third and fourth lines. Taking the first integral,

$$I_a \approx \int_0^1 du\, u^2(1-u(1-S))^{-3}(1-uT)^{-1}\left(1 + 2\epsilon \sum_{k\geq 1} \frac{(1-u)^k}{k} - 2\epsilon \sum_{k\geq 1} \frac{u^k(1-S)^k}{k}\right), \tag{5.140}$$

where the leading order term is simply $\frac{1}{3}F_1(3; 3, 1; 4; 1-S, T)$ which is simple to evaluate. The first $\mathcal{O}(\epsilon)$ term goes as

$$2\epsilon \frac{\partial}{\partial X} \sum_{k\geq 1} \int_0^1 du\, u^2(1-u(1-S))^{-3}(1-uT)^{-1}\frac{(1-u)^k X^k}{k}$$

$$= 2\epsilon \sum_{k\geq 0} \int_0^1 du\, u^2(1-u(1-S))^{-3}(1-uT)^{-1}(1-u)^{k+1}X^k$$

$$= 2\epsilon \sum_{k\geq 0} \frac{\Gamma[3]\Gamma[2+k]X^k}{\Gamma[5+k]}F_1[3; 3, 1; 5+k; 1-S, T]$$

$$= 2\epsilon S^{-3}(1-T)^{-1}\sum_{k\geq 0} \frac{\Gamma[3]\Gamma[2+k]X^k}{\Gamma[5+k]}F_1\left[2+k; 3, 1; 5+k; \frac{S-1}{S}, \frac{T}{T-1}\right]$$

$$= 2\epsilon S^{-3}(1-T)^{-1}\sum_{k\geq 0}\sum_{m\geq 0}\sum_{n\geq 0} \frac{\Gamma[3]\Gamma[2+k+m+n](3)_m(1)_k(1)_n}{\Gamma[5+k+m+n]}\frac{X^k(\frac{S-1}{S})^m(\frac{T}{T-1})^n}{k!m!n!}.$$

Closing the k and n sums

$$= 2\epsilon \frac{\Gamma[3]S^{-3}(1-T)^{-1}}{\Gamma[5]}\sum_{m\geq 0} \frac{(2)_m(3)_m(\frac{S-1}{S})^m}{(5)_m m!}F_1\left[2+m; 1, 1; 5+m; X, \frac{T}{T-1}\right]. \tag{5.141}$$

We can reduce the F_1 by partial fractioning and then a reordering of the sums into $m \pm n$ as

before,

$$F_1[a; 1, 1; 3 + a; x, y] = \frac{\Gamma[3+a]}{\Gamma[a]} \sum_{m \geq 0} \sum_{n \geq 0} \frac{x^m y^n}{(a + 2 + m + n)(a + 1 + m + n)(a + m + n)}$$

$$= \frac{\Gamma[3+a]}{\Gamma[a]} \sum_{m \geq 0} \sum_{n \geq 0} x^m y^n \left(\frac{1}{2(2 + a + m + n)} - \frac{1}{1 + a + m + n} + \frac{1}{2(a + m + n)} \right)$$

$$= \frac{\Gamma[3+a]}{\Gamma[a]} \sum_{s \geq 0} \sum_{\Delta = 0}^{s} x^\Delta y^{s - \Delta} \left(\frac{1}{2(2 + a + s)} - \frac{1}{1 + a + s} + \frac{1}{2(a + s)} \right)$$

$$= \frac{\Gamma[3+a]}{\Gamma[a]} \sum_{s \geq 0} \left(\frac{x^{s+1} - y^{s+1}}{x - y} \right) \times \left(\frac{1}{2(2 + a + s)} - \frac{1}{1 + a + s} + \frac{1}{2(a + s)} \right)$$

$$= \frac{\Gamma[2+a]}{2\Gamma[a]} \frac{x\,_2F_1[1, 2 + a; 3 + a; x] - y\,_2F_1[1, 2 + a; 3 + a; y]}{x - y}$$

$$- \frac{\Gamma[3+a]\Gamma[1+a]}{\Gamma[2+a]\Gamma[a]} \frac{x\,_2F_1[1, 1 + a; 2 + a; x] - y\,_2F_1[1, 1 + a; 2 + a; y]}{x - y}$$

$$+ \frac{\Gamma[3+a]}{2\Gamma[1+a]} \frac{x\,_2F_1[1, a; 1 + a; x] - y\,_2F_1[1, a; 1 + a; y]}{x - y}. \tag{5.142}$$

Applying this to (5.141) we have (with $Y = \frac{T}{T-1}$)

$$2\epsilon \frac{\Gamma[3]S^{-3}(1 - T)^{-1}}{\Gamma[5]} \sum_{m \geq 0} \frac{(2)_m (3)_m (\frac{S-1}{S})^m}{(5)_m m!}$$

$$\times \left(\frac{\Gamma[4+m]}{2\Gamma[2+m]} \frac{X\,_2F_1[1, 4 + m; 5 + m; X] - Y\,_2F_1[1, 4 + m; 5 + m; Y]}{X - Y} \right.$$

$$- \frac{\Gamma[5+m]\Gamma[3+m]}{\Gamma[2+m]\Gamma[4+m]} \frac{X\,_2F_1[1, 3 + m; 4 + m; X] - Y\,_2F_1[1, 3 + m; 4 + m; Y]}{X - Y}$$

$$+ \left. \frac{\Gamma[5+m]}{2\Gamma[3+m]} \frac{X\,_2F_1[1, 2 + m; 3 + m; X] - Y\,_2F_1[1, 2 + m; 3 + m; Y]}{X - Y} \right)$$

$$= 2\epsilon \frac{S^{-3}(1 - T)^{-1}}{2(X - Y)}$$

$$\times \left(\frac{\Gamma[4]}{\Gamma[5]} X F_1 \left[4; 3, 1; 5; \frac{S-1}{S}, X \right] - 2\frac{\Gamma[3]}{\Gamma[4]} F_1 \left[3; 3, 1; 4; \frac{S-1}{S}, X \right] + \frac{\Gamma[2]}{\Gamma[3]} F_1 \left[2; 3, 1; 3; \frac{S-1}{S}, X \right] \right.$$

$$\left. - \frac{\Gamma[4]}{\Gamma[5]} Y F_1 \left[4; 3, 1; 5; \frac{S-1}{S}, Y \right] + 2\frac{\Gamma[3]}{\Gamma[4]} Y F_1 \left[3; 3, 1; 4; \frac{S-1}{S}, Y \right] - \frac{\Gamma[2]}{\Gamma[3]} Y F_1 \left[2; 3, 1; 3; \frac{S-1}{S}, Y \right] \right)$$

$$\tag{5.143}$$

From here we can integrate these F_1's with respect to X between boundaries $[0, 1 - S]$, again not being too careful about the Riemann sheet here. For the next piece we can simply use derivative tricks to push the arguments of the F_1 function around. For example it is easy to

show

$$F_1[a+1; b+1, b'; c+1; x, y] = \frac{c}{ab} \frac{\partial}{\partial x} F_1[a; b, b'; c; x, y],$$

$$F_1[a+1; b, b'+1; c+1; x, y] = \frac{c}{ab'} \frac{\partial}{\partial y} F_1[a; b, b'; c; x, y], \qquad (5.144)$$

as well as a general result

$$F_1[a; 1+N+\delta, b'; c; x, y] = \frac{1}{(1+\delta)_N} \frac{1}{x^\delta} \frac{\partial^N}{\partial x^N} \left[x^{N+\delta} F_1[a; 1+\delta, b'; c; x, y] \right]. \qquad (5.145)$$

With these results in mind we can calculate the last part of the expansion of I_{55a}

$$-2\epsilon \frac{\partial}{\partial X} \sum_{k \geq 1} \int_0^1 du\, u^{2+k} (1 - u(1-S))^{-3} (1-uT)^{-1} \frac{X^k}{k}$$

$$= -2\epsilon \sum_{k \geq 0} \int_0^1 du\, u^{3+k} (1 - u(1-S))^{-3} (1-uT)^{-1} X^k$$

$$= 2\epsilon \sum_{k \geq 0} \frac{\Gamma[4+k] X^k}{\Gamma[5+k]} F_1(4+k; 3, 1; 5+k; 1-S, T)$$

$$= \epsilon \sum_{k \geq 0} \frac{(1)_k (2)_k X^k}{(3)_k k!} \frac{\partial_2}{\partial^2 Y} F_1(2+k; 1, 1; 3+k; Y, T)$$

$$= \epsilon \frac{\partial_2}{\partial^2 Y} \sum_{k \geq 0} \frac{(1)_k (2)_k X^k}{(3)_k l!} \left(\frac{T\, {}_2F_1(2+k, 1; 3+k; T) - Y\, {}_2F_1(2+k, 1; 3+k; Y)}{T-Y} \right)$$

$$= \epsilon \frac{\partial_2}{\partial^2 Y} \left(\frac{T F_1(2; 1, 1; 3; X, T) - Y F_1(2; 1, 1; 3; X, Y)}{T-Y} \right). \qquad (5.146)$$

We know that $F_1(2; 1, 1; 3; x, y) = \frac{2(x\log[1-y] - y\log[1-x])}{xy(x-y)}$ so this expression can be integrated with respect to X between boundaries $[0, 1-S]$, and then differentiated with respect to Y and set $Y \to 1 - S$. I_b does not provide any other tricks so we will stop this example here, but needless to say these are easy to generalise and adapt from one problem to another. It is also apparent that many of the same F_1 functions will appear so these expansions become very quick to perform.

The final term in the $\nu_{\hat{1}} = 1$ and $\nu_2 = 1$ cases can largely be dealt with by converting the hypergeometric function into its integral form and performing the same tricks. Care must be taken when looking at the integral representation as it diverges for some arguments of the function. In these cases we found it easier to expand the hypergeometric function using nested sums and then perform the u integration after. Nested sums quickly become cumbersome as the value of their arguments increase but most of the problematic terms we find have simple arguments. We will now review this approach.

5.5.2 Nested Sums and Expansions of Hypergeometric functions

This technique is explored in more detail in [108]. Appendix B has a detailed calculation of an Appell F_2 expansion using nested sums. It is clear from this that while it may be possible to automate the nested sums approach it takes a lot more computing power than necessary

when the integral representations are easily expanded. We will review the necessary steps for the present calculation.

We define the sums

$$Z_\mu[n] = S_\mu[n] = \sum_{i=1}^{n} \frac{1}{i^\mu},$$

$$Z_{\mu\nu}[n] = \sum_{1 \le i < j \le n} \frac{1}{i^\mu j^\nu},$$

and

$$S_{\mu\nu}[n] = \sum_{1 \le i \le j \le n} \frac{1}{i^\mu j^\nu} = Z_{\mu\nu}[n] + Z_{\mu+\nu}[n]. \tag{5.147}$$

Note the difference in the double sum between Z and S is simply $i < j$ instead of $i \le j$. The gamma function for positive integer a is

$$\Gamma[a + \epsilon] = (a - 1 + \epsilon)(a - 2 + \epsilon) \ldots (1 + \epsilon)\Gamma(1 + \epsilon). \tag{5.148}$$

Extracting the ϵ coefficients we have

$$\Gamma[a + \epsilon] = \Gamma[1 + \epsilon]\Gamma[a] \left(1 + \epsilon Z_1[a - 1] + \epsilon^2 Z_{11}[a - 1] + \ldots\right) \tag{5.149}$$

and the reciprocal expansion

$$\frac{1}{\Gamma[a + \epsilon]} = \frac{1}{\Gamma[1 + \epsilon]\Gamma[a]} \left(1 - \epsilon S_1[a - 1] + \epsilon^2 S_{11}[a - 1] + \ldots\right). \tag{5.150}$$

For hypergeometric expansions we will need the more general nested sum

$$Z[n; m_1, \ldots, m_k; x_1, \ldots, x_k] = \sum_{i=1}^{n} \frac{x_1^i}{i^{m_1}} Z[i - 1; m_2, \ldots, m_k; x_2, \ldots, x_k] \tag{5.151}$$

and

$$S[n; m_1, \ldots, m_k; x_1, \ldots, x_k] = \sum_{i=1}^{n} \frac{x_1^i}{i^{m_1}} S[i; m_2, \ldots, m_k; x_2, \ldots, x_k] \tag{5.152}$$

We also define $Z[n] = 1$ for $n \ge 0$, $Z[n] = 0$ for $n < 0$ and $S[n] = 1$ for $n > 0$, $S[n] = 0$ for $n \le 0$. We finally need the special case of

$$Z[\infty; m_1, \ldots, m_k; x_1, \ldots, x_k] = \mathrm{Li}_{m_k, \ldots, m_1}[x_k, \ldots, x_1], \tag{5.153}$$

where $\mathrm{Li}_{m_k, \ldots, m_1}[x_k, \ldots, x_1]$ are the multiple polylogarithms of Gonochorov [109]. These are a whole subject to themselves and while more work was done on them in Appendix B, we did not need to go very far with them for the final version of the calculation. What we will need to know is that a subset of these multiple polylogarithms are Nielsen's generalised polylogarithms [110]

$$S_{n,p}[x] = \mathrm{Li}_{1,1,\ldots,1,n+1}[1, \ldots, 1, x] \tag{5.154}$$

where there are p arguments of Li so there are $(p-1)$ "1's". These functions are very well documented and can be easily related to the standard polylogarithms. For cases where $m_i \neq 1$ but with all but the last $x_i = 1$, we have the harmonic polylogarithms of Remiddi and Vermaseren [111]

$$H_{m_1,\ldots,m_k}[x] = \mathrm{Li}_{m_k,\ldots,m_1}[1,1,\ldots,1,x], \tag{5.155}$$

noting the reversed orderings of the subscript labellings between Z, Li and H. They have the useful property that you can find simple enough ways of manipulating the order of m_i using relations like

$$H_{m_1+1,m_2,\ldots,m_k}[x] = \int_0^x \mathrm{d}x_1 \, f_0[x_1] H_{m_1,m_2,\ldots,m_k}[x_1] \tag{5.156}$$

and

$$H_{\pm 1,m_2,\ldots,m_k}[x] = \int_0^x \mathrm{d}x_1 \, f_{\pm 1}[x_1] H_{m_2,\ldots,m_k}[x_1] \tag{5.157}$$

where

$$f_0[x] = \frac{1}{x}, \qquad f_{\pm 1}[x] = \frac{1}{1 \mp x}. \tag{5.158}$$

We can then combine all of these definitions to calculate some hypergeometric expansions where we rewrite the hypergeometric $_2F_1$ as

$$_2F_1[a,b;c;x] = 1 + \frac{\Gamma[c]}{\Gamma[a]\Gamma[b]} \sum_{i \geq 1} x^i \frac{\Gamma[i+a]\Gamma[i+b]}{\Gamma[i+c]\Gamma[i+1]}, \tag{5.159}$$

and we can then use all of the above together to perform this expansion. For example we have a box with parameters as before, $\{1, -1+\epsilon, 1, 2, 6-2\epsilon, -1\}$. The spinor coefficient from the first integral is finite and the box looks like

$$
\begin{aligned}
& I^D_{4,\nu_{\tilde{1}}=1}[1, -1+\epsilon, 1, 2, 6-2\epsilon, -1] \\
&= -\frac{(-1)^{-2\epsilon}(M^2)^{-2\epsilon}S^{2-2\epsilon}T^{-2\epsilon}\Gamma[3-2\epsilon]\Gamma[-\epsilon]\Gamma[2\epsilon]}{\Gamma[3-3\epsilon]\Gamma[\epsilon]} \\
&\quad \times \int_0^1 \mathrm{d}u\, u^{1-2\epsilon}(1-u(1-S))^{-3+2\epsilon} \, _2F_1\left[2\epsilon, 1; \epsilon, \frac{uT-1}{uT}\right] \\
&= -\frac{(-1)^{-2\epsilon}(M^2)^{-2\epsilon}S^{2-2\epsilon}T^{-2\epsilon}\Gamma[3-2\epsilon]\Gamma[-\epsilon]\Gamma[2\epsilon]}{\Gamma[3-3\epsilon]\Gamma[\epsilon]} \\
&\quad \times \int_0^1 \mathrm{d}u\, u^{1-2\epsilon}(1-u(1-S))^{-3+2\epsilon}\left(1 - 2(1-uT)(1+\epsilon\log[uT])\right) + \mathcal{O}(\epsilon^2) \tag{5.160}
\end{aligned}
$$

where we have used nested sums to rewrite the hypergeometric function as

$$
\begin{aligned}
_2F_1[a\epsilon, 1; b\epsilon; x] &= 1 + \frac{\Gamma[b\epsilon]}{\Gamma[a\epsilon]} \sum_{i=1}^\infty \frac{x^i \Gamma[i+a\epsilon]}{\Gamma[i+b\epsilon]} \\
&= 1 + \frac{\Gamma[1+a\epsilon]\Gamma[b\epsilon]}{\Gamma[1+b\epsilon]\Gamma[a\epsilon]} \sum_{i=1}^\infty x^i \left(1 + (a-b)\epsilon Z_1[i-1] + a\epsilon^2 Z_{11}[i-1] + b\epsilon^2 S_{11}[i-1] + \ldots\right) \\
&= 1 + \frac{a}{b}\frac{x}{1-x}\left(1 + (b-a)\epsilon\log[1-x]\right) + \mathcal{O}(\epsilon^2). \tag{5.161}
\end{aligned}
$$

The coefficient is finite and the box goes as $\mathcal{O}(\epsilon^{-1})$, so we only needed to go to $\mathcal{O}(\epsilon)$ but had we needed to go to $\mathcal{O}(\epsilon^2)$ then we could rewrite $S_{11}[i-1] = Z_{11}[i-1] + Z_2[i-1]$ and each of these cases can be related to a Nielsen's polylogarithm. We find similar results

$$_2F_1(1+a\epsilon, 1; 1+b\epsilon; x) = \frac{1}{1-x} + \epsilon(b-a)\frac{\log[1-x]}{1-x} + \ldots, \tag{5.162}$$

$$_2F_1(-1+a\epsilon, 1; -1+b\epsilon; x)$$
$$= 1 + \frac{\Gamma[-1+b\epsilon]}{\Gamma[-1+a\epsilon]} \sum_{i=1}^{\infty} x^i \frac{\Gamma[-1+i+a\epsilon]}{\Gamma[-1+i+b\epsilon]}$$
$$= 1 + x(1+(b-a)\epsilon) + x\frac{\Gamma[-1+b\epsilon]}{\Gamma[-1+a\epsilon]} \sum_{i=1}^{\infty} x^i \frac{\Gamma[i+a\epsilon]}{\Gamma[i+b\epsilon]}$$
$$= 1 + x(1+(b-a)\epsilon) + x\frac{a(a\epsilon-1)}{b(b\epsilon-1)} \sum_{i=1}^{\infty} x^i(1+(a-b)\epsilon Z_1[i-1])$$
$$= 1 + x(1+(b-a)\epsilon) + \frac{ax^2}{b(1-x)}\Big(1+\epsilon(b-a)(1+\log[1-x])\Big), \tag{5.163}$$

and

$$_2F_1(2+a\epsilon, b\epsilon; 1+c\epsilon; x)$$
$$= 1 + (b\epsilon - ab\epsilon^2)\left(\frac{x}{1-x} - \log[1-x]\right)$$
$$+ ab\epsilon^2\left(-2\log[1-x] - \frac{x\log[1-x]}{1-x} + \frac{1}{2}\log[1-x]^2 + \text{Li}_2[x]\right)$$
$$+ b^2\epsilon^2(\text{Li}_{-1,2}[1,x] + \text{Li}_{0,2}[1,x]) - bc\epsilon^2\left(-\log[1-x] - \frac{x\log[1-x]}{1-x} + \frac{1}{2}\log[1-x]^2 + \text{Li}_2[x]\right). \tag{5.164}$$

This last expansion was needed to $\mathcal{O}(\epsilon^2)$ for the box $\{-1+\epsilon, 1, 1, 1, 4-2\epsilon, -1\}$ which we will briefly discuss. The spinor coefficient of the box is finite and the box goes as

$$I^D_{4,\nu_2=1}[-1+\epsilon, 1, 1, 1, 4-2\epsilon, -1]$$
$$= \frac{(-1)^{-2\epsilon}(M^2)^{-2\epsilon}S^{1-2\epsilon}\Gamma[2-2\epsilon]\Gamma[-\epsilon]\Gamma[2\epsilon]}{\Gamma[2-3\epsilon]\Gamma[\epsilon]} \int_0^1 du(1-u(1-S))^{-2+2\epsilon} {}_2F_1(2\epsilon, 1; \epsilon; 1-uT)$$
$$= \frac{(-1)^{-2\epsilon}(M^2)^{-2\epsilon}S^{1-2\epsilon}\Gamma[2-2\epsilon]\Gamma[-\epsilon]\Gamma[2\epsilon]}{\Gamma[2-3\epsilon]\Gamma[\epsilon]}$$
$$\times \int_0^1 du(uT)^{-1}(1-u(1-S))^{-2+2\epsilon} {}_2F_1\left(-\epsilon, 1; \epsilon; \frac{uT-1}{uT}\right)$$
$$= \frac{(-1)^{-2\epsilon}(M^2)^{-2\epsilon}S^{1-2\epsilon}\Gamma[2-2\epsilon]\Gamma[-\epsilon]\Gamma[2\epsilon]}{\Gamma[2-3\epsilon]\Gamma[\epsilon]}$$
$$\times \int_0^1 du(uT)^{-1}(1-u(1-S))^{-2+2\epsilon}\Big(2-uT-2\epsilon(1-uT)\log[uT]\Big), \tag{5.165}$$

but there is a convergence issue at $u = 0$. This is an issue with our general box result but we can take a step back to earlier results for this. We have

$$I_D^{\{q_1,q_2\}} + I^{\{p_4,q_2\}}|_{\nu_4=1} = (M^2)^{\frac{D}{2}-\sigma}(S)^{\frac{D}{2}-\nu_{123}}\frac{\Gamma[\frac{D}{2}-\nu_{12}]\Gamma[\sigma-\frac{D}{2}]\Gamma[\frac{D}{2}-\nu_{234}]}{\Gamma[\nu_1]\Gamma[\nu_{34}]\Gamma[D-\sigma]}$$

$$\sum_{n\geq0}\frac{(\nu_2)_n(\nu_4)_n}{(\nu_{34})_n}\frac{T^n}{n!}\,{}_2F_1\left(\frac{D}{2}-\nu_{12},\nu_4+n;\nu_{34}+n;1-S\right)$$

$$= (M^2)^{\frac{D}{2}-\sigma}(S)^{\frac{D}{2}-\nu_{123}}\frac{\Gamma[\frac{D}{2}-\nu_{12}]\Gamma[\sigma-\frac{D}{2}]\Gamma[\frac{D}{2}-\nu_{234}]}{\Gamma[\nu_1]\Gamma[\nu_{34}]\Gamma[D-\sigma]}F_1\left(\nu_4;\frac{D}{2}-\nu_{12},\nu_2;\nu_{34};1-S,T\right),$$
$$(5.166)$$

and given that for this box we have $\nu_2 = \nu_3 = \nu_4$ we have some freedom to relabel things (this is very much not general!). $\nu_4 = 1$ gives cancellations and so we write

$$I_D^{\{p_1,q_1\}} + I^{\{p_1,p_4\}}|_{\nu_2=1} = (T)^{\frac{D}{2}-\nu_{234}}(M^2)^{\frac{D}{2}-\sigma}(S)^{\frac{D}{2}-\nu_{123}}\frac{\Gamma[\frac{D}{2}-\nu_{12}]\Gamma[\nu_{234}-\frac{D}{2}]\Gamma[\frac{D}{2}-\nu_{23}]\Gamma[\frac{D}{2}-\nu_{34}]}{\Gamma[\nu_2]\Gamma[\nu_4]\Gamma[D-\sigma]\Gamma[\frac{D}{2}-\nu_2]}$$

$$\sum_{n\geq0}\frac{(\frac{D}{2}-\nu_{23})_n(\nu_1)_n}{(\frac{D}{2}-\nu_2)_n}\frac{T^n}{n!}\,{}_2F_1\left(\frac{D}{2}-\nu_{12},\frac{D}{2}-\nu_{23}+n;\frac{D}{2}-\nu_2+n;1-S\right)$$

$$= (T)^{\frac{D}{2}-\nu_{234}}(M^2)^{\frac{D}{2}-\sigma}(S)^{\frac{D}{2}-\nu_{123}}\frac{\Gamma[\frac{D}{2}-\nu_{12}]\Gamma[\nu_{234}-\frac{D}{2}]\Gamma[\frac{D}{2}-\nu_{23}]\Gamma[\frac{D}{2}-\nu_{34}]}{\Gamma[\nu_2]\Gamma[\nu_4]\Gamma[D-\sigma]\Gamma[\frac{D}{2}-\nu_2]}$$

$$\times F_1\left(\frac{D}{2}-\nu_{23};\frac{D}{2}-\nu_{12},\nu_1;\frac{D}{2}-\nu_2;1-S,T\right).$$
$$(5.167)$$

These results then look like

$$I_D^{\{p_1,q_1\}} + I^{\{p_1,p_4\}} = \frac{(M^2)^{-2\epsilon}S^{1-2\epsilon}T^{-1-\epsilon}\Gamma[2-2\epsilon]\Gamma[-\epsilon]^2\Gamma[1+\epsilon]}{\Gamma[2-3\epsilon]\Gamma[1-\epsilon]}$$

$$\times F_1(-\epsilon;2-2\epsilon,-1+\epsilon;1-\epsilon;1-S,T)$$

$$= \frac{(M^2)^{-2\epsilon}S^{1-2\epsilon}T^{-1-\epsilon}\Gamma[2-2\epsilon]\Gamma[-\epsilon]^2\Gamma[1+\epsilon]}{\Gamma[2-3\epsilon]\Gamma[1-\epsilon]}$$

$$\times (1-T)^\epsilon\,{}_2F_1\left(2-2\epsilon,-\epsilon;1-\epsilon;\frac{1-S-T}{1-T}\right) \qquad (5.168)$$

and

$$I_D^{\{q_1,q_2\}} + I^{\{p_4,q_2\}}$$

$$= \frac{(M^2)^{-2\epsilon}S^{1-2\epsilon}\Gamma[2-2\epsilon]\Gamma[-1-\epsilon]\Gamma[2\epsilon]}{\Gamma[2-3\epsilon]\Gamma[-1+\epsilon]}F_1(1,2-2\epsilon,1,2,1-S,T). \qquad (5.169)$$

The Appell function is easily expanded using the integral representation and we now have the nested sums results to expand the hypergeometric function. This was the only case of (5.117) not converging properly and there were only four cases where nested sums were needed at all. Everything else was expanded using (5.118) and we used the other tricks covered in this section in some rare cases. With the boxes done we can now look at two-mass and one-mass triangles.

5.5.3 Triangles

We take the triangles to be special cases of our general box result (5.117). We have already done something similar for $\kappa = -1$ cases earlier but now we can do the same for Mellin-Barnes expanded cases.

$$
I_{3,2m}^{D,MB} = I_{4,\nu_3 \to 0}^{D,MB}
$$

$$
= \lim_{\nu_3 \to 0} (-1)^{\frac{D}{2}+1+\kappa} (M^2)^{\frac{D}{2}-\sigma} S^{\frac{D}{2}-\nu_{123}} \frac{\Gamma[\frac{D}{2}-\nu_{12}]\Gamma[\hat{\sigma}-\frac{D}{2}]\Gamma[\frac{D}{2}-\nu_{34}]}{\Gamma[\nu_3]\Gamma[\nu_4]\Gamma[\nu_{\hat{1}2}]\Gamma[D-\sigma]}
$$

$$
\times \sum_{m \geq 0} \frac{(\hat{\sigma}-\frac{D}{2})_m (\nu_2)_m}{(\nu_{\hat{1}2})_m m!} \int_0^1 du\, u^{\nu_4-1}(1-u)^{\nu_3-1}(1-u(1-S))^{\nu_{12}-\frac{D}{2}}(1-uT)^{m-1-\kappa}
$$

$$
= \lim_{\nu_3 \to 0} (-1)^{\frac{D}{2}+1+\kappa} (M^2)^{\frac{D}{2}-\sigma} S^{\frac{D}{2}-\nu_{123}} \frac{\Gamma[\frac{D}{2}-\nu_{12}]\Gamma[\hat{\sigma}-\frac{D}{2}]\Gamma[\frac{D}{2}-\nu_{34}]}{\Gamma[\nu_3]\Gamma[\nu_4]\Gamma[\nu_{\hat{1}2}]\Gamma[D-\sigma]}
$$

$$
\times \sum_{m \geq 0} \frac{(\hat{\sigma}-\frac{D}{2})_m (\nu_2)_m}{(\nu_{\hat{1}2})_m m!} \frac{\Gamma[\nu_3]\Gamma[\nu_4]}{\Gamma[\nu_{34}]} F_1\left(\nu_4; \frac{D}{2}-\nu_{12}, 1+\kappa-m; \nu_{34}; 1-S, T\right) \quad (5.170)
$$

Take the $\nu_3 \to 0$ limit and get

$$
I_{3,2m}^{D,MB} = (-1)^{\frac{D}{2}+1+\kappa} (M^2)^{\frac{D}{2}-\sigma} \frac{\Gamma[\frac{D}{2}-\nu_{12}]\Gamma[\hat{\sigma}-\frac{D}{2}]\Gamma[\frac{D}{2}-\nu_4]}{\Gamma[\nu_4]\Gamma[\nu_{\hat{1}2}]\Gamma[D-\sigma]}
$$

$$
\times \sum_{m \geq 0} \frac{(\hat{\sigma}-\frac{D}{2})_m (\nu_2)_m (1-T)^{m-1-\kappa}}{(\nu_{\hat{1}2})_m m!}
$$

$$
= (-1)^{\frac{D}{2}} (M^2)^{\frac{D}{2}-\sigma} (T-1)^{-1-\kappa} \frac{\Gamma[\frac{D}{2}-\nu_{12}]\Gamma[\hat{\sigma}-\frac{D}{2}]\Gamma[\frac{D}{2}-\nu_4]}{\Gamma[\nu_4]\Gamma[\nu_{\hat{1}2}]\Gamma[D-\sigma]}
$$

$$
\times \,_2F_1\left(\hat{\sigma}-\frac{D}{2}, \nu_2; \nu_{\hat{1}2}; 1-T\right) \quad (5.171)
$$

and for the one-mass triangle with $\nu_4 \to 0$

$$
I_{3,1m}^{D,MB} = (-1)^{\frac{D}{2}+1+\kappa} S^{\frac{D}{2}-\nu_{123}} \frac{\Gamma[\frac{D}{2}-\nu_{12}]\Gamma[\hat{\sigma}-\frac{D}{2}]\Gamma[\frac{D}{2}-\nu_{23}]}{\Gamma[\nu_3]\Gamma[\nu_{\hat{1}}]\Gamma[D-\sigma]}. \quad (5.172)
$$

Recalling we used a box shift to avoid tensor triangles, we expect cases of $\nu_4 = -1$ with $\nu_3 = 1$. With this in mind, we will need to use

$$
\frac{1}{\Gamma[0]} F_1(-1; a, b; 0; x, y) = -(ax + by), \quad (5.173)
$$

144

which is easy enough to derive using the summation representation, to give

$$I_{4,\nu_3=1,\nu_4=-1}^{D,MB}$$

$$= (-1)^{\frac{D}{2}+1+\kappa}(M^2)^{\frac{D}{2}-\sigma}S^{\frac{D}{2}-\nu_{123}}\frac{\Gamma[\frac{D}{2}-\nu_{12}]\Gamma[\hat{\sigma}-\frac{D}{2}]\Gamma[\frac{D}{2}-\nu_{34}]}{\Gamma[\nu_{\hat{1}2}]\Gamma[D-\sigma]}$$

$$\times \sum_{m\geq 0}\frac{(\hat{\sigma}-\frac{D}{2})_m(\nu_2)_m}{(\nu_{\hat{1}2})_m m!}\frac{1}{\Gamma[0]}F_1\left(-1;\frac{D}{2}-\nu_{12},1+\kappa-m;0;1-S,T\right)$$

$$= (-1)^{\frac{D}{2}+1+\kappa}(M^2)^{\frac{D}{2}-\sigma}S^{\frac{D}{2}-\nu_{123}}\frac{\Gamma[\frac{D}{2}-\nu_{12}]\Gamma[\hat{\sigma}-\frac{D}{2}]\Gamma[\frac{D}{2}-\nu_{34}]}{\Gamma[\nu_{\hat{1}2}]\Gamma[D-\sigma]}$$

$$\times \sum_{m\geq 0}\frac{(\hat{\sigma}-\frac{D}{2})_m(\nu_2)_m}{(\nu_{\hat{1}2})_m m!}\left((1-S)\left(\nu_{12}-\frac{D}{2}\right)+T(m-1-\kappa)\right)$$

$$= (-1)^{\frac{D}{2}+1+\kappa}(M^2)^{\frac{D}{2}-\sigma}S^{\frac{D}{2}-\nu_{123}}\frac{\Gamma[\frac{D}{2}-\nu_{12}]\Gamma[\hat{\sigma}-\frac{D}{2}]\Gamma[\frac{D}{2}-\nu_2]}{\Gamma[D-\sigma]\Gamma[\nu_{\hat{1}}]}\left((1-S)\left(\nu_{12}-\frac{D}{2}\right)-T(1+\kappa)\right)$$

$$+ (-1)^{\frac{D}{2}+1+\kappa}(M^2)^{\frac{D}{2}-\sigma}S^{\frac{D}{2}-\nu_{123}}\frac{\Gamma[\frac{D}{2}-\nu_{12}]\Gamma[\hat{\sigma}-\frac{D}{2}]\Gamma[\frac{D}{2}-\nu_{34}]}{\Gamma[\nu_{\hat{1}2}]\Gamma[D-\sigma]}\sum_{m\geq 0}\frac{(\hat{\sigma}-\frac{D}{2})_m(\nu_2)_m}{(\nu_{\hat{1}2})_m(m-1)!}T$$

$$= (-1)^{\frac{D}{2}+1+\kappa}(M^2)^{\frac{D}{2}-\sigma}S^{\frac{D}{2}-\nu_{123}}\frac{\Gamma[\frac{D}{2}-\nu_{12}]\Gamma[\hat{\sigma}-\frac{D}{2}]\Gamma[\frac{D}{2}-\nu_2]}{\Gamma[D-\sigma]\Gamma[\nu_{\hat{1}}]}\left((1-S)\left(\nu_{12}-\frac{D}{2}\right)-T(1+\kappa)\right)$$

$$+ (-1)^{\frac{D}{2}+1+\kappa}(M^2)^{\frac{D}{2}-\sigma}S^{\frac{D}{2}-\nu_{123}}\frac{\nu_2\Gamma[\frac{D}{2}-\nu_{12}]\Gamma[1+\hat{\sigma}-\frac{D}{2}]\Gamma[\frac{D}{2}-\nu_{34}]}{\Gamma[1+\nu_{\hat{1}2}]\Gamma[D-\sigma]}\sum_{m\geq 0}\frac{(1+\hat{\sigma}-\frac{D}{2})_m(1+\nu_2)_m}{(1+\nu_{\hat{1}2})_m m!}T$$

$$= (-1)^{\frac{D}{2}+1+\kappa}(M^2)^{\frac{D}{2}-\sigma}S^{\frac{D}{2}-\nu_{123}}\frac{\Gamma[\frac{D}{2}-\nu_{12}]\Gamma[\hat{\sigma}-\frac{D}{2}]\Gamma[\frac{D}{2}-\nu_2]}{\Gamma[D-\sigma]\Gamma[\nu_{\hat{1}}]}\left((1-S)\left(\nu_{12}-\frac{D}{2}\right)-T(1+\kappa)\right)$$

$$+ (-1)^{\frac{D}{2}+1+\kappa}(M^2)^{\frac{D}{2}-\sigma}S^{\frac{D}{2}-\nu_{123}}\frac{\nu_2\Gamma[\frac{D}{2}-\nu_{12}]\Gamma[1+\hat{\sigma}-\frac{D}{2}]\Gamma[\frac{D}{2}-\nu_2-1]}{\Gamma[\nu_{\hat{1}}]\Gamma[D-\sigma]}T. \tag{5.174}$$

These were the only exceptional cases, the remaining one-mass and two-mass triangles were easy enough to expand using methods outlined previously or even just Mathematica's inbuilt Series function. Now that we have introduced all of the tools necessary for the ϵ-expansions, we can discuss how the Riemann sheets were fixed.

5.5.4 Riemann Sheet Problems and Solutions

We know what our target solution is from [2] but there are other tests that our solution must satisfy. We know that the IR piece is (5.3) but we also know a priori how the transcendentality of the result should look. If we define τ to mean the order of transcendentality, i.e. τ^0 implies rational functions, τ^1 implies logarithms and π's etc, then we expect the amplitude to have *maximum* transcendentality

$$\sum_{i=0}^{2}\frac{\tau^i}{\epsilon^{2-i}}, \tag{5.175}$$

where we say maximum transcendality because we also expect rational pieces at $\mathcal{O}(\epsilon^{-1})$ and rational and τ^1 terms at $\mathcal{O}(\epsilon^0)$. This was the first clue that we were on the wrong Riemann sheet as we will discuss shortly. Looking back to (5.12) these expansions were all performed

for the general arguments $\{k, \overline{a}, i, j, \omega\}$ with the aim of summing over all configurations after the expansion was performed. We chose to work in the fundamental region but we were intentionally careless about kinematic regions when expanding the boxes, making sure they worked for $0 < S < 1$, $0 < T < 1$ and $S + T < 1$ only. This does not cover the whole fundamental region but we will see this is fine.

After completing all of the expansions and summing all of the contributions, we first found that the $\mathcal{O}(\epsilon^{-3})$ vanished, we had the correct $\mathcal{O}(\epsilon^{-2})$ terms but there were problems beyond this. There were τ^2 terms at $\mathcal{O}(\epsilon^{-1})$ and τ^3 terms at $\mathcal{O}(\epsilon^0)$. For the kinematic region that we were expanding in these pieces were numerically zero, but taking the result outside of this region we found non-zero results. We of course expect zero to analytically continue to zero so this was a good first test to ensure we were on the right Riemann sheet.

To resolve this, we can make a few observations. Firstly, the result from [2] tells us a posteri that it can be presented in terms of six-dimensional boxes. One can therefore write code that would give the initial alphabet of arguments in the polylogarithms and try to manipulate them in such a way that reduces them to only having arguments $\{1 - S, 1 - T\}$ for the dilogarithms and explicitly vanishing τ^3 terms. The ambiguity would then lie in the logarithms, where $\log[x] \to \log[-x] + ci\pi$, where we are uncertain of which value from $c = \{-1, 0, 1\}$ should be taken on a logarithm to logarithm case. We hereby take c to mean that each logarithm gets a tag $c_i \in c$ and we hope to constrain all of the c_i's to give us the correct Riemann sheet.

Secondly, the form of (5.117) makes it clear that for $0 < S < 1$, $0 < T < 1$ and $S + T < 1$, the boxes will be completely real apart from the $(-1)^{\frac{D}{2}}$ factor. Removing this factor allows us to track any time a branch cut was crossed and therefore some imaginary value would be picked up. The idea here is that the final result should be completely real in this kinematic region, so if we could isolate the imaginary contributions after bringing the result into a form with the correct alphabet in this region then we could test for a solution of c which caused this imaginary part to vanish, and what was left over would be the result on the correct Riemann sheet.

First we looked at the boxes individually. For example if we take the box with Glover parameters $\{\nu_1 = 0, \nu_2 = \epsilon, \nu_3 = 1, \nu_4 = 1, D = 4 - 2\epsilon, \kappa = 0\}$, we find that there are only three dilogarithms present, $\{\text{Li}_2[1 - S], \text{Li}_2\left[\frac{S}{1-T}\right], \text{Li}_2\left[\frac{S+T-1}{S}\right]\}$. Noticing that $\frac{S+T-1}{S} = 1 - \left(\frac{1-T}{S}\right)$ and using

$$\text{Li}_2[z] + \text{Li}_2[1 - z] = -\log[1 - z]\log[z] + \frac{\pi^2}{6}, \tag{5.176}$$

followed by

$$\text{Li}_2[z] + \text{Li}_2\left[\frac{1}{z}\right] = -\frac{1}{2}\log[-z]^2 - \frac{\pi^2}{6}, \tag{5.177}$$

we get to

$$\text{Li}_2\left[\frac{S+T-1}{S}\right]$$
$$\to \text{Li}_2\left[\frac{S}{1-T}\right] + \frac{1}{2}\log\left[\frac{T-1}{S}\right]^2 - \log\left[\frac{1-T}{S}\right]\log\left[\frac{S+T-1}{S}\right] + \frac{\pi^2}{3}. \tag{5.178}$$

This did not cancel the existing $\text{Li}_2\left[\frac{S}{1-T}\right]$, but if we create a list of all boxes whose coefficients from the first integral were equal to each other up to some real rational factors, then the sum

146

of these boxes reduced to only having $\text{Li}_2[1-S]$. Again we are being intentionally careless with kinematic regions, (5.177) requires $z \notin (0,1)$ and it is unclear where $\frac{1-T}{S}$ lies in the this range, but we press on. Now that we have this combination of boxes reduced to only having dilogarithms $\text{Li}_2[1-S]$, we can look at the logarithms. We again are focusing on the region $0 < S < 1$, $0 < T < 1$ and $S + T < 1$ so we can rewrite the logarithms in a way that they would be real and then include a tagged $i\pi$ as previously mentioned. For example

$$\log\left[\frac{S+T-1}{S}\right] \to \log[1-S-T] - \log[S] + c(i\pi) \tag{5.179}$$

where c is just a tag to keep track of these pieces. Rewriting all of the logarithms this way then the combination of boxes reduced to

$$\sum_{i\in\mathcal{B}_1} C_i I_{4,i}^{D,MB}$$
$$= f\left(\log[s], \log[t], \log[M^2], \text{Li}_2[1-S], \text{Li}_2[1-T], (ci\pi)^2\right) + g\left(ci\pi\log[1-T]\right) \tag{5.180}$$

where $\mathcal{B}_1 = \{1, 2, 3, 4, 10, 11, 13\}$. What is interesting here is that when crossing branch cuts and going between kinematic regions (and therefore picking up an imaginary part), we see the entire imaginary part is contained in the function g, and in fact g is entirely this imaginary part. f is therefore the real part and the piece that matches the expansion for $0 < S < 1$, $0 < T < 1$ and $S + T < 1$. There is a non-trivial solution for all of the tags c that eliminates g and this is the solution that puts us on the correct Riemann sheet, practically translating to just keeping f. It is important that it is non-trivial as f contains $(ci\pi)^2 = -|c|^2\pi^2$ and which requires $|c| = 1$ in the final result.

This is essentially the procedure that was used for all boxes but we will highlight a case which made use of a further identity. The box with Glover parameters $\{\nu_1 = 1, \nu_2 = \epsilon, \nu_3 = 1, \nu_4 = 2, D = 6 - 2\epsilon, \kappa = 1\}$ has the dilogarithms

$$\left\{\text{Li}_2(1-S), \text{Li}_2(1-T), \text{Li}_2\left(\frac{S}{1-T}\right), \text{Li}_2\left(\frac{T}{S+T-1}\right), \text{Li}_2\left(\frac{ST}{S+T-1}\right)\right\}, \tag{5.181}$$

upon expansion, and again we collect all boxes with similar coefficients. Noting the identity

$$\text{Li}_2(wz) + \text{Li}_2\left(\frac{z(1-w)}{1-wz}\right) + \text{Li}_2\left(\frac{w(1-z)}{1-wz}\right)$$
$$= \text{Li}_2(w) + \text{Li}_2(z) - \log\left(\frac{1-w}{1-wz}\right)\log\left(\frac{1-z}{1-wz}\right), \tag{5.182}$$

we can use $1 - \frac{ST}{S+T-1} = \frac{(1-S)(1-T)}{1-S-T}$ and the solve for $\left\{\frac{T}{S+T-1} = \frac{z(1-w)}{1-wz}, \frac{(1-S)(1-T)}{1-S-T} = \frac{w(1-z)}{1-wz}\right\}$ which gives us $\left\{w = 1-T, z = \frac{1}{S}\right\}$. We then use (5.177) on the $\text{Li}_2(z)$ and $\text{Li}_2(wz)$ terms. This successfully reduces these boxes to having only $\text{Li}_2(1-S)$ and $\text{Li}_2(1-T)$.

We earlier mentioned the existence of τ^3 terms at $\mathcal{O}(\epsilon^0)$. We performed the exact same tricks but making use of identities such as

$$\text{Li}_3[z] = \text{Li}_3\left[\frac{1}{z}\right] - \frac{1}{6}\log^3[-z] - \frac{\pi^2}{6}\log[-z] \tag{5.183}$$

and

$$\text{Li}_3[z] + \text{Li}_3\left[\frac{z}{z-1}\right] + \text{Li}_3[1-z]$$

$$= \frac{1}{6}\log^3[1-z] - \frac{1}{2}\log[z]\log^2[1-z] + \frac{\pi^2}{6}\log[1-z] + \zeta(3). \tag{5.184}$$

We were generally aiming for the alphabet $\left\{\frac{S}{S+T-1}, \frac{T}{S+T-1}, \frac{ST}{S+T-1}\right\}$ as these seemed like common arguments across all boxes. We found that using these identities and reaching this alphabet would lead to these trilogarithms having vanishing coefficients, and then rewriting the logarithms as discussed above lead to all τ^3 terms explicitly vanishing. With these techniques discussed we can look closer at the structure of the results.

5.6   A Summary of Results

We can break down the possible contributions in terms of powers of ϵ and transcendental weight, as shown in (5.175) and in Table 5.1. We will quickly discuss the contributions to each piece and summarise how the genuine two-loop diagrams and inserts interact to give the amplitude.

	ϵ^{-4}	ϵ^{-3}	ϵ^{-2}	ϵ^{-1}	ϵ^0
τ^3	✓	✓	✓	✓	✓
τ^2	✓	✓	✓	✓	✓
τ^1	✓	✓	✓	✓	✗
τ^0	✓	✓	✓	✓	✗

Table 5.1: A table to show the current results compared to the results presented in [2]. ϵ refers to the dimensional regulation scalar and τ^i are terms of transcendental weight i.

ϵ^{-4}

We expect vanishing coefficient at $\mathcal{O}(\epsilon^{-4})$ and indeed we get no contributions at all to this order.

ϵ^{-3}

We also expect vanishing coefficient for $\mathcal{O}(\epsilon^{-3})$. We do get individual contributions to $\mathcal{O}(\epsilon^{-3})$ from the one-mass triangles coming from $\eta = \{K21\}$. These contributions arise only from the "a in middle" part of this structure and we find they cancel amongst themselves leaving us with an overall zero coefficient.

ϵ^{-2}, τ^0

We expect $\mathcal{O}(\epsilon^{-2})$ to follow the universal IR equation (5.3). We see that all contributions that come from the box and two mass triangle inserts cancel with each other, and the whole IR contribution comes from the triple cuts on the one-mass triangle inserts. All contributions from the genuine two-loop structures cancel amongst themselves.

ϵ^{-1}, τ^1 and τ^0

We again expect this to follow the universal IR equation (5.3). We can expect interaction between the genuine two-loop and insert pieces here. This is because double cuts on the inserts will provide rational contributions to this piece, but the IR function is only made of logarithms at this order in ϵ. The double cuts should then be completely cancelled by the genuine two loop integrals. Indeed, we see the double cuts are completely cancelled by the one-mass triangles $\eta = \{stt, K21\}$. The box-like second integrals of $\eta = \{tbx, K31\}$ and two-mass triangle-like $\eta = \{K12\}$ have completely cancelling divergent pieces amongst themselves.

ϵ^0, τ^0

We already know that this will not get all contributions due to four-dimensional unitarity losing rational pieces and so we can discard these for now, where we will use augmented recursion to calculate this contribution at a later date.

ϵ^0, τ^2

We find full agreement with [2]. We get contributions from the box cuts on the inserts and then contributions from $\eta = \{tbx, stt, K31, K21\}$.

ϵ^0, τ^1

We find agreement with three of these pieces, as demonstrated in Table 5.2. Interestingly, the π contributions match which suggests the correct Riemann sheet has been found.

The pieces that we do not find agreement are the logarithms of Mandelstam variables including only positive helicity legs. This immediately suggests that the possible bug comes from the one-mass triangles as these vanish or integrate to zero if either of the massless legs are the negative helicity leg. Further evidence of this is found by sitting near kinematic poles. As an example, if we extract the coefficient for the $\log[s_{bc}]$ from our result and the result of [2], we can then numerically evaluate them near various poles, finding that if

$$\mathcal{I}_{stt}^{(2)}|_{\langle x\,y\rangle \to 0} \sim \langle x\,y\rangle^i$$

then the difference between the two results is also $\mathcal{O}\big(\langle x\,y\rangle^i\big)$. This is true for all poles for each of the mismatching logarithm coefficients, suggesting that either the bug is contained within the $\eta = stt$ structure or that there is a piece elsewhere that should be consistently cancelling this $\eta = stt$ piece.

π		$\log[s_{ab}]$	$\log[s_{ea}]$	$\log[s_{bc}]$	$\log[s_{cd}]$	$\log[s_{de}]$
✓		✓	✓	✗	✗	✗

Table 5.2: A table showing the present agreement with the results given in [2] for ϵ^0. Here the helicity assignment is $\{a^-, b^+, c^+, d^+, e^+\}$.

If there was a mistake in the insert calculations, it could only come from the bubble cuts.

We would need there to be contributions of the form,

$$C(p_a, p_b, p_c, p_d, p_e) \times \big(I_2(s_{bc}) + I_2(s_{de}) - 2I_2(s_{cd})\big), \qquad (5.185)$$

or any such combination of bubble integrals that have cancelling $\frac{1}{\epsilon}$ terms but non-cancelling logarithmic terms where C is some common kinematic coefficient that can be factorised out. This would provide transcendental one terms at finite order without effecting the already correct IR singular terms.

We already have flip symmetry checks on the results that are all satisfied. We have also recalculated them using a different method; where we initially had $\ell_1 = \ell_2 + P$ and generally tried to write things in terms of ℓ_1, we decided to calculate the double cuts again with most things written in terms of ℓ_2. This required a completely different series of algebraic manipulations and required different types of canonical forms and we found complete agreement with the first set of results. This leads us to strongly believe that the insert calculations are correct and therefore that the problem must lie either in genuine two-loop integrals or in something more fundamental.

There are numerical checks at every step of the automated two-loop integral and coefficient generator. These checks allowed us to track down errors in the $\frac{1}{\epsilon^3}$ calculation. The new checks lead us to also believe that the generation of the lists of box/triangle integrals and their associated coefficient is also working correctly. Much of this stage has also been checked by hand and found to match.

The unitarity stage also has extensive numerical checks, and so the most likely location of a calculational error would be the epsilon expansions and integrals themselves. The expansions of the boxes have been checked numerically against the explicit Appell functional forms (5.78) from [1] for kinematic points $0 < S < 1$, $|T| < 1$ and $S+T < 1$. The final form of the expanded boxes after the Riemann sheet cleanup has also been tested numerically and found to be the correct to $\mathcal{O}(\epsilon)$ in this region.

For the triangles, these tests are harder to perform due to slow convergence of the sums if comparing specifically against the form (5.64). There are forms of the one-mass and two-mass triangles presented in [102] that we may compare against for triangles that do not need a Mellin-Barnes expansion. Alternative derivations of the Mellin-Barnes expanded triangles are given in Appendix C. All integrals are then tested numerically and found to have the correct expansions.

There are a few other consistency checks we performed: changing the algebra for generating the list of one-mass triangles such that we had a new list with a different set of triangles and coefficients, but the final expanded result matched the previous list. We see in the "a in middle" part of the $\eta = K21$ numerator that the two terms are flips of each other, and integrating one side first necessarily gives us a scalar triangle as the first integration. We isolated this piece and changed the order of integration such that there was always an x_3 Feynman parameter in the numerator but found this to match as well. The specific integrand,

$$\frac{\ell_z^2}{P^2 Q^2 L_1^2}, \qquad (5.186)$$

provides the case of $\nu_4 = -1$ and $\nu_3 = 1$ case which was presented earlier. This integral is calculated explicitly using triangle parametrisations as a tensor integral in Appendix C.

One last note is that while there are no checks stated in [2], the coefficients generated for the all-plus logarithms in our calculation are certainly incorrect. Sitting on the collinear

limit $a^- \sim b^+$, we expect the result to have the limit

$$\lim_{a||b} A^{(2)}_{5:1}(a^-, b^+, c^+, d^+, e^+) = \sum_{\ell=0}^{2} \sum_{\lambda} S^{(\ell)}_{\lambda}(a^-, b^+) \times A^{(2-\ell)}_{4:1}(-K^{-\lambda}, c^+, d^+, e^+). \quad (5.187)$$

The flip symmetry here implies that in this limit we should expect the coefficient of $\log[s_{cd}]$ and $\log[s_{de}]$, defined as C_{cd} and C_{de} respectively, to obey

$$\lim_{a||b} C_{cd} = -\lim_{a||b} C_{de}, \quad (5.188)$$

and indeed the coefficient in [2] obeys this whereas our coefficients do not.

With hundreds of integrals needed to be calculated, there is of course the possibility that one of these tests has not been performed correctly, and indeed this is likely to be the case. If this is not the case, then the technique must have a more fundamental problem that we have overlooked, although with so many of the pieces being correct in highly non-trivial ways, it is more likely the case that there is some undiscovered bug in the code. Unfortunately, the author ran out of time in locating this bug.

5.7   Conclusion

In this calculation we

- Used four-dimensional unitarity and triple cuts to constrain some numerators for various two-loop structures.

- Used double cuts to find one-loop insert type structures built into one-loop structures.

- Used existing and developed new one-loop techniques to calculate the inserts.

- Used dimension shifting, a new representation of generalised scalar one-mass boxes and new techniques in $\epsilon-$expansions to calculate the genuine two-loop integrals to finite order.

- Summed these results over all diagrams.

We have unfortunately not been able to calculate the correct coefficient for the all-plus logarithms at finite order, but we are hopeful that this is simply an overlooked bug in the code. Should this be the case, then the technique will in theory scale well to higher multiplicities. The existence of a compact n-point tree amplitude for the MHV configurations means that numerators for the genuine two-loop structures are able to be calculated for n-points, and indeed they have been calculated [100]. The challenge would then be to calculate the loop inserts, calculate a compact form for general two-mass easy boxes and extend augmented recursion to the single-minus configuration. This is of course academic until the technique can be proven to work for the five-point case.

Regardless, this calculation has uncovered many new results for generalised hypergeometric functions, for general scalar integrals and ϵ-expansions, as well as a simple method for fixing the Riemann sheets. While it is disappointing that the final result was not able to be calculated in time for this thesis, the investigation has been interesting and has felt like a very worthwhile endeavour.

It is worth noting that some steps have already been taken towards future calculations and they are showing some promising results. Pieces of the augmented recursion for the single-minus calculation have already been calculated and a set of numerators for the genuine two-loop structures has been calculated at n-points. This set of numerators has been built in a way that require generalised two-mass easy boxes and so the next stage of the calculation would be to find a compact form of this ready for ϵ-expanding. The initial steps for this, as well as some notes on augmented recursion for the single-minus amplitude, are included in Appendix D.

Chapter 6

Conclusion

In this thesis we have calculated new and existing results using four-dimensional unitarity and augmented recursion. The technique scales very well to higher multiplicities. The largely algebraic nature of the calculations allow close inspection of the intermediate steps and uncovers interesting relations between different structures. Augmented recursion has previously been used to calculate the full rational piece of amplitudes of various theories, and we extend this technique to the full colour, pure Yang-Mills case for all-plus helicities. It continues to prove the most promising method of calculating rational contributions containing double poles.

In Chapter 2, we calculated the full colour, five-point all-plus amplitude at two loops, agreeing with the previously calculated result. This involved extending the pseudo one-loop calculation to one which included the full colour one-loop insert, made easier by the compact forms of the subleading in colour amplitudes presented. The rational calculation also extended the augmented recursion technique to full colour, instead opting to use the decoupling identities to express each subleading in colour current in terms of two independent leading in colour currents.

Chapter 3 calculated the two-loop, six-point, full colour, all-plus amplitude using the same techniques as for five-point. This was a new result and required functional reconstruction of the rational piece.

Chapter 4 calculated the cut-constructible part of the full two-loop, all-plus amplitude at n-points. We also conjecture the rational part of the $A^{(2)}_{n:1B}$ amplitude for all-plus helicities, completing this partial amplitude. The conjecture matches the explicit calculation for up to seven gluons.

Finally, in Chapter 5 we present a new technique for calculating the cut-constructible part of the five-point single-minus amplitude at two-loops. This leading in colour calculation has not been completed, although the IR divergent piece and finite, transcendental two pieces are correctly calculated which are highly non-trivial results. Only the finite order, all-plus helicity logarithms are incorrect, and an extensive list of consistency checks has been presented. Several new results are calculated for generalised hypergeometric functions, for general scalar integrals and ϵ-expansions, as well as a simple method for fixing the Riemann sheets.

Appendix A

Bubble Structures and Inserts

A.1   Genuine Two-Loop Bubble Contributions

We showed in Chapter 5 that all contributions of bubbles in propagators vanish upon integration. They are still required for the unitarity checks and so we will list the numerators here. Starting with $\eta = fbbx$ for completeness,

$$\mathcal{N}_{nfbbx} = \langle a\,\bar{a}\rangle\,[\bar{a}|\ell_\omega|\omega\rangle\langle a|L_A L_B|a\rangle[\omega|\ell_z\ell_\omega L_A|a\rangle. \tag{A.1}$$
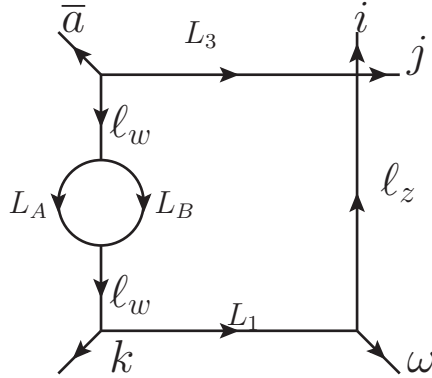

Figure A.1: Bubble in box between two null corners. $\eta = fbbx$ for no pinched propagators, $\eta = pbbx$ for ℓ_w pinched towards $\bar{a}$. No contributions for both ℓ_w propagators pinched.

$$\mathcal{N}_{npbbx} = \langle a\,\bar{a}\rangle\,[\bar{a}|\ell_\omega L_1\omega|a\rangle\langle a|L_A L_B|a\rangle, \tag{A.2}$$

154
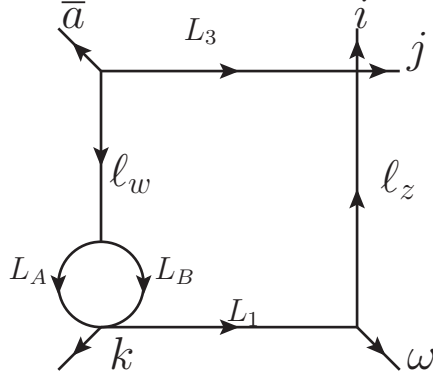
Figure A.2: Bubble in box between two null corners with a pinched propagator. $\eta = npbbx$. No contribution for the other ℓ_w being pinched.

$$\mathcal{N}_{mfbbx} = \langle a\,\overline{a}\rangle\,[\overline{a}|\ell_\omega|\omega\rangle\langle a|L_A L_B|a\rangle[\omega|\ell_z L_3 L_A|a\rangle. \tag{A.3}$$

Figure A.3: Bubble in box between two massive corners. $\eta = mfbbx$.

$$\mathcal{N}_{mpbbx} = \langle a\,\overline{a}\rangle\,[\overline{a}|\ell_\omega|\omega\rangle\langle a|L_A L_B|a\rangle[\omega|\ell_z L_3 L_A|a\rangle. \tag{A.4}$$
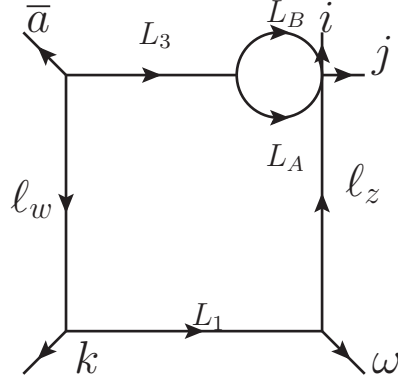
Figure A.4: Bubble in box between two massive corners. $\eta = mpbbx$. No contributions for both L_3 propagators pinched.

$$\mathcal{N}_{mft1m} = \langle a\,\bar{a}\rangle\,[\bar{a}|L_M L_S L_A|a\rangle\langle a|L_A L_B|a\rangle, \tag{A.5}$$
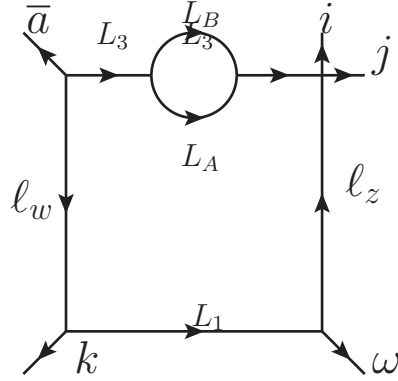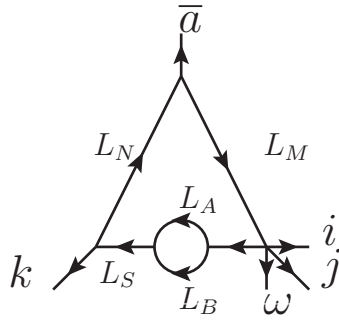

Figure A.5: Bubble in one-mass triangle between a massive corner and null corner. $\eta = mft1m$

$$\mathcal{N}_{mpt1m} = (\delta_a^i + \delta_a^\omega)\langle a|\bar{a}k|a\rangle\langle a|L_A L_B|a\rangle, \tag{A.6}$$

where δ_a^i and δ_a^ω are one when the single minus gluon is in position i or ω respectively and zero in all other cases.
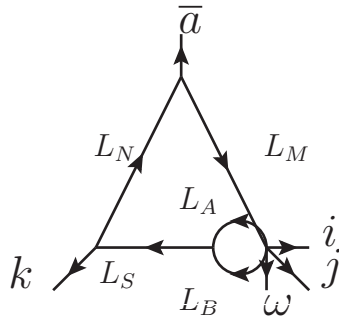
Figure A.6: Bubble in one-mass triangle between a massive corner and null corner with a pinched propagator. $\eta = mpt1m$. No contribution for doubly pinched bubbles.

$$\mathcal{N}_{nft1m} = [\bar{a}|k|\bar{a}\rangle(\langle a|L_A L_B|a\rangle)^2, \tag{A.7}$$
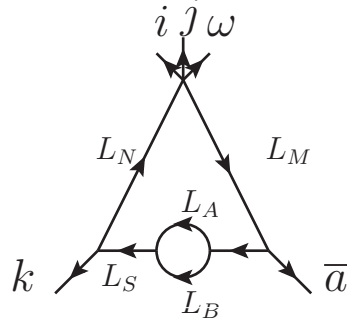
Figure A.7: Bubble in one-mass triangle between two null corners. $\eta = nft1m$

$$\mathcal{N}_{npt1m} = -\langle a|kL_A|a\rangle\langle a|L_S L_B|a\rangle + \langle a|\bar{a}L_A|a\rangle\langle a|L_S L_B|a\rangle, \tag{A.8}$$
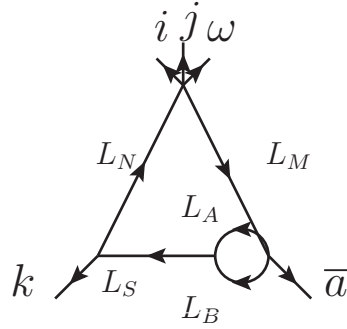
Figure A.8: Bubble in one-mass triangle between two null corners with a pinched propagator. $\eta = npt1m$. No contributions from doubly pinched propagators.

$$\mathcal{N}_{ft2m} = \langle a|\bar{a}L_A|a\rangle\langle a|L_B L_A|a\rangle, \tag{A.9}$$
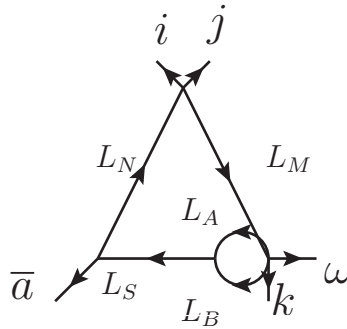
Figure A.9: Bubble in two-mass triangle between a null corner and a massive corner with a pinched propagator. $\eta = ft2m$. No other contributions.

A.2 Inserts

The following inserts contribute to multiple double cuts, with the loop insert being indicated by the vertex in the corresponding figure. The following is for $\{a^-, b^+, c^+, d^+, e^+\}$ and the propagators are left out of the equations but are indicated by the corresponding figure. There is also a Parke-Taylor denominator factorised out $1/(\langle a\,b\rangle \langle b\,c\rangle \langle c\,d\rangle \langle d\,e\rangle \langle e\,a\rangle)$.

$$Ib_1 = \frac{(P_1 + d)^2 \langle a\,d\rangle^2 \langle a\,c\rangle [a|P_1|c\rangle [c|(P_1 + P_{de})|a\rangle \langle e\,a\rangle}{6 \langle c\,d\rangle \langle d\,e\rangle}$$
$$- \frac{\langle a\,b\rangle \langle e\,a\rangle s_{bc}[b|c|d\rangle [c|P_1|a\rangle [b|(P_1 + P_{de})|c\rangle}{6 [a\,b] \langle d\,e\rangle} \tag{A.10}$$

Figure A.10: Insert diagram corresponding to Ib_1. The vertex on the massive corner indicates the one-loop insertion.

$$Ib_2 = -\frac{\langle a\,b\rangle^2 \langle a\,c\rangle^2 [a|P_1|c\rangle [c|(P_1 + P_{de})|a\rangle [b\,c]}{6 \langle b\,c\rangle}$$
$$+ \frac{\langle a\,b\rangle \langle a\,c\rangle^2 \langle a\,d\rangle [a|P_1|c\rangle [c|(P_1 + P_{de})|a\rangle [b\,c]}{6 \langle c\,d\rangle} \tag{A.11}$$

Figure A.11: Insert diagram corresponding to Ib_2. The vertex on the massive corner indicates the one-loop insertion.

$$Ib_3 = \frac{(P_1 + b)^2 \langle a\,c \rangle^2 \langle a\,d \rangle\,[a|(P_1 + P_{bc})|d\rangle[d|P_1|a\rangle\,\langle b\,a \rangle}{6\,\langle b\,c \rangle\,\langle c\,d \rangle}$$

$$- \frac{\langle e\,a \rangle\,\langle a\,b \rangle\,s_{de}[e|d|c\rangle[d|(P_1 + P_{bc})|a\rangle\,[e|P_1|d\rangle}{6\,[e\,a]\,\langle b\,c \rangle} \tag{A.12}$$

Figure A.12: Insert diagram corresponding to Ib_3. The vertex on the massive corner indicates the one-loop insertion.

$$Ib_4 = -\frac{\langle e\,a \rangle^2\,\langle a\,d \rangle^2\,[d|P_1|a\rangle[a|(P_1 + P_{bc})|d\rangle\,[d\,e]}{6\,\langle d\,e \rangle}$$

$$+ \frac{\langle e\,a \rangle\,\langle a\,d \rangle^2\,\langle a\,c \rangle\,[a|(P_1 + P_{bc})|d\rangle[d|P_1|a\rangle\,[d\,e]}{6\,\langle c\,d \rangle} \tag{A.13}$$

Figure A.13: Insert diagram corresponding to Ib_4. The vertex on the massive corner indicates the one-loop insertion.

$$Ib_5 = \frac{\langle e\,a \rangle^2\,\langle c\,e \rangle\,[e|(P_1 + P_{ab}|a\rangle[e|P_1 + P_{ab}|a\rangle[c|P_1|d\rangle}{6\,\langle d\,e \rangle} \tag{A.14}$$

Figure A.14: Insert diagram corresponding to Ib_5. The vertex on the massive corner indicates the one-loop insertion.

$$Ib_6 = -\frac{\langle a\,c\rangle^2\,\langle d\,e\rangle\,[c|P_1|a\rangle[c|P_1|a\rangle[e|(P_1+P_{ab})|c\rangle}{6\,\langle c\,d\rangle}$$
$$+\frac{\langle a\,b\rangle\,\langle a\,c\rangle\,\langle d\,e\rangle\,[d|P_1|a\rangle[c|P_1|a\rangle[e|(P_1+P_{ab})|c\rangle}{6\,\langle b\,c\rangle} \tag{A.15}$$
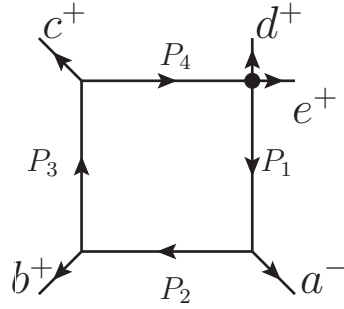

Figure A.15: Insert diagram corresponding to Ib_6. The vertex on the massive corner indicates the one-loop insertion.

$$Ib_7 = -\frac{\langle a\,b\rangle\,\langle a\,c\rangle\,\langle e\,a\rangle\,[a|P_1|a\rangle[c|P_1|a\rangle[e|(P_1+P_{ab})|c\rangle}{6\,\langle b\,c\rangle} \tag{A.16}$$

Figure A.16: Insert diagram corresponding to Ib_7. The vertex on the massive corner indicates the one-loop insertion.

$$Ib_8 = \frac{\langle a\,b\rangle^2 \langle d\,b\rangle\, [b|P_1|a\rangle [b|P_1|a\rangle [d|(P_1 + P_{ea})|c\rangle}{6\,\langle b\,c\rangle} \tag{A.17}$$
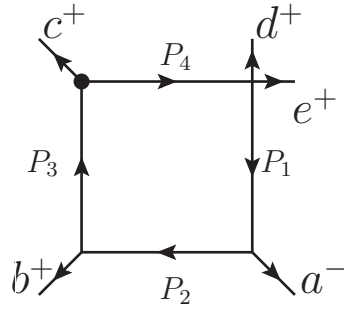

Figure A.17: Insert diagram corresponding to Ib_8. The vertex on the massive corner indicates the one-loop insertion.

$$Ib_9 = \frac{\langle a\,d\rangle^2 \langle b\,c\rangle\, [d|(P_1 + P_{ea})|a\rangle [d|(P_1 + P_{ea})|a\rangle [b|P_1|d\rangle}{6\,\langle c\,d\rangle}$$
$$+ \frac{\langle e\,a\rangle \langle a\,d\rangle \langle b\,c\rangle\, [c|(P_1 + P_{ea})|a\rangle [d|(P_1 + P_{ea})|a\rangle [b|P_1|d\rangle}{6\,\langle d\,e\rangle} \tag{A.18}$$

Figure A.18: Insert diagram corresponding to Ib_9. The vertex on the massive corner indicates the one-loop insertion.

$$Ib_{10} = -\frac{\langle e\,a\rangle \langle a\,d\rangle \langle a\,b\rangle\, [a|(P_1 + P_{ea})|a\rangle [d|(P_1 + P_{ea})|a\rangle [b|P_1|d\rangle}{6\,\langle d\,e\rangle} \tag{A.19}$$
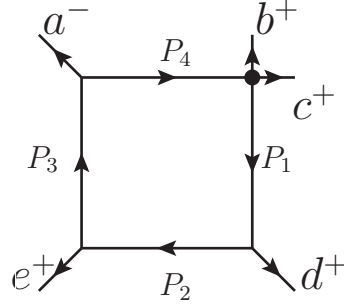
Figure A.19: Insert diagram corresponding to Ib_{10}. The vertex on the massive corner indicates the one-loop insertion.

$$Ib_{11} = \frac{\langle a\,b\rangle^2}{6\,\langle b\,c\rangle}\bigg(\langle e\,c\rangle\,[e|P_1|a\rangle[a|b|a\rangle[b|(P_1+P_{cd})|a\rangle + [e|P_1|e\rangle\,\langle e\,c\rangle\,[e|b|a\rangle[b|(P_1+P_{cd})|a\rangle$$

$$- (P1)^2\,\langle e\,c\rangle\,[e|b|a\rangle[b|P_1+P_{cd}|a\rangle + [b|(P_1+P_{cd})|b\rangle\,\langle e\,c\rangle\,[e|P_1|a\rangle[b|(P_1+P_{cd})|a\rangle$$

$$- [e|P_1|e\rangle\,\langle b\,c\rangle\,[b|(P_1+P_{cd})|a\rangle[b(P_1+P_{cd}|a\rangle\bigg) \tag{A.20}$$
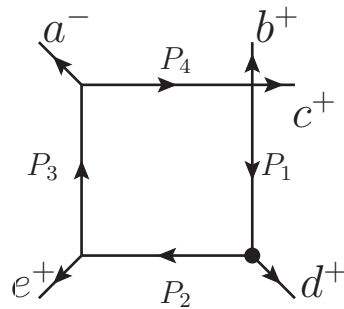

Figure A.20: Insert diagram corresponding to Ib_{11}. The vertex on the massive corner indicates the one-loop insertion.

$$Ib_{12} = \frac{\langle a\,b\rangle^2\,\langle e\,c\rangle\,[b|(P_1+P_{cd})|a\rangle[b|(P_1-e)|c\rangle[c|P_1|d\rangle[e|P_1|c\rangle}{6\,\langle b\,c\rangle\,\langle c\,d\rangle\,[a\,b]}$$

$$+ \frac{\langle e\,a\rangle^2\,\langle b\,d\rangle\,[e|P_1|a\rangle[e|(P_1-a)|d\rangle}{12\,\langle c\,d\rangle\,\langle d\,e\rangle\,[e\,a]}$$

$$\times\bigg(-(P_4)^2[b|P_1|c\rangle + \big((P_1+c)^2 - [d|P_1|d\rangle\big)[b|(P_1+P_{cd})|c\rangle + [b|(P_1+P_{cd})P_1d|c\rangle\bigg)$$

$$- \frac{\langle a\,b\rangle\,\langle e\,a\rangle\,\langle b\,c\rangle\,\langle d\,e\rangle\,[b\,e]^3}{6\,\langle c\,d\rangle\,[a\,b]\,[e\,a]}\bigg(((P_1)^2 - (P_2)^2)[b|P_1|b\rangle - (P_1)^2[e|b|e\rangle + [b|P_1|e\rangle[e|P_{cd}|b\rangle\bigg) \tag{A.21}$$
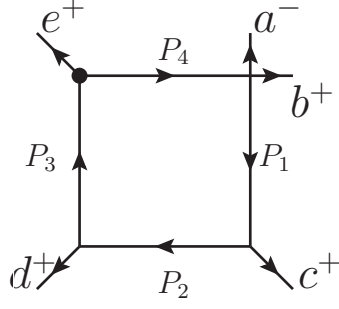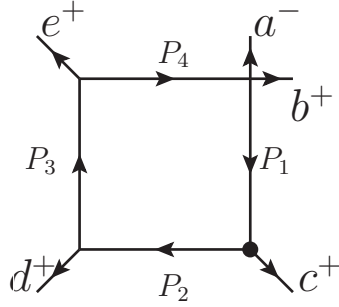
162

Figure A.21: Insert diagram corresponding to Ib_{12}. The vertex on the massive corner indicates the one-loop insertion.

$$
\begin{aligned}
Ib_{13} = {} & \frac{\langle e\,a\rangle^2\,[e|P_1|a\rangle}{6\,\langle d\,e\rangle} \times \Bigg(-(P_1)^2\,\langle a\,b\rangle\,[b|(P_1 + P_{cd})|d\rangle \\
& + (P_2)^2\big(\,\langle b\,d\rangle\,\langle e\,a\rangle\,[e\,b] + \langle a\,b\rangle\,[b|(P_1 + P_{cd})|d\rangle\big) \\
& - \langle e\,a\rangle\,\big(\,\langle b\,d\rangle\,[a\,b]\,[e|P_1|a\rangle + ((P_3)^2 - (P_4)^2)[e|P_1|d\rangle \Bigg)
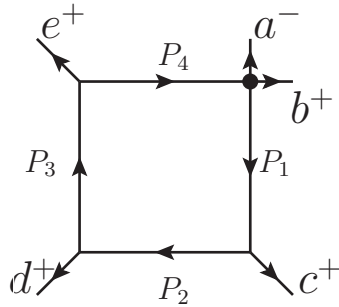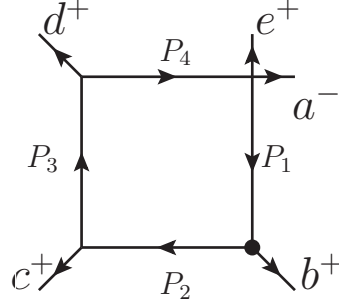\end{aligned}
\tag{A.22}
$$

Figure A.22: Insert diagram corresponding to Ib_{13}. The vertex on the massive corner indicates the one-loop insertion.

$$
\begin{aligned}
Ib_{14} = {} & \frac{\langle a\,c\rangle^2\,[c|P_1|a\rangle}{6\,\langle b\,c\rangle\,\langle c\,d\rangle}\Big(\langle b\,c\rangle\,(-\langle c\,d\rangle\,[c|P_1|a\rangle + \langle d\,a\rangle\,[c|(P_1 + P_{ab}|c\rangle \\
& + \langle a\,b\rangle\,\langle c\,d\rangle\,([d|(P_1 + P_{ab})|d\rangle + [e|(P_1 + P_{ab}|e\rangle\Big)
\end{aligned}
\tag{A.23}
$$

Figure A.23: Insert diagram corresponding to Ib_{14}. The vertex on the massive corner indicates the one-loop insertion.

$$
\begin{aligned}
Ib_{15} = -\frac{\langle e\,a\rangle\,[c|P_1|a\rangle}{6s_{de}\,\langle d\,e\rangle\,[a\,b]}\Big(&2\,\langle d\,e\rangle\,[b|(P_1+P_{ab})|c\rangle[e|(P_1+P_{ab}|a\rangle[e|(P_1+P_{ab})|e\rangle \\
&- s_{de}\,\langle a\,c\rangle\,[a\,b]\,\big(\,\langle d\,e\rangle\,[e|(P_1+P_{ab}|a\rangle - 2\,\langle e\,a\rangle\,[e|(P_1+P_{ab})|d\rangle \\
&\qquad + \langle d\,a\rangle\,(s_{de}+[e|(P_1+P_{ab})|e\rangle)\big) \\
&+ s_{de}\,\langle a\,d\rangle\,(\langle d\,a\rangle\,\langle e\,c\rangle\,[a\,b]\,[d\,e] + 2[b|(P_1+P_{ab})|c\rangle[e|(P_1+P_{ab})|e\rangle))\Big)
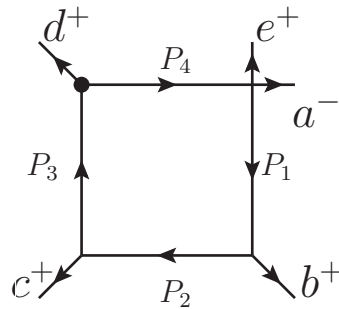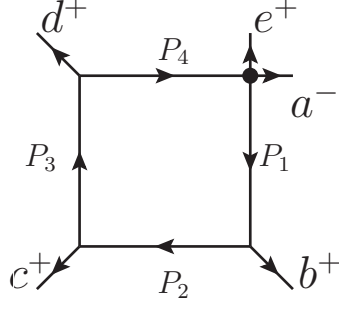\end{aligned}
$$
(A.24)

Figure A.24: Insert diagram corresponding to Ib_{15}. The vertex on the massive corner indicates the one-loop insertion.

$$
Ib_{16} = \frac{\langle e\,a\rangle}{6\,\langle c\,d\rangle\,\langle d\,e\rangle\,[a\,b]}\Big(\langle a\,c\rangle\,\langle a\,d\rangle^2\,\langle a\,e\rangle\,[a\,b]\,[d\,e]\,[a|P_1|d\rangle + s_{bc}\,\langle a\,b\rangle\,\langle c\,d\rangle^2\,[b\,c]\,[b|P_1|a\rangle\Big)
$$
(A.25)

164

Figure A.25: Insert diagram corresponding to Ib_{16}. The vertex on the massive corner indicates the one-loop insertion.

$$Ib_{17} = -\frac{\langle a\,b\rangle}{6\,\langle b\,c\rangle}\left(\frac{\langle a\,b\rangle\,\langle a\,c\rangle^2\,\langle a\,d\rangle\,[b\,c]\,[a|P_1|c\rangle}{\langle c\,d\rangle} + \frac{s_{de}\,\langle e\,a\rangle\,\langle c\,d\rangle\,[d\,e]\,[e|P_1|a\rangle}{[e\,a]}\right) \tag{A.26}$$

Figure A.26: Insert diagram corresponding to Ib_{17}. The vertex on the massive corner indicates the one-loop insertion.

$$Ib_{18} = \frac{\langle e\,a\rangle^2\,[e|P_1|a\rangle^2}{6} \tag{A.27}$$

Figure A.27: Insert diagram corresponding to Ib_{18}. The vertex on the massive corner indicates the one-loop insertion.

$$Ib_{19} = \frac{\langle a\,b\rangle \langle e\,a\rangle \, [b|(P_1 + P_{cd})|a\rangle [e|P_1|a\rangle}{6} \tag{A.28}$$
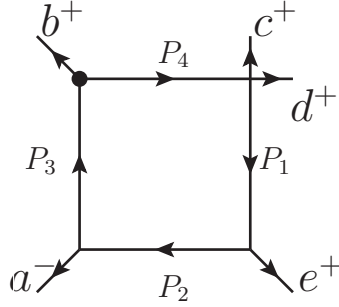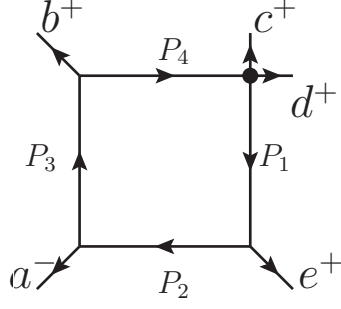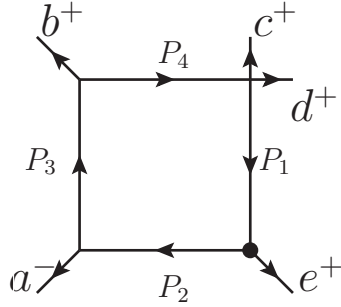

Figure A.28: Insert diagram corresponding to Ib_{19}. The vertex on the massive corner indicates the one-loop insertion.

$$
\begin{aligned}
Ib_{20} = -\frac{1}{6 s_{cd} \langle b\,c\rangle \langle c\,d\rangle \langle d\,e\rangle \, [a\,b]\,[e\,a]} \\
\Big(\langle a\,c\rangle \langle c\,d\rangle \langle d\,e\rangle \, [e\,a]\,[b|(P_1 + P_{cd})|e\rangle [d|(P_1 + P_{cd}|a\rangle [e|P_1|d\rangle \\
\times\, (\langle b\,c\rangle\,[c|(P_1 + P_{cd}|a\rangle - \langle a\,b\rangle\,[c|(P_1 + P_{cd}|c\rangle) \\
+ s_{cd}\,\langle b\,c\rangle\,[b|(P_1 + P_{cd})|d\rangle [e|P_1|a\rangle \\
\times\, \big(\langle d\,a\rangle s_{ea} \langle d\,e\rangle\,[d|(P_1 + P_{cd}|c\rangle - \langle c\,d\rangle \langle e\,a\rangle\,(\langle d\,e\rangle\,[c\,e]\,[d|P_1|c\rangle + s_{ea}[d|(P_1 + P_{cd})|d\rangle)\big) \\
+ s_{cd}\,\langle c\,a\rangle \langle d\,e\rangle\,[a\,b]\,[e\,a] \\
\times\, \big(\langle a\,d\rangle \langle a\,b\rangle \langle c\,e\rangle\,[d|(P_1 + P_{cd})|a\rangle [e|P_1|d\rangle \\
+ \langle e\,a\rangle \langle c\,d\rangle\,(\langle b\,c\rangle\,[c|(P_1 + P_{cd})|a\rangle [e|P_1|a\rangle + \langle a\,b\rangle\,[d|(P_1 + P_{cd})|a\rangle [e|P_1|d\rangle)\big)\Big)
\end{aligned}
\tag{A.29}
$$
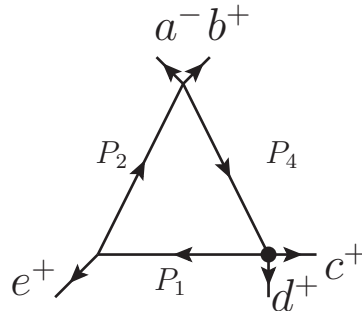
Figure A.29: Insert diagram corresponding to Ib_{20}. The vertex on the massive corner indicates the one-loop insertion.

$$Ib_{21} = \frac{\langle d\,a \rangle^2 \, [d|P_1|a \rangle (\langle e\,a \rangle \, \langle c\,d \rangle \, ([b|(P_1 + P_{bc})|b \rangle + [c|(P_1 + P_{bc}|c \rangle))}{6 \, \langle c\,d \rangle \, \langle d\,e \rangle}$$

$$- \frac{\langle d\,a \rangle^2 \, [d|P_1|a \rangle (\langle c\,d \rangle \, [d|P_1|a \rangle + \langle c\,a \rangle \, [d|(P_1 + P_{bc})|d \rangle)}{6 \, \langle c\,d \rangle} \tag{A.30}$$
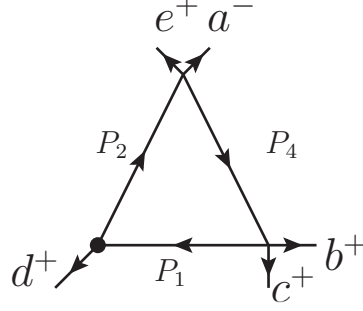
Figure A.30: Insert diagram corresponding to Ib_{21}. The vertex on the massive corner indicates the one-loop insertion.

$$Ib_{22} = \frac{\langle a\,b \rangle \, [d|P_1|a \rangle}{6s_{bc} \, \langle b\,c \rangle \, [e\,a]} \Big(-2 \, \langle b\,c \rangle \, [b|(P_1 + P_{bc}|a \rangle [b|(P_1 + P_{bc}|b \rangle [e|(P_1 + P_{bc})|d \rangle$$

$$- s_{bc} \, \langle a\,c \rangle^2 \, \langle b\,d \rangle \, [e\,a] \, [b\,c]$$

$$- s_{bc} \, \langle a\,d \rangle \, [e\,a] \, (\langle b\,c \rangle \, [b|(P_1 + P_{bc}|a \rangle - 2 \, \langle a\,b \rangle \, [b|(P_1 + P_{bc})|c \rangle)$$

$$+ s_{bc} \, \langle a\,c \rangle \, \Big(\langle a\,d \rangle \, [e\,a] \, (s_{bc} - [b|(P_1 + P_{bc})|b \rangle) + 2[b|(P_1 + P_{bc})|b \rangle [e|(P_1 + P_{bc})|d \rangle) \Big) \tag{A.31}$$
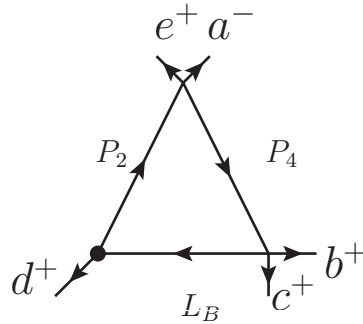
Figure A.31: Insert diagram corresponding to Ib_{22}. The vertex on the massive corner indicates the one-loop insertion.

$$Ib_{23} = -\frac{\langle a\,b \rangle^2 \, [b|P_1|a \rangle^2}{6} \tag{A.32}$$
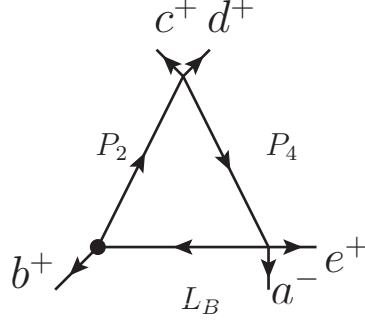
Figure A.32: Insert diagram corresponding to Ib_{23}. The vertex on the massive corner indicates the one-loop insertion.

$$Ib_{24} = \frac{\langle a\,b\rangle\,\langle e\,a\rangle\,[b|P_1|a\rangle[e|P_1|a\rangle}{6} \tag{A.33}$$
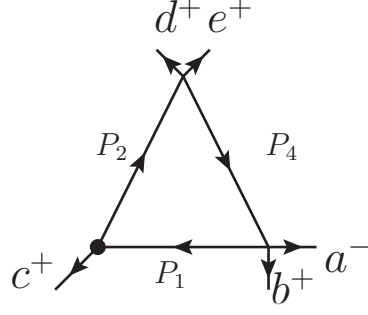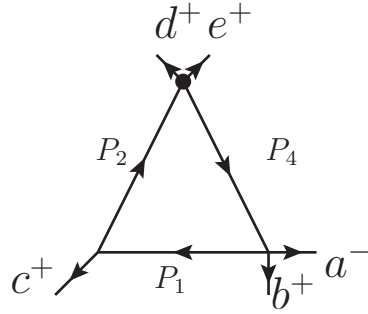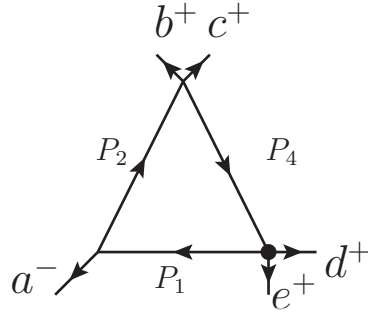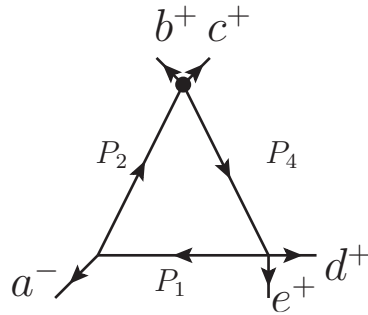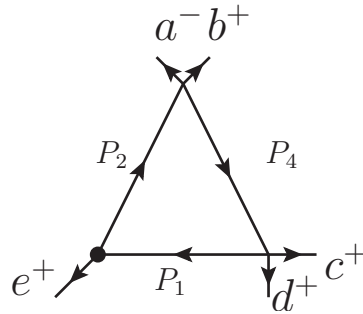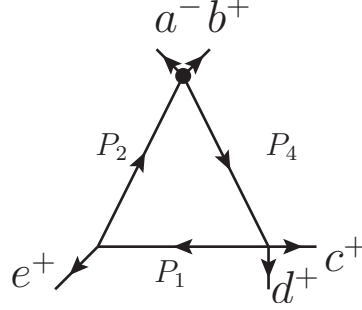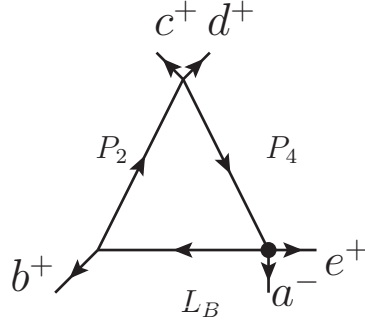

Figure A.33: Insert diagram corresponding to Ib_{24}. The vertex on the massive corner indicates the one-loop insertion.

$$
\begin{aligned}
Ib_{25} = {}& -\frac{1}{6s_{cd}\,\langle b\,c\rangle\,\langle c\,d\rangle\,\langle d\,e\rangle\,[a\,b]\,[e\,a]}\\
& \Big(\langle a\,d\rangle\,\langle b\,c\rangle\,\langle c\,d\rangle\,[a\,b]\,[b|P_1|e\rangle[c|(P_1+P_{ea}|a\rangle[e|(P_1+P_{ea})|b\rangle\\
& \qquad \times (\langle d\,e\rangle\,[d|(P_1+P_{ea}|a\rangle - \langle e\,a\rangle\,[d|(P_1+P_{ea}|d\rangle)\\
& + s_{cd}\,\langle c\,a\rangle\,\langle b\,c\rangle\,[a\,b]\\
& \qquad \times \big(\langle a\,d\rangle\,\langle b\,d\rangle\,s_{ea}[b|P_1|c\rangle[c|(P_1+P_{ea})|a\rangle\\
& \qquad\quad + \langle a\,b\rangle\,\langle d\,e\rangle\,[b|P_1|a\rangle[c|(P_1+P_{ea})|d\rangle[e|(P_1+P_{ea})|c\rangle\big)\\
& - s_{cd}\,\langle c\,d\rangle\,\langle a\,b\rangle\,\langle a\,d\rangle\,\langle b\,c\rangle\,[a\,b]\,[e\,a]\\
& \qquad \times (\langle e\,a\rangle\,[b|P_1|c\rangle[c|(P_1+P_{ea})|a\rangle + \langle d\,e\rangle\,[b|P_1|a\rangle[d|(P_1+P_{ea})|a\rangle)\\
& + s_{cd}\,\langle c\,d\rangle\,\langle a\,b\rangle\,\langle d\,e\rangle\,[b|P_1|a\rangle\\
& \qquad \times (s_{ab}[c|(P_1+P_{ea})|c\rangle[e|(P_1+P_{ea})|c\rangle + \langle b\,c\rangle\,[b\,d]\,[c|(P_1+P_{ea})|d\rangle[e|(P_1+P_{ea}|c\rangle)\Big)
\end{aligned}
\tag{A.34}
$$

168
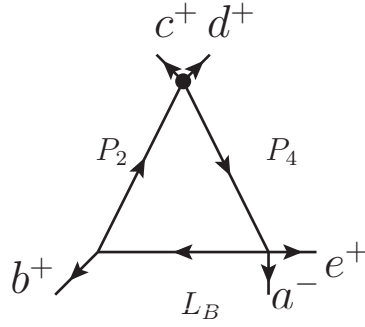
Figure A.34: Insert diagram corresponding to Ib_{25}. The vertex on the massive corner indicates the one-loop insertion.

The remaining inserts are either one-mass triangles or one-mass bubbles, both of which only contribute to one channel on a four-dimensional double cut. As an example, for $A_4^{(0)}(a^-, b^+, \ell_1, \ell_2) \times \ldots$ we denote the insert It_{ab} whereas the $A_4^{(1)}(a^-, b^+, \ell_1, \ell_2) \times \ldots$ is denoted $I\ell_{ab}$. We define ℓ_1 and ℓ_2 to be going away from the massless corners. We present the insert as they appear on the cut, with cut propagators removed and, in the case of the one-mass triangle, the uncut propagator remaining. We still factorise out the Parke-Taylor denominator.

$$I\ell_{ab} = -\frac{\langle a\,b\rangle^2 \langle a\,\ell_1\rangle \langle \ell_2\,c\rangle\, [\ell_2|\ell_1|a\rangle}{6 \langle b\,c\rangle \langle b\,\ell_1\rangle} \tag{A.35}$$

It_{ab}

$$= \frac{1}{6}\left(\frac{\langle b\,a\rangle\,\langle c\,a\rangle\,\langle \ell_1\,a\rangle^2\,\langle \ell_2\,d\rangle\,[b\,\ell_1]}{\langle c\,d\rangle\,\langle \ell_1\,\ell_2\rangle} + \frac{\langle a\,c\rangle\,\langle a\,e\rangle\,\langle d\,a\rangle\,\langle e\,a\rangle\,[c\,e]}{\langle d\,e\rangle} \right.$$

$$- \frac{\langle a\,c\rangle\,\langle b\,a\rangle\,\langle \ell_1\,a\rangle^2\,\langle \ell_2\,c\rangle\,[c\,\ell_1]}{\langle b\,c\rangle\,\langle \ell_1\,\ell_2\rangle} - \frac{\langle a\,c\rangle\,\langle b\,a\rangle\,\langle d\,b\rangle\,\langle \ell_1\,a\rangle^3\,\langle \ell_2\,c\rangle^2\,[c\,\ell_1]}{\langle b\,\ell_1\rangle\,\langle c\,b\rangle\,\langle c\,d\rangle\,\langle \ell_1\,\ell_2\rangle\,\langle \ell_2\,a\rangle}$$

$$+ \frac{\langle b\,c\rangle\,\langle c\,d\rangle\,\langle e\,a\rangle\,\langle \ell_2\,a\rangle\,[b\,\ell_2]\,[c\,b]\,[c\,\ell_2]}{\langle d\,e\rangle\,[a\,b]\,[a\,\ell_2]} + \frac{\langle a\,c\rangle\,\langle e\,a\rangle\,\langle \ell_1\,a\rangle^2\,\langle \ell_2\,d\rangle^2\,[d\,c]}{\langle d\,e\rangle\,\langle \ell_1\,\ell_2\rangle\,\langle \ell_2\,\ell_1\rangle}$$

$$- \frac{\langle a\,c\rangle\,\langle d\,a\rangle\,\langle e\,a\rangle\,\langle \ell_1\,a\rangle\,\langle \ell_2\,d\rangle\,[d\,e]}{\langle c\,d\rangle\,\langle \ell_1\,\ell_2\rangle} - \frac{\langle a\,c\rangle\,\langle e\,a\rangle\,\langle \ell_1\,a\rangle^2\,\langle \ell_2\,d\rangle^2\,[d\,e]}{\langle c\,d\rangle\,\langle \ell_1\,\ell_2\rangle\,\langle \ell_2\,\ell_1\rangle}$$

$$+ \frac{\langle b\,a\rangle\,\langle c\,e\rangle\,\langle e\,a\rangle\,\langle \ell_1\,a\rangle^3\,\langle \ell_2\,d\rangle^3\,[d\,e]}{\langle b\,\ell_1\rangle\,\langle c\,d\rangle\,\langle d\,e\rangle\,\langle \ell_1\,\ell_2\rangle\,\langle \ell_2\,a\rangle\,\langle \ell_2\,\ell_1\rangle} + \frac{\langle a\,d\rangle\,\langle d\,a\rangle\,\langle e\,a\rangle\,\langle \ell_1\,a\rangle\,[d\,\ell_1]}{\langle d\,e\rangle}$$

$$- \frac{\langle a\,c\rangle\,\langle d\,a\rangle^2\,\langle e\,a\rangle\,\langle \ell_1\,a\rangle\,\langle \ell_2\,d\rangle\,[d\,\ell_1]}{\langle c\,d\rangle\,\langle d\,e\rangle\,\langle \ell_2\,a\rangle} + \frac{\langle b\,d\rangle\,\langle d\,a\rangle\,\langle e\,a\rangle\,\langle \ell_1\,c\rangle\,\langle \ell_1\,d\rangle\,\langle \ell_2\,a\rangle\,[b\,e]\,[d\,\ell_1]}{\langle c\,d\rangle\,\langle d\,e\rangle\,\langle \ell_1\,\ell_2\rangle\,[a\,e]}$$

$$- \frac{\langle a\,c\rangle\,\langle b\,a\rangle\,\langle c\,a\rangle\,\langle \ell_1\,a\rangle\,\langle \ell_2\,d\rangle\,[c\,\ell_2]\,[d\,\ell_1]}{\langle b\,c\rangle\,\langle c\,d\rangle\,[c\,d]} - \frac{\langle a\,b\rangle\,\langle a\,\ell_1\rangle\,\langle e\,a\rangle\,\langle \ell_2\,a\rangle\,[e\,\ell_2]}{\langle b\,\ell_1\rangle}$$

$$+ \frac{\langle e\,a\rangle\,\langle \ell_1\,a\rangle\,\langle \ell_2\,a\rangle^2\,[e\,\ell_2]}{\langle \ell_1\,\ell_2\rangle} + \frac{\langle b\,e\rangle\,\langle e\,a\rangle\,\langle \ell_1\,a\rangle\,\langle \ell_1\,d\rangle\,\langle \ell_2\,a\rangle^2\,[e\,\ell_2]}{\langle b\,\ell_1\rangle\,\langle d\,e\rangle\,\langle \ell_1\,\ell_2\rangle}$$

$$+ \frac{\langle a\,d\rangle\,\langle e\,a\rangle\,\langle \ell_1\,a\rangle\,\langle \ell_2\,a\rangle\,\langle \ell_2\,e\rangle\,[e\,\ell_2]}{\langle d\,e\rangle\,\langle \ell_1\,\ell_2\rangle} - \frac{\langle c\,a\rangle^2\,\langle \ell_1\,a\rangle^2\,\langle \ell_2\,d\rangle\,[\ell_1\,c]}{\langle c\,d\rangle\,\langle \ell_1\,\ell_2\rangle}$$

$$- \frac{\langle b\,c\rangle\,\langle e\,a\rangle\,\langle \ell_1\,a\rangle\,\langle \ell_1\,d\rangle^3\,\langle \ell_2\,a\rangle^2\,[\ell_1\,d]}{\langle b\,\ell_1\rangle\,\langle c\,d\rangle\,\langle d\,e\rangle\,\langle \ell_1\,\ell_2\rangle^2} + \frac{\langle a\,d\rangle\,\langle e\,a\rangle\,\langle \ell_1\,a\rangle\,\langle \ell_2\,a\rangle\,[\ell_1\,\ell_2]}{\langle d\,e\rangle}$$

$$+ \frac{\langle a\,b\rangle^2\,\langle c\,a\rangle\,\langle \ell_1\,a\rangle\,\langle \ell_2\,c\rangle\,\langle \ell_2\,d\rangle\,[\ell_2\,b]}{\langle b\,c\rangle\,\langle c\,d\rangle\,\langle \ell_1\,\ell_2\rangle} + \frac{\langle a\,\ell_2\rangle\,\langle c\,a\rangle\,\langle e\,a\rangle\,\langle \ell_2\,d\rangle\,[c\,\ell_2]\,[\ell_2\,b]}{\langle d\,e\rangle\,[a\,b]}$$

$$- \frac{\langle c\,a\rangle\,\langle \ell_1\,a\rangle\,\langle \ell_2\,a\rangle\,\langle \ell_2\,d\rangle\,[c\,\ell_2]\,[d\,\ell_1]\,[\ell_2\,b]}{\langle c\,d\rangle\,[a\,b]\,[c\,d]} - \frac{\langle b\,a\rangle\,\langle c\,a\rangle\,\langle \ell_1\,a\rangle\,\langle \ell_2\,c\rangle\,\langle \ell_2\,d\rangle\,[c\,\ell_2]\,[d\,\ell_1]\,[\ell_2\,b]}{\langle b\,c\rangle\,\langle c\,d\rangle\,[a\,b]\,[c\,d]}$$

$$- \frac{\langle b\,c\rangle\,\langle e\,a\rangle\,\langle \ell_1\,d\rangle^3\,\langle \ell_2\,a\rangle^3\,[\ell_2\,d]}{\langle b\,\ell_1\rangle\,\langle c\,d\rangle\,\langle d\,e\rangle\,\langle \ell_1\,\ell_2\rangle^2} - \frac{\langle b\,c\rangle\,\langle c\,d\rangle\,\langle e\,a\rangle\,\langle \ell_1\,a\rangle\,\langle \ell_2\,a\rangle^2\,[c\,\ell_2]^2}{\langle b\,\ell_1\rangle\,\langle d\,e\rangle\,\langle \ell_1\,\ell_2\rangle\,[\ell_2\,\ell_1]}$$

$$+ \frac{\langle a\,b\rangle\,\langle a\,c\rangle\,\langle \ell_1\,a\rangle\,\langle \ell_2\,a\rangle\,[\ell_2\,\ell_1]}{\langle b\,c\rangle} + \frac{\langle a\,b\rangle\,\langle b\,c\rangle\,\langle d\,e\rangle\,\langle e\,a\rangle\,[e\,b]^3\,[b|\ell_2|b\rangle}{[b|\ell_1|b\rangle\,\langle c\,d\rangle\,[a\,b]\,[e\,a]}$$

$$- \frac{\langle b\,c\rangle\,\langle d\,e\rangle\,\langle e\,a\rangle\,\langle \ell_1\,a\rangle\,(3[e|b|a\rangle^2 + 3[e|b|a\rangle[e|\ell_2|a\rangle + [e|\ell_2|a\rangle^2}{\langle b\,\ell_1\rangle\,\langle c\,d\rangle\,\langle \ell_1\,\ell_2\rangle\,[\ell_2\,\ell_1]}$$

$$\left. + \frac{2\,\langle e\,a\rangle\,\langle \ell_1\,a\rangle\,\langle \ell_2\,a\rangle\,[\ell_1\,e]\,[\ell_2\,b]\,[e|\ell_2|e\rangle}{\langle d\,e\rangle\,[a\,b]\,[d\,e]} + \frac{\langle a\,c\rangle\,\langle d\,a\rangle\,\langle e\,a\rangle\,\langle \ell_1\,e\rangle\,\langle \ell_2\,a\rangle\,[c\,e]}{\langle d\,e\rangle\,\langle \ell_1\,\ell_2\rangle} \right) \tag{A.36}$$

$$I\ell_{bc} = \frac{1}{6}\Bigg(\frac{\langle a\,b\rangle\,\langle c\,a\rangle\,\langle a|\ell_2\ell_1|a]}{\langle b\,c\rangle} + \frac{\langle a\,b\rangle^2\,\langle a\,c\rangle^2\,[b\,c]}{\langle b\,c\rangle}$$

$$- \frac{\langle a\,b\rangle\,\langle a\,c\rangle\,\langle a\,d\rangle\,\langle\ell_2\,c\rangle\,[c\,\ell_2]\,[b|c|a\rangle}{s_{bc}\,\langle c\,d\rangle} - \frac{\langle a\,b\rangle\,\langle a\,c\rangle^2\,\langle d\,a\rangle\,[b|\ell_1|b\rangle}{\langle b\,c\rangle\,\langle c\,d\rangle}$$

$$+ \frac{\langle a\,b\rangle\,\langle c\,a\rangle\,\langle\ell_1\,b\rangle\,[e\,\ell_1]\,[b|\ell_2|a\rangle}{\langle c\,b\rangle\,[e\,a]} + \frac{2\,\langle a\,b\rangle^2\,\langle\ell_1\,c\rangle\,[e\,\ell_1]\,[b|\ell_2|a\rangle}{\langle c\,b\rangle\,[e\,a]}$$

$$+ \frac{\langle a\,b\rangle\,\langle a\,c\rangle\,\langle a\,d\rangle\,[b|\ell_1|b\rangle[b|\ell_2|a\rangle}{s_{bc}\,\langle c\,d\rangle} + \frac{\langle a\,b\rangle\,\langle\ell_1\,a\rangle\,[e\,\ell_1]\,[b|\ell_1|b\rangle[b|\ell_2|a\rangle}{s_{bc}\,[e\,a]}$$

$$- \frac{\langle a\,b\rangle\,\langle b\,a\rangle\,[b|\ell_2|a\rangle^2}{s_{bc}} - \frac{\langle a\,b\rangle\,\langle\ell_1\,b\rangle\,[e\,\ell_1]\,[b|\ell_2|a\rangle^2}{s_{bc}\,[e\,a]}$$

$$+ \frac{2\,\langle a\,b\rangle\,\langle a\,c\rangle\,\langle a\,\ell_1\rangle\,[e\,\ell_1]\,[b|\ell_2|b\rangle}{\langle b\,c\rangle\,[e\,a]} - \frac{\langle a\,b\rangle\,\langle a\,c\rangle\,\langle c\,a\rangle\,[c|\ell_1|a\rangle}{\langle b\,c\rangle}$$

$$+ \frac{\langle a\,b\rangle\,\langle a\,c\rangle\,\langle a\,d\rangle\,\langle\ell_2\,c\rangle\,[b\,\ell_2]\,[c|\ell_1|a\rangle}{s_{bc}\,\langle c\,d\rangle} - \frac{\langle a\,b\rangle\,\langle a\,c\rangle\,\langle c\,b\rangle\,[b|c|a\rangle[c|\ell_1|a\rangle}{[c|\ell_1|c\rangle\,\langle b\,c\rangle}$$

$$- \frac{\langle a\,b\rangle\,\langle a\,c\rangle\,[b|\ell_1|a\rangle[c|\ell_1|a\rangle}{s_{bc}} + \frac{\langle a\,b\rangle\,\langle a\,c\rangle\,[b|\ell_2|a\rangle[c|\ell_1|a\rangle}{[c|\ell_1|c\rangle}$$

$$+ \frac{\langle a\,b\rangle\,\langle a\,c\rangle\,\langle a\,d\rangle\,[b|\ell_2|c\rangle[c|\ell_2|a\rangle}{[c|\ell_1|c\rangle\,\langle c\,d\rangle} + \frac{\langle a\,b\rangle\,\langle c\,b\rangle\,[b|\ell_2|a\rangle^2[c|\ell_2|a\rangle}{s_{bc}[b|\ell_2|b\rangle}\Bigg) \qquad (A.37)$$

$$It_{bc} = \frac{1}{6}\Bigg($$

$$-\frac{\langle a\,b\rangle\,\langle a\,d\rangle\,\langle a\,e\rangle\,\langle d\,\ell_2\rangle\,\langle e\,a\rangle\,[d\,e]}{\langle d\,e\rangle\,\langle \ell_2\,b\rangle} - \frac{\langle a\,d\rangle^2\,\langle a\,e\rangle\,\langle c\,b\rangle\,\langle d\,\ell_2\rangle\,\langle e\,a\rangle\,[d\,e]}{\langle c\,d\rangle\,\langle d\,e\rangle\,\langle \ell_2\,b\rangle}$$

$$-\frac{\langle a\,d\rangle^3\,\langle c\,b\rangle\,\langle c\,\ell_2\rangle\,\langle e\,a\rangle\,\langle \ell_1\,e\rangle\,[d\,e]}{\langle c\,d\rangle\,\langle c\,\ell_1\rangle\,\langle d\,e\rangle\,\langle \ell_2\,b\rangle} - \frac{s_{bc}\,\langle a\,b\rangle\,\langle c\,d\rangle\,\langle e\,a\rangle\,[b\,c]\,[e\,b]}{\langle d\,e\rangle\,[a\,b]\,[e\,a]}$$

$$+\frac{\langle a\,b\rangle\,\langle d\,a\rangle\,\langle \ell_1\,a\rangle\,\langle \ell_2\,a\rangle\,[\ell_1\,d]}{\langle \ell_2\,b\rangle} + \frac{2\,\langle a\,b\rangle\,\langle a\,\ell_1\rangle\,\langle e\,a\rangle\,\langle \ell_2\,d\rangle\,[e\,d]\,[\ell_1\,e]}{\langle \ell_2\,b\rangle\,[e\,a]}$$

$$+\frac{\langle a\,b\rangle\,\langle d\,\ell_2\rangle\,\langle e\,a\rangle\,\langle \ell_1\,a\rangle^2\,[\ell_1\,a]\,[\ell_1\,e]}{\langle d\,e\rangle\,\langle \ell_2\,b\rangle\,[a\,e]} + \frac{\langle a\,b\rangle\,\langle a\,c\rangle\,\langle a\,\ell_1\rangle^2\,\langle c\,\ell_2\rangle\,\langle d\,e\rangle\,\langle d\,\ell_2\rangle\,[\ell_1\,\ell_2]}{\langle c\,d\rangle\,\langle c\,\ell_1\rangle\,\langle e\,d\rangle\,\langle \ell_2\,b\rangle}$$

$$-\frac{\langle a\,b\rangle\,\langle d\,\ell_2\rangle\,\langle e\,a\rangle\,\langle \ell_2\,d\rangle\,[e\,d]^2\,[\ell_2\,e]}{\langle \ell_2\,b\rangle\,[e\,a]^2} - \frac{\langle a\,b\rangle\,\langle d\,\ell_2\rangle\,\langle e\,a\rangle\,\langle \ell_1\,a\rangle\,\langle \ell_2\,d\rangle\,[d\,e]\,[\ell_1\,a]\,[\ell_2\,e]}{\langle d\,e\rangle\,\langle \ell_2\,b\rangle\,[e\,a]^2}$$

$$-\frac{\langle a\,b\rangle\,\langle c\,\ell_2\rangle\,\langle d\,\ell_2\rangle\,\langle e\,a\rangle\,\langle \ell_1\,a\rangle\,[\ell_1\,e]\,[\ell_2\,e]}{\langle c\,d\rangle\,\langle \ell_2\,b\rangle\,[e\,a]} - \frac{\langle a\,b\rangle\,\langle c\,\ell_2\rangle\,\langle d\,\ell_2\rangle\,\langle e\,a\rangle\,\langle \ell_2\,d\rangle\,[d\,e]\,[\ell_2\,e]^2}{\langle c\,d\rangle\,\langle \ell_2\,b\rangle\,[e\,a]^2}$$

$$+\frac{\langle a\,b\rangle\,\langle d\,\ell_2\rangle\,\langle e\,a\rangle\,\langle \ell_1\,\ell_2\rangle\,\langle \ell_2\,d\rangle\,[d\,e]\,[\ell_1\,a]\,[\ell_2\,e]^2}{\langle d\,e\rangle\,\langle \ell_2\,b\rangle\,[e\,a]^3} - \frac{\langle a\,b\rangle\,\langle c\,\ell_2\rangle\,\langle d\,\ell_2\rangle\,\langle e\,a\rangle\,\langle \ell_1\,\ell_2\rangle\,[\ell_1\,e]\,[\ell_2\,e]^2}{\langle c\,d\rangle\,\langle \ell_2\,b\rangle\,[e\,a]^2}$$

$$+\frac{\langle a\,b\rangle\,\langle d\,\ell_2\rangle\,\langle e\,a\rangle\,\langle \ell_1\,\ell_2\rangle^2\,[\ell_1\,a]\,[\ell_1\,e]\,[\ell_2\,e]^2}{\langle d\,e\rangle\,\langle \ell_2\,b\rangle\,[e\,a]^3} + \frac{\langle a\,d\rangle\,\langle a\,\ell_2\rangle\,\langle e\,a\rangle\,\langle \ell_1\,a\rangle\,[\ell_2\,\ell_1]}{\langle d\,e\rangle}$$

$$+\frac{\langle a\,b\rangle\,\langle d\,\ell_2\rangle\,\langle e\,a\rangle\,\langle \ell_1\,\ell_2\rangle^2\,[\ell_1\,e]\,[\ell_2\,e]\,[\ell_2\,\ell_1]}{\langle d\,e\rangle\,\langle \ell_2\,b\rangle\,[e\,a]^2} - \frac{s_{bc}\,\langle a\,b\rangle\,\langle a\,d\rangle\,\langle e\,a\rangle\,[e\,b]\,[c|\ell_2|c\rangle}{[c|\ell_1|c\rangle\,\langle d\,e\rangle\,[e\,a]}$$

$$-\frac{\langle a\,b\rangle\,\langle b\,c\rangle\,\langle e\,a\rangle\,[b\,e]\,[c\,b]\,[e\,b]\,[c|\ell_2|c\rangle}{[c|\ell_1|c\rangle\,[a\,b]\,[e\,a]} - \frac{s_{bc}\,\langle a\,b\rangle\,\langle a\,d\rangle\,\langle e\,a\rangle\,[b\,c]\,[e|\ell_2|c\rangle}{[c|\ell_1|c\rangle\,\langle d\,e\rangle\,[e\,a]}$$

$$-\frac{\langle a\,c\rangle\,\langle a\,d\rangle^2\,\langle e\,a\rangle\,[c|\ell_1|e\rangle[e|\ell_2|c\rangle}{[c|\ell_1|c\rangle\,\langle c\,d\rangle\,\langle d\,e\rangle} - \frac{\langle a\,b\rangle\,\langle d\,a\rangle\,\langle e\,a\rangle\,[b\,c]\,[e|\ell_2|c\rangle^2}{[c|\ell_1|c\rangle\,\langle c\,d\rangle\,[e\,a]}\Bigg) \qquad (A.38)$$

$$I\ell_{cd} = \frac{1}{6}\Bigg($$

$$-\frac{\langle a\,c\rangle\,\langle a\,d\rangle\,\langle a|\ell_2\ell_1|a\rangle}{\langle c\,d\rangle} + \frac{\langle a\,d\rangle^2\,\langle a\,e\rangle\,\langle\ell_1\,a\rangle\,\langle\ell_1\,c\rangle\,[c\,\ell_1]\,[d\,\ell_1]}{s_{cd}\,\langle d\,e\rangle}$$

$$-\frac{\langle a\,b\rangle\,\langle b\,c\rangle\,\langle d\,e\rangle\,\langle e\,a\rangle\,[b\,e]^3}{\langle c\,d\rangle\,[a\,b]\,[e\,a]} + \frac{\langle a\,b\rangle\,\langle e\,c\rangle\,\langle\ell_1\,c\rangle\,\langle\ell_1\,d\rangle\,\langle\ell_2\,a\rangle\,[c\,\ell_1]\,[d\,\ell_2]\,[e\,b]\,[e\,\ell_1]}{s_{cd}\,\langle c\,b\rangle\,[a\,b]\,[e\,a]}$$

$$+\frac{\langle a\,b\rangle\,\langle e\,c\rangle\,\langle\ell_1\,c\rangle\,\langle\ell_2\,a\rangle\,\langle\ell_2\,d\rangle\,[c\,\ell_2]\,[d\,\ell_1]\,[e\,b]\,[e\,\ell_2]}{s_{cd}\,\langle c\,b\rangle\,[a\,b]\,[e\,a]} + \frac{\langle a\,d\rangle\,\langle\ell_1\,a\rangle^2\,\langle\ell_1\,c\rangle\,[c\,\ell_1]\,[d\,\ell_1]\,[\ell_1\,b]}{s_{cd}\,[a\,b]}$$

$$-\frac{\langle a\,e\rangle\,\langle\ell_1\,a\rangle\,\langle\ell_1\,c\rangle\,\langle\ell_2\,d\rangle\,[c\,\ell_2]\,[d\,\ell_2]\,[e\,c]\,[\ell_1\,b]}{\langle d\,e\rangle\,[a\,b]\,[c\,d]\,[e\,a]} - \frac{\langle a\,c\rangle\,\langle a\,d\rangle\,\langle\ell_1\,a\rangle\,\langle\ell_2\,a\rangle\,[\ell_1\,\ell_2]}{\langle c\,d\rangle}$$

$$+\frac{\langle a\,d\rangle\,\langle c\,a\rangle\,\langle\ell_1\,a\rangle\,\langle\ell_1\,c\rangle\,[c\,\ell_1]\,[\ell_2\,b]}{\langle c\,d\rangle\,[a\,b]} + \frac{\langle a\,d\rangle\,\langle\ell_1\,a\rangle^2\,\langle\ell_1\,c\rangle\,[c\,\ell_1]\,[d\,\ell_1]\,[\ell_2\,b]}{s_{cd}\,[a\,b]}$$

$$+\frac{\langle a\,e\rangle\,\langle\ell_1\,a\rangle\,\langle\ell_1\,c\rangle\,\langle\ell_2\,d\rangle\,[c\,\ell_1]\,[d\,\ell_2]\,[e\,c]\,[\ell_2\,b]}{\langle d\,e\rangle\,[a\,b]\,[c\,d]\,[e\,a]} - \frac{\langle a\,e\rangle^2\,\langle\ell_1\,a\rangle\,\langle\ell_2\,d\rangle\,[c\,\ell_1]\,[e\,b]\,[\ell_2\,d]}{\langle d\,e\rangle\,[a\,b]\,[c\,d]}$$

$$+\frac{\langle a\,d\rangle^2\,\langle a\,e\rangle\,\langle\ell_1\,c\rangle\,[d\,\ell_2]\,[c|\ell_1|a\rangle}{s_{cd}\,\langle d\,e\rangle} - \frac{\langle a\,b\rangle\,\langle\ell_1\,a\rangle\,\langle\ell_2\,a\rangle\,[d\,\ell_2]\,[e\,\ell_1]\,[c|\ell_1|c\rangle}{\langle c\,b\rangle\,[d\,c]\,[e\,a]}$$

$$-\frac{3\,\langle c\,a\rangle^2\,\langle d\,a\rangle\,[d\,c]\,[c|\ell_2|a\rangle}{[c|\ell_2|c\rangle} - \frac{3\,\langle c\,a\rangle\,\langle d\,a\rangle^2\,[c\,d]\,[d|\ell_1|a\rangle}{[c|\ell_1|c\rangle} - \frac{\langle a\,c\rangle\,\langle a\,d\rangle\,[c|\ell_2|a\rangle[d|\ell_2|a\rangle}{s_{cd}}$$

$$-\frac{\langle a\,c\rangle\,\langle a\,d\rangle\,[c|\ell_1|a\rangle[d|\ell_1|a\rangle}{s_{cd}} - \frac{\langle a\,d\rangle\,\langle a\,e\rangle\,\langle d\,c\rangle\,[c|\ell_1|a\rangle[d|\ell_1|a\rangle}{s_{cd}\,\langle d\,e\rangle}$$

$$+\frac{\langle a\,d\rangle\,\langle\ell_1\,c\rangle\,[e\,\ell_2]\,[c|\ell_1|a\rangle[d|\ell_1|a\rangle}{s_{cd}\,[e\,a]} + \frac{\langle a\,d\rangle\,\langle a\,e\rangle\,\langle\ell_1\,c\rangle\,[e\,\ell_2]\,[c|\ell_1|a\rangle[d|\ell_1|d\rangle}{s_{cd}\,\langle d\,e\rangle\,[e\,a]}$$

$$+\frac{\langle a\,b\rangle\,\langle a\,c\rangle^2\,\langle\ell_1\,d\rangle\,[c\,\ell_1]\,[d|\ell_2|a\rangle}{s_{cd}\,\langle c\,b\rangle} - \frac{\langle a\,b\rangle\,\langle a\,c\rangle\,\langle\ell_1\,d\rangle\,[\ell_1\,b]\,s_{cd}[d|\ell_2|a\rangle}{s_{cd}\,\langle c\,b\rangle\,[a\,b]}$$

$$-\frac{\langle a\,b\rangle\,\langle\ell_2\,a\rangle\,[e\,\ell_2]\,[c|\ell_1|c\rangle[d|\ell_2|a\rangle)}{\langle c\,b\rangle\,[d\,c]\,[e\,a]} - \frac{\langle a\,b\rangle\,\langle a\,c\rangle\,\langle\ell_1\,d\rangle\,[\ell_1\,b]\,[c|\ell_1|c\rangle[d|\ell_2|a\rangle}{s_{cd}\,\langle c\,b\rangle\,[a\,b]}$$

$$-\frac{\langle a\,b\rangle\,\langle a\,c\rangle\,\langle c\,d\rangle\,[c|\ell_2|a\rangle[d|\ell_2|a\rangle}{s_{cd}\,\langle c\,b\rangle} + \frac{\langle a\,c\rangle\,\langle\ell_1\,d\rangle\,[\ell_1\,b]\,[c|\ell_2|a\rangle[d|\ell_2|a\rangle}{s_{cd}\,[a\,b]}\Bigg) \tag{A.39}$$

$$It_{cd} = \frac{1}{6}\Bigg($$

$$-\frac{\langle a\,b\rangle\,\langle a\,c\rangle\,\langle a\,\ell_2\rangle^2\,\langle d\,b\rangle\,\langle e\,a\rangle\,\langle\ell_1\,c\rangle\,[b\,\ell_2]}{\langle a\,e\rangle\,\langle c\,b\rangle\,\langle d\,\ell_1\rangle\,\langle\ell_1\,c\rangle} - \frac{\langle a\,b\rangle\,\langle b\,c\rangle\,\langle d\,e\rangle\,\langle e\,a\rangle\,\langle\ell_1\,\ell_2\rangle\,[b\,e]^3}{\langle d\,\ell_1\rangle\,\langle\ell_1\,c\rangle\,[a\,b]\,[e\,a]}$$

$$+\frac{\langle a\,d\rangle\,\langle a\,\ell_1\rangle^2\,\langle c\,e\rangle\,\langle d\,\ell_2\rangle\,\langle e\,a\rangle\,[e\,\ell_1]}{\langle d\,e\rangle\,\langle d\,\ell_1\rangle\,\langle\ell_1\,c\rangle} + \frac{\langle a\,c\rangle\,\langle e\,a\rangle\,\langle\ell_1\,a\rangle\,\langle\ell_2\,a\rangle\,[\ell_1\,e]}{\langle\ell_1\,c\rangle}$$

$$-\frac{\langle a\,b\rangle\,\langle a\,c\rangle\,\langle a\,\ell_2\rangle^2\,\langle\ell_1\,c\rangle\,[\ell_1\,\ell_2]}{\langle c\,b\rangle\,\langle\ell_1\,c\rangle} + \frac{\langle a\,d\rangle\,\langle b\,a\rangle\,\langle\ell_1\,a\rangle\,\langle\ell_2\,a\rangle\,[\ell_2\,b]}{\langle\ell_1\,d\rangle}$$

$$-\frac{\langle a\,d\rangle\,\langle a\,e\rangle\,\langle a\,\ell_1\rangle^2\,\langle\ell_2\,d\rangle\,[\ell_2\,\ell_1]}{\langle d\,e\rangle\,\langle\ell_1\,d\rangle}\Bigg) \tag{A.40}$$

173

$$
I\ell_{de} = \frac{1}{6}\Bigg(
$$

$$
-\frac{\langle a\,c\rangle\,\langle a\,d\rangle^2\,\langle a\,e\rangle\,\langle \ell_1\,d\rangle\,[d\,\ell_1]}{\langle d\,c\rangle\,\langle e\,d\rangle}
+\frac{\langle a\,d\rangle\,\langle a\,e\rangle^2\,\langle d\,a\rangle\,[e\,d]}{\langle d\,e\rangle}
$$

$$
+\frac{\langle a\,c\rangle\,\langle a\,d\rangle\,\langle a\,e\rangle\,\langle \ell_1\,d\rangle\,[e\,\ell_1]\,[d|\ell_2|a\rangle)}{s_{de}\,\langle d\,c\rangle}
+\frac{2\,\langle a\,e\rangle\,\langle \ell_2\,a\rangle\,[\ell_2\,b]\,[e|d|a\rangle}{[a\,b]}
$$

$$
+\frac{2\,\langle a\,e\rangle\,\langle \ell_2\,a\rangle\,[\ell_2\,b]\,[e|\ell_1|a\rangle}{[a\,b]}
+\frac{\langle a\,d\rangle\,\langle a\,e\rangle\,[d|\ell_2|a\rangle[e|\ell_1|a\rangle}{[d|l2|d\rangle}
$$

$$
-\frac{\langle a\,e\rangle\,\langle e\,a\rangle\,[e|\ell_1|a\rangle^2}{s_{de}}
+\frac{\langle a\,e\rangle\,\langle d\,e\rangle\,[d|\ell_1|a\rangle[e|\ell_1|a\rangle^2}{s_{de}[e|\ell_1|e\rangle}
$$

$$
+\frac{\langle a\,c\rangle\,\langle a\,d\rangle\,\langle a\,e\rangle\,[d|\ell_2|a\rangle[e|\ell_1|d\rangle}{[d|l2|d\rangle\,\langle d\,c\rangle}
-\frac{\langle a\,d\rangle\,\langle a\,e\rangle\,[d|e|a\rangle[d|\ell_2|a\rangle[e|\ell_1|d\rangle}{s_{de}[d|l2|d\rangle}
$$

$$
-\frac{\langle a\,c\rangle\,\langle a\,d\rangle\,\langle a\,e\rangle\,\langle \ell_2\,e\rangle\,[e\,\ell_2]\,[e|\ell_2|a\rangle}{s_{de}\,\langle d\,c\rangle}
-\frac{2\,\langle a\,e\rangle\,\langle \ell_2\,a\rangle\,\langle \ell_2\,e\rangle\,[e\,\ell_2]\,[\ell_2\,b]\,[e|\ell_2|a\rangle}{s_{de}\,[a\,b]}
$$

$$
+\frac{\langle a\,d\rangle\,\langle a\,e\rangle\,[d|\ell_1|d\rangle[d|\ell_2|a\rangle[e|\ell_2|a\rangle}{s_{de}[d|l2|d\rangle}
-\frac{\langle a\,e\rangle\,\langle d\,a\rangle\,\langle \ell_2\,a\rangle\,[\ell_2|\ell_1|a\rangle}{\langle d\,e\rangle}\Bigg)
\tag{A.41}
$$

174

$$It_{de} = \frac{1}{6}\Bigg($$

$$-\frac{\langle a\,b\rangle\,\langle a\,c\rangle\,\langle a\,e\rangle\,\langle b\,a\rangle\,\langle c\,\ell_1\rangle\,[c\,b]}{\langle c\,b\rangle\,\langle \ell_1\,e\rangle} - \frac{\langle a\,b\rangle\,\langle a\,c\rangle^2\,\langle b\,a\rangle\,\langle c\,\ell_1\rangle\,\langle d\,e\rangle\,[c\,b]}{\langle c\,b\rangle\,\langle d\,c\rangle\,\langle \ell_1\,e\rangle}$$

$$-\frac{\langle a\,c\rangle^3\,\langle b\,a\rangle\,\langle d\,e\rangle\,\langle d\,\ell_1\rangle\,\langle \ell_2\,b\rangle\,[c\,b]}{\langle c\,b\rangle\,\langle d\,c\rangle\,\langle d\,\ell_2\rangle\,\langle \ell_1\,e\rangle} - \frac{\langle a\,e\rangle\,\langle b\,a\rangle\,\langle c\,a\rangle\,\langle d\,\ell_2\rangle\,[e\,d]\,[e\,\ell_2]}{\langle c\,b\rangle\,[e\,a]}$$

$$+\frac{\langle a\,c\rangle^2\,\langle a\,d\rangle\,\langle b\,a\rangle\,\langle d\,\ell_1\rangle\,\langle \ell_2\,b\rangle\,[\ell_1\,b]}{\langle c\,b\rangle\,\langle d\,c\rangle\,\langle d\,\ell_2\rangle} - \frac{\langle a\,e\rangle\,\langle b\,a\rangle\,\langle c\,\ell_1\rangle\,\langle \ell_1\,c\rangle\,[b\,c]^2\,[\ell_1\,b]}{\langle \ell_1\,e\rangle\,[b\,a]^2}$$

$$-\frac{s_{de}\,\langle a\,e\rangle\,\langle b\,a\rangle\,\langle c\,\ell_1\rangle\,\langle d\,\ell_1\rangle\,[e\,b]\,[\ell_1\,b]}{\langle d\,c\rangle\,\langle \ell_1\,e\rangle\,[b\,a]\,[e\,a]} - \frac{\langle a\,e\rangle\,\langle b\,a\rangle\,\langle c\,\ell_1\rangle\,\langle d\,\ell_1\rangle\,\langle \ell_1\,c\rangle\,[c\,b]\,[\ell_1\,b]^2}{\langle d\,c\rangle\,\langle \ell_1\,e\rangle\,[b\,a]^2}$$

$$+\frac{s_{de}\,\langle a\,e\rangle\,\langle b\,a\rangle\,\langle c\,b\rangle\,\langle d\,\ell_1\rangle^2\,[e\,b]\,[\ell_1\,b]^2}{[e|\ell_1|e\rangle\,\langle d\,c\rangle\,\langle d\,e\rangle\,[b\,a]\,[e\,a]} + \frac{\langle a\,c\rangle^2\,\langle a\,d\rangle\,\langle a\,\ell_1\rangle\,[\ell_1\,c]}{\langle d\,c\rangle}$$

$$-\frac{\langle a\,d\rangle\,\langle a\,\ell_1\rangle\,\langle c\,a\rangle^2\,[\ell_1\,c]}{\langle d\,c\rangle} + \frac{\langle a\,c\rangle\,\langle a\,\ell_1\rangle\,\langle b\,a\rangle\,\langle \ell_2\,a\rangle\,[\ell_1\,\ell_2]}{\langle c\,b\rangle}$$

$$+\frac{s_{de}\,\langle a\,e\rangle\,\langle b\,a\rangle\,\langle c\,\ell_1\rangle\,\langle \ell_2\,\ell_1\rangle\,[e\,b]\,[\ell_1\,\ell_2]}{\langle c\,b\rangle\,\langle \ell_1\,e\rangle\,[b\,a]\,[e\,a]} - \frac{\langle a\,e\rangle\,\langle b\,a\rangle\,\langle c\,\ell_1\rangle\,\langle \ell_1\,c\rangle\,\langle \ell_2\,a\rangle\,[c\,b]\,[\ell_1\,b]\,[\ell_2\,a]}{\langle c\,b\rangle\,\langle \ell_1\,e\rangle\,[a\,b]^2}$$

$$+\frac{\langle a\,e\rangle\,\langle b\,a\rangle\,\langle c\,\ell_1\rangle\,\langle \ell_1\,c\rangle\,\langle \ell_2\,\ell_1\rangle\,[c\,b]\,[\ell_1\,b]^2\,[\ell_2\,a]}{\langle c\,b\rangle\,\langle \ell_1\,e\rangle\,[b\,a]^3} + \frac{2\,\langle a\,e\rangle\,\langle a\,\ell_2\rangle\,\langle b\,a\rangle\,\langle \ell_1\,c\rangle\,[b\,c]\,[\ell_2\,b]}{\langle \ell_1\,e\rangle\,[b\,a]}$$

$$+\frac{s_{de}\,\langle a\,e\rangle\,\langle b\,a\rangle\,\langle c\,\ell_1\rangle\,\langle \ell_2\,\ell_1\rangle\,[\ell_1\,b]\,[\ell_2\,b]}{\langle c\,b\rangle\,\langle \ell_1\,e\rangle\,[b\,a]^2} - \frac{\langle a\,e\rangle\,\langle b\,a\rangle\,\langle c\,\ell_1\rangle\,\langle d\,\ell_1\rangle\,\langle \ell_2\,a\rangle\,[\ell_1\,b]\,[\ell_2\,b]}{\langle d\,c\rangle\,\langle \ell_1\,e\rangle\,[b\,a]}$$

$$-\frac{\langle a\,e\rangle\,\langle b\,a\rangle\,\langle c\,\ell_1\rangle\,\langle d\,\ell_1\rangle\,\langle \ell_2\,\ell_1\rangle\,[\ell_1\,b]^2\,[\ell_2\,b]}{\langle d\,c\rangle\,\langle \ell_1\,e\rangle\,[b\,a]^2} + \frac{\langle a\,e\rangle\,\langle b\,a\rangle\,\langle c\,\ell_1\rangle\,\langle \ell_2\,a\rangle^2\,[\ell_2\,a]\,[\ell_2\,b]}{\langle c\,b\rangle\,\langle \ell_1\,e\rangle\,[a\,b]}$$

$$+\frac{\langle a\,e\rangle\,\langle b\,a\rangle\,\langle c\,\ell_1\rangle\,\langle \ell_2\,\ell_1\rangle^2\,[\ell_1\,b]^2\,[\ell_2\,a]\,[\ell_2\,b]}{\langle c\,b\rangle\,\langle \ell_1\,e\rangle\,[b\,a]^3} + \frac{\langle a\,e\rangle\,\langle c\,a\rangle\,\langle \ell_1\,a\rangle\,\langle \ell_2\,a\rangle\,[\ell_1\,c]}{\langle \ell_1\,e\rangle}$$

$$+\frac{\langle a\,d\rangle\,\langle a\,e\rangle\,\langle a\,\ell_2\rangle^2\,\langle c\,b\rangle\,\langle c\,\ell_1\rangle\,\langle d\,\ell_1\rangle\,[\ell_2\,\ell_1]}{\langle b\,c\rangle\,\langle d\,c\rangle\,\langle d\,\ell_2\rangle\,\langle \ell_1\,e\rangle} - \frac{s_{de}\,\langle a\,c\rangle\,\langle a\,e\rangle\,\langle b\,a\rangle\,\langle d\,\ell_1\rangle\,[\ell_1\,b]\,[e|\ell_2|d\rangle}{[e|\ell_1|e\rangle\,\langle d\,c\rangle\,\langle d\,e\rangle\,[e\,a]}$$

$$+\frac{s_{de}\,\langle a\,e\rangle\,\langle b\,a\rangle\,\langle c\,a\rangle\,\langle d\,\ell_1\rangle\,[\ell_1\,d]\,[e|\ell_2|d\rangle}{[e|\ell_1|e\rangle\,\langle c\,b\rangle\,\langle d\,e\rangle\,[e\,a]}\Bigg) \tag{A.42}$$

$$I\ell_{ea} = -\frac{\langle a\,e\rangle^2\,\langle e\,a\rangle\,\langle \ell_1\,d\rangle\,[e\,\ell_1]\,[e|\ell_2|a\rangle}{6\,\langle e\,d\rangle\,\langle e\,\ell_2\rangle\,[\ell_2\,e]} \tag{A.43}$$

$$It_{ea} = \frac{1}{6}\Bigg($$

$$\frac{\langle a\,b\rangle^2 \langle c\,\ell_2\rangle \langle e\,d\rangle \langle \ell_1\,a\rangle^2 \langle \ell_1\,c\rangle^2 [b\,c]}{\langle c\,b\rangle \langle d\,c\rangle \langle e\,\ell_2\rangle \langle \ell_2\,\ell_1\rangle^2} - \frac{\langle a\,e\rangle \langle a\,\ell_2\rangle \langle b\,a\rangle \langle \ell_1\,a\rangle [b\,\ell_1]}{\langle e\,\ell_2\rangle}$$

$$+ \frac{\langle b\,a\rangle \langle e\,c\rangle \langle \ell_1\,a\rangle^2 \langle \ell_2\,a\rangle \langle \ell_2\,b\rangle [b\,\ell_1]}{\langle c\,b\rangle \langle e\,\ell_2\rangle \langle \ell_2\,\ell_1\rangle} + \frac{\langle a\,b\rangle \langle a\,c\rangle \langle b\,a\rangle \langle \ell_2\,a\rangle [b\,\ell_2]}{\langle c\,b\rangle}$$

$$+ \frac{\langle a\,c\rangle \langle b\,a\rangle \langle d\,a\rangle \langle \ell_1\,c\rangle \langle \ell_2\,a\rangle [c\,b]}{\langle d\,c\rangle \langle \ell_1\,\ell_2\rangle} + \frac{\langle b\,a\rangle \langle d\,a\rangle \langle \ell_1\,c\rangle^2 \langle \ell_2\,a\rangle^2 [c\,b]}{\langle d\,c\rangle \langle \ell_1\,\ell_2\rangle \langle \ell_2\,\ell_1\rangle}$$

$$+ \frac{\langle b\,a\rangle \langle d\,b\rangle \langle e\,a\rangle \langle \ell_1\,c\rangle^3 \langle \ell_2\,a\rangle^3 [c\,b]}{\langle c\,b\rangle \langle d\,c\rangle \langle e\,\ell_2\rangle \langle \ell_1\,a\rangle \langle \ell_1\,\ell_2\rangle \langle \ell_2\,\ell_1\rangle} - \frac{\langle a\,c\rangle \langle b\,a\rangle \langle d\,a\rangle \langle \ell_1\,c\rangle \langle \ell_2\,a\rangle [c\,d]}{\langle c\,b\rangle \langle \ell_1\,\ell_2\rangle}$$

$$+ \frac{\langle a\,c\rangle^2 \langle b\,a\rangle \langle d\,a\rangle \langle \ell_1\,c\rangle \langle \ell_2\,a\rangle [c\,\ell_2]}{\langle c\,b\rangle \langle d\,c\rangle \langle \ell_1\,a\rangle} - \frac{\langle b\,a\rangle \langle d\,a\rangle \langle e\,d\rangle \langle \ell_1\,a\rangle^2 \langle \ell_1\,c\rangle^3 [d\,c]}{\langle c\,b\rangle \langle d\,c\rangle \langle e\,\ell_2\rangle \langle \ell_2\,\ell_1\rangle^2}$$

$$- \frac{2\,\langle a\,c\rangle \langle b\,a\rangle \langle d\,a\rangle \langle \ell_2\,a\rangle [d\,\ell_2]}{\langle c\,b\rangle} - \frac{\langle a\,d\rangle \langle e\,a\rangle \langle \ell_1\,d\rangle \langle \ell_2\,a\rangle^2 [d\,\ell_2]}{\langle e\,d\rangle \langle \ell_2\,\ell_1\rangle}$$

$$- \frac{\langle a\,d\rangle \langle c\,e\rangle \langle e\,a\rangle \langle \ell_1\,d\rangle^2 \langle \ell_2\,a\rangle^3 [d\,\ell_2]}{\langle d\,c\rangle \langle d\,e\rangle \langle e\,\ell_2\rangle \langle \ell_1\,a\rangle \langle \ell_2\,\ell_1\rangle} + \frac{\langle b\,a\rangle \langle d\,a\rangle \langle \ell_1\,c\rangle^2 \langle \ell_2\,a\rangle [c\,d] [e\,\ell_1]}{\langle c\,b\rangle \langle \ell_1\,\ell_2\rangle [e\,a]}$$

$$+ \frac{\langle b\,a\rangle \langle d\,c\rangle \langle e\,d\rangle \langle \ell_1\,a\rangle^2 \langle \ell_2\,a\rangle [d\,\ell_1]^2}{\langle c\,b\rangle \langle e\,a\rangle \langle \ell_2\,\ell_1\rangle [\ell_1\,a]} - \frac{2\,\langle d\,a\rangle \langle \ell_1\,c\rangle \langle \ell_2\,a\rangle^2 [d\,\ell_2] [e\,\ell_2] [\ell_1\,c]}{\langle d\,c\rangle [d\,c] [e\,a]}$$

$$- \frac{\langle d\,a\rangle^2 \langle \ell_1\,c\rangle \langle \ell_2\,a\rangle \langle \ell_2\,e\rangle [d\,\ell_2] [e\,\ell_2] [\ell_1\,c]}{\langle d\,c\rangle \langle e\,d\rangle [d\,c] [e\,a]} + \frac{\langle a\,\ell_1\rangle \langle b\,a\rangle \langle \ell_1\,b\rangle \langle \ell_2\,a\rangle [b\,\ell_2] [\ell_1\,b] [\ell_1\,e]}{\langle c\,b\rangle [c\,b] [e\,a]}$$

$$+ \frac{\langle a\,d\rangle \langle a\,e\rangle \langle \ell_1\,a\rangle \langle \ell_2\,a\rangle [\ell_1\,\ell_2]}{\langle e\,d\rangle} + \frac{\langle d\,a\rangle^2 \langle e\,a\rangle \langle \ell_1\,c\rangle \langle \ell_2\,a\rangle [\ell_1\,\ell_2]}{\langle d\,c\rangle \langle e\,d\rangle}$$

$$- \frac{s_{de}\,\langle b\,a\rangle \langle d\,c\rangle \langle \ell_1\,a\rangle \langle \ell_2\,a\rangle [d\,\ell_1] [\ell_1\,\ell_2]}{\langle c\,b\rangle \langle e\,a\rangle [a\,e] [\ell_1\,a]} + \frac{\langle b\,a\rangle \langle c\,a\rangle \langle \ell_1\,b\rangle \langle \ell_2\,a\rangle [\ell_1\,e] [\ell_2\,b]}{\langle c\,b\rangle [e\,a]}$$

$$+ \frac{\langle a\,d\rangle \langle b\,a\rangle \langle \ell_1\,b\rangle \langle \ell_2\,a\rangle [b\,d] [\ell_1\,e] [\ell_2\,b]}{\langle c\,b\rangle [c\,b] [e\,a]} - \frac{\langle a\,\ell_2\rangle \langle b\,a\rangle \langle \ell_1\,b\rangle \langle \ell_2\,a\rangle [b\,\ell_2] [\ell_1\,e] [\ell_2\,b]}{\langle c\,b\rangle [c\,b] [e\,a]}$$

$$- \frac{\langle d\,a\rangle^2 \langle \ell_1\,c\rangle \langle \ell_2\,a\rangle^2 [\ell_2\,d]}{\langle d\,c\rangle \langle \ell_2\,\ell_1\rangle} + \frac{\langle b\,a\rangle \langle c\,a\rangle \langle \ell_1\,b\rangle \langle \ell_2\,a\rangle [b\,\ell_1] [\ell_2\,e]}{\langle c\,b\rangle [e\,a]}$$

$$- \frac{\langle b\,a\rangle \langle c\,\ell_1\rangle \langle d\,a\rangle \langle \ell_2\,a\rangle [\ell_1\,d] [\ell_2\,e]}{\langle c\,b\rangle [e\,a]}$$

$$- \frac{\langle b\,a\rangle \langle c\,b\rangle \langle e\,d\rangle \langle \ell_2\,a\rangle \left(3[b|e|a\rangle^2 + 3[b|e|a\rangle[b|\ell_1|a\rangle + [b|\ell_1|a\rangle^2\right)}{\langle d\,c\rangle \langle e\,\ell_2\rangle \langle \ell_2\,\ell_1\rangle [\ell_1\,\ell_2]}$$

$$+ \frac{\langle a\,b\rangle \langle a\,c\rangle \langle e\,c\rangle \langle \ell_2\,d\rangle [b\,e] [e\,\ell_2] [c|\ell_2|c\rangle}{\langle c\,b\rangle \langle d\,c\rangle [a\,b] [a\,e]} - \frac{\langle b\,a\rangle \langle c\,b\rangle \langle e\,a\rangle \langle e\,d\rangle [b\,e]^3 [e|\ell_1|e\rangle}{[e|\ell_2|e\rangle \langle d\,c\rangle [a\,b] [e\,a]} \Bigg) \tag{A.44}$$

Appendix B

F_2 Expansion via Nested Sums

We consider the expansion of $F_2(1+\delta_1; 1, 1; 2+\delta_2, 2+\delta_3; x, y)$ using a nested sums approach, mainly to demonstrate how much more efficient the integral method is. Writing it as

$$
F_2(1+\delta_1; 1, 1; 2+\delta_2, 2+\delta_3; x, y)
$$

$$
= 1 + \frac{\Gamma(2+\delta_2)}{\Gamma(1+\delta_1)} \sum_{i=1}^{\infty} x^i \frac{\Gamma(i+1+\delta_1)}{\Gamma(i+2+\delta_2)} + \frac{\Gamma(2+\delta_3)}{\Gamma(1+\delta_1)} \sum_{i=1}^{\infty} y^i \frac{\Gamma(i+1+\delta_1)}{\Gamma(i+2+\delta_3)}
$$

$$
- \frac{\Gamma(2+\delta_2)\Gamma(2+\delta_3)}{\Gamma(1+\delta_1)} \sum_{n=1}^{\infty} \frac{\Gamma(n+1+\delta_1)}{\Gamma(n+1)}
$$

$$
\times (-1) \sum_{i=1}^{n-1} \binom{n}{i} (-1)^i (-x)^i \frac{\Gamma(i+1)}{\Gamma(i+2+\delta_2)} y^{n-i} \frac{\Gamma(n-i+1)}{\Gamma(n-i+2+\delta_3)}. \tag{B.1}
$$

we start by defining

$$
Z_\mu[n] = S_\mu[n] = \sum_{i=1}^{n} \frac{1}{i^\mu},
$$

$$
Z_{\mu\nu}[n] = \sum_{1 \le i < j \le n} \frac{1}{i^\mu j^\nu},
$$

$$
S_{\mu\nu}[n] = \sum_{1 \le i \le j \le n} \frac{1}{i^\mu j^\nu} = Z_{\mu\nu}[n] + Z_{\mu+\nu}[n]. \tag{B.2}
$$

We also define $Z[n] = 1$ for $n \ge 0$, $Z[n] = 0$ for $n < 0$ and $S[n] = 1$ for $n > 0$, $S[n] = 0$ for $n \le 0$. The gamma functions expand to

$$
\binom{n}{i} (-1)^i (-x)^i y^{n-i} \frac{\Gamma(i+1)\Gamma(n-i+1)\Gamma(2+\delta_2)\Gamma(2+\delta_3)\Gamma(n+1+\delta_1)}{\Gamma(i+2+\delta_2)\Gamma(n-i+2+\delta_3)\Gamma(n+1)\Gamma(1+\delta_1)}
$$

$$
= \binom{n}{i} \frac{(-1)^i(-x)^i y^{n-i}}{(i+1)(n-i+1)} \times \Big(1 + \delta_2(1 - Z_1[i+1]) + \delta_3(1 - Z_1[n-i+1]) + \delta_1 Z_1[n]
$$

$$
+ \delta_1 Z_1[n](\delta_2(1 - Z_1[i+1]) + \delta_3(1 - Z_1[n-i+1])) + \delta_2\delta_3(1 + Z_1[i+1]Z_1[n-i+1])
$$

$$
- (\delta_2 + \delta_3)(\delta_2 Z_1[i+1] + \delta_3 Z_1[n-i+1]) + \delta_1^2 Z_{11}[n] + \delta_2^2 S_{11}[i+1] + \delta_3^2 S_{11}[n-i+1] \Big)
$$

$$
\to \binom{n}{i} \frac{(-1)^i(-x)^i y^{n-i}}{(i+1)(n+2)} \times \big(\dots \big) + \{x \leftrightarrow y, \delta_2 \leftrightarrow \delta_3\} \tag{B.3}
$$

where the last line has made use of the partial fractioning as before. We can reduce the denominator $(i+1) \to i$ via

$$\sum_{i=1}^{n-1} \binom{n}{i} (-1)^i \frac{x^i}{(i+c)^m} S[i,\ldots] = \left(-\frac{1}{x}\right) \frac{1}{n+1} \sum_{i=1}^{n+1-1} \binom{n+1}{i} (-1)^i \frac{x^i}{i+c-1} iS[i-1,\ldots].$$

(B.4)

B.1 Leading

For this case we have (B.4) with $S[i]$ of zero depth. Therefore the $i = 1$ term in the RHS vanishes.

$$\sum_{n=1}^{\infty} \sum_{i=1}^{n-1} \binom{n}{i} \frac{y^n (-1)^i (-\frac{x}{y})^i}{(i+1)(n+2)} = \left(\frac{y}{x}\right) \sum_{n=1}^{\infty} \sum_{i=2}^{n} \binom{n+1}{i} \frac{y^n (-1)^i (-\frac{x}{y})^i}{(n+2)(n+1)}$$

$$= \sum_{n=1}^{\infty} \frac{1}{(n+1)(n+2)} \left(\frac{y}{x}(y+x)^n - \frac{y^{n+1}}{x} + (y+x)^n - x^n - (1+n)y^n\right).$$ (B.5)

We are therefore left with sums of the form

$$\sum_{n=1}^{\infty} \frac{1}{(n+2)} X^n = -\left(\frac{1}{2} + \frac{1}{X} + \frac{\text{Log}(1-X)}{X^2}\right)$$

and

$$\sum_{n=1}^{\infty} \frac{1}{(n+1)(n+2)} X^n = \frac{(1-X)\text{Log}(1-X) + X}{X^2} - \frac{1}{2}$$ (B.6)

The leading part of the binomial piece is therefore

$$\frac{(1-y-x)\text{Log}(1-y-x)}{x(x+y)} - \frac{y(1-x)\text{Log}(1-x) + x(1-y)\text{Log}(1-y) + xy}{x^2 y}$$

$$+ \frac{1}{2} + \frac{1}{y} + \frac{\text{Log}(1-y)}{y^2} + x \leftrightarrow y$$ (B.7)

The leading result for the first 3 terms in F_2 give in total

$$1 + \sum_{i=1}^{\infty} \left(\frac{\Gamma(2+\delta_2)}{\Gamma(1+\delta_1)} x^i \frac{\Gamma(i+1+\delta_1)}{\Gamma(i+2+\delta_2)} + \frac{\Gamma(2+\delta_3)}{\Gamma(1+\delta_1)} y^i \frac{\Gamma(i+1+\delta_1)}{\Gamma(i+2+\delta_3)}\right)$$

$$= -1 - \frac{\text{Log}(1-x)}{x} - \frac{\text{Log}(1-y)}{y} + \mathcal{O}(\epsilon)$$ (B.8)

Putting both results together and simplifying yields

$$F_2(1+\delta_1; 1, 1; 2+\delta_2, 2+\delta_3; x, y)$$

$$= \frac{(1-x-y)\text{Log}(1-x-y) - (1-x)\log(1-x) - (1-y)\log(1-y)}{xy} + \mathcal{O}(\epsilon)$$ (B.9)

B.2 $\mathcal{O}(\delta)$ Terms

We have for the binomial bit

$$\sum_{n=1}^{\infty}\sum_{i=1}^{n-1}\binom{n}{i}\frac{y^n(-1)^i(-\frac{x}{y})^i}{(i+1)(n+2)}\left(\delta_2+\delta_3+\delta_1 Z_1[n]-\delta_2 Z_1[i+1]-\delta_3 Z_1[n-i+1]\right) \quad \text{(B.10)}$$

The first two terms are given by (B.7) so we'll focus on the Z_1 sums.

δ_1

The δ_1 term has no i-dependence so is given by (B.5)$\times\delta_1 Z[n]$. We therefore have terms like

$$\sum_{n=1}^{\infty}\frac{Z_1[n]}{(n+2)}X^n = \sum_{n=1}^{\infty}\frac{Z_1[n-1]}{(n+2)}X^n + \sum_{n=1}^{\infty}\frac{1}{(n+2)n}X^n$$

$$= \frac{1}{X}\left[\frac{1}{X}\sum_{i=1}^{\infty}\frac{X^n}{n}Z_1[n-1]-\sum_{n=1}^{\infty}\frac{X^n}{(n)(n+1)}\right] = \frac{S_0^2(X)}{X^2} - \frac{(1-X)\log(1-X)}{X^2} - \frac{1}{X}$$

$$= \frac{\log(1-X)^2}{2X^2} - \frac{(1-X)\log(1-X)}{X^2} - \frac{1}{X} \quad \text{(B.11)}$$

and

$$\sum_{n=1}^{\infty}\frac{Z_1[n]}{(n+1)(n+2)}X^n = \sum_{i=1}^{\infty}\left[\frac{Z_1[n]}{(n+1)}X^n - \frac{Z_1[n]}{(n+2)}X^n\right]$$

$$= \frac{(X-1)\log(1-X)^2}{2X^2} + \frac{(1-X)\log(1-X)}{X^2} + \frac{1}{X}. \quad \text{(B.12)}$$

We then have from the non-binomial terms

$$\sum_{i=1}^{\infty}\frac{x^i}{(i+1)}Z_1[i] = \frac{\log(1-x)^2}{2x} \quad \text{(B.13)}$$

In total this comes to

$$F_2(1+\delta_1;1,1;2+\delta_2,2+\delta_3;x,y)|_{\delta_1}$$

$$= \frac{\delta_1}{2xy}\Bigg((1-x)\log(1-x)\times(\log(1-x)-2)+(1-y)\log(1-y)\times(\log(1-y)-2)$$

$$-(1-x-y)\log(1-x-y)\times(\log(1-x-y)-2)\Bigg) \quad \text{(B.14)}$$

179

B.2.1 δ_2

We will begin by considering just the first set of terms in (B.3) ie will include the $\{x \leftrightarrow y, \delta_2 \leftrightarrow \delta_3\}$ after. Starting with the binomial term

$$\sum_{n=1}^{\infty} \frac{y^n}{(n+2)} \sum_{i=1}^{n-1} \binom{n}{i} \frac{(-1)^i(-\frac{x}{y})^i}{(i+1)} Z_1[i+1]$$

$$= \sum_{n=1}^{\infty} \frac{y^n}{(n+2)(n+1)} \left(\frac{y}{x}\right) \sum_{i=1}^{n} \binom{n+1}{i} (-1)^i \left(-\frac{x}{y}\right)^i Z_1[i] - \sum_{n=1}^{\infty} \frac{y^n}{(n+2)}$$

$$= \sum_{n=1}^{\infty} \frac{y^n}{(n+2)(n+1)} \left(\frac{y}{x}\right) \sum_{i=1}^{n+1} \binom{n+1}{i} (-1)^i \left(-\frac{x}{y}\right)^i Z_1[i]$$

$$- \sum_{n=1}^{\infty} \frac{x^n}{(n+2)(n+1)} Z_1[n+1] - \sum_{n=1}^{\infty} \frac{y^n}{(n+2)} \tag{B.15}$$

The first term can be evaluated by introducing raising and lowering operators

$$(\mathbf{x}^+)^m \cdot 1 = \frac{1}{m} \ln^m(x)$$

$$\mathbf{x}^+ \cdot f(x) = \int_0^x \frac{f(x')}{x'} dx'$$

$$\mathbf{x}^- \cdot f(x) = x \frac{d}{dx} f(x) \tag{B.16}$$

and then redefining the $Z_1[i] = S_1[i]$ via

$$S_1[i] = S_1[N] - \sum_{j=i+1}^{N} \frac{x_1^j}{j} \tag{B.17}$$

where we will take an $N \to \infty$ limit and an $x_1 \to 1$ limit at the end. Consider the second term and rewrite the sum using the raising operator

$$-\sum_{n=1}^{\infty} \frac{y^n}{(n+2)(n+1)} \left(\frac{y}{x}\right) \mathbf{x}_1^+ \sum_{i=1}^{n+1} \binom{n+1}{i} (-1)^i \left(-\frac{x}{y}\right)^i \sum_{j=i+1}^{N} x_1^j \tag{B.18}$$

The j-sum is evaluated using

$$\sum_{j=i+1}^{N} x_1^j = \frac{x_1}{1-x_1} x_1^i - \frac{x_1}{1-x_1} x_1^N \tag{B.19}$$

where the second term can be neglected as it vanishes under the $\mathbf{x}_1^+$ operator in the $N \to \infty$. Calling $X = \frac{x}{y}$ for convience we have

$$-\sum_{n=1}^{\infty} \frac{y^n}{X(n+2)(n+1)} \mathbf{x}_1^+ \frac{x_1}{1-x_1} \sum_{i=1}^{n+1} \binom{n+1}{i} (Xx_1)^i$$

$$= -\sum_{n=1}^{\infty} \frac{y^n}{X(n+2)(n+1)} \mathbf{x}_1^+ \frac{x_1}{1-x_1} ((1+Xx_1)^{n+1} - 1)$$

$$= \sum_{n=1}^{\infty} \frac{y^n}{X(n+2)(n+1)} \left(-(1+X)^{n+1} \sum_{i=1}^{n+1} \frac{1}{i} \left(\frac{1}{1+X} \right)^i \times (1 - (1+Xx_1)^i) \right.$$

$$\left. -((1+X)^{n+1} - 1) \sum_{i=1}^{N} \frac{1}{j} \right) \tag{B.20}$$

The last line cancels the $S_1[N]$ from (B.17). NOTE typo in eq.(57) of [108] where sum to ∞ should be a sum to n. Taking the $x_1 \to 1$ limit leaves us with

$$\sum_{n=1}^{\infty} \frac{y^n}{(n+2)(n+1)} \left(\frac{y}{x} \right) \sum_{i=1}^{n+1} \binom{n+1}{i} (-1)^i \left(-\frac{x}{y} \right)^i Z_1[i]$$

$$-\sum_{n=1}^{\infty} \frac{x^n}{(n+2)(n+1)} Z_1[n+1] - \sum_{n=1}^{\infty} \frac{y^n}{(n+2)}$$

$$= \sum_{n=1}^{\infty} \frac{(x+y)^{n+1}}{x(n+2)(n+1)} \left(Z_1[n+1] - \sum_{i=1}^{n+1} \frac{1}{i(1+\frac{x}{y})^i} \right)$$

$$-\sum_{n=1}^{\infty} \frac{x^n}{(n+2)(n+1)} Z_1[n+1] - \sum_{n=1}^{\infty} \frac{y^n}{(n+2)} \tag{B.21}$$

Focusing on the second term we need to first define the general nested sums

$$Z[N; m_1, m_2, \ldots, m_k; x_1, x_2, \ldots, x_k] := \sum_{i=1}^{N} \frac{x_1^i}{i^{m_1}} Z[N-1; m_2, \ldots, m_k; x_2, \ldots, x_k] \tag{B.22}$$

$$S[N; m_1, m_2, \ldots, m_k; x_1, x_2, \ldots, x_k] := \sum_{i=1}^{N} \frac{x_1^i}{i^{m_1}} S[N; m_2, \ldots, m_k; x_2, \ldots, x_k] \tag{B.23}$$

allowing us to write the second term as

$$-\sum_{n=1}^{\infty} \frac{(x+y)^{n+1}}{x(n+2)(n+1)} Z\left[n+1; 1; \frac{y}{x+y}\right]$$

$$= -\sum_{n=1}^{\infty} \frac{(x+y)^{n+1}}{x(n+2)(n+1)} \left(Z\left[n-1; 1; \frac{y}{x+y}\right] + \frac{y^n}{n(x+y)^n} Z[n-1] + \frac{y^{n+1}}{(n+1)(x+y)^{n+1}} Z[n-1] \right).$$

$$\tag{B.24}$$

The first term goes as

$$-\sum_{n=1}^{\infty} \frac{(x+y)^{n+1}}{x(n+2)(n+1)} Z\left[n-1;1;\frac{y}{x+y}\right]$$

$$= -\frac{(x+y)}{x} \sum_{n=1}^{\infty} (x+y)^n \left(\frac{1}{n+1} - \frac{1}{n+2}\right) Z\left[n-1;1;\frac{y}{x+y}\right] \tag{B.25}$$

Leaving us with terms

$$\sum_{n=1}^{\infty} \frac{(x+y)^n}{(n+1)} Z\left[n-1;1;\frac{y}{x+y}\right]$$

$$= \frac{1}{(x+y)} \sum_{n=1}^{\infty} \frac{(x+y)^n}{n} Z\left[n-1;1;\frac{y}{x+y}\right] - \sum_{n=1}^{\infty} \frac{y^n}{n(n+1)} Z[n-1]$$

$$= \frac{1}{(x+y)} Z\left[\infty;1,1;x+y,\frac{y}{x+y}\right] + \frac{\log(1-x-y)}{x+y} + 1$$

$$= \frac{1}{(x+y)} \mathrm{Li}_{1,1}\left(\frac{y}{x+y},x+y\right) + \frac{\log(1-x-y)}{x+y} + 1. \tag{B.26}$$

The multipolylogarithm is defined as

$$\mathrm{Li}_{m_1,\ldots,m_n}(x_1,\ldots,x_n) = \sum_{0<i_1<i_2<\ldots<i_n} \frac{x_1^{i_1}}{i_1^{m_1}} \frac{x_2^{i_2}}{i_2^{m_2}} \cdots \frac{x_n^{i_n}}{i_n^{m_n}} \tag{B.27}$$

We can evaluate the Multiple Polylogarithm (MPL) $\mathrm{Li}_{11}(\frac{y}{x+y},x+y)$ by considering it's relation to Generalised Polylogarithms (GPL) [112]

$$G(a_1,\ldots,a_n;x) = \int_0^x \frac{\mathrm{d}y}{y-a_1} G(a_2,\ldots,a_n;y) \tag{B.28}$$

$$G(;x) \equiv 1 \tag{B.29}$$

$$\mathrm{Li}_{m_n,\ldots,m_2,m_1}(z_n,\ldots,z_2,z_1) = (-1)^n G\left(\underbrace{0,\ldots,0}_{m_1-1},\frac{1}{z_1},\underbrace{0,\ldots,0}_{m_2-1},\frac{1}{z_1 z_2},\ldots,\underbrace{0,\ldots,0}_{m_n-1},\frac{1}{\prod_{i=1}^n z_i};1\right) \tag{B.30}$$

and so evaluating the integral gives us (within the fundamental region $|x|+|y|<1$)

$$\mathrm{Li}_{1,1}\left(z_1,z_2\right) = \log\left(\frac{z_1-z_1 z_2}{z_1-1}\right)\log\left(1-z_1 z_2\right) + \mathrm{Li}_2\left(\frac{1-z_1 z_2}{1-z_1}\right) - \mathrm{Li}_2\left(\frac{1}{1-z_1}\right)$$

$$\mathrm{Li}_{1,1}\left(\frac{y}{x+y},x+y\right) = \log(1-y)\log\left(\frac{x}{(x+y-1)}\right) + \mathrm{Li}_2\left(\frac{1-y}{(1-x-y)}\right) - \mathrm{Li}_2\left(\frac{1}{(1-x-y)}\right). \tag{B.31}$$

Returning to (B.25) we have the term

$$\sum_{n=1}^{\infty} \frac{(x+y)^n}{(n+2)} Z\left[n-1;1;\frac{y}{x+y}\right]$$

$$= \frac{1}{(x+y)} \sum_{n=1}^{\infty} \frac{(x+y)^n}{(n+1)} Z\left[n-1;1;\frac{y}{x+y}\right] - \sum_{n=1}^{\infty} \frac{y^n}{n(n+2)} Z[n-1] \tag{B.32}$$

the first of which has been evaluated and the second is standard.

B.2.2 δ_3 piece

Finally we have

$$-\sum_{n=1}^{\infty}\sum_{i=1}^{n-1}\binom{n}{i}\frac{y^n(-1)^i(-\frac{x}{y})^i}{(i+1)(n+2)}Z_1[n-i+1]$$

$$=-\sum_{n=1}^{\infty}\sum_{i=1}^{n-1}\binom{n}{i}\frac{y^n(-1)^i(-\frac{x}{y})^i}{(i+1)(n+2)}\left(Z_1[n-i]+\frac{1}{(n-i+1)}\right) \tag{B.33}$$

where the second term partial fractions to

$$-\sum_{n=1}^{\infty}\sum_{i=1}^{n-1}\binom{n}{i}\frac{y^n(-1)^i(-\frac{x}{y})^i}{(n+2)^2}\left(\frac{1}{(i+1)}+\frac{1}{(n-i+1)}\right)$$

$$=-\sum_{n=1}^{\infty}\frac{y^n}{(n+2)^2}\left(\frac{(x+y)^{n+1}}{x(n+1)y^n}-\frac{x^n}{y^n(n+1)}-\frac{y}{x(1+n)}-1\right)+\{x\leftrightarrow y\}$$

$$=\sum_{n=1}^{\infty}\left(\frac{x^n}{(n+2)^2(n+1)}+\frac{y}{x}\frac{y^n}{(n+2)^2(n+1)}+\frac{y^n}{(n+2)^2}-\frac{(x+y)}{x}\frac{(x+y)^n}{(n+2)^2(n+1)}\right)$$

$$+\{x\leftrightarrow y\}. \tag{B.34}$$

These easily evaluate to polylogarithms. The other term is

$$-\sum_{n=1}^{\infty}\sum_{i=1}^{n-1}\binom{n}{i}\frac{y^n(-1)^i(-\frac{x}{y})^i}{(i+1)(n+2)}Z_1[n-i]$$

$$=-\sum_{n=1}^{\infty}\frac{y^{n+1}}{x(n+1)(n+2)}\sum_{i=2}^{n}\binom{n+1}{i}(-1)^i\left(-\frac{x}{y}\right)^i Z_1[n+1-i]$$

$$=-\sum_{n=1}^{\infty}\frac{y^n}{xn(n+1)}\sum_{i=2}^{n-1}\binom{n}{i}(-1)^i\left(-\frac{x}{y}\right)^i Z_1[n-i]$$

$$=-\sum_{n=1}^{\infty}\frac{y^n}{xn(n+1)}\sum_{i=1}^{n-1}\binom{n}{i}(-1)^i\left(-\frac{x}{y}\right)^i Z_1[n-i]+\sum_{n=1}^{\infty}\frac{y^n}{(n+2)}Z_1[n] \tag{B.35}$$

where we have reduced the $i+1$ denominator, the $i=1$ term vanishes due to an implicit $S[i-1]$ term in the second line and we relabel $n \to n-1$ in the third line. We've evaluated the last term before, and upon relabelling $i \to n-i$ and using the result implicitely derived in the δ_2 section

$$\sum_{i=1}^{n}\binom{n}{i}x^i Z_1[i]=(1+x)^n Z_1[n]-(1+x)^n Z\left[n-1;1;\frac{1}{(1+x)}\right]-\frac{1}{n} \tag{B.36}$$

we can rewrite (B.35) as (dropping the last sum)

$$
-\sum_{n=1}^{\infty} \frac{y^n}{xn(n+1)} \sum_{i=1}^{n-1} \binom{n}{i} \left(\frac{x}{y}\right)^{n-i} Z_1[i]
$$

$$
= \sum_{n=1}^{\infty} \frac{x^{n-1}}{n(n+1)} \left(\left(\frac{y}{x}\right)^n Z_1[n] + \frac{1}{n} + \left(\frac{x+y}{x}\right)^n Z\left[n-1;1;\frac{x}{x+y}\right] - \left(\frac{x+y}{x}\right)^n Z_1[n] \right)
$$

$$
= \frac{1}{x} \sum_{n=1}^{\infty} \left(\frac{x^n}{n^2(n+1)} + \frac{y^n}{n(n+1)} Z_1[n] + \frac{(x+y)^n}{n(n+1)} Z\left[n-1;1;\frac{x}{x+y}\right] - \frac{(x+y)^n}{n(n+1)} Z_1[n] \right).
$$
(B.37)

We now have all of the $\mathcal{O}(\delta)$ pieces for the binomial terms. Returning to the non-binomial bit we have

$$
\frac{\Gamma(2+\delta_2)}{\Gamma(1+\delta_1)} \sum_{n=1}^{\infty} x^n \frac{\Gamma(n+1+\delta_1)}{\Gamma(n+2+\delta_2)}
$$

$$
= \sum_{n=1}^{\infty} \frac{x^n}{(n+1)} (1+\delta_2) \times (1 + \delta_1 Z_1[n] + \delta_1^2 Z_{11}[n] + \delta_1^3 Z_{111}[n] + \ldots)
$$

$$
\times (1 - \delta_2 S_1[n+1] + \delta_2^2 S_{11}[n+1] - \delta_2^3 S_{111}[n+1])
$$
(B.38)

which can be evaluated easily.

B.3 $\mathcal{O}(\delta^2)$ terms

B.3.1 δ_1^2

Starting with non-binomial terms we have

$$
\sum_{n=1}^{\infty} \frac{x^n}{(n+1)} Z_{11}[n] = \sum_{n=1}^{\infty} \frac{x^n}{(n+1)} \left(Z_{11}[n-1] + \frac{1}{n} Z_1[n-1] \right)
$$

$$
= \sum_{n=1}^{\infty} \left(\frac{1}{x} \frac{x^n}{n} Z_{11}[n-1] - \frac{x^n}{n(n+1)} Z_1[n-1] + \frac{x^n}{(n+1)} \frac{1}{n} Z_1[n-1] \right)
$$

$$
= \frac{1}{x} \operatorname{Li}_{111}(1,1,x) = -\frac{\log(1-x)^3}{6x} + \{x \leftrightarrow y\}.
$$
(B.39)

From the binomial we have terms like

$$
\sum_{n=1}^{\infty} \frac{X^n}{(n+2)} Z_{11}[n] = \sum_{n=1}^{\infty} \frac{1}{X} \frac{X^n}{(n+1)} Z_{11}[n-1]
$$

$$
= -\frac{\log(1-X)^3}{6X^3} - \frac{1}{X} \sum_{n=1}^{\infty} \left(\frac{X^n}{n} Z_1[n-1] - \frac{X^n}{(n+1)} Z_1[n-1] \right)
$$

$$
= -\frac{\log(1-X)^3}{6X^3} - \frac{\log(1-X)^2}{2X} + \frac{1}{X} \sum_{n=1}^{\infty} \left(\frac{1}{X} \frac{X^n}{n} Z_1[n-1] - \frac{X^n}{n(n+1)} \right)
$$
(B.40)

184

all of which are previous results. The other terms to consider are

$$\sum_{n=1}^{\infty} \frac{X^n}{(n+1)(n+2)} Z_{11}[n] = \sum_{n=1}^{\infty} \left(\frac{X^n}{(n+1)} - \frac{X^n}{(n+2)} \right) Z_{11}[n] \tag{B.41}$$

both of which have been calculated.

B.3.2 δ_2^2

We need to consider

$$= \sum_{n=1}^{\infty} \sum_{i=1}^{n-1} \binom{n}{i} \frac{(-1)^i(-x)^i y^{n-i}}{(i+1)(n-i+1)} \times \delta_2^2(S_{11}[i+1] - S_1[i+1])$$

$$\rightarrow \sum_{n=1}^{\infty} \sum_{i=1}^{n-1} \binom{n}{i} \frac{(-1)^i(-x)^i y^{n-i}}{(i+1)(n+2)} \times \delta_2^2(S_{11}[i+1] - S_1[i+1]) + \{x \leftrightarrow y, \delta_2 \leftrightarrow \delta_3\} \tag{B.42}$$

where the $S_1[i+1]$ term was previously evaluated so first consider

$$\sum_{i=1}^{n-1} \binom{n}{i} (-1)^i \frac{X^i}{(i+1)} \times S_{11}[i+1] = \sum_{i=1}^{n} \binom{n}{i} (-1)^i \frac{X^i}{(i+1)} \times S_{11}[i+1] - \frac{(-X)^n}{(n+1)} S_{11}[n+1].$$
$$\tag{B.43}$$

where we'll first consider

$$\sum_{i=1}^{n} \binom{n}{i} (-1)^i \frac{X^i}{(i+1)} \times S_{11}[i+1] = \left(-\frac{1}{X} \right) \frac{1}{(n+1)} \sum_{i=1}^{n+1} \binom{n+1}{i} (-1)^i X^i S_{11}[i] - 1. \tag{B.44}$$

As before we redefine

$$S_{11}[i] = S_{11}[N] - S_1[N] \sum_{i_1=i+1}^{N} \frac{x_1^{i_1}}{i_1} + \sum_{i_1=i+1}^{N} \sum_{i_2=i_1+1}^{N} \frac{x_1^{i_1}}{i_1} \frac{x_2^{i_2}}{i_2} \tag{B.45}$$

where we will take the $i_1, i_2 \to 1$ and $N \to \infty$ limits at the end. The fist term can be rewritten as

$$S_{11}[N] = \left(Z_{11}[N] + \sum_{i=1}^{N} \frac{1}{i^2} \right)\Big|_{N\to\infty} = \frac{\log(1-x_1)^2}{2}\Big|_{x_1\to 1} + \frac{\pi^2}{6} = \frac{S_1[N]^2}{2} + \frac{\pi^2}{6}. \tag{B.46}$$

The second term is similar to the $\mathcal{O}(\delta_2)$ term. Let's generalise this.

$$\sum_{i=1}^{n} \binom{n}{i} (-1)^i X^i \sum_{i_1=i+1}^{N} \frac{x_1^{i_1}}{i_1} = \sum_{i=1}^{n} \mathbf{x}_1^+ \binom{n}{i} (-1)^i (Xx_1)^i \frac{x_1}{1-x_1} = -\mathbf{x}_1^+ \frac{x_1}{1-x_1} \left(1 - (1-Xx_1)^n \right)$$

$$= (1-X)^n \sum_{i=1}^{n} \frac{1}{i} \left(\frac{1}{1-X} \right)^i \left[1 - (1-X)^i \right] - \left(1 - (1-X)^n \right) S_1[N]$$

$$= (1-X)^n \left(S\left[n; 1; \frac{1}{1-X} \right] - S_1[n] \right) - \left(1 - (1-X)^n \right) S_1[N] \tag{B.47}$$

The last term contains terms like

$$\mathbf{x}_2^+ \cdot \mathbf{x}_1^+ \cdot \frac{x_2}{1 - x_2} \frac{x_1 x_2}{1 - x_1 x_2} \left[1 - (1 - X x_1 x_2)^{n+1} \right]$$

$$= -(1 - X)^{n+1} \sum_{i=1}^{n+1} \frac{1}{i} \left(\frac{1}{1 - X} \right)^i \mathbf{x}_2^+ \cdot \frac{x_2}{1 - x_2} [1 - (1 - X x_2)^i]$$

$$+ \left(1 - (1 - X)^{n+1} \right) \sum_{i=1}^{N} \sum_{i_2 = i+1}^{N} \frac{x_1^i}{i} \frac{x_2^{i_2}}{i_2}. \tag{B.48}$$

The last line cancels the $S_{11}[N]$ contribution from (B.46). The operator $\mathbf{x}_2^+$ acts as

$$\mathbf{x}_2^+ \cdot \frac{x_2}{1 - x_2} \left[1 - (1 - X x_2)^i \right] = \left(1 - (1 - X)^i \right) S_1[N]$$

$$+ \left(1 - (1 - X)^i \right) \mathbf{x}_2^+ \cdot \frac{x_2}{1 - x_2} x_2^N - (1 - X)^i \sum_{j=1}^{i} \frac{1}{j} \left(\frac{1}{1 - X} \right)^j \left[1 - (1 - X x_2)^j \right]. \tag{B.49}$$

The second term vanishes as discussed earlier as

$$\mathbf{x}_2^+ \frac{x_2}{1 - x_2} x_2^N = \sum_{i=N+1}^{\infty} \frac{x_2}{i} \tag{B.50}$$

so vanishes in the $N \to \infty$ limit. (B.48) therefore reduces to

$$(1 - X)^{n+1} S_1[n+1] S_1[N] - (1 - X)^{n+1} S_1[N] S\left[n + 1; 1; \frac{1}{1 - X} \right]$$

$$+ (1 - X)^{n+1} \sum_{i=1}^{n+1} \left(\frac{1}{i} \left(S\left[i; 1; \frac{1}{1 - X} \right] - S_1[i] \right) \right)$$

$$= (1 - X)^{n+1} S_1[n+1] S_1[N] - (1 - X)^{n+1} S_1[N] S\left[n + 1; 1; \frac{1}{1 - X} \right]$$

$$+ (1 - X)^{n+1} \left(S\left[n + 1; 1, 1; 1, \frac{1}{1 - X} \right] - S_{11}[n+1] \right) \tag{B.51}$$

The first line cancels the $S_1[N] \sum_{i_1 = i+1}^{\infty} \frac{x_1^{i_1}}{i_1}$ contribution and we are left with

$$\sum_{i=1}^{n} \binom{n}{i} (-1)^i \frac{X^i}{(i+1)} \times S_{11}[i+1]$$

$$= \left(-\frac{1}{X} \right) \frac{1}{(n+1)} (1 - X)^{n+1} \left(\sum_{i=1}^{n+1} \sum_{j=1}^{i} \frac{1}{i} \frac{1}{j} - \sum_{i=1}^{n+1} \sum_{j=1}^{i} \frac{1}{i} \frac{1}{j(1 - X)^j} \right) - 1$$

$$= \left(-\frac{1}{X} \right) \frac{1}{(n+1)} (1 - X)^{n+1} \left(S_{11}[n+1] - S\left[n + 1; 1, 1; 1, \frac{1}{1 - X} \right] \right) - 1. \tag{B.52}$$

186

Returning to the original problem we have

$$\sum_{n=1}^{\infty} \frac{y^n}{(n+2)} \left(\sum_{i=1}^{n} \binom{n}{i} (-1)^i \frac{X^i}{(i+1)} \times S_{11}[i+1] - \frac{(-X)^n}{(n+1)} S_{11}[n+1]. \right)|_{X \to -\frac{x}{y}}$$

$$= \sum_{n=1}^{\infty} \frac{y^n}{(n+2)(n+1)} \left(\left(-\frac{1-X}{X} \right)(1-X)^n \left(S_{11}[n+1] - S\left[n+1; 1, 1; 1, \frac{1}{1-X}\right] \right) \right.$$

$$\left. - (-X)^n S_{11}[n+1] - (n+1) \right)|_{X \to -\frac{x}{y}}. \quad \text{(B.53)}$$

First we look at terms like

$$\sum_{n=1}^{\infty} \frac{X^n}{(n+2)(n+1)} S_{11}[n+1] = \sum_{n=1}^{\infty} \frac{X^n}{(n+2)(n+1)} \left(Z_{11}[n+1] + Z_2[n+1] \right)$$

$$= \sum_{n=1}^{\infty} \frac{X^n}{(n+2)(n+1)} \left(\frac{1}{(n+1)^2} + \frac{1}{n^2} + Z_{11}[n] + \frac{1}{(n+1)} Z_1[n] + Z_2[n-1] \right). \quad \text{(B.54)}$$

We consider terms

$$\sum_{n=1}^{\infty} \frac{X^n}{n} Z_2[n-1] = Z[\infty; 1, 2; X, 1] = \text{Li}_{2,1}(1, X) = H_{1,2}(X) \quad \text{(B.55)}$$

where $H_{m_1, \dots}(x)$ are the harmonic polylogarithms [111] which we evaluate in Section B.4. We also look at

$$\sum_{n=1}^{\infty} \frac{X^n}{(n+1)^2(n+2)} Z_1[n] = \sum_{n=1}^{\infty} X^n \left(\frac{1}{(n+1)^2} - \frac{1}{(n+1)(n+2)} \right) Z_1[n]. \quad \text{(B.56)}$$

We've evaluated the second term before so look at

$$\sum_{n=1}^{\infty} \frac{X^n}{(n+1)^2} Z_1[n] = \frac{1}{X} \sum_{n=1}^{\infty} \frac{X^n}{n^2} Z_1[n-1] = \frac{\text{Li}_{1,2}(1, X)}{X} = \frac{S_1^2(X)}{X}. \quad \text{(B.57)}$$

where $S_\nu^\rho(x)$ is the Nielsen generalised polylogarithm. Next we consider terms of the form

$$\sum_{n=1}^{\infty} \frac{(X \cdot Y)^n}{(n+2)(n+1)} S[n+1; 1, 1; 1, \frac{1}{X}] \quad \text{(B.58)}$$

where first we rewrite in terms of useful Z sums via

$$S[n+1; 1, 1; 1, X] = Z[n+1; 1, 1; 1, X] + Z[n+1; 2; X]$$

$$= Z[n-1; 1, 1; 1, X] + \left(\frac{1}{n} + \frac{1}{(n+1)} \right) Z[n-1; 1; X] + \frac{X^n}{n(n+1)}$$

$$+ Z[n-1; 2; X] + \frac{X^{n+1}}{(n+1)^2} + \frac{X^n}{n^2} \quad \text{(B.59)}$$

187

and so we will need to look at terms

$$\sum_{n=1}^{\infty} \frac{(X \cdot Y)^n}{n} Z\left[n - 1; 1, 1; 1, \frac{1}{X}\right] = \text{Li}_{1,1,1}\left(\frac{1}{X}, 1, X \cdot Y\right) = -G\left(\frac{1}{XY}, 1, \frac{1}{Y}; 1\right), \quad \text{(B.60)}$$

$$\sum_{n=1}^{\infty} \frac{(X \cdot Y)^n}{n} Z\left[n - 1; 2; \frac{1}{X}\right] = \text{Li}_{2,1}\left(\frac{1}{X}, X \cdot Y\right) = G\left(0, \frac{1}{X \cdot Y}, \frac{1}{Y}; 1\right), \quad \text{(B.61)}$$

$$\sum_{n=1}^{\infty} \frac{(X \cdot Y)^n}{n} Z\left[n - 1; 1; \frac{1}{X}\right] = \text{Li}_{1,1}(\frac{1}{X}, X \cdot Y) = G\left(\frac{1}{XY}, \frac{1}{Y}; 1\right) \quad \text{(B.62)}$$

and

$$\sum_{n=1}^{\infty} \frac{(X \cdot Y)^n}{n^2} Z\left[n - 1; 1; \frac{1}{X}\right] = \text{Li}_{1,2}(\frac{1}{X}, X \cdot Y) = G\left(\frac{1}{XY}, 0, \frac{1}{Y}; 1\right). \quad \text{(B.63)}$$

B.3.3 δ_3^2

We look at

$$= \sum_{n=1}^{\infty} \sum_{i=1}^{n-1} \binom{n}{i} \frac{(-1)^i (-x)^i y^{n-i}}{(i+1)(n-i+1)} \times \delta_3^2 S_{11}[n - i + 1]$$

$$\rightarrow \sum_{n=1}^{\infty} \sum_{i=1}^{n-1} \binom{n}{i} \frac{(-1)^i (-x)^i y^{n-i}}{(i+1)(n+2)} \times \delta_3^2 S_{11}[n - i + 1] + \{x \leftrightarrow y, \delta_2 \leftrightarrow \delta_3\}$$

$$\text{(B.64)}$$

As previously seen we can evaluate this by reducing the S sum

$$\sum_{n=1}^{\infty} \sum_{i=1}^{n-1} \binom{n}{i} \frac{(-1)^i (-x)^i y^{n-i}}{(i+1)(n+2)} \times \delta_3^2 \left(S_{11}[n - i] + \frac{1}{(n-i+1)} S_1[n - i + 1]\right) \quad \text{(B.65)}$$

and starting with the second term we partial fraction to give

$$\sum_{n=1}^{\infty} \sum_{i=1}^{n-1} \binom{n}{i} \frac{(-1)^i (-x)^i y^{n-i}}{(n+2)^2} \left(\frac{1}{(n-i+1)} + \frac{1}{(i+1)}\right) S_1[n - i + 1] \quad \text{(B.66)}$$

where here the first term can be related to (B.47) via a relabeling and the second term goes as (B.35) where we reduce the denominator offset and then relabel. We are thus left with the term

$$\sum_{n=1}^{\infty} \sum_{i=1}^{n-1} \binom{n}{i} \frac{(-1)^i (-x)^i y^{n-i}}{(n+2)(i+1)} S_{11}[n - i]$$

$$= \left(\frac{y}{x}\right) \sum_{n=1}^{\infty} \frac{y^n}{(n+1)(n+2)} \sum_{i=2}^{n} \binom{n+1}{i} (-1)^i \left(-\frac{x}{y}\right)^i S_{11}[n - i + 1]$$

$$= \left(\frac{y}{x}\right) \sum_{n=1}^{\infty} \frac{y^n}{(n+1)(n+2)} \sum_{i=1}^{n} \binom{n+1}{i} (-1)^i \left(-\frac{x}{y}\right)^i S_{11}[n - i + 1] - \sum_{n=1}^{\infty} \frac{y^n}{(n+2)} S_{11}[n]$$

$$= \frac{1}{x} \sum_{n=1}^{\infty} \frac{x^n}{n(n+1)} \sum_{i=1}^{n-1} \binom{n}{i} \left(\frac{y}{x}\right)^i S_{11}[i] - \sum_{n=1}^{\infty} \frac{y^n}{(n+2)} S_{11}[n]. \quad \text{(B.67)}$$

188

Generalising from earlier

$$\sum_{i=1}^{n-1} \binom{n}{i} X^i S_{11}[i] = \sum_{i=1}^{n} \binom{n}{i} X^i S_{11}[i] - X^n S_{11}[n]$$

$$= -(1+X)^n \left(S\left[n; 1, 1; 1, \frac{1}{1+X}\right] - S_{11}[n] \right) - X^n S_{11}[n] \tag{B.68}$$

reducing the problem to

$$\frac{1}{x} \sum_{n=1}^{\infty} \frac{x^n}{n(n+1)} \left(\frac{(x+y)^n}{x^n} \left(S_{11}[n] - S\left[n; 1, 1; 1, \frac{x}{x+y}\right] \right) - \left(\frac{y}{x}\right)^n S_{11}[n] \right) - \sum_{n=1}^{\infty} \frac{y^n}{(n+2)} S_{11}[n] \tag{B.69}$$

which can be evaluated by converting S sums to Z sums and reducing denominators etc. For completeness we'll look at (B.66) more explicitly. Taking the first term

$$\sum_{n=1}^{\infty} \sum_{i=1}^{n-1} \binom{n}{i} \frac{(-1)^i(-x)^i y^{n-i}}{(n+2)^2} \frac{1}{(n-i+1)} S_1[n-i+1]$$

$$= \sum_{n=1}^{\infty} \frac{x^n}{(n+2)^2} \sum_{i=1}^{n-1} \binom{n}{i} \frac{(\frac{y}{x})^i}{(i+1)} S_1[i+1]$$

$$= \sum_{n=1}^{\infty} \frac{x^n}{(n+2)^2} \left(\frac{x}{y} \frac{1}{(n+1)} \sum_{i=1}^{n} \binom{n+1}{i} \left(\frac{y}{x}\right)^i S_1[i] - 1 \right)$$

$$= \frac{1}{y} \sum_{n=1}^{\infty} \frac{x^n}{n(n+1)^2} \sum_{i=1}^{n} \binom{n}{i} \left(\frac{y}{x}\right)^i S_1[i] - \frac{1}{y} \sum_{n=1}^{\infty} \frac{y^n}{n(n+1)^2} S_1[n] - \sum_{n=1}^{\infty} \frac{x^n}{(n+2)^2} \tag{B.70}$$

all of which have been previously evaluated. The second piece is

$$\sum_{n=1}^{\infty} \sum_{i=1}^{n-1} \binom{n}{i} \frac{(-1)^i(-x)^i y^{n-i}}{(n+2)^2} \frac{1}{(i+1)} S_1[n-i+1] \tag{B.71}$$

which is same as (B.33) except with $(n+2) \to (n+2)^2$ but otherwise has the exact same procedure. Finally we have the non-binomial terms for both δ_2^2 and δ_3^2

$$= \sum_{n=1}^{\infty} \frac{x^n}{(n+1)} (S_{11}[n+1] - S_1[n+1]) = \frac{1}{x} \sum_{n=1}^{\infty} \frac{x^n}{n} (S_{11}[n] - S_1[n]) \tag{B.72}$$

which have already been evaluated.

B.3.4 $\delta_1 \delta_2$ and $\delta_1 \delta_3$

Starting with the non-binomial term we have

$$\delta_1 \delta_2 \sum_{n=1}^{\infty} \frac{x^n}{(n+1)} (Z_1[n] - Z_1[n] Z_1[n+1]) + \{x \leftrightarrow y, \delta_2 \leftrightarrow \delta_3\} \tag{B.73}$$

where we have evaluated the first term before and the second term required us to deal with products of Z-sums for the first time. This can be done by reducing the argument to the same value and using the formula

$$
Z[n; m_1, \ldots, m_k; x_1, \ldots, x_k] \times Z[n; m'_1, \ldots, m'_l; x'_1, \ldots, x'_\ell]
$$
$$
= \sum_{i=1}^{n} \frac{x_1^i}{i^{m_1}} Z[i-1; m_2, \ldots, m_k; x_2, \ldots, x_k] Z[i-1; m'_1, \ldots, m'_\ell; x'_1, \ldots, x'_\ell]
$$
$$
+ \sum_{i=1}^{n} \frac{x_1'^i}{i^{m'_1}} Z[i-1; m_1, \ldots, m_k; x_1, \ldots, x_k] Z[i-1; m'_2, \ldots, m'_\ell; x'_2, \ldots, x'_\ell]
$$
$$
+ \sum_{i=1}^{n} \frac{(x_1 x'_1)^i}{i^{m_1+m'_1}} Z[i-1; m_2, \ldots, m_k; x_2, \ldots, x_k] Z[i-1; m'_2, \ldots, m'_\ell; x'_2, \ldots, x'_\ell] \qquad \text{(B.74)}
$$

which reduces $Z_1[n]^2$ to $2Z_{11}[n] + Z_2[n]$. For the binomial piece we have

$$
\delta_1 \delta_2 \sum_{n=1}^{\infty} \sum_{i=1}^{n-1} \binom{n}{i} \frac{(-1)^i(-x)^i y^{n-i}}{(i+1)(n+2)} \times Z_1[n](1 - Z_1[i+1])
$$
$$
+ \delta_1 \delta_3 \sum_{n=1}^{\infty} \sum_{i=1}^{n-1} \binom{n}{i} \frac{(-1)^i(-x)^i y^{n-i}}{(i+1)(n+2)} \times Z_1[n](1 - Z_1[n-i+1]) + \{x \leftrightarrow y,\ \delta_2 \leftrightarrow \delta_3\} \quad \text{(B.75)}
$$

The first term for both $\delta_1\delta_2$ and $\delta_1\delta_3$ has been evaluated previously and the second term of $\delta_1\delta_2$ can be derived from (B.21).

$$
\sum_{n=1}^{\infty} \frac{(x+y)^{n+1}}{x(n+2)(n+1)} Z_1[n] \left(Z_1[n+1] - \sum_{i=1}^{n+1} \frac{1}{i(1+\frac{x}{y})^i} \right)
$$
$$
- \sum_{n=1}^{\infty} \frac{x^n}{(n+2)(n+1)} Z_1[n] Z_1[n+1] - \sum_{n=1}^{\infty} \frac{y^n}{(n+2)} Z_1[n]
$$
$$
= \sum_{n=1}^{\infty} \frac{(x+y)^{n+1}}{x(n+2)(n+1)^2} Z_1[n] + \sum_{n=1}^{\infty} \frac{(x+y)^{n+1}}{x(n+2)(n+1)} (2Z_{11}[n] + Z_2[n]) - \sum_{n=1}^{\infty} \frac{y^{n+1}}{x(n+2)(n+1)^2} Z_1[n]
$$
$$
- \sum_{n=1}^{\infty} \frac{(x+y)^{n+1}}{x(n+2)(n+1)} \left(Z\left[n; 1, 1; 1, \frac{y}{x+y}\right] + Z\left[n; 1, 1; \frac{y}{x+y}, 1\right] + Z\left[n; 2; \frac{y}{x+y}\right] \right)
$$
$$
- \sum_{n=1}^{\infty} \frac{x^n}{(n+2)(n+1)} (2Z_{11}[n] + Z_2[n]) - \sum_{n=1}^{\infty} \frac{x^n}{(n+2)(n+1)^2} Z_1[n] - \sum_{n=1}^{\infty} \frac{y^n}{(n+2)} Z_1[n]
$$
$$
\text{(B.76)}
$$

all of which have previously been evaluated. Looking at the second term of $\delta_1\delta_3$ we use (B.34) and (B.37) to split it into two parts

$$
\sum_{n=1}^{\infty} Z_1[n-1] \left(\frac{1}{x} \frac{x^n}{n(n+1)^2} + \frac{1}{x} \frac{y^n}{n(n+1)^2} + \frac{1}{y} \frac{y^n}{(n+1)^2} - \frac{1}{x} \frac{(x+y)^n}{n(n+1)^2} \right) + \{x \leftrightarrow y\}. \quad \text{(B.77)}
$$

and

$$= \frac{1}{x} \sum_{n=1}^{\infty} Z_1[n-1] \Big(\frac{x^n}{n^2(n+1)} + \frac{y^n}{n(n+1)} Z_1[n] + \frac{(x+y)^n}{n(n+1)} Z\Big[n-1;1;\frac{x}{x+y}\Big] - \frac{(x+y)^n}{n(n+1)} Z_1[n] \Big)$$

$$+ \sum_{n=1}^{\infty} \frac{y^n}{(n+2)} Z_1[n]Z_1[n]. \tag{B.78}$$

B.3.5 $\quad \delta_2\delta_3$

This goes as

$$\delta_2\delta_3 \sum_{n=1}^{\infty} \sum_{i=1}^{n-1} \binom{n}{i} \frac{(-1)^i(-x)^i y^{n-i}}{(i+1)(n+2)} \times \Big(1 - Z_1[i+1] - Z_1[n-i+1] + Z_1[i+1]Z_1[n-i+1] \Big)$$

$$+ \{x \leftrightarrow y, \delta_2 \leftrightarrow \delta_3\} \tag{B.79}$$

The first three terms have been previously calculated so we consider the last term. This cannot be reduced to product sums of the same limit so we need a new technique. First we reduce the Z-sums to

$$\sum_{n=1}^{\infty} \sum_{i=1}^{n-1} \binom{n}{i} \frac{(-1)^i(-x)^i y^{n-i}}{(i+1)(n+2)} \Big(Z_1[i]Z_1[n-i] + \frac{Z_1[i+1]}{(n-i+1)} + \frac{Z_1[n-i+1]}{(i+1)} - \frac{1}{(i+1)(n-i+1)} \Big)$$

$$\tag{B.80}$$

We reduce the offset of the denominator for the first term

$$\sum_{n=1}^{\infty} \sum_{i=1}^{n-1} \binom{n}{i} \frac{(-1)^i(-x)^i y^{n-i}}{(i+1)(n+2)} Z_1[i]Z_1[n-i] = \frac{1}{x} \sum_{n=1}^{\infty} \frac{y^n}{n(n+1)} \sum_{i=1}^{n-1} \binom{n}{i} \Big(\frac{x}{y}\Big)^i Z_1[i-1]Z_1[n-i]$$

$$= \frac{1}{x} \sum_{n=1}^{\infty} \frac{y^n}{n(n+1)} \sum_{i=1}^{n-1} \binom{n}{i} \Big(\frac{x}{y}\Big)^i \Big(Z_1[i]Z_1[n-i] - \frac{Z_1[n-i]}{i} \Big) \tag{B.81}$$

and look at the first term which can be rewritten using [108]

$$\sum_{i=1}^{n-1} \binom{n}{i} X^i S[i;m_1,\ldots]S[n-i;m'_1,\ldots]$$

$$= (1+X)^n \sum_{j=1}^{n} \frac{1}{j(1+X)^j} \sum_{i=1}^{j-1} \binom{j}{i} \frac{(Xx_1)^i}{i^{m_1-1}} S[i;m_2,\ldots]S[n-i;m'_1,\ldots]$$

$$+ (1+X)^n \sum_{j=1}^{n} \frac{1}{j(1+X)^j} \sum_{i=1}^{j-1} \binom{j}{i} \frac{(X)^i x_1'^{j-i}}{(n-i)^{m'_1-1}} S[i;m_1,\ldots]S[n-i;m'_2,\ldots] \tag{B.82}$$

to

$$\frac{1}{x}\sum_{n=1}^{\infty}\frac{y^n}{n(n+1)}\sum_{i=1}^{n-1}\binom{n}{i}\left(\frac{x}{y}\right)^i Z_1[i]Z_1[n-i]$$

$$=\frac{1}{x}\sum_{n=1}^{\infty}\frac{y^n}{n(n+1)}\left(\left(\frac{x+y}{y}\right)^n\sum_{j=1}^{n}\frac{y^j}{j(x+y)^j}\sum_{i=1}^{j-1}\binom{j}{i}\left[\left(\frac{x}{y}\right)^i+\left(\frac{x}{y}\right)^{j-i}\right]Z_1[i]\right)$$

$$=-\frac{1}{x}\sum_{n=1}^{\infty}\frac{(x+y)^n}{n(n+1)}\sum_{j=1}^{n}\frac{1}{j}\left(\frac{y}{x+y}\right)^j$$

$$\times\left(\left(\frac{x+y}{y}\right)^j\left(S\left[j;1;\frac{y}{x+y}\right]+S\left[j;1;\frac{x}{x+y}\right]-2S_1[j]\right)+\left[\left(\frac{x}{y}\right)^j+1\right]S_1[j]\right)\qquad(\text{B}.83)$$

all of which can be rewritten as $Z[\infty;\ldots]$ after some algebra. We next look at

$$-\frac{1}{x}\sum_{n=1}^{\infty}\frac{y^n}{n(n+1)}\sum_{i=1}^{n-1}\binom{n}{i}\left(\frac{x}{y}\right)^i\frac{Z_1[n-i]}{i}$$

$$=-\frac{1}{x}\sum_{n=1}^{\infty}\frac{y^n}{n(n+1)}\sum_{j=1}^{n}\frac{1}{j}\sum_{i=1}^{j-1}\binom{j}{i}\left[\left(\frac{x}{y}\right)^{j-i}Z_1[i]+\frac{1}{i}\left(\frac{x}{y}\right)^i\right]\qquad(\text{B}.84)$$

which requires the evaluation of

$$\sum_{i=1}^{j-1}\binom{j}{i}\frac{X^i}{i}=\mathbf{x_0}+\sum_{i=1}^{j}\binom{j}{i}X^i-\frac{X^j}{j}$$

$$=\sum_{i=1}^{j}\left(\frac{(1+X)^i-1}{i}\right)-\frac{X^j}{j}=Z[j;1,1+X]-Z[j,1,1]-\frac{X^j}{j}\qquad(\text{B}.85)$$

and the rest has been previously evaluated. Returning to (B.80) we next to consider

$$\sum_{n=1}^{\infty}\sum_{i=1}^{n-1}\binom{n}{i}\frac{(-1)^i(-x)^iy^{n-i}}{(i+1)(n+2)}\frac{Z_1[i]}{(n-i+1)}$$

$$=\sum_{n=1}^{\infty}\sum_{i=1}^{n-1}\binom{n}{i}\frac{(-1)^i(-x)^iy^{n-i}}{(n+2)^2}Z_1[i]\left(\frac{1}{(i+1)}+\frac{1}{(n-i+1)}\right)\qquad(\text{B}.86)$$

which is simply (B.66). The third term of (B.80) involves reducing the Z-sum arguments, reducing the offset of the denominator and then various partial fractions and denominator reductions but overall introduces no new techniques or general results. The last term is

$$-\sum_{n=1}^{\infty}\sum_{i=1}^{n-1}\binom{n}{i}\frac{(-1)^i(-x)^iy^{n-i}}{(i+1)(n+2)}\frac{1}{(i+1)(n-i+1)}$$

$$=-\sum_{n=1}^{\infty}\sum_{i=1}^{n-1}\binom{n}{i}\frac{(-1)^i(-x)^iy^{n-i}}{(n+2)^2}\left(\frac{1}{(i+1)^2}+\left[\frac{1}{(i+1)(n+2)}+\{x\leftrightarrow y\}\right]\right)\qquad(\text{B}.87)$$

where again we've done enough that this introduces nothing new. We now have all of the $\mathcal{O}(\epsilon^2)$ terms. Clearly the integral method is better.

B.4 Multiple and Harmonic Polylogarithms

A few results are given here

$$G(y, y, xy; 1) = -\frac{1}{2}\log\left[\frac{x}{(x-1)}\right]\log[-y]^2$$

$$-\frac{1}{2}\log[1-y]^2(\log[-xy] - \log[1-xy] + \log\left[\frac{(xy-1)}{((-1+x)y)}\right]) - \log[-y]\operatorname{Li}_2\left[\frac{1}{(1-x)}\right]$$

$$+ \log[1-y](\log\left[\frac{x}{(x-1)}\right]\log[-y] + \operatorname{Li}_2\left[\frac{1}{(1-x)}\right]) + \operatorname{Li}_3\left[\frac{1}{(1-x)}\right] - \operatorname{Li}_3\left[\frac{(1-y)}{(x-1)}\right] \quad (B.88)$$

Looking at $\operatorname{Li}_{2,1}(1, X)$ we have

$$\int_0^1 \frac{\mathrm{d}x_1}{x_1 - \frac{1}{X}} \int_0^{x_1} \frac{\mathrm{d}x_2}{x_2} \int_0^{x_2} \frac{\mathrm{d}x_3}{x_3 - 1} = \int_0^1 \frac{\mathrm{d}x_1}{x_1 - \frac{1}{X}} \int_0^{x_1} \frac{\log(1-x_2)\mathrm{d}x_2}{x_2}$$

$$= -\int_0^1 \frac{\operatorname{Li}_2(x_1)}{x_1 - \frac{1}{X}}\mathrm{d}x_1 = X \int_0^1 \frac{\operatorname{Li}_2(x_1)}{1 - Xx_1}\mathrm{d}x_1. \quad (B.89)$$

Alternatively noticing this is a Harmonic polylogarithm we can use the relations

$$H_{m_1+1,m_2,...,m_k}(x) = \int_0^x \mathrm{d}x_1 f_0(x_1) H_{m_1,m_2,...,m_k}(x_1) \quad (B.90)$$

and

$$H_{\pm 1,m_2,...,m_k}(x) = \int_0^x \mathrm{d}x_1 f_{\pm 1}(x_1) H_{m_2,...,m_k} \quad (B.91)$$

where

$$f_0(x) = \frac{1}{x}, \qquad f_{\pm 1}(x) = \frac{1}{1 \mp x}. \quad (B.92)$$

We therefore have

$$H_{1,2}(x) = \int_0^x \mathrm{d}x_1 f_1(x_1) \int_0^{x_1} \mathrm{d}x_2 f_0(x_2) H_1(x_2) = \int_0^x \mathrm{d}x_1 \frac{\operatorname{Li}_2(x_1)}{1 - x_1}$$

$$= \log[1-x]\operatorname{Li}_2[x] - 2\operatorname{Li}_3[x] - 2\operatorname{Li}_3\left[\frac{x}{(x-1)}\right] + \frac{1}{3}\log[1-x]^3. \quad (B.93)$$

We also need

$$H_{1,3}(x) = \int_0^x \mathrm{d}x_1 f_1(x_1)\operatorname{Li}_3(x) = \quad (B.94)$$

$$H_{2,2}(x) = \int_0^x \mathrm{d}x_1 f_0(x_1) H_{1,2}(x_2)$$

$$= -\frac{1}{2}\operatorname{Li}_2[x]^2 - 2\operatorname{Li}_4[x] \quad (B.95)$$

We similarly calculate $H_{1,1,2}(x)$ and $H_{1,2,1}(x)$.

Appendix C

Mellin-Barnes Expansions of Triangles and a Specific Triangle Integral

C.1   Mellin-Barnes Expanded Triangles

First the two-mass triangle. Starting from (5.96) we close the contour on the left side of the complex plane (after performing the initial Gauss shift)

$$
I_{3,MB}^D(\nu_1,\nu_2,\nu_4;t,M^2) = (-1)^{\frac{D}{2}+1+\kappa}(M^2)^{\frac{D}{2}-\sigma}\frac{\Gamma[\frac{D}{2}-\nu_{12}]\Gamma[\sigma-\frac{D}{2}]\Gamma[\frac{D}{2}-\nu_4]}{\Gamma[\nu_4]\Gamma[\nu_{12}]\Gamma[D-\sigma]}
$$

$$
\times \sum_{N\geq 0}\frac{(1+\kappa)_N}{\Gamma[1+N]}\,{}_2F_1\left(\sigma-\frac{D}{2},\nu_2-N;\nu_{12};1-T\right)
$$

$$
= (-1)^{\frac{D}{2}+1+\kappa}(M^2)^{\frac{D}{2}-\sigma}T^{\frac{D}{2}-\nu_{24}}\frac{\Gamma[\frac{D}{2}-\nu_{12}]\Gamma[\sigma-\frac{D}{2}]\Gamma[\frac{D}{2}-\nu_4]}{\Gamma[\nu_4]\Gamma[\nu_{12}]\Gamma[D-\sigma]}
$$

$$
\times \sum_{N\geq 0}\frac{(1+\kappa)_N}{\Gamma[1+N]}T^N\,{}_2F_1\left(\frac{D}{2}-\nu_4,\nu_1+N;\nu_{12};1-T\right)
$$

$$
= (-1)^{\frac{D}{2}+1+\kappa}(M^2)^{\frac{D}{2}-\sigma}T^{\frac{D}{2}-\nu_{24}}\frac{\Gamma[\frac{D}{2}-\nu_{12}]\Gamma[\sigma-\frac{D}{2}]\Gamma[\frac{D}{2}-\nu_4]}{\Gamma[\nu_4]\Gamma[\nu_{12}]\Gamma[D-\sigma]}
$$

$$
\times \sum_{N,m\geq 0}\frac{(\nu_1)_{m+N}(1+\kappa)_N(\frac{D}{2}-\nu_4)_m}{(\nu_1)_N(\nu_{12})_m\Gamma[1+N]\Gamma[1+m]}T^N(1-T)^m
$$

$$
= (-1)^{\frac{D}{2}+1+\kappa}(M^2)^{\frac{D}{2}-\sigma}T^{\frac{D}{2}-\nu_{24}}\frac{\Gamma[\frac{D}{2}-\nu_{12}]\Gamma[\sigma-\frac{D}{2}]\Gamma[\frac{D}{2}-\nu_4]}{\Gamma[\nu_4]\Gamma[\nu_{12}]\Gamma[D-\sigma]}
$$

$$
\times F_2\left[\nu_1;1+\kappa,\frac{D}{2}-\nu_4;\nu_1,\nu_{12};T,1-T\right]
$$

$$
= (-1)^{\frac{D}{2}+1+\kappa}(M^2)^{\frac{D}{2}-\sigma}T^{\frac{D}{2}-\nu_{24}}\frac{\Gamma[\frac{D}{2}-\nu_{12}]\Gamma[\sigma-\frac{D}{2}]\Gamma[\frac{D}{2}-\nu_4]}{\Gamma[\nu_4]\Gamma[\nu_{12}]\Gamma[D-\sigma]}
$$

$$
\times (1-T)^{-1-\kappa}F_1\left[\frac{D}{2}-\nu_4;1+\kappa,\nu_{\hat 1};\nu_{12};1,1-T\right]
$$

$$
= (-1)^{\frac{D}{2}+1+\kappa}(M^2)^{\frac{D}{2}-\sigma}T^{\frac{D}{2}-\nu_{24}}\frac{\Gamma[\frac{D}{2}-\nu_{12}]\Gamma[\sigma-\frac{D}{2}]\Gamma[\frac{D}{2}-\nu_4]}{\Gamma[\nu_4]\Gamma[\nu_{12}]\Gamma[D-\sigma]}
$$

$$
\times (1-T)^{-1-\kappa}\,{}_2F_1\left[\frac{D}{2}-\nu_4,\nu_{\hat 1};\nu_{\hat{1}2};1-T\right]\frac{\Gamma[\hat\sigma-\frac{D}{2}]\Gamma[\nu_{12}]}{\Gamma[\nu_{\hat{1}2}]\Gamma[\sigma-\frac{D}{2}]}
$$

$$
= (-1)^{\frac{D}{2}+1+\kappa}(M^2)^{\frac{D}{2}-\sigma}\frac{\Gamma[\frac{D}{2}-\nu_{12}]\Gamma[\hat\sigma-\frac{D}{2}]\Gamma[\frac{D}{2}-\nu_4]}{\Gamma[\nu_4]\Gamma[\nu_{\hat{1}2}]\Gamma[D-\sigma]}
$$

$$
\times (1-T)^{-1-\kappa}\,{}_2F_1\left[\hat\sigma-\frac{D}{2},\nu_2;\nu_{\hat{1}2};1-T\right]. \tag{C.1}
$$

For the one-mass triangles we similarly have

$$I_{3,MB}^D(\nu_1, \nu_2, \nu_3; M^2) = (-1)^{\frac{D}{2}+1+\kappa} s^{\frac{D}{2}-\sigma} \frac{\Gamma[\frac{D}{2} - \nu_1 - \nu_2]\Gamma[\frac{D}{2} - \nu_2 - \nu_3]\Gamma[\sigma - \frac{D}{2}]}{\Gamma[\nu_1]\Gamma[\nu_3]\Gamma[D - \sigma]}$$

$$\times \sum_{N \geq 0} \frac{(1 + \kappa)_N (\frac{D}{2} - \nu_2 - \nu_3)_N}{(\nu_1)_N}$$

$$= (-1)^{\frac{D}{2}+1+\kappa} s^{\frac{D}{2}-\sigma} \frac{\Gamma[\frac{D}{2} - \nu_1 - \nu_2]\Gamma[\frac{D}{2} - \nu_2 - \nu_3]\Gamma[\sigma - \frac{D}{2}]}{\Gamma[\nu_1]\Gamma[\nu_3]\Gamma[D - \sigma]}$$

$$\times \frac{\Gamma[\nu_1]\Gamma[\hat{\sigma} - \frac{D}{2}]}{\Gamma[\nu_{\hat{1}}]\Gamma[\sigma - \frac{D}{2}]}$$

$$= (-1)^{\frac{D}{2}+1+\kappa} s^{\frac{D}{2}-\sigma} \frac{\Gamma[\frac{D}{2} - \nu_1 - \nu_2]\Gamma[\frac{D}{2} - \nu_2 - \nu_3]\Gamma[\hat{\sigma} - \frac{D}{2}]}{\Gamma[\nu_{\hat{1}}]\Gamma[\nu_3]\Gamma[D - \sigma]}. \quad (C.2)$$

C.2 A Tensor Integral

There is a tensor integral of the form

$$\int dP \frac{(P - P_{k\omega})^2}{(P^2)^{\nu_2}(P + \bar{a})^{2\nu_1}(P - k)^{2\nu_3}} \rightarrow \frac{\Gamma[\sigma]}{\Gamma[\nu_1]\Gamma[\nu_2]\Gamma[\nu_3]} \int dP\{dx_i\} x_2^{\nu_1 - 1} x_3^{\nu_3 - 1} x_1^{\nu_2 - 1}$$

$$\times \frac{(P - x_2\bar{a} + x_3 k - P_{k\omega})^2}{(P^2 + x_2 x_3 s_{k\bar{a}})^\sigma}$$

$$= \frac{\Gamma[\sigma]}{\Gamma[\nu_1]\Gamma[\nu_2]\Gamma[\nu_3]} \int dP\{dx_i\} \frac{P^2 + (1 - x_3)s_{k\omega} + x_2[\bar{a}|P_{k\omega}|\bar{a}\rangle - x_2 x_3 s_{k\bar{a}}}{(P^2 + x_2 x_3 s_{k\bar{a}})^\sigma}$$

$$= I_3^t + s_{k\omega}\left(I_3^{D=4-2\epsilon}(\nu_1, \nu_2, \nu_3) - \frac{(-1)\Gamma[1 + \nu_3]}{\Gamma[\nu_3]} I_3^{D=6-2\epsilon}(\nu_1, \nu_2, 1 + \nu_3)\right)$$

$$+ [\bar{a}|P_{k\omega}|\bar{a}\rangle \frac{(-1)\Gamma[1 + \nu_1]}{\Gamma[\nu_1]} I_3^{D=6-2\epsilon}(\nu_1 + 1, \nu_2, \nu_3)$$

$$- s_{k\bar{a}} \frac{\Gamma[1 + \nu_1]\Gamma[1 + \nu_3]}{\Gamma[\nu_1]\Gamma[\nu_3]} I_3^{D=8-2\epsilon}(1 + \nu_1, \nu_2, 1 + \nu_3) \quad (C.3)$$

where the triangle mass is $s_{k\bar{a}}$ and

$$I_3^t = \frac{\Gamma[\sigma]}{\Gamma[\nu_1]\Gamma[\nu_2]\Gamma[\nu_3]} \int dP\{dx_i\} x_2^{\nu_1 - 1} x_3^{\nu_3 - 1} \frac{P^2}{(P^2 + x_2 x_3 s_{k\bar{a}})^\sigma}$$

$$= \frac{\Gamma[\sigma]}{\Gamma[\nu_1]\Gamma[\nu_2]\Gamma[\nu_3]} (-1)^{1+\sigma} \frac{\Gamma[1 + \frac{D}{2}]\Gamma[\sigma - 1 - \frac{D}{2}]}{\Gamma[\frac{D}{2}]\Gamma[\sigma]}$$

$$\times \int \{dx_i\} x_2^{\nu_1 - 1} x_3^{\nu_3 - 1} (1 - x_2 - x_3)^{\nu_2 - 1} (-x_2 x_3 s_{k\bar{a}})^{1 + \frac{D}{2} - \sigma}$$

$$= \frac{\Gamma[\sigma]}{\Gamma[\nu_1]\Gamma[\nu_2]\Gamma[\nu_3]} (-1)^{1+\sigma} \frac{\Gamma[3 - \epsilon]\Gamma[\sigma + \epsilon - 3]}{\Gamma[2 - \epsilon]\Gamma[\sigma]} (-s_{k\bar{a}})^{3 - \epsilon - \sigma}$$

$$\times \int \{dx_i\} x_2^{\nu_1 - 1} x_3^{\nu_3 - 1} (1 - x_2 - x_3)^{\nu_2 - 1} (x_2 x_3)^{3 - \epsilon - \sigma}$$

$$= (-1)^{-\epsilon} \frac{\Gamma[3 - \epsilon]\Gamma[\sigma + \epsilon - 3]}{\Gamma[2 - \epsilon]\Gamma[\nu_1]\Gamma[\nu_3]} s_{k\bar{a}}^{3 - \epsilon - \sigma} \frac{\Gamma[3 - \epsilon - \nu_1 - \nu_2]\Gamma[3 - \epsilon - \nu_2 - \nu_3]}{\Gamma[6 - 2\epsilon - \sigma]}. \quad (C.4)$$

This agrees with the box result presented in the main body of the thesis when setting $\nu_4 = -1$.

Appendix D

Starting Points for Future Calculations

D.1   General Two-Mass-Easy Box

We can add in the second mass to the derivation of the generalised one-mass box. $\{Q_i^2\}$ from (5.66) now contains $\{s, t, M_1^2, M_2^2\}$.
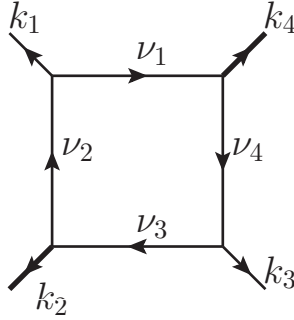

Figure D.1: A generalised two-mass easy box with $k_4^2 = M_1^2$, $k_2^2 = M_2^2$ and all other $k_i^2 = 0$. The internal propagators $\{A_1, A_2, A_3, A_4\}$ have arbitrary powers $\{\nu_1, \nu_2, \nu_3, \nu_4\}$.

This extends to the two-mass case as follows:

$$\mathcal{P} = x_1 + x_2 + x_3 + x_4, \tag{D.1}$$

and

$$\mathcal{Q} = x_1 x_3 s + x_2 x_4 t + x_1 x_4 M_1^2 + x_2 x_3 M_2^2. \tag{D.2}$$

The proceeding multinomial expansion can be written as,

$$
\begin{aligned}
&I_4^D(\nu_1, \nu_2, \nu_3, \nu_4; s, t, M^2) \\
&= \int \mathcal{D}x \sum_{n_1, n_2, n_3, n_4 \geq 0} \int \frac{\mathrm{d}^D \ell}{i\pi^{\frac{D}{2}}} \frac{(x_1 A_1)^{n_1}}{n_1!} \frac{(x_2 A_2)^{n_2}}{n_2!} \frac{(x_3 A_3)^{n_3}}{n_3!} \frac{(x_4 A_4)^{n_4}}{n_4!} \\
&= \int \mathcal{D}x \sum_{\mathcal{S} \geq 0} \frac{(x_1 x_3 s)^{q_1} (x_2 x_4 t)^{q_2} (x_1 x_4 M_1^2)^{q_3} (x_2 x_3 M_2^2)^{q_4}}{q_1! q_2! q_3!} \frac{x_1^{p_1} x_2^{p_2} x_3^{p_3} x_4^{p_4}}{p_1! p_2! p_3! p_4!} \times (p_1 + p_2 + p_3 + p_4)!,
\end{aligned}
\tag{D.3}
$$

$\mathcal{S} = \{q_1, q_2, q_3, q_4, p_1, p_2, p_3, p_4\}$ and with the constraint

$$q_1 + q_2 + q_3 + q_4 + p_1 + p_2 + p_3 + p_4 = -\frac{D}{2}, \tag{D.4}$$

which ensures the powers of $\mathcal{P}$ and $\mathcal{Q}$ are correct. Calling $\nu_i = -n_i$ we can take the $x_i^{-\nu_i}$ coefficients and compare these with the other side of the equality, extracting the Schwinger integrand to give

$$I_4^{D,2m}(\nu_1, \nu_2, \nu_3, \nu_4; s, t, M_1^2, M_2^2) = \sum_{\mathcal{S} \geq 0} \frac{\Gamma[1 + p_1 + p_2 + p_3 + p_4]}{\Gamma[1 + q_1]\Gamma[1 + q_2]\Gamma[1 + q_3]\Gamma[1 + q_4]}$$
$$\times \left(\prod_{i=1}^{4} \frac{\Gamma[1 - \nu_i]}{\Gamma[1 + p_i]} \right) s^{q_1} t^{q_2} (M_1^2)^{q_3} (M_2^2)^{q_4}, \tag{D.5}$$

where we can read off the constraints

$$q_1 + q_3 + p_1 = -\nu_1,$$
$$q_2 + q_4 + p_2 = -\nu_2,$$
$$q_1 + q_4 + p_3 = -\nu_3,$$
$$q_2 + q_3 + p_4 = -\nu_4,$$
$$q_1 + q_2 + q_3 + p_1 + p_2 + p_3 + p_4 = -\frac{D}{2}. \tag{D.6}$$

There are 56 potential solutions to $\mathcal{S}$ under these constraints but there are only 35 existing solutions. There is plenty to explore here, both in terms of kinematic regions and in pushing the results to a single, compact form such as with (5.117), and the result will be required for pushing our single-minus technique further to higher multiplicities.

D.2   Augmented Recursion for Single-Minus Amplitudes

This thesis has not touched upon the rational part of the single-minus amplitudes. We expect that we can use the BCFW shift for this amplitude which will reduce the number of factorisations needed to be considered, and indeed with the results known this has been tested and the rational contribution does vanish for large z under this shift.

In the all-plus case, there were double poles originating from the all-plus, three-point, one-loop vertex. There was no contributions from the two-loop vertex because the tree amplitude in the factorisation vanished for the all-plus configuration. The single-minus amplitude will contain contributions from the two-loop vertex as now the tree becomes an MHV tree. We could look at all of the two-loop diagrams that would contribute double poles individually but it might be easier to take two separate currents as shown in Figure D.2.
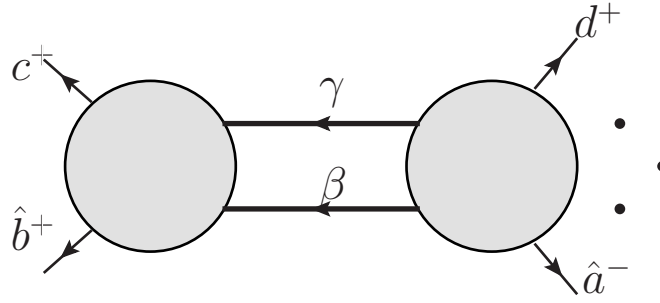
Figure D.2: Schematic diagram for the (two-loop)-(tree) channel containing the double pole contribution which comes from the two-loop, all-plus, three point vertex. The LHS circle indicates a doubly off-shell two-loop, four-point current. The RHS circle indicates a doubly off-shell n-point, tree amplitude. The external legs are BCFW shifted on legs $\hat{a}^-$ and $\hat{b}^+$.

The remaining channels either contain simple poles and only need standard recursion, or use the same methods as seen for the all-plus configuration.

Bibliography

[1] C. Anastasiou, E. Glover, and C. Oleari, "Application of the negative-dimension approach to massless scalar box integrals," *Nuclear Physics B*, vol. 565, no. 1, pp. 445–467, 2000.

[2] S. Badger, C. Brønnum-Hansen, H. B. Hartanto, and T. Peraro, "Analytic helicity amplitudes for two-loop five-gluon scattering: the single-minus case," *JHEP*, vol. 01, p. 186, 2019.

[3] C.-N. Yang and R. L. Mills, "Conservation of Isotopic Spin and Isotopic Gauge Invariance," *Phys. Rev.*, vol. 96, pp. 191–195, 1954.

[4] G. 't Hooft and M. Veltman, "Regularization and renormalization of gauge fields," *Nuclear Physics B*, vol. 44, no. 1, pp. 189–213, 1972.

[5] R. Feynman, "The Theory of positrons," *Phys. Rev.*, vol. 76, pp. 749–759, 1949.

[6] J. E. Paton and H.-M. Chan, "Generalized veneziano model with isospin," *Nucl. Phys.*, vol. B10, pp. 516–520, 1969.

[7] M. L. Mangano, S. J. Parke, and Z. Xu, "Duality and Multi - Gluon Scattering," *Nucl. Phys.*, vol. B298, pp. 653–672, 1988.

[8] F. A. Berends and W. Giele, "The Six Gluon Process as an Example of Weyl-Van Der Waerden Spinor Calculus," *Nucl. Phys.*, vol. B294, pp. 700–732, 1987.

[9] P. de Causmaecker, *Fotonen en Gluonen bij Hoge Energie*. PhD thesis, Katholieke Universiteit Leuven, 1983.

[10] P. De Causmaecker, R. Gastmans, W. Troost, and T. T. Wu, "Multiple Bremsstrahlung in Gauge Theories at High-Energies. 1. General Formalism for Quantum Electrodynamics," *Nucl. Phys.*, vol. B206, pp. 53–60, 1982.

[11] F. A. Berends, R. Kleiss, P. De Causmaecker, R. Gastmans, W. Troost, and T. T. Wu, "Multiple Bremsstrahlung in Gauge Theories at High-Energies. 2. Single Bremsstrahlung," *Nucl. Phys.*, vol. B206, pp. 61–89, 1982.

[12] F. A. Berends, R. Kleiss, P. de Causmaecker, R. Gastmans, W. Troost, and T. T. Wu, "Multiple Bremsstrahlung in Gauge Theories at High-energies. 3. Finite Mass Effects in Collinear Photon Bremsstrahlung," *Nucl. Phys.*, vol. B239, pp. 382–394, 1984.

[13] F. A. Berends, R. Kleiss, P. de Causmaecker, R. Gastmans, W. Troost, and T. T. Wu, "Multiple Bremsstrahlung in Gauge Theories at High-Energies. 4. The Process e+ e- —¿ gamma gamma gamma gamma," *Nucl. Phys.*, vol. B239, pp. 395–409, 1984.

[14] D. Danckaert, P. De Causmaecker, R. Gastmans, W. Troost, and T. T. Wu, "Four Jet Production in e^+e^- Annihilation," *Phys. Lett.*, vol. 114B, pp. 203–207, 1982.

[15] Z. Xu, D.-H. Zhang, and L. Chang, "Helicity Amplitudes for Multiple Bremsstrahlung in Massless Non-Abelian Gauge Theories," *Nucl. Phys.*, vol. B291, pp. 392–428, 1987.

[16] J. Henn and J. Plefka, *Scattering Amplitudes in Gauge Theories*, vol. 883. Springer, 11 2013.

[17] S. J. Parke and T. R. Taylor, "Amplitude for n Gluon Scattering," *Phys. Rev. Lett.*, vol. 56, p. 2459, 1986.

[18] F. A. Berends and W. T. Giele, "Recursive Calculations for Processes with n Gluons," *Nucl. Phys.*, vol. B306, pp. 759–808, 1988.

[19] M. L. Mangano and S. J. Parke, "Soft and Collinear Behavior of Dual Amplitudes," in *High-energy physics. Proceedings, International Europhysics Conference, Uppsala, Sweden, June 25 - July 1, 1987. Vols. 1, 2*, 1987.

[20] F. A. Berends and W. T. Giele, "Multiple Soft Gluon Radiation in Parton Processes," *Nucl. Phys.*, vol. B313, pp. 595–633, 1989.

[21] R. Britto, F. Cachazo, and B. Feng, "New recursion relations for tree amplitudes of gluons," *Nucl. Phys.*, vol. B715, pp. 499–522, 2005.

[22] R. Britto, F. Cachazo, B. Feng, and E. Witten, "Direct proof of tree-level recursion relation in Yang-Mills theory," *Phys. Rev. Lett.*, vol. 94, p. 181602, 2005.

[23] K. Risager, "A Direct proof of the CSW rules," *JHEP*, vol. 12, p. 003, 2005.

[24] D. Melrose, "Reduction of Feynman diagrams," *Nuovo Cim.*, vol. 40, pp. 181–213, 1965.

[25] G. Passarino and M. J. G. Veltman, "One Loop Corrections for e+ e- Annihilation Into mu+ mu- in the Weinberg Model," *Nucl. Phys.*, vol. B160, pp. 151–207, 1979.

[26] W. van Neerven and J. Vermaseren, "Large Loop Integrals," *Phys. Lett. B*, vol. 137, pp. 241–244, 1984.

[27] G. van Oldenborgh and J. Vermaseren, "New Algorithms for One Loop Integrals," *Z. Phys. C*, vol. 46, pp. 425–438, 1990.

[28] Z. Bern, L. J. Dixon, and D. A. Kosower, "Dimensionally regulated one loop integrals," *Phys. Lett.*, vol. B302, pp. 299–308, 1993. [Erratum: Phys. Lett.B318,649(1993)].

[29] Z. Bern, L. J. Dixon, and D. A. Kosower, "Dimensionally regulated pentagon integrals," *Nucl. Phys.*, vol. B412, pp. 751–816, 1994.

[30] R. G. Stuart, "Algebraic Reduction of One Loop Feynman Diagrams to Scalar Integrals," *Comput. Phys. Commun.*, vol. 48, pp. 367–389, 1988.

[31] R. G. Stuart and A. Gongora, "Algebraic Reduction of One Loop Feynman Diagrams to Scalar Integrals. 2.," *Comput. Phys. Commun.*, vol. 56, pp. 337–350, 1990.

[32] Z. Kunszt, A. Signer, and Z. Trocsanyi, "Singular terms of helicity amplitudes at one loop in QCD and the soft limit of the cross-sections of multiparton processes," *Nucl. Phys.*, vol. B420, pp. 550–564, 1994.

[33] S. Catani, "The Singular behavior of QCD amplitudes at two loop order," *Phys. Lett.*, vol. B427, pp. 161–171, 1998.

[34] G. 't Hooft, "A Planar Diagram Theory for Strong Interactions," *Nucl. Phys.*, vol. B72, p. 461, 1974. [,337(1973)].

[35] D. Zeppenfeld, "Diagonalization of Color Factors," *Int. J. Mod. Phys.*, vol. A3, pp. 2175–2179, 1988.

[36] V. Del Duca, A. Frizzo, and F. Maltoni, "Factorization of tree QCD amplitudes in the high-energy limit and in the collinear limit," *Nucl. Phys.*, vol. B568, pp. 211–262, 2000.

[37] V. Del Duca, L. J. Dixon, and F. Maltoni, "New color decompositions for gauge amplitudes at tree and loop level," *Nucl. Phys.*, vol. B571, pp. 51–70, 2000.

[38] S. G. Naculich, "All-loop group-theory constraints for color-ordered SU(N) gauge-theory amplitudes," *Phys. Lett.*, vol. B707, pp. 191–197, 2012.

[39] A. C. Edison and S. G. Naculich, "SU(N) group-theory constraints on color-ordered five-point amplitudes at all loop orders," *Nucl. Phys.*, vol. B858, pp. 488–501, 2012.

[40] Z. Bern, L. J. Dixon, and D. A. Kosower, "A Two loop four gluon helicity amplitude in QCD," *JHEP*, vol. 01, p. 027, 2000.

[41] R. J. Eden, P. V. Landshoff, D. I. Olive, and J. C. Polkinghorne, *The analytic S-matrix*. Cambridge: Cambridge Univ. Press, 1966.

[42] R. E. Cutkosky, "Singularities and discontinuities of Feynman amplitudes," *J. Math. Phys.*, vol. 1, pp. 429–433, 1960.

[43] W. van Neerven, "Dimensional Regularization of Mass and Infrared Singularities in Two Loop On-shell Vertex Functions," *Nucl. Phys. B*, vol. 268, pp. 453–488, 1986.

[44] Z. Bern and A. G. Morgan, "Massive loop amplitudes from unitarity," *Nucl. Phys.*, vol. B467, pp. 479–509, 1996.

[45] Z. Bern, L. J. Dixon, and D. A. Kosower, "Progress in one loop QCD computations," *Ann. Rev. Nucl. Part. Sci.*, vol. 46, pp. 109–148, 1996.

[46] Z. Bern, L. J. Dixon, D. C. Dunbar, and D. A. Kosower, "One loop selfdual and N=4 superYang-Mills," *Phys. Lett.*, vol. B394, pp. 105–115, 1997.

[47] W. T. Giele, Z. Kunszt, and K. Melnikov, "Full one-loop amplitudes from tree amplitudes," *JHEP*, vol. 04, p. 049, 2008.

[48] C. Anastasiou, R. Britto, B. Feng, Z. Kunszt, and P. Mastrolia, "D-dimensional unitarity cut method," *Phys. Lett.*, vol. B645, pp. 213–216, 2007.

[49] C. Anastasiou, R. Britto, B. Feng, Z. Kunszt, and P. Mastrolia, "Unitarity cuts and Reduction to master integrals in d dimensions for one-loop amplitudes," *JHEP*, vol. 03, p. 111, 2007.

[50] R. Britto, F. Cachazo, and B. Feng, "Generalized unitarity and one-loop amplitudes in N=4 super-Yang-Mills," *Nucl. Phys.*, vol. B725, pp. 275–305, 2005.

[51] P. Mastrolia and G. Ossola, "On the Integrand-Reduction Method for Two-Loop Scattering Amplitudes," *JHEP*, vol. 11, p. 014, 2011.

[52] D. A. Kosower and K. J. Larsen, "Maximal Unitarity at Two Loops," *Phys. Rev. D*, vol. 85, p. 045017, 2012.

[53] S. Badger, H. Frellesvig, and Y. Zhang, "Hepta-Cuts of Two-Loop Scattering Amplitudes," *JHEP*, vol. 04, p. 055, 2012.

[54] Y. Zhang, "Integrand-Level Reduction of Loop Amplitudes by Computational Algebraic Geometry Methods," *JHEP*, vol. 09, p. 042, 2012.

[55] S. Badger, H. Frellesvig, and Y. Zhang, "An Integrand Reconstruction Method for Three-Loop Amplitudes," *JHEP*, vol. 08, p. 065, 2012.

[56] P. Mastrolia, E. Mirabella, G. Ossola, and T. Peraro, "Scattering Amplitudes from Multivariate Polynomial Division," *Phys. Lett. B*, vol. 718, pp. 173–177, 2012.

[57] P. Mastrolia, E. Mirabella, G. Ossola, and T. Peraro, "Integrand-Reduction for Two-Loop Scattering Amplitudes through Multivariate Polynomial Division," *Phys. Rev. D*, vol. 87, no. 8, p. 085026, 2013.

[58] P. Mastrolia, E. Mirabella, G. Ossola, and T. Peraro, "Multiloop Integrand Reduction for Dimensionally Regulated Amplitudes," *Phys. Lett. B*, vol. 727, pp. 532–535, 2013.

[59] S. Caron-Huot and K. J. Larsen, "Uniqueness of two-loop master contours," *JHEP*, vol. 10, p. 026, 2012.

[60] P. Mastrolia, T. Peraro, and A. Primo, "Adaptive Integrand Decomposition in parallel and orthogonal space," *JHEP*, vol. 08, p. 164, 2016.

[61] T. Peraro, "Scattering amplitudes over finite fields and multivariate functional reconstruction," *JHEP*, vol. 12, p. 030, 2016.

[62] S. Abreu, F. Febres Cordero, H. Ita, M. Jaquier, and B. Page, "Subleading Poles in the Numerical Unitarity Method at Two Loops," *Phys. Rev. D*, vol. 95, no. 9, p. 096011, 2017.

[63] Z. Bern, G. Chalmers, L. J. Dixon, and D. A. Kosower, "One loop N gluon amplitudes with maximal helicity violation via collinear limits," *Phys. Rev. Lett.*, vol. 72, pp. 2134–2137, 1994.

[64] D. C. Dunbar, J. H. Ettle, and W. B. Perkins, "Augmented Recursion For One-loop Gravity Amplitudes," *JHEP*, vol. 06, p. 027, 2010.

[65] S. D. Alston, D. C. Dunbar, and W. B. Perkins, "n-point amplitudes with a single negative-helicity graviton," *Phys. Rev.*, vol. D92, no. 6, p. 065024, 2015.

[66] D. C. Dunbar and W. B. Perkins, "$\mathcal{N} = 4$ supergravity next-to-maximally-helicity-violating six-point one-loop amplitude," *Phys. Rev.*, vol. D94, no. 12, p. 125027, 2016.

[67] D. C. Dunbar and W. B. Perkins, "Two-loop five-point all plus helicity Yang-Mills amplitude," *Phys. Rev.*, vol. D93, no. 8, p. 085029, 2016.

[68] D. C. Dunbar, G. R. Jehu, and W. B. Perkins, "Two-loop six gluon all plus helicity amplitude," *Phys. Rev. Lett.*, vol. 117, no. 6, p. 061602, 2016.

[69] D. C. Dunbar, J. H. Godwin, G. R. Jehu, and W. B. Perkins, "Analytic all-plus-helicity gluon amplitudes in QCD," *Phys. Rev.*, vol. D96, no. 11, p. 116013, 2017.

[70] D. C. Dunbar, J. H. Godwin, W. B. Perkins, and J. M. W. Strong, "Color Dressed Unitarity and Recursion for Yang-Mills Two-Loop All-Plus Amplitudes," *Phys. Rev. D*, vol. 101, no. 1, p. 016009, 2020.

[71] A. R. Dalgleish, D. C. Dunbar, W. B. Perkins, and J. M. W. Strong, "Full color two-loop six-gluon all-plus helicity amplitude," *Phys. Rev. D*, vol. 101, no. 7, p. 076024, 2020.

[72] D. A. Kosower, "Light Cone Recurrence Relations for QCD Amplitudes," *Nucl. Phys.*, vol. B335, pp. 23–44, 1990.

[73] C. Schwinn and S. Weinzierl, "Scalar diagrammatic rules for Born amplitudes in QCD," *JHEP*, vol. 05, p. 006, 2005.

[74] D. Vaman and Y.-P. Yao, "The Space-Cone Gauge, Lorentz Invariance and On-Shell Recursion for One-Loop Yang-Mills amplitudes," in *8th Workshop on Continuous Advances in QCD (CAQCD-08)*, pp. 41–55, 5 2008.

[75] D. C. Dunbar, W. B. Perkins, and J. M. Strong, "n-point QCD two-loop amplitude," *Phys. Rev. D*, vol. 101, no. 7, p. 076001, 2020.

[76] S. Caron-Huot, L. J. Dixon, F. Dulat, M. von Hippel, A. J. McLeod, and G. Papathanasiou, "Six-Gluon amplitudes in planar $\mathcal{N} = 4$ super-Yang-Mills theory at six and seven loops," *JHEP*, vol. 08, p. 016, 2019.

[77] J. L. Bourjaily, E. Herrmann, C. Langer, A. J. McLeod, and J. Trnka, "All-Multiplicity Non-Planar MHV Amplitudes in sYM at Two Loops," 2019.

[78] E. W. N. Glover, C. Oleari, and M. E. Tejeda-Yeomans, "Two loop QCD corrections to gluon-gluon scattering," *Nucl. Phys.*, vol. B605, pp. 467–485, 2001.

[79] Z. Bern, A. De Freitas, and L. J. Dixon, "Two loop helicity amplitudes for gluon-gluon scattering in QCD and supersymmetric Yang-Mills theory," *JHEP*, vol. 03, p. 018, 2002.

[80] T. Ahmed, J. Henn, and B. Mistlberger, "Four-particle scattering amplitudes in QCD at NNLO to higher orders in the dimensional regulator," *JHEP*, vol. 12, p. 177, 2019.

[81] S. Badger, H. Frellesvig, and Y. Zhang, "A Two-Loop Five-Gluon Helicity Amplitude in QCD," *JHEP*, vol. 12, p. 045, 2013.

[82] S. Badger, G. Mogull, A. Ochirov, and D. O'Connell, "A Complete Two-Loop, Five-Gluon Helicity Amplitude in Yang-Mills Theory," *JHEP*, vol. 10, p. 064, 2015.

[83] T. Gehrmann, J. M. Henn, and N. A. Lo Presti, "Analytic form of the two-loop planar five-gluon all-plus-helicity amplitude in QCD," *Phys. Rev. Lett.*, vol. 116, no. 6, p. 062001, 2016. [Erratum: Phys. Rev. Lett.116,no.18,189903(2016)].

[84] S. Abreu, J. Dormans, F. Febres Cordero, H. Ita, B. Page, and V. Sotnikov, "Analytic Form of the Planar Two-Loop Five-Parton Scattering Amplitudes in QCD," *JHEP*, vol. 05, p. 084, 2019.

[85] D. Chicherin, T. Gehrmann, J. M. Henn, P. Wasser, Y. Zhang, and S. Zoia, "All Master Integrals for Three-Jet Production at Next-to-Next-to-Leading Order," *Phys. Rev. Lett.*, vol. 123, no. 4, p. 041603, 2019.

[86] H. A. Chawdhry, M. A. Lim, and A. Mitov, "Two-loop five-point massless QCD amplitudes within the integration-by-parts approach," *Phys. Rev.*, vol. D99, no. 7, p. 076011, 2019.

[87] S. Badger, D. Chicherin, T. Gehrmann, G. Heinrich, J. M. Henn, T. Peraro, P. Wasser, Y. Zhang, and S. Zoia, "Analytic form of the full two-loop five-gluon all-plus helicity amplitude," *Phys. Rev. Lett.*, vol. 123, no. 7, p. 071601, 2019.

[88] S. D. Alston, D. C. Dunbar, and W. B. Perkins, "Complex Factorisation and Recursion for One-Loop Amplitudes," *Phys. Rev.*, vol. D86, p. 085022, 2012.

[89] Z. Bern, L. J. Dixon, and D. A. Kosower, "On-shell recurrence relations for one-loop QCD amplitudes," *Phys. Rev.*, vol. D71, p. 105013, 2005.

[90] Z. Bern, L. J. Dixon, and D. A. Kosower, "One loop corrections to five gluon amplitudes," *Phys. Rev. Lett.*, vol. 70, pp. 2677–2680, 1993.

[91] D. C. Dunbar, W. B. Perkins, and E. Warrick, "The Unitarity Method using a Canonical Basis Approach," *JHEP*, vol. 06, p. 056, 2009.

[92] D. C. Dunbar, G. R. Jehu, and W. B. Perkins, "The two-loop n-point all-plus helicity amplitude," *Phys. Rev.*, vol. D93, no. 12, p. 125006, 2016.

[93] J. Henn, B. Power, and S. Zoia, "Conformal Invariance of the One-Loop All-Plus Helicity Scattering Amplitudes," *JHEP*, vol. 02, p. 019, 2020.

[94] R. Ellis and G. Zanderighi, "Scalar one-loop integrals for QCD," *JHEP*, vol. 02, p. 002, 2008.

[95] S. Badger, G. Mogull, and T. Peraro, "Local integrands for two-loop all-plus Yang-Mills amplitudes," *JHEP*, vol. 08, p. 063, 2016.

[96] G. Mahlon, "Multi - gluon helicity amplitudes involving a quark loop," *Phys. Rev.*, vol. D49, pp. 4438–4453, 1994.

[97] "Private Conversations with supervisor Prof. David Dunbar," 2020.

[98] D. Cangemi, "Selfdual Yang-Mills theory and one loop like - helicity QCD multi - gluon amplitudes," *Nucl. Phys.*, vol. B484, pp. 521–537, 1997.

[99] G. Chalmers and W. Siegel, "The Selfdual sector of QCD amplitudes," *Phys. Rev.*, vol. D54, pp. 7628–7633, 1996.

[100] "Private Conversations with supervisor Dr. Warren Perkins," 2020.

[101] D. Forde, "Direct extraction of one-loop integral coefficients," *Phys. Rev. D*, vol. 75, p. 125019, 2007.

[102] C. Anastasiou, E. Glover, and C. Oleari, "Scalar one-loop integrals using the negative-dimension approach," *Nuclear Physics B*, vol. 572, no. 1, pp. 307–360, 2000.

[103] I. Halliday and R. Ricotta, "Negative dimensional integrals. i. feynman graphs," *Physics Letters B*, vol. 193, no. 2, pp. 241–246, 1987.

[104] R. M. Ricotta, "Negative dimensions in quantum field theory," *J.J. Giambiagi Festschrif*, p. 350, Dec 1989.

[105] A. T. Suzuki and A. G. M. Schmidt, "Negative dimensional integration," *Journal of High Energy Physics*, vol. 1997, pp. 002–002, sep 1997.

[106] H. Bateman, "Higher Transcendental Functions [Volumes I-III]," 1953.

[107] N. Lebedev and R. Silverman, *Special Functions and Their Applications*. Dover Books on Mathematics, Dover Publications, 1972.

[108] S. Moch, P. Uwer, and S. Weinzierl, "Nested sums, expansion of transcendental functions and multiscale multiloop integrals," *J. Math. Phys.*, vol. 43, pp. 3363–3386, 2002.

[109] A. B. Goncharov, "Multiple polylogarithms and mixed Tate motives," *arXiv Mathematics e-prints*, p. math/0103059, Mar. 2001.

[110] N. Nielsen, *Der eulersche dilogarithmus und seine verallgemeinerungen*. W. Engelmann in Leipzig in Komm., 1909.

[111] E. Remiddi and J. Vermaseren, "Harmonic polylogarithms," *Int. J. Mod. Phys. A*, vol. 15, pp. 725–754, 2000.

[112] H. Frellesvig, "Generalized Polylogarithms in Maple," 6 2018.